

# **Experimental Investigation on Crack Formation in Filter Cakes with Wide Particle Size Distribution**

To the Faculty of Mechanical, Process and Energy Engineering  
of the Technische Universität Bergakademie Freiberg

approved

## **DISSERTATION**

to attain the academic degree of

Doctor of Engineering (Dr.-Ing)

Submitted

By M.Eng. Thanh Hai Pham

born on the 14<sup>th</sup> of September 1986 in Quang Ninh, Vietnam

Reviewers: Prof. Dr. -Ing. Urs Alexander Peuker, Freiberg, Germany

Prof. Dr.-Ing. Bernhard Hoffner, Mannheim, Germany

Date of the award: 29<sup>th</sup> January 2021

### **Declaration**

I, at this moment, declare that I completed this work without any improper help from a third party and without using any aids other than those cited. All ideas derived directly or indirectly from other sources are identified. In the selection and use of materials and the writing of the manuscript, I received support from Prof. Dr.-Ing. Urs Alexander Peuker.

Persons other than those above did not contribute to the writing of this thesis. I did not seek the help of a professional doctorate-consultant. Only those identified as having done so received no financial payment from me for any work done for me.

This thesis has not previously been published in the same or a similar form in Germany or abroad.

Date: 23<sup>rd</sup> September 2020

M.Eng. Thanh Hai Pham

## **Abstract**

Cua Ong Coal Washing Plant (CCWP) is operated by Vietnam National Coal-Mineral Industries Holding Corporation Limited and located in Quang Ninh coal basin of north-eastern Vietnam. The plant begins its operation since 1924 by French and washing anthracite coal to produce coal with different size ranges and ash content. After washing by Jigging, dense medium Cyclone, coal is separated into various sizes such as 0.5-6 mm; 6-15 mm; 15-35 mm; 35-50 mm; 50-100 mm. A large amount of fine coal, below 0.5 mm fine coal is dewatering by thickening before going to filtration by high-pressure filters.

Currently, the filtration process is inefficient in achieving the desired product with low moisture of the coal that makes it is suitable for mixing with other good quality coal before sending it to power stations, other domestic consumers, and export or storage. The residual moisture content of dewatered fine coals is still higher (20 – 22%) in some periods up to 25%, makes them too difficult to be mixed with other coals. Otherwise, water in filter cake cannot be recycled and reused, leading to higher overall production costs, higher transport costs, and reducing product value. From the above production situations, Vietnamese coal is selected as the primary research material. The research work does not only contribute the academic values but also solving current problems.

Besides the Vietnam coal as the primary material, two kinds of limestone KS12 (fine material which the particle size below 12  $\mu\text{m}$ ) and KS100 (coarser material, which the particle size below 100  $\mu\text{m}$ ) are used. They are pure limestone for laboratory experiments, which are provided accessible by commercial companies. The purpose is experiment execution as a different kind of material to reference, compare the results, and confirm assumptions.

From previous literature, one of the reasons for the imperfect dewatering process is shrinkage cracking, that is encountered frequently during filtration of the fine particulate filter cake. The consequence of the cracks is a significant disadvantage about the economy (the gas/wash water consumption is mostly increased by order of magnitude) and process results (higher moisture content/lower purity). The idea for research work is whether or not the crack formation on the coal filter cake, the change of the degree of cracking, and residual moisture content under various operating parameters. Base on the collected experimental result, some assumptions would be given for explanation. Otherwise, steam pressure filtration also would be suggested as a new method to avoid crack formation as well as improve the dewatering process.

Operation parameters using for research are particle size distribution, especially the proportion of fine particles, the solid volume concentration of slurry, the height of filter cake, and the applied pressure difference. By the change step by step each parameter, the effect of variables on the crack formation, and residual moisture content are collected. The increase in the percentage of fine particles and filter cake height leads to the probability and degree of crack rise up. Meanwhile, the opposite trends occur in the growth of solid volume fraction and pressure difference. The change of residual moisture content witnessed a different trend but, in general, achieved a lower value when cracking does not occur or the reduction of its degree. The dependence of tensile strengths and liquid distribution on the system, which can be characterized by saturation, the packing of agglomerated fine particles, wall effect, and the transition of stress, are using theories for interpretation. Because the almost explained phenomenon leads to a more precise understanding of the mechanism of shrinkage cracking, it is the basis for proposing new approaches as well as applicable over a wide range.

Steam pressure filtration is also applied to survey the crack formation and dewatering efficiency. Research showed the different probability and degree of cracking, the efficiency of dewatering compare with traditional filtration. Both experimental results are interpreted with suitability and acceptance.



## **Acknowledgment**

First of all, I would like to thank Prof. Dr.-Ing. Urs Alexander Peuker for giving me an opportunity to pursue doctoral studies at TU Bergakademie Freiberg and also as my supervisor, for his support during the whole period of my research work as well as his guidance. Thanks so much for his caring, advice, and tolerance. It was an enjoyable experience working with him.

Moreover, extended thanks go to all colleagues at the Institute of Mechanical Process Engineering and Mineral Processing, TU Bergakademie Freiberg, especially Thomas Buchwald, Sabine Seupel, Sophie Kühne, Erik Löwer, Thomas Leißner, Simon Esser, Silke Thümmeler, Annett Kästner, Yvonne Volkmar, Thomas Hanstusch and Hoang Huu Duong for their discussion, assistance, and support.

At CCWP, my heartfelt thanks go to Van Khoi Dang (Director) and Thu Thuy Bui (Coal Washing Science and Technology Department) for allowing me to conduct this research at the process plant between August and September 2019. The engineer's team and all employees of the plant are also appreciated.

I am also highly indebted to the Vietnam International Education Development (VIED) – Ministry of Education and Training for financial support through the 911 Project. Further, thank the German Academic Exchange Service (DAAD) and World University System (WUS) for their support in Germany. The Hanoi University of Mining and Geology is also appreciated for the support and permission to attend this doctoral program.

More special thanks go to my parents for their encouragement. I am also thankful to all my relatives and close friends for their support in different ways.

Lastly, but very importance, I am grateful to my wife Thi Oanh Do and our wonderful children Thuy Duong Pham and Binh Minh Pham for their patience and understanding in times when I was not with them because of this work. Their company and emotional support have made this possible.

## **Contents**

<b>Abstract</b> .....	iii
<b>Acknowledgment</b> .....	v
<b>Contents</b> .....	vi
<b>List of Figure</b> .....	viii
<b>List of Tables</b> .....	xvi
<b>List of Symbols</b> .....	xvii
<b>Abbreviation</b> .....	xix
<b>1. Background</b> .....	1
1.1. The Filtration process .....	1
1.2. Conventional pressure filtration and steam pressure filtration.....	3
1.3. Filtration theory .....	6
1.4. Cake deliquoring - immiscible fluid displacement in porous media.....	16
1.5. Tensile stress between particles .....	20
1.6. Coal processing/ washing.....	24
<b>2. Literature review</b> .....	34
2.1. Cracking on filter cake and the dewatering process with and without cracking .....	34
2.2. Summary and focus of research .....	47
<b>3. Material, methods and the result of capillary pressure curve and tensile stress versus saturation</b> .....	51
3.1. Material used.....	51
3.1.1. Limestone.....	51
3.1.2. Vietnam Coal .....	52
3.2. Conventional filtration rig and steam pressure filtration rig .....	55
3.2.1. Conventional filtration rig.....	55
3.2.2. Steam pressure filtration rig.....	57
3.3. Filtration experimental.....	58
3.4. Relevant parameter .....	59
3.5. Analyze technique.....	65
3.6. Tensile stresses depend on saturation during deliquoring.....	66

<b>4. The influence of operating parameters on cracks formation in case of limestone</b>	<b>69</b>
4.1. Capillary pressure curve and tensile stress during the filtration in the case of limestone	69
4.2. Test were conducted using conventional pressure filtration .....	76
4.2.1. Particle size distribution effect.....	76
4.2.2. The solid volume fraction of suspension effect .....	82
4.2.3. Height of filter cake (filter cake deep/ filter cake thickness) effect .....	92
4.2.4. Pressure difference effect.....	101
4.3. The difference in the crack formation by using steam pressure filtration.....	111
4.4. General conclusion.....	116
<b>5. The influence of operating parameters on cracks formation in the case of Vietnam coal .....</b>	<b>118</b>
5.1. Capillary pressure curve and tensile stress during filtration in case of Vietnam coal	118
5.2. Test were conducted using conventional pressure filtration .....	122
5.2.1. The influence of the solid volume fraction on crack formation and saturation	122
5.2.2. The influence of the height of filter cake on crack formation and saturation ...	127
5.2.3. The influence of pressure difference on crack formation and saturation .....	134
5.3. Estimate the efficiency dewatering as well as the crack formation using steam pressure filtration .....	139
5.4. General conclusion.....	146
<b>6. Overall conclusion and recommendation .....</b>	<b>148</b>
6.1. Overall conclusion .....	148
6.2. Recommendation .....	150
<b>References .....</b>	<b>152</b>
<b>Appendices .....</b>	<b>156</b>
Appendix A: Data from CCWP. ....	156
Appendix B: Data from the crack formation with various operation parameters using conventional pressure filtration (CPF).....	159
Appendix C: Data from steam pressure filtration. ....	167
Appendix D: Miscellaneous Information.....	177

## List of Figure

Figure 1. Diagram describes the main process phases during conventional pressure filtration and steam pressure filtration [8].	4
Figure 2. The deposition of solid during filtration [1].	7
Figure 3. Chart for the cumulative volume of filtrate and filtration time [1].	9
Figure 4. The relationship between the volume of filtrate and the volume of filter cake during filtration [1].	9
Figure 5. The linear relationship between cake resistance and mass of solid deposited on filter cake [1].	10
Figure 6. The linear diagram between $t/V$ versus $V$ [17, 18].	14
Figure 7. Types of deviation occur during filtration [17, 18].	15
Figure 8. Deliquoring by gas pressure – the residual saturation as a function of time [17].	17
Figure 9. Types of capillary pressure curve for imbibition and deliquoring [17, 23].	17
Figure 10. The relative permeability as a function of degree saturation [17].	19
Figure 11. Types state of group particles depending on the amount of liquid [29, 30].	21
Figure 12. Theoretical tensile strength of agglomerates with different bonding mechanisms [29, 31].	22
Figure 13. Tensile stress and capillary pressure as a function of saturation [32].	23
Figure 14. Types of coal [36].	25
Figure 15. Coal reserves in regions [36].	25
Figure 16. The distribution of coal reserves in Vietnam [37-40].	26
Figure 17. The distribution of coal reserves in Quang Ninh [37-40].	27
Figure 18. Major coal mines around the Cam Pha - Quang Ninh region [37, 38].	27
Figure 19. The data and prediction of supply and demand of coal [41].	28
Figure 20. Flow sheet of Factory I – Cua Ong Washing Plant (data from Coal Technical department – Cua Ong Coal Washing Plant).	31

Figure 21. Flow sheet of Factory II – Cua Ong Washing Plant (data from Coal Technical department – Cua Ong Coal Washing Plant). .....	32
Figure 22. Flowsheet of Dewatering plant (Environment plant) – Cua Ong Washing Plant (data from Coal Technical department – Cua Ong Coal Washing Plant). .....	33
Figure 23. Diagram and picture for micro-cracking and macro-cracking on filter cake during the mechanical displacement phase. ....	34
Figure 24. Diagram and images for cracking horizontally due to sedimentation. ....	35
Figure 25. Constructive measure for suppression of crack formation [42]. ....	35
Figure 26. Schematic illustration of the liquid bridge between two particles and the corresponding effective capillary forces (adhesion $F_A$ and capillary suction $F_{CS}$ ) [5]. ....	36
Figure 27. Characteristic shrinkage curve with three sections [5]. ....	37
Figure 28. The shrinkage potential of filter cake against the compressive pressure at variety of surface tension [5]. ....	38
Figure 29. No crack and no shrinkage at the higher pressure minimum compressive pressure [5]. ....	38
Figure 30. The particle size distribution of some test materials [5]. ....	39
Figure 31. Comparison of the shrinkage behaviour of different organic and inorganic test products [5]. ....	39
Figure 32. Confined and non-confined shrinkage of a filter cake [16, 42]. ....	40
Figure 33. Cake cracking during pressure and hyperbaric vacuum filtration of PbS ore [42]. ....	40
Figure 34. Cake cracking during pressure and hyperbaric vacuum filtration of ZnS ore [42]. ....	41
Figure 35. The probability of cake cracking in the difference of filter cake area and cake thickness for circular and rectangular filter plate [42]. ....	41
Figure 36. Illustration saturation distribution curves [43]. ....	42
Figure 37. For high suction potential filter cake [43]. ....	43
Figure 38. For moderate suction potential filter cake [43]. ....	43
Figure 39. The particle size distribution of KS12 and KS100. ....	51

Figure 40. SEM pictures for KS100 (left) and KS12 (right).....	52
Figure 41. The sedimentation curve of coal in different solid volume concentration of the suspension (cv).....	53
Figure 42. The particle size distribution of fine coal. ....	54
Figure 43. SEM images for coal particles. ....	55
Figure 44. Images for the Nutsche apparatus (according to VDI 2762-2) [18]. ....	56
Figure 45. Schematic diagram of the experimental setup. ....	56
Figure 46. Diagram of steam pressure filtration according to VDI 2762/2, [12, 13, 18]. .....	57
Figure 47. Steam pressure filtration apparatus [12, 13]. ....	58
Figure 48. The mass of filtrate from the moment the gas breaking through for SPF (blue line) and CPF (blue dash line) and the temperature profile of filter cloth when using SPF (orange line). ....	64
Figure 49. Schematic of capillary and tensile strength against saturation. ....	66
Figure 50. Images for lab-scale compression permeable cell. ....	68
Figure 51. Capillary pressure and tensile stresses against saturation for KS12.....	70
Figure 52. The saturation and residual moisture content of KS12 filter cake at 3 bar capillary pressure as the function of the volume fraction. ....	71
Figure 53. Capillary pressure and tensile stresses against saturation for KS100.....	74
Figure 54. The saturation and residual moisture content of KS100 filter cake at 3 bar capillary pressure as the function of the volume fraction. ....	75
Figure 55. Water is pushed out of the large and small capillaries. ....	76
Figure 56. Permeability ratio of fine limestone KS 12 and coarse limestone KS 100 filter cakes at some volume fraction values; “1-1 bar” of pressure difference; 50 grams of solid content. ....	77
Figure 57. Saturation and residual moisture content of KS 12 and KS 100 filter cakes at some volume fraction values; “1-1 bar” of pressure difference; 50 gram of solid content. ....	78

Figure 58. The specific resistance of KS 12 and KS 100 filter cakes at some volume fraction values; 1 bar of pressure difference in the cake formation phase; 50 gram of solid content.....	80
Figure 59. The porosity of KS 12 and KS 100 filter cakes at some volume fraction values; 1 bar of pressure difference in the cake formation phase; 50 gram of solid content. ....	80
Figure 60. Images for the top and bottom of coarse material (KS100) and fine material (KS12) filter cake; “1-1 bar” of the pressure difference ( $\Delta p$ ); 18 mm of filter cake thickness.....	81
Figure 61. Permeability ratio of KS100 filter cake in variety of solid volume fraction of suspension; 18 mm of filter cake thickness; “1-1 bar” and “1-3 bar” of pressure difference. ....	83
Figure 62. Saturation and residual moisture content of KS100 filter cake in variety of solid volume fraction of suspension; 18 mm of filter cake thickness; “1-1 bar” and “1-3 bar” of pressure difference. ....	84
Figure 63. Specific resistance and porosity of KS100 filter cake in variety of solid volume fraction of suspension; 18 mm of filter cake thickness; 1 bar of pressure difference in the cake formation phase.....	85
Figure 64. The ratio of filtration time and filtrate volume ( $t/V$ ) as a function of filtrate volume for KS100 in various volume fraction; 18 mm of filter cake thickness; 1 bar of pressure difference in the cake formation phase. ....	86
Figure 65. Median particle size on top and bottom layers of KS100 filter cake; 1 bar of pressure difference in the cake formation phase; 18 mm of filter cake thickness. ....	86
Figure 66. Permeability ratio for KS12 filter cake in various solid volume fraction; 18 mm of filter cake thickness; “1-1 bar” and “1-3 bar” of pressure difference. ....	88
Figure 67. Saturation and residual moisture content for KS12 filter cake; 18 mm of filter cake thickness; “1-1 bar” and “1-3 bar” of pressure difference.....	90
Figure 68. Specific resistance and porosity of KS12 filter cake; 18 mm of filter cake thickness, 1 bar of pressure difference in the cake formation phase.....	90
Figure 69. Median particle size on top and bottom layers of KS12 filter cake; 1 bar of pressure difference in the cake formation phase; 18 mm of filter cake thickness. ....	91

Figure 70. The ratio of filtration time and filtrate volume ( $t/V$ ) as a function of filtrate volume for KS12 in various volume fraction; 18 mm of filter cake thickness; 1 bar of pressure difference in the cake formation phase. ....	91
Figure 71. Images for KS100 (upper) and KS12 (lower) top and bottom filter cakes with the different volume concentrations of the suspension; the height of filter cake 18 mm; “1-1 bar” of pressure difference. ....	92
Figure 72. Permeability ratio of KS100 filter cake using “1-1 bar” and “1-3 bar” of pressure difference; 0.3 of solid volume fraction.....	93
Figure 73. Saturation and residual moisture content of KS100 filter cake using “1-1 bar” and “1-3 bar” of pressure difference; 0.3 of solid volume fraction. ....	94
Figure 74. Specific resistance and porosity of KS100 filter cake using “1-1 bar” and “1-3 bar” of pressure difference; 0.3 of solid volume fraction. ....	95
Figure 75. Images for KS100 filter cake with difference height; 0.3 of solid volume fraction. ....	97
Figure 76. Permeability ratio of KS12 filter cake using “1-1 bar” and “1-3 bar” of pressure difference; 0.1 of solid volume fraction. ....	98
Figure 77. Diagram $t/V$ versus $V$ of filter cake with the various filter cake deep; 0.1 of solid volume fraction; 1 bar of pressure difference in the cake formation phase. ....	98
Figure 78. Saturation and residual moisture content of KS12 filter cake using “1-1 bar” and “1-3 bar” of pressure difference; 0.1 of solid volume fraction. ....	100
Figure 79. Specific resistance and porosity of KS12 filter cake; 1 bar of pressure difference in the cake formation phase; 0.1 of solid volume fraction.....	100
Figure 80. Images for KS12 filter cake with different height; 0.1 of volume fraction. ....	101
Figure 81. Permeability ratio of KS100 (coarse material) filter cake using the variety of pressure difference; 18 mm of filter cake thickness.....	102
Figure 82. Images for KS100 filter cake in the variety of pressure difference; 18 mm of filter cake thickness.....	103
Figure 83. Saturation and residual moisture content of KS100 (coarse material) filter cake using the variety of pressure difference; 18 mm of filter cake thickness.....	105



Figure 84. Specific resistance and porosity of KS100 (coarse material) filter cake using the variety of pressure difference; 18 mm of filter cake thickness. ....	106
Figure 85. Permeability ratio of KS12 (fine material) filter cake using the variety of pressure difference; 18 mm of filter cake thickness.....	107
Figure 86. Images for KS12 filter cake in the variety of applied pressure difference; 18 mm of filter cake thickness. ....	108
Figure 87. Saturation and residual moisture content of KS12 (fine material) filter cake using the variety of pressure difference; 18 mm of filter cake thickness.....	109
Figure 88. Specific resistance and porosity of KS12 (fine material) filter cake using the variety of pressure difference; 18 mm of filter cake thickness. ....	110
Figure 89. Permeability ratio of KS12 filter cake using conventional pressure filtration (CPF) and steam pressure filtration (SPF) in various volume fraction; “3 -3 bar” of pressure difference; 18 mm of filter cake height. ....	112
Figure 90. Saturation and residual moisture content of KS12 filter cake in various volume fraction; ; using SPF and CPF ; “3-3 bar” of pressure difference; 18 mm of filter cake height.....	113
Figure 91. Permeability ratio of KS12 filter cake in various filter cake height; using SPF and CPF; “3-3 bar” of pressure difference; 0.1 of volume fraction. ....	114
Figure 92. Saturation and residual moisture content of KS12 filter cake in the variety of filter cake height; using SPF and CPF; “3-3 bar” of pressure difference; 0.1 of volume fraction. ....	115
Figure 93. Capillary pressure and tensile stresses against saturation for VN Coal.....	121
Figure 94. The saturation and residual moisture content of VN coal filter cake at 3 bar capillary pressure as the function of the volume fraction. ....	122
Figure 95. Permeability ratio of VN coal filter cake in the variety of volume fraction; 15 mm of filter cake height. ....	122
Figure 96. The median particle size of the upper and bottom layer filter cake; 15 mm of filter cake height; 1 bar and 3 bar of pressure difference in the cake formation phase.	123
Figure 97. Diagram of $t/V$ versus $V$ ; in the variety of volume fraction; 15 mm of filter cake height; 1 bar and 3 bar of pressure difference in the cake formation phase. ....	123

Figure 98. Saturation and residual moisture content of VN coal filter cake in the variety of volume fraction; 15 mm of filter cake height. ....	125
Figure 99. Specific resistance and porosity of VN coal filter cake in the variety of volume fraction; 15 mm of filter cake height; 1 bar and 3 bar of pressure difference in the cake formation phase. ....	126
Figure 100. Permeability ratio of VN coal filter cake in the variety of filter cake height; 0.1 and 0.3 of volume fraction. ....	128
Figure 101. Images for coal filter cake in various filter cake height, 0.1 and 0.3 of volume fraction. ....	130
Figure 102. Saturation of VN coal filter cake in the variety of filter cake height; 0.1 and 0.3 of volume fraction. ....	131
Figure 103. The residual moisture content of VN coal filter cake in the variety of filter cake height; 0.1 and 0.3 of volume fraction. ....	132
Figure 104. The specific resistance of VN coal filter cake in the variety of filter cake height; 0.1 and 0.3 of volume fraction; 1 bar and 3 bar of pressure difference in the cake formation phase. ....	133
Figure 105. The porosity of VN coal filter cake in the variety of filter cake height; 0.1 and 0.3 of volume fraction; 1 bar and 3 bar of pressure difference in the cake formation phase. ....	134
Figure 106. Permeability ratio of filter cake in the variety of pressure difference; 15 mm of filter cake thickness; using CPF. ....	135
Figure 107. Images for filter cake in the 1.5 and 3.5 bar of pressure difference; 0.1 of solid volume fraction; 15 mm of filter cake thickness. ....	136
Figure 108. Saturation and residual moisture content of filter cake in the variety of pressure difference; 15 mm of filter cake thickness. ....	137
Figure 109. Particle size distribution on the top and bottom layer of the filter cake; 1 bar and 3 bar of pressure difference in the cake formation phase. ....	139
Figure 110. Permeability ratio of VN coal filter cake in the variety of volume fraction; 15 mm of filter cake height; using steam pressure filtration (SPF) and conventional pressure filtration (CPF). ....	140

Figure 111. Images for coal filter cake using steam pressure filtration (SPF) and conventional pressure filtration (CPF). .....	141
Figure 112. Saturation of VN coal filter cake in the variety of volume fraction; 15 mm of filter cake height; using SPF and CPF. ....	142
Figure 113. The residual moisture content of VN coal filter cake in the variety of volume fraction; 15 mm of filter cake height; using SPF and CPF. ....	143
Figure 114. Permeability ratio of VN coal filter cake in the variety of height; using SPF and CPF; 0.3 of volume fraction, “1-3 bar” of pressure difference. ....	144
Figure 115. Images for VN coal filter cake in various height; using SPF and CPF; 0.3 of volume fraction; “1-3 bar” of pressure difference. ....	144
Figure 116. Saturation and residual moisture content of VN coal filter cake in the variety of height ; using SPF and CPF; 0.3 of volume fraction, “1-3 bar” of pressure difference. ....	146

## **List of Tables**

Table 1. Types of cake filtration and types of equipment [1]. .....	2
Table 2. The mean particle size of batches of Calcium carbonate is used [4]. .....	45
Table 3. Summarize influence elements from literature. ....	47
Table 4. Sedimentation of coal corresponding to the concentration of the suspension. .	53
Table 5. Coal particles properties. ....	54
Table 6. The viscosity of water corresponding to the temperature. ....	61

## List of Symbols

Symbols	Description	Units
$\Delta p$	Pressure differential	Pa ( $\text{N m}^{-2}$ ) ( $10^{-5}$ bar)
L or H or h	Bed deep	m
$\mu$	Dynamic viscosity	Pa.s
A	Cross-section area	$\text{m}^2$
$\varepsilon$	Porosity	-
$S_v$	Specific surface area per unit volume of the particles	$\text{m}^2 \text{m}^{-3}$
K	Kozenny constant	-
$\beta$	Filter cake to filtrate volume ratio	-
K	Filter cake permeability	-
V	Volume of filtrate	$\text{m}^3$
C or $c_v$	Solid concentration by volume fraction	-
$\rho_s$	Solid density	$\text{kg m}^{-3}$
W	Mass dry solid depositing on filter cake per unit area of the filter	$\text{kg m}^{-2}$
$\alpha$ or $\alpha_m$	Solid mass related filter cake specific resistance	$\text{m kg}^{-1}$
$R_c$	Filter cake resistance	$\text{m}^{-1}$
$\Delta p_c$	Pressure differential over the filter cake	$\text{N m}^{-2}$
$\Delta p_m$	Pressure differential over the filter medium	$\text{N m}^{-2}$
$R_m$	Medium resistance	$\text{m}^{-1}$
c	Mass of dry cake deposited per unit volume of filtrate	$\text{kg m}^{-3}$
T	Time	s
$\alpha_H$ or $r_c$	Cake thickness related filter cake specific resistance	$\text{m}^{-2}$
S	Saturation	-
$p_{ce}$	Capillary pressure entry	Pa
$\sigma$ or $\gamma$	Surface tension	N/m
$\delta$	Contact angle	o
$d_{\text{pore, neck}}$	Diameter of the neck of the pores	m
$k_{\text{rel,w}}$	Relative permeability for wetting fluid	
$k_{\text{rel,n}}$	Relative permeability for non-wetting fluid	-
$S_{\infty}$	Irreducible saturation	-

$\lambda$	Pore size distribution index	-
$p_b$	Threshold pressure	Pa
$p_c$	Capillary pressure	Pa
$k_{rg}$	Relative permeability for gas	-
$k_{rl}$	Relative permeability for liquid	-
$\sigma_t$	Tensile stress	$N\ m^{-2}$
$F^*$	Mean adhesion force transmitted at a contact point	N
$x$	Mean particle size	m
$F_H$	Dimensions adhesion number	-
$\sigma_B$	Tensile stress cause by the liquid bridge	$N\ m^{-2}$
$\sigma'_B$	Tensile stress cause by the liquid bridge in the funicular state	$N\ m^{-2}$
$\sigma'_k$	Tensile stress cause by the capillary state in the funicular state	$N\ m^{-2}$
$B_g$ or $K_g$	Gas permeability	$m^2$
$B_l$ or $K_l$	Liquid permeability	$m^2$
$V_l$	Liquid volume flowrate	$m^3\ h^{-1}$
$V_g$	Gas volume flowrate	$m^3\ h^{-1}$
$\mu_l$	Dynamic viscosity of the liquid	Pa s
$\mu_g$	Dynamic viscosity of the gas	Pa s
$\beta^*$	Permeability ratio	-
$K_{ST}$	Steam permeability	$m^2$

Note: When alternative units are used, these will be stated

## **Abbreviation**

DI water	Distilled water
L15	Lower 15 $\mu\text{m}$
CCWP	Cua Ong Coal Washing Plant
ROM coal	Run Of Mine coal
SEM	Scanning Electron Microcope
VDI	Verein Deutscher Ingenieure
G	Gas
ST	Steam
L	Liquid
CPF	Conventional Pressure Filtration
SPF	Steam Pressure Filtration

## **1. Background**

Nowadays, solid-fluid separations are more popular and occur in the almost large-scale industrial process. They are usually based on two principles of separation, are filtration and separation by sedimentation or settling. Meanwhile, the sedimentation process separates liquid and solid, based on the difference in phase of densities. Filtration, essentially, is a separation of the amount of solid and fluid mixture (suspension or slurry) in which the fluid (liquid/filtrate or air) flows directly toward and through the medium (screen, paper, woven cloth, membrane, etc.) while the solids are retained, either on the surface or within the medium [1, 2].

It can be said that filtration is a long-standing technology, which uses from ancient to now with its underlying principles. In the entire solid-liquid process, filtration is an indispensable step and always has an important position in almost the industry process. The application of filter and filtration can be divided into two main categories. The first one is the removal of contaminant or solid from a useful or valuable fluid such as drinking water, ambient office air, fuel, lubricating fluid, compressed air, process water, emission from other processes, to prolong the lifetime of the equipment or prevent fouling of other equipment (electrolytic cell in a chloralkali process). The second one is recovery one or more valuable phase from a mixture of phases such as the recovery of valuable solid (products of mining and mineral processing) or removal the residue from a product in solution (chemical, metals, and pharmaceutical, etc.) [3]. For the latter application, shrinkage cracking is an undesired phenomenon that is encountered frequently during conventional pressure filtration, especially of the fine particulate filter cake. Once a cake has cracked, channels are formed, and gas permeability increases significantly as the gas preferentially flows through the crack rather than through the pores in the filter cake [4]. The consequence of the cracks is a significant disadvantage concerning the economy (the gas/washing water consumption is mostly increased by orders of magnitude) and process results (higher moisture content/lower purity). In an adverse case, the disadvantages mentioned compel more expensive dewatering processes [5, 6]. The result of research gives further insight into the mechanism of crack formation (including micro- and macro-cracking), giving assumptions as reasons caused shrinkage cracking. That information is the basis for proposing steam pressure filtration as a new approach, for avoiding the crack formation as well as improve the dewatering process.

### **1.1. The Filtration process**



Filtration can be understood as a process in the equipment named filter, in which slurry or suspension is directed toward a tissue with a very small pore size called medium. The medium can be the screen, paper, woven cloth, or membrane. The liquid that was collected during filtration, is named filtrate. Solids are retained on or in the filter medium.

There are two kinds of filtration, cake filtration, and deep bed filtration. In the case of cake filtration, particles are deposited above medium and build the filter cake. For deep bed filtration, the deposition of particles occurs inside of the pores of the filter medium, where they are retained and become a part of the filter medium.

Table 1 shows the affected forces and separation techniques available in the filtration process [1].

Table 1. Types of cake filtration and types of equipment [1].

Filtration	Force cause pressure difference	Discharge	Typical Machinery
	Gravity	Discontinuous	Strainer or Nutsche; Sand-Charcoal Filter (deep filtration)
		Continuous	Grids: Sieve Bends; Rotary screen; Vibratory screen
	Vacuum	Discontinuous	Nutsche Filter, Candle, and Cartridge
		Continuous	Table or Pan Filter, Rotary Drum or Disc Filter, Horizontal Belt
	Pressure	Discontinuous	Pressure Nutsche; Press and Frame Filter; Tube, Candle and Leaf Filter; Cartridge Filter
		Continuous	Belt Press; Screw Press
	Centrifugal	Discontinuous	Basket: three-column Centrifuge; Peeler Centrifuge
		Continuous	Pusher, Vibratory and Tumbler Centrifuge; Helical Conveyor; Conical and Cylindrical; Basket Centrifuge

The relationship between pressure drop and the flow rate of liquid passing through the packed filter cake was the first to report by Darcy in 1856 [1, 7]. The liquid flow through the open spaces on the filter cake, which is called pore or void in the bed. He also shows the importance of the amount of solid on filter cake. The greater this leads to the larger surface, the higher the pressure drop will be as a result of friction. There are two kinds of drag on the solid surface, skin friction (viscous drag) and form drag. Skin friction occurs because of friction between solid and liquid, which is a stable layer of liquid around the solid. Form drag is due to turbulent of higher flow rate. It leads to additional pressure losses and breaks down the linearity between flow rate and pressure drop. Because of the complication related to the high flow rate of liquid, the research is just only focused in the laminar regime. It is not only due to the simple approach that Darcy can be used; we also have low Re-number due to the fine particles. These avoid the occurrence of turbulence.

#### 1.2. Conventional pressure filtration and steam pressure filtration

The filtration process can be divided into three main phases: cake formation, mechanical displacement, and drying[8].

For the first steps, the slurry is fed and distributed over the filter cloth. The pressure gradient for filtration is applied. These forces are compressed air, vacuum, or even gravity as well as centrifugal pressure. Filtrate begins to pass through the filter medium, and filter cake starts to grow. At this period, the resistance of the system increases gradually. The cake formation phase finishes when the pores of the filter cake are fully filled with mother liquid but no more water is on the surface of the filter cake.

When the cake is exposed directly to driving de-watering forces, the water is pushed out of the pores of the filter cake. The difference between the conventional pressure filtration and steam pressure filtration is in the mechanical displacement phase. For the conventional filtration, compressed air is applied and penetrates the pores. When the pressure difference between the upper side and the lower side exceeds the capillary entry pressure, the mother liquid drains. The model of capillaries describes the mechanical displacement of a liquid out of a porous system. The displacement in pores with different sizes has different velocities. The larger the pore, the faster the flow becomes. The air breaks through in the gas flow in the largest pore resulting in higher gas consumption. The mechanical displacement in smaller pores is decelerated after the breakthrough of air. This phase also finishes when the air flow through the filter cake and

the system achieves a dynamic equilibrium. Most tests in this thesis are investigated in the mechanical displacement phase, which can be realized by the no water flowing through the filter cake. The drying phase using the air is not conducted in order to avoid the drying effect, which also can affect the result of cracking. The residual moisture content is measured at the end of this mechanical phase.

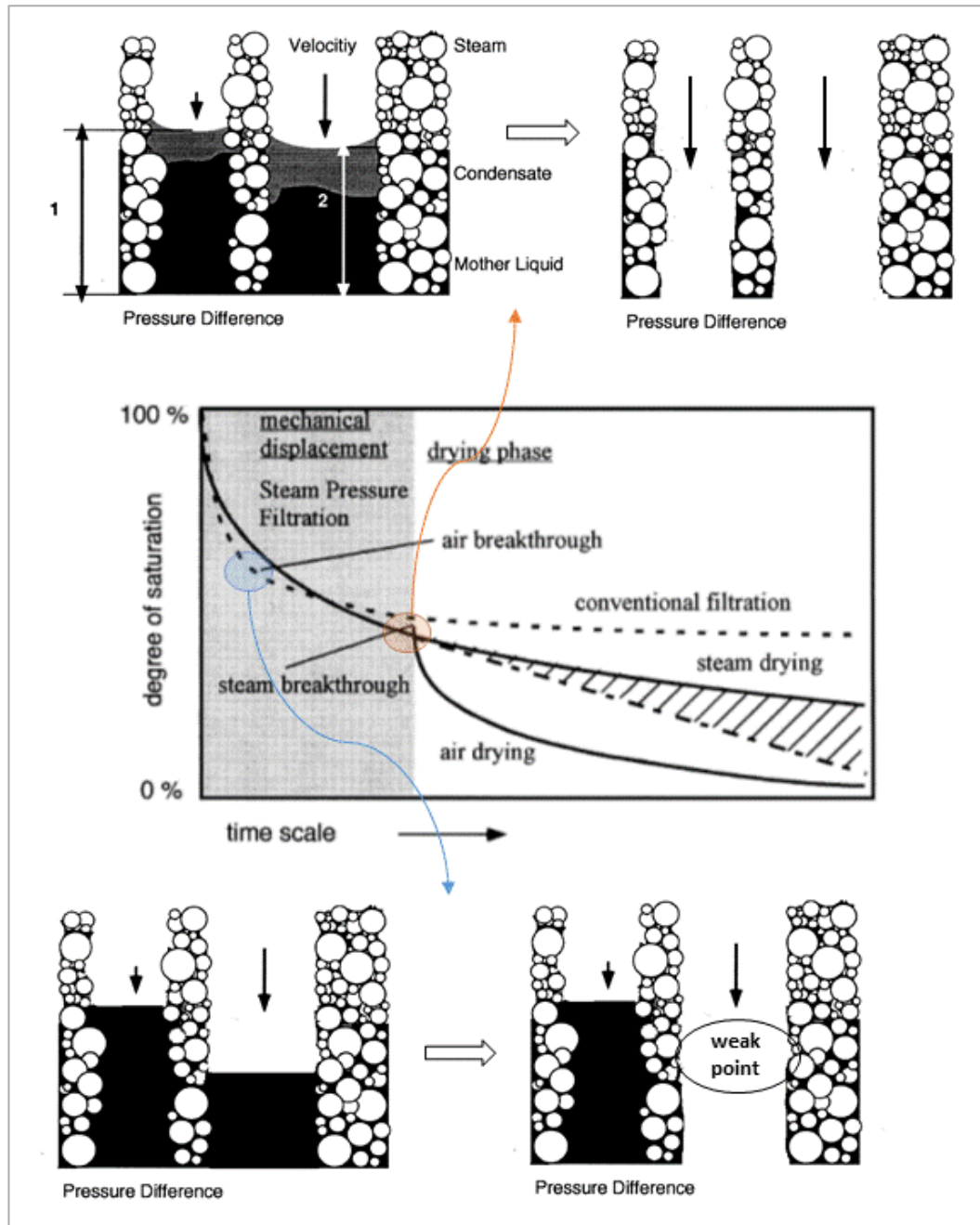


Figure 1. Diagram describes the main process phases during conventional pressure filtration and steam pressure filtration [8].

For steam pressure filtration, steam pressure is applied and firstly get in contact with the cold surface of the filter cake. The superheated [9] or the saturated steam is used

in order to replace the air pressure in conventional pressure filtration [8, 10, 11], as also mentioned in the research of Esser and Peuker [12, 13]. No air is permitted in this system because air can not condensate. Condensation of steam creates a displacement front [8, 14]. Steam intrudes the filter cake and condenses continuously during advancing. The displacement front moves down through the system of the filter cake and starts pushing the filtrate out of filter cake.

Two different stabilizing effects lead to the sharp and even mechanical displacement front, which is characteristic of steam pressure filtration. Due to condensation and steam consumption, the volume of steam reduces. This issue provokes the fast steam flow from the surface to the front. As the description of Peuker and Stahl [8], because of the pressure drop of the steam flow, the effective pressure at the front is lower at the fast-moving of steam. There is a dynamic equilibrium between the velocity of the liquid inside the filter cake and the steam flow above it. The speed of the displacement front decreases, and with it, the reduction of pressure of the steam flow. The local pressure at the front increases and the front is accelerated again. The model of capillaries of different sizes is also able to describe the displacement of mother liquid. At larger pores with lower capillary pressure, the mother liquid is accelerated, so that the cold surface is exposed to steam. At the surface of larger pores, more steam condenses. The decrease of steam volume leads to the lower local pressure and the deceleration of liquid. The liquid is still kept in large pores. At other smaller pores, less steam is consumed leading to higher local pressure. When the system is heated up, no more steam is consumed, both liquids in large and small pores are pushed out. The condensed water refills continuously mainly into large pores and prevents steam breakthrough only through the large pores [8]. This characteristic is the notable difference in comparison with conventional pressure filtration and is showed clearly in Figure 1.

The even displacement front provokes the related gas breakthrough compared to conventional pressure filtration. The high temperature leads to lower viscosity as well as surface tension. Less water remains in the liquid bridge between particles and the volume of the liquid bridge decreases due to small surface tension. The result is that during mechanical displacement, the residual moisture content is lower compared to conventional pressure filtration [8].

The successive phase in steam pressure filtration can be applied in two ways. The first one is the application of pressurized air after the breakthrough of steam. This way is

more effective, rapid, and economical. The remaining water on the filter cake is evaporated due to the stored latent heat. The air treatment after the steam breakthrough is the optimal process to reduce the moisture to the maximal extent. The second way is the maintain the saturated or superheated steam during the second and third process phases. Steam pressure filtration should be operated in this way in case of washing and extraction of the volatile component in the filter cake and the residual moisture content [8, 12, 13].

In this thesis, in order to observe the crack formation in the mechanical displacement phase as well as the degree of the reduction of the residual moisture content in this phase, most tests are just stopped when the gas breaks through the filter cake. The further drying can lead to the drying effect, which affects as much the shrinkage on filter cake. Moreover, there is unnecessary to survey the drying phase because the dewatering efficiency in the mechanical displacement phase would be a precursor to reducing the moisture further in the successive phases.

### 1.3. Filtration theory

According to Rushton [1], the deposition of solid on filter medium or septum is shown schematically in Figure 2. The filter medium has a long-lasting effect on the filter cake structure and properties throughout the filtration cycle. This one will be discussed more below. The mathematical description of the process starts with the neglect of septum resistance. For the low flow rate through the porous system, the relationship between pressure drop and flow rate of liquid was first reported by Darcy in 1856 [7], called Darcy's law. It can be regarded as fluid flow through a porous media analogous to Ohm's law for the flow of electric current.

$$\frac{\Delta p}{L} = \frac{\mu \cdot dV \cdot 1}{k \cdot dt \cdot A} \quad (1)$$

Where  $\Delta p$  is a pressure drop;  $L$  is the bed deep (height of filter cake);  $\mu$  is the liquid dynamic viscosity;  $dV$  is the volume flowing in time  $dt$  and  $A$  is the cross-section area of the bed (area of filter cake).

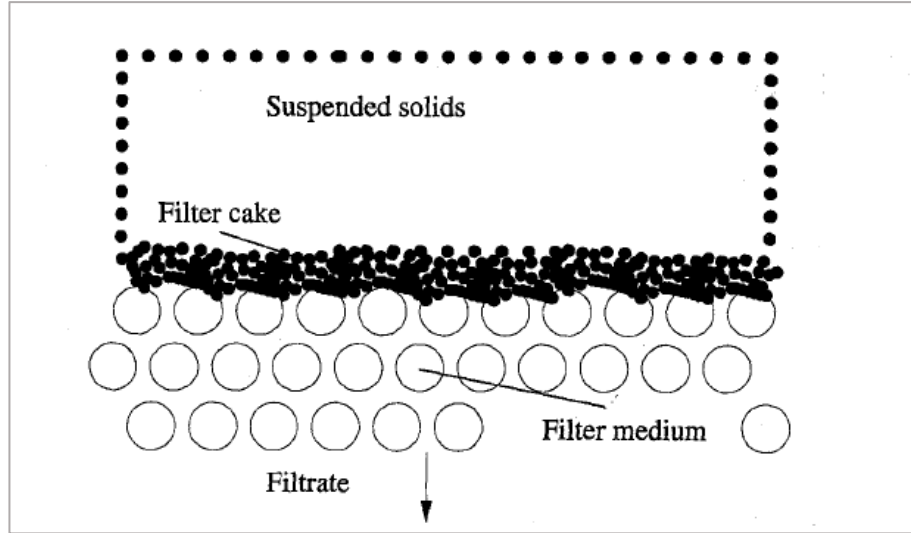


Figure 2. The deposition of solid during filtration [1].

During filtration, the solid deposited on the surface of the filter medium leads to the cake deep (height of filter cake) increase. The change of cake deep is accompanied to the shift in pressure differentially, fluid flow rate, as well as the increasing of filtration time. Even if there are remain constant of the material's permeability, the viscosity of the liquid, and the filter cake area, the Equation (1) still has four variables. The constant system permeability is obtained when the particle size distribution and porosity do not change. This issue got a good agreement with Kozeny [15] about the permeability – one of the critical parameter which characterizes the ease with which liquid will flow within a porous medium, including filter cake.

$$k = \frac{\varepsilon^3}{K(1 - \varepsilon)^2 \cdot S_V^2} \quad (2)$$

Where  $S_V$  is the specific surface area per unit volume of the particles and  $K$  is Kozeny constant (which is usually take 5 and 3.36 for slowly and rapidly depositing, respectively);  $\varepsilon$  is the porosity of the porous system.

The total volume  $V_{tot}$  of the porous filter cake includes the volume of solid  $V_s$  and the void volume  $V_{void}$ , which is defined at first as voids between compact particles. The void volume is typically not given in absolute value, instead of the relative value of the void volume, also known as the porosity  $\varepsilon$  [16].

$$V_{tot} = V_s + V_{void}$$

$$\varepsilon = \frac{V_{void}}{V_{tot}} = \frac{V_{void}}{V_s + V_{void}} = \frac{V_{tot} - V_s}{A \cdot h_c} = \frac{A \cdot h_c - \frac{m_s}{\rho_s}}{A \cdot h_c} = 1 - \frac{m_s}{A \cdot h_c \cdot \rho_s}$$

Actually, the meaning of porosity is the volume available for fluid flow. In many solid-liquid separations, the use of solid concentration  $C$  is often preferred than the porosity. The porosity is the void volume fraction, so the sum of those factors to unity. The solid volume fraction therefore can be defined [1]:

$$C = 1 - \varepsilon$$

A material displays the constant's filter cake concentration (or no change in the porosity of filter cake), named incompressible material. This type of filtration is incompressible cake filtration, and all the result of the thesis belongs to this limitation.

For incompressible filtration, the cake concentration is, thus for each volume unit of suspension filtered, the amount volume of filtrate increases uniformly and constantly. However, because of particles deposit continuously on the bed surface, liquid has to flow through the new layer on the filter cake, the total resistance increases (when the pressure difference does not change), resulting in the filtration rate declines as shown in Figure 3. Otherwise, the uniform of the volume of filtrate  $V_L$  and the volume of the filter cake  $V_C$  is also described in Figure 4. The constants  $\beta$  can be used to give an equation for cake deep at any instant time.

$$\beta = \frac{V_C}{V_L} = \frac{L \cdot A}{V_L} \quad (3)$$

Darcy's law can be rewritten is:

$$\frac{dV_L}{dt} = \frac{A^2 \cdot \Delta p \cdot k}{\beta \cdot V_L \cdot \mu} \quad (4)$$

By multiplying both the numerator and denominator to solid concentration  $C$  and density  $\rho_s$ , this equation is rearranged and give a new form:

$$\frac{dV_L}{dt} = \left( \frac{A}{\beta \cdot V_L \cdot C \cdot \rho_s} \right) \cdot \left( \frac{k \cdot C \cdot \rho_s}{1} \right) \cdot \left( \frac{A \cdot \Delta p}{\mu} \right) \quad (5)$$

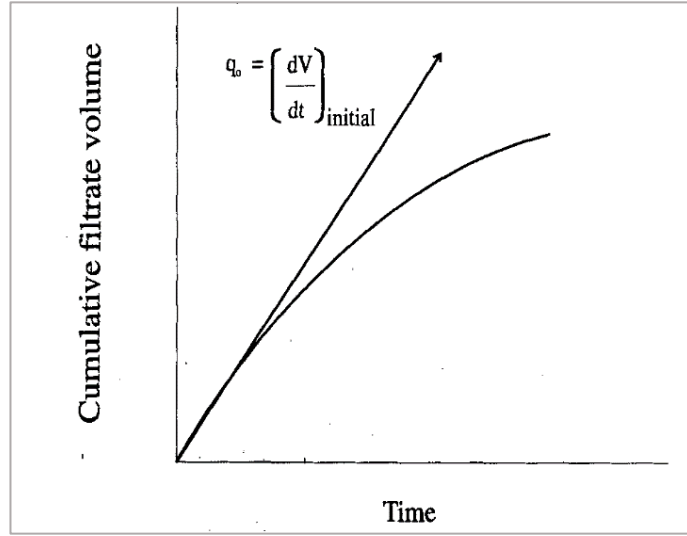


Figure 3. Chart for the cumulative volume of filtrate and filtration time [1].

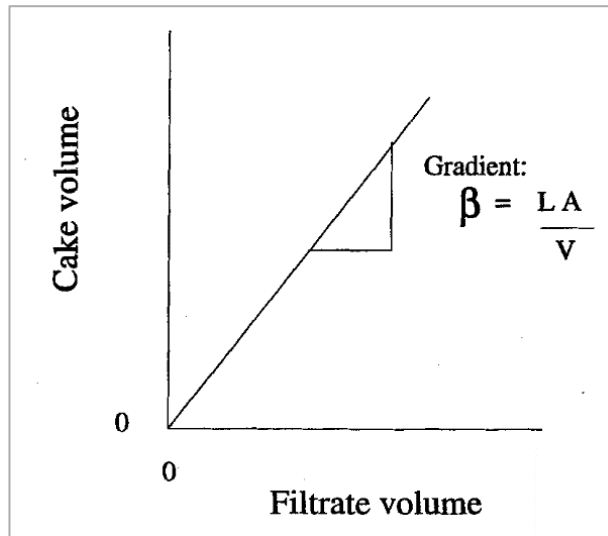


Figure 4. The relationship between the volume of filtrate and the volume of filter cake during filtration [1].

In another way, the mass of dry solid depositing on the bed surface ( $A \cdot L \cdot C \cdot \rho_s$ ) is equaled ( $\beta \cdot V_L \cdot C \cdot \rho_s$ ). The term “mass dry solid depositing on filter cake per unit area of filter ( $w$ )” can be calculated:

$$w = \frac{\beta \cdot V_L \cdot C \cdot \rho_s}{A} \quad (6)$$



Because of incompressible filter cake, the permeability, density, and solid concentration are constant and can be replaced by specific resistance cake  $\alpha$  which has a unit m/kg.

$$\alpha = \frac{1}{k \cdot C \cdot \rho_s} \quad (7)$$

Substitution Equation (6) and Equation (7) to Equation (5), Darcy law has a new form:

$$\frac{dV_L}{dt} = \frac{A \cdot \Delta p}{w \cdot \alpha \cdot \mu} \quad (8)$$

If only cake resistance is considered in Darcy's law, the pressure drop can be defined according to Equation (9):

$$\Delta p_c = \mu \cdot R_c \cdot \frac{dV_L}{dt} \cdot \frac{1}{A} \quad (9)$$

Where:

$$R_c = \alpha \cdot w \quad (10)$$

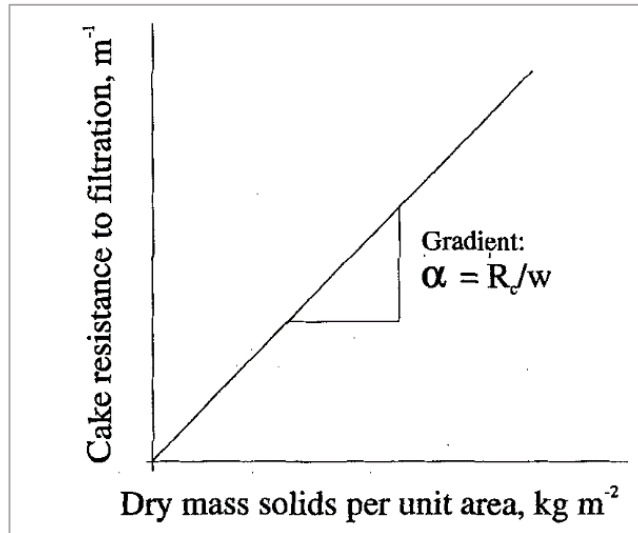


Figure 5. The linear relationship between cake resistance and mass of solid deposited on filter cake [1].

The overall resistance is increased during particle deposition. The rate of increase of cake resistance linear concerning the mass of dry solid deposited on filter cake and specific resistance cake is the ratio of two terms, as shown in Figure 5.

In case of the term,  $c$  represents the mass of dry cake deposited per unit volume of filtrate, and the volume of filtrate are similar with the volume of liquid in slurry (for incompressible filtration), the mass of dry solid is calculated:

$$w \cdot A = c \cdot V_L \quad (11)$$

Which rearranges to give:

$$w = \frac{c \cdot V_L}{A} \quad (12)$$

Substitution Equation (12) into the Equation (8) gives:

$$\frac{dV_L}{dt} = \frac{A^2 \cdot \Delta p}{c \cdot V_L \cdot \alpha \cdot \mu} \quad (13)$$

This equation has three variables and four constants. The variables are pressure difference, time, and the volume of filtrate. The filter area, specific resistance cake, dynamic viscosity, and concentration are mentioned constants, where the concentration and specific resistance cake are constant in case of incompressible filtration. However, the pressure loss due to the flow of filtrate through the filter cake and filter medium. Total pressure drop is the sum of pressure drop over the filter cake  $\Delta p_c$  and pressure drop in the medium  $\Delta p_m$ . Likewise, the total resistance  $R$  is the sum of the cake resistance  $R_c$  and the filter medium resistance  $R_m$ .

$$\Delta p = \Delta p_m + \Delta p_c \quad (14)$$

$$R = R_m + R_c$$

Darcy's law is applied for both and can be rewritten:

$$\begin{aligned} \frac{dV_L}{dt} &= \frac{A^2 \cdot \Delta p}{c \cdot V_L \cdot \alpha \cdot \mu} = \frac{A^2 \cdot (\Delta p_m + \Delta p_c)}{c \cdot V_L \cdot \alpha \cdot \mu} \\ \Delta p &= \Delta p_m + \Delta p_c = \mu \cdot \frac{\alpha \cdot c \cdot V_L}{A} \cdot \frac{dV_L}{dt} \cdot \frac{1}{A} = \mu \cdot (R_c + R_m) \cdot \frac{dV_L}{dt} \cdot \frac{1}{A} \end{aligned} \quad (15)$$

$$\Delta p = \mu \cdot R_c \cdot \frac{dV_L}{dt} \cdot \frac{1}{A} + \mu \cdot R_m \cdot \frac{dV_L}{dt} \cdot \frac{1}{A}$$

Substitution Equation (10) on this equation gives:

$$\Delta p = \mu \cdot w \cdot \alpha \cdot \frac{dV_L}{dt} \cdot \frac{1}{A} + \mu \cdot R_m \cdot \frac{dV_L}{dt} \cdot \frac{1}{A} = \mu \cdot c \cdot \alpha \cdot V_L \cdot \frac{dV_L}{dt} \cdot \frac{1}{A^2} + \mu \cdot R_m \cdot \frac{dV_L}{dt} \cdot \frac{1}{A}$$

Rearrange this equation and integrate, gives:

$$\begin{aligned} dt &= \frac{\mu \cdot c \cdot \alpha}{\Delta p \cdot A^2} \cdot V_L \cdot dV_L + \frac{\mu \cdot R_m}{A \cdot \Delta p} \cdot dV_L \\ \Leftrightarrow \int_0^t dt &= \int_0^V \frac{\mu \cdot c \cdot \alpha}{\Delta p \cdot A^2} \cdot V_L \cdot dV_L + \int_0^V \mu \cdot R_m \cdot \frac{1}{A \cdot \Delta p} \cdot dV_L \\ \Leftrightarrow \frac{t}{V_L} &= \frac{\mu \cdot c \cdot \alpha}{2 \cdot A^2 \cdot \Delta p} \cdot V_L + \frac{\mu \cdot R_m}{A \cdot \Delta p} \end{aligned} \quad (16)$$

Which  $c = \frac{m_s}{V_L}$

Equation (16) is the straight line, where  $t/V_L$  is the dependent, and  $V_L$  is the independent variable. The graph of the experimental data points of  $t/V_L$  against  $V_L$  permits calculating the gradient and intercept. Which:

$$\text{Gradient} = \frac{\mu \cdot c \cdot \alpha}{2 \cdot A^2 \cdot \Delta p} \quad (17)$$

$$\text{Intercept} = \frac{\mu \cdot R_m}{A \cdot \Delta p} \quad (18)$$

Thus if the liquid viscosity, cross-section area of the filter, pressure difference, and the ratio between the mass of dry cake and volume of filtrate are known, the chart can be used to calculate specific resistance cake and filter medium resistance.

In order to extend the filtration model, Walter Gösele [17] introduced to the specific resistance cake follow the equation of Darcy:

$$\Delta p_1 = \left( \frac{\dot{V}}{A} \right) \cdot H \cdot \mu \cdot \alpha_H \quad (19)$$

The SI unit is

$$\text{Pa} = \frac{\text{m}^3/\text{s}}{\text{m}^2} \cdot \text{m} \cdot \text{Pa} \cdot \text{s} \cdot \text{m}^{-2}$$

The unit of  $\alpha_H$  must be  $\text{m}^{-2}$  in order to satisfy the Darcy equation. The reciprocal of the filter resistance  $\alpha_H$  is also called permeability  $k = \frac{1}{\alpha_H} [\text{m}^2]$ . Sometimes it is more comfortable to define the height of filter cake in terms of solid mass per unit area and lead to a little difference in the definition of cake resistance.

$$\Delta p_1 = \frac{\dot{V}_L}{A} \cdot \frac{m}{A} \cdot \mu \cdot \alpha_m \quad (20)$$

In this case, the unit of specific resistance has the unit “m/kg” and is called solid mass related filter cake specific resistance. The  $\alpha_H$  named cake thickness related filter cake specific resistance. The relationship between the two kinds of resistance can be calculated by the equation:

$$\alpha_H \cdot H = \alpha_m \cdot \frac{m}{A} \quad (21)$$

$$\alpha_m = \alpha_H \cdot \frac{H \cdot A}{m} = \alpha_H \cdot \frac{V_{\text{total}}}{V_s \cdot \rho_s} = \alpha_H \cdot \frac{1}{(1 - \varepsilon) \cdot \rho_s} \quad (22)$$

Equation (17) shows how to calculate the specific resistance cake  $\alpha$  related to the solid mass. In order to calculate the  $\alpha_H$ , Equation (17) can be rewritten:

$$\text{Gradient} = \frac{\mu \cdot c \cdot \alpha_H \cdot H \cdot A}{2 \cdot A^2 \cdot \Delta p \cdot m} \quad (23)$$

By the define the concentration parameter  $\kappa$ , as is defined in appendix D1, the Equation (23) gives:

$$\text{Gradient} = \frac{\mu \cdot \alpha_H \cdot \kappa}{2 \cdot A^2 \cdot \Delta p} \quad (24)$$

Which

$$\kappa = \frac{c_v}{1 - \varepsilon - c_v} \quad (25)$$

Thus, while Equation (16) is the integrated form of Darcy’s law with the solid mass related filter cake resistance (specific resistance cake  $\alpha$  has the unit kg/m), the

integrated form of Darcy's law with the thickness cake related filter cake resistance (specific resistance cake  $\alpha_H$  has the unit  $\text{m}^{-2}$ ) can be given:

$$\frac{t}{V_L} = \frac{\mu \cdot \alpha_H \cdot \kappa}{2 \cdot A^2 \cdot \Delta p} \cdot V_L + \frac{\mu \cdot R_m}{A \cdot \Delta p} \quad (26)$$

In practical, by collecting the amount of filtrate in time, the experimental result is plotted in the form of  $\frac{t}{V_L} = f(V_L)$ .

Which  $f(V_L)$  is the integrated form of Darcy's law.

The linear diagram is shown in Figure 6.

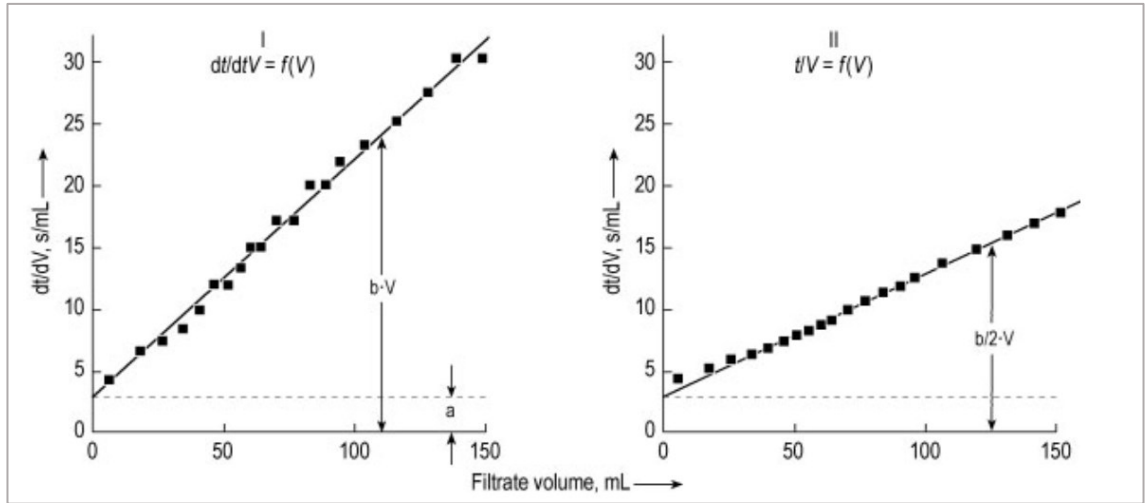


Figure 6. The linear diagram between  $t/V$  versus  $V$  [17, 18].

However, the experimental data often differs from the ideal linear characteristic, as shown in Figure 6. The kind of deviation indicates the second effect, which occurred during filtration and is shown in Figure 7.

The reason for errors can be explained according to [17, 18]:

A: Theoretical curve without secondary effect.

B: Some solid has settled before filtration start and increases the filter medium resistance.

C: At the beginning of filtration, there is turbidity in the filtrate. The solid loss reduces the amount of cake, clearly indicates the negative of filter medium resistance. In case no turbid filtrate is found, the fine solid could deposit inside the filter medium,

blocking it in the long run. This curve also indicates the floating solid, where the clear filtrate is filtered at the beginning of filtration.

D: The solid settled out completely, increasing the speed of cake growth. At the end of filtration, the filtrate is filtered with the constant resistance cake.

E: Only the coarse particles are settled out. After that, the remaining fine particles are filtered, and the resistance increases. This case also sees when the time for filtration is long and wide particle size distribution.

F: The fine particles trickle through the filter cake, maybe blocks the pores, even blocks the filter medium. The process can be described as a blocking filtration. On the other hand, the non-linear ( $t/V$  vs.  $V$ ) data also derived from the formation and behavior of the skin even is accepted than the idea of the migration of particles. This permeability of the skin could decrease throughout filtration, result in grow up specific resistance in time [19-21].

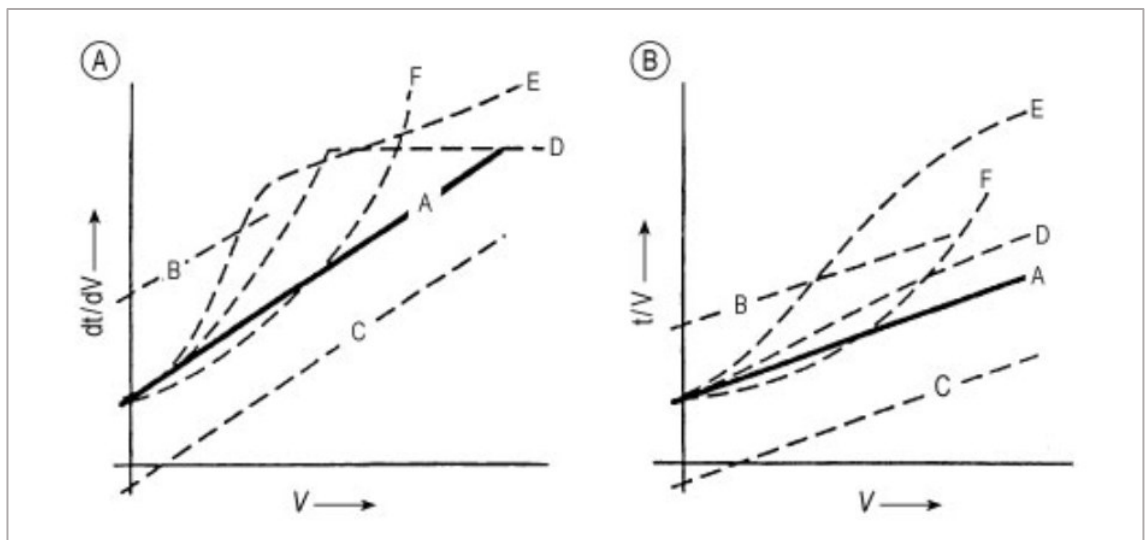


Figure 7. Types of deviation occur during filtration [17, 18].

A further cause of deviations might be:

- The determination of the begin or the end of filtration. This endpoint is particularly difficult without the sight glass. Therefore, some last points of filtration are skipped.
- Unusual properties of suspension like foam bubbles, oil droplet, non-Newtonian rheology of liquid, or nonisometric of particles.

- The sediment may be so voluminous that it fills the whole suspension. The deviations maybe come from the precipitation to new solid, continuing of agglomeration that changes the effect of particle size.

#### 1.4. Cake deliquoring - immiscible fluid displacement in porous media

According to Wakeman and Tarleton [22], after filtration, one of the methods to dewater filter cake is to replace the retained water that has been in cake pores by an immiscible fluid. The second fluid is gas, with air being used most commonly. Typically, the term “deliquoring” is used in case of dewatering of filter cake by mean of a gas pressure differential to reduce the moisture remaining in the voids. In the deliquoring process, the filter cake is mentioned as a matrix of solid particles in a liquid and gas mixture, and the mode of removal liquid reduces one or two-phase flow through the porous medium. One of the fluids is usually liquid (filtrate) in feed slurry, will tend to wet solid in preference to incoming gas. As a result, the wetting fluid (liquid) flows through the solid and prevents the non-wetting fluid (gas) getting contact with the solid. The gas flows through the remaining voids spaces and contacts the retained liquid rather than with solid. The shape of the flow channel is considerably modified by the presence of liquid and the extent of saturation of the cake by the liquid. The saturation,  $S$ , is defined by:

$$S = \frac{\text{the volume of liquid in the cake}}{\text{the volume of voids in the cake}} \quad (27)$$

The liquid tends to smooth the surface of the channel. Thus gas does not experience such a sharp change in direction like it would if the cake were completely dry.

According to Ullmann's Encyclopedia of Industrial Chemistry - Filtration [17], the residual saturation with moisture as a function of time and then asymptotically approach the equilibrium value as a presence in Figure 8.

Thus, an equilibrium value is established with regard to the mechanical displacement of liquid. Thermal drying by airflow will reduce further to the total dryness of filter cake if the airflow is maintained long enough. Nevertheless, generally, the thermal effect is minimal as compared to the mechanical impact because of the low mass of air flowing through the filter cake [16]. The final “equilibrium” moisture for mechanical dewatering depends on the nature of the cake, the applied pressure difference.

The initial deliquoring speed also depends on cake thickness. For both values, the flow rate of gas is not important if it is not produced pressure difference [16].

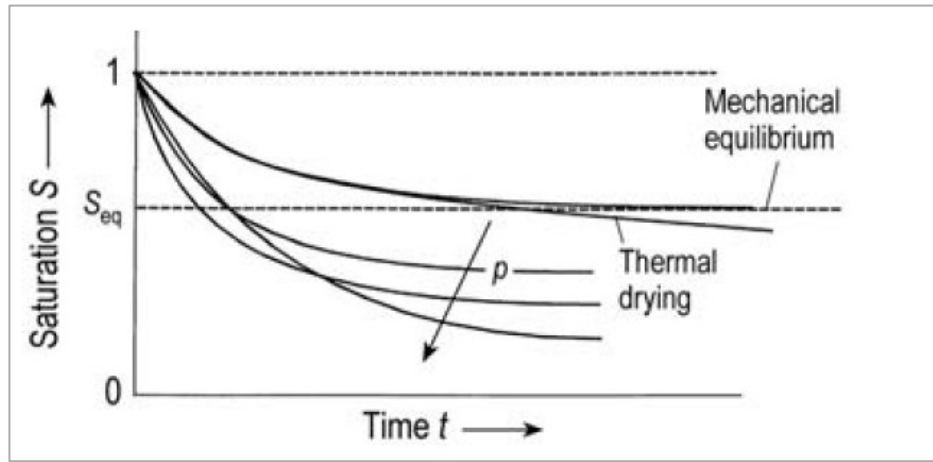


Figure 8. Deliquoring by gas pressure – the residual saturation as a function of time [17].

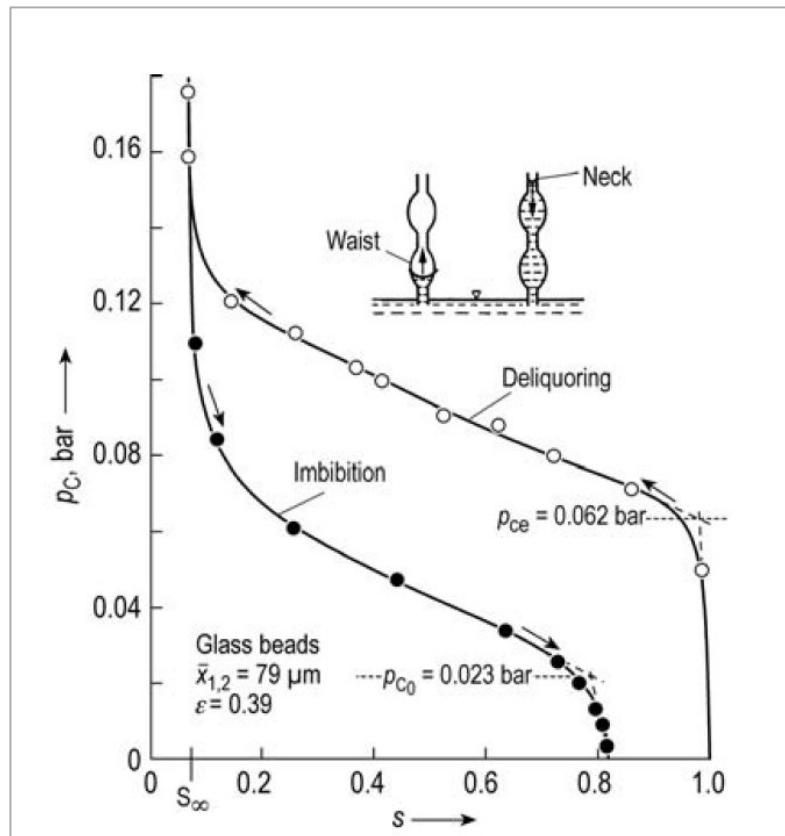


Figure 9. Types of capillary pressure curve for imbibition and deliquoring [17, 23].

For the same material as well as cake thickness, at each pressure difference, the saturation has defined value at equilibrium state. A plot of saturation of the cake and pressure difference in this state is called a capillary pressure curve. The saturated filter cake is placed in the filter on the filter medium (semipermeable membrane – this



membrane is permeable for liquid and impermeable for gas at the applied pressure. The quantity of filtrate displaced from filter cake is collected. A typical capillary pressure curve is shown in Figure 9. The curve starts from a completely saturated cake (saturation = 1). The pressure difference increases slowly. At each set point of the equilibrium state, the quantity of displaced liquid is registered, yielding one point in the capillary pressure curve. The liquid is displaced for the first out of filter cake when the pressure exceeds a certain threshold pressure. This pressure value is capillary pressure entry ( $p_{ce}$ ) [16, 24]. Each time, when a pore is emptied, the gas pressure overcome the capillary pressure at the neck of the pores, with diameter  $d_{pore, neck}$ . This is the traditional 2D-view on filter pores.

$$p_{ce} = \frac{4 \cdot \sigma \cdot \cos \delta}{d_{pore, neck}} \quad (28)$$

Further increasing the pressure difference, liquid in the fine pore is displaced, and the moisture is reduced to irreducible saturation after infinite time beyond at which no further reduction is reached. The residual moisture corresponds to the amount of liquid that is trapped in isolated domains within the filter cake (internal water) [17, 25].

In most cases, there is no semipermeable membrane below the filter cake, normally that is a permeable filter medium for gas as well as liquid, such as filter cloth. Gas and liquid flow simultaneously through the filter cake. A gas exerts capillary force onto the adjacent liquid, both gas and liquid flow in the same direction, however with the different speed and different pressure (local pressure between gas and liquid is equal to local capillary pressure). The difference saturation between the top and bottom of the incompressible filter cake is small.

The permeability of saturated filter cake is the same if either gas or liquid flow through the pores. However, pores filled liquid and pore filled gas form two separate capillary systems, each of them with reduced permeability. The local permeabilities (for liquid or air) about the permeability of the saturated cake are called relative permeability. They depend on the degree of saturation and can be calculated as:

For the wetting fluid (the liquid)

$$k_{rel, w} = \frac{k_w}{k} = \frac{\alpha}{\alpha_w} \quad (29)$$

For non-wetting fluid (gas)

$$k_{rel,n} = \frac{k_n}{k} = \frac{\alpha}{\alpha_n} \quad (30)$$

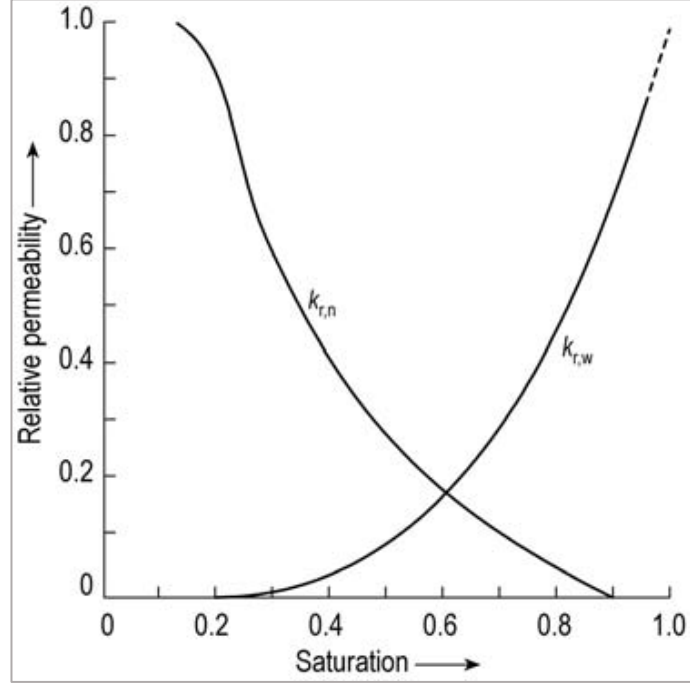


Figure 10. The relative permeability as a function of degree saturation [17].

Relative permeability is shown in Figure 10 as a function of degree saturation of filter cake. For the wetting phase, relative permeability reduces from 1 to 0 when the saturation decline to irreducible saturation. At the other extreme, the flow of air reaches 0 when the degree of saturation is 0.9 and has a maximal value at irreducible saturation [17].

The capillary pressure acts to retain liquid inside the pores of the cake and is dependent on the saturation of the filter cake and the range of pore sizes that exist therein. The most useful relationship is obtained by measuring a capillary pressure curve for the porous medium or filter cake and then plotting the capillary pressure against saturation. After defining the reduced saturation,  $S_R$ , as [22]:

$$S_R = \frac{S - S_\infty}{1 - S_\infty} \quad (31)$$

Which  $S_\infty$  is irreducible saturation, the resulting data can generally be described by Brook and Corey [26]; Wakeman [27, 28].

$$S_R = \left(\frac{p_b}{p_c}\right)^\lambda \text{ for } p_b \geq p_c \quad (32)$$

Where  $\lambda$  is a pore size distribution index which characterizes the range of pore size in filter cake,  $p_c$  is the capillary pressure and  $p_b$  is the threshold pressure.

The threshold pressure increase as the mean size of particles in the cake decreases, and as the size range increases, the value of  $\lambda$  does not follow any trend of particle size, probably because it also depends on the size range of the particles in the distribution. The variation in the value of  $\lambda$  is not significant for smaller particles, and the change leads only to a small variation in the relative permeability [22, 28]. Therefore, the pore size distribution  $\lambda$  is suggested 5 to be a reasonable value for practical purposes [22].

One of the expression for the relative permeabilities in term of the pore size distribution index  $\lambda$  has been described by Wakeman [22]:

$$k_{rg} = (1 - S_R)^2 \cdot \left(1 - S_R^{\frac{(2+\lambda)}{\lambda}}\right) = \left(1 - \left(\frac{p_b}{p_c}\right)^\lambda\right)^2 \left(1 - \left(\frac{p_b}{p_c}\right)^{2+\lambda}\right) \quad (33)$$

$$k_{rl} = S_R^{(2+3\lambda)/\lambda} = \left(\frac{p_b}{p_c}\right)^{2+3\lambda} \quad (34)$$

### 1.5. Tensile stress between particles

The study of particles gives the different types of interparticle forces and their relative importance as a function of particle size. Interparticle forces can be listed Van der Waals forces, forces due to adsorbed liquid layers, forces due to the liquid bridge, electrostatic forces, and solid bridge.

*Van der Waals forces* exist between all solid molecularly based attractive forces collectivity. The energy of these forces is of the order of 9.1 eV, and the range is broad compared with chemical bonds.

*Forces due to adsorbed liquid layers* are kind of force occurring because of the condensable vapor adsorbed layer on the solid's surface. The strength of the bond depends on the area of contact and the tensile strength of adsorbed layers.

*The electrostatic force* occurs because of the transfer of electrons between the bodies, which results from friction when the particles collide or the frequent rubbing of

particles against the equipment's surface. This force may be attractive or repulsive, do not require contact between particles, and acts in long distance.

*The solid bridge* may take three forms: crystalline bridge, liquid binder bridges, and solid binder bridges. It is the permanent bonding within the granule as the liquid is removed from the original granule. Forces due to liquid bridges (liquid bridge force) are specifically crucial in the granulation process. Although the adsorbed liquid layer forces exist and increasing particle-particle contact and reducing the interparticle distance, these forces are usually negligible in comparison with liquid bridge forces, which is form by the presence of sufficient magnitude of liquid. There are four types of the state, depending on the proportion of liquid present between groups of particles. They are pendular, funicular, capillary and droplet, as shown in Figure 11 [29, 30].

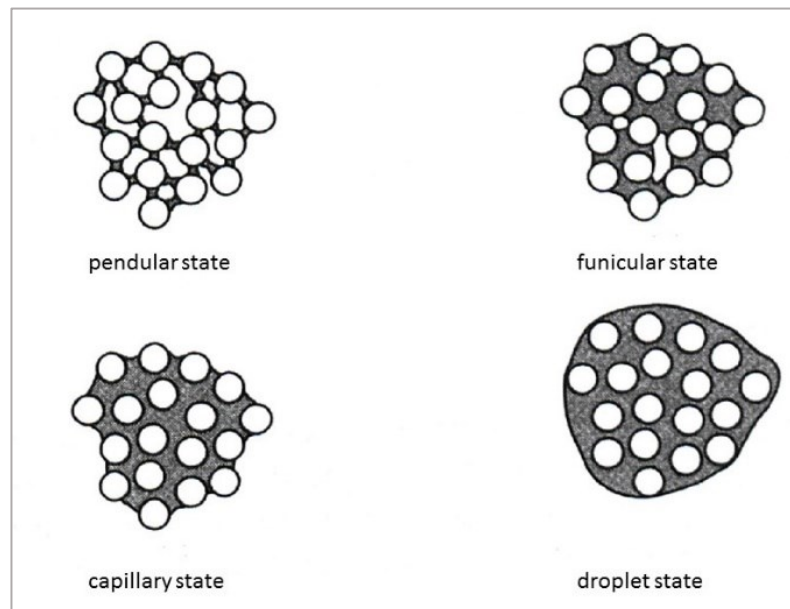


Figure 11. Types state of group particles depending on the amount of liquid [29, 30].

In the pendular state, the liquid is presented as a point contact in the bridge neck between particles. They are separated and independent with others. The interstitial space between particles is porosity. As the proportion of liquid to particles is increased, the liquid is free to move, and the surface tension boundary attractive force between particles decreases upon increasing separation. This state is funicular. By increasing the amount of liquid, then capillary state occurs where the pores are filled by liquid. There are fewer curved liquid surface and fewer boundaries for surface tension to act on. Finally, when the particles are entirely dispersed on liquid, the regime is called a droplet state, where the strength of the structure is very low [29]. Because the author is just only mentioned

the attractive force caused by the liquid bridge, result in when there is sufficient liquid to completely fill the interstitial pores between the particles (capillary), the granule strength falls further as there are fewer curved liquid surfaces and fewer boundaries for surface tension forces to act on. Moreover, the particles are completely dispersed in the liquid (droplet), the strength of the structure is very low. Some studies also showed the comparison and interaction between forces, as can be seen in Figure 12.

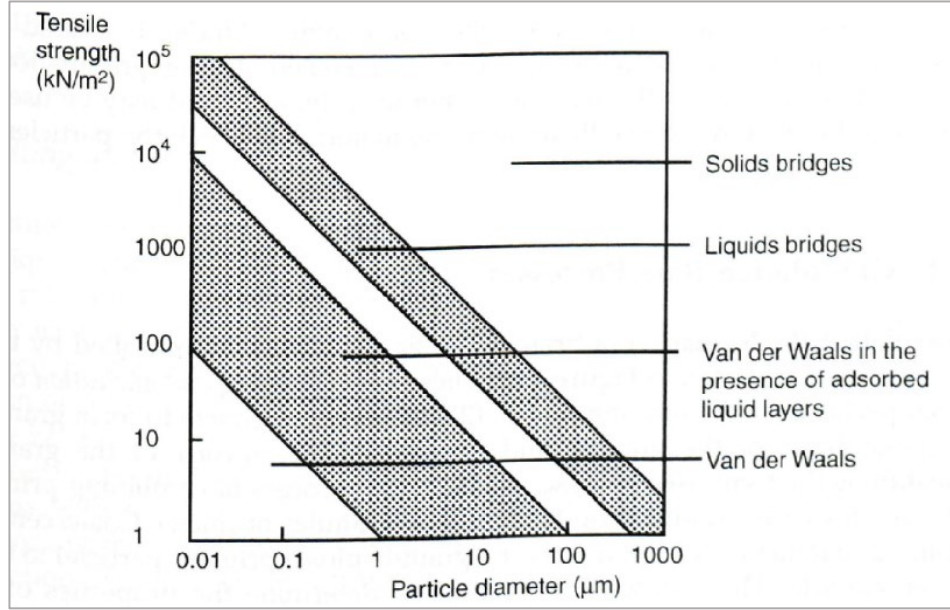


Figure 12. Theoretical tensile strength of agglomerates with different bonding mechanisms [29, 31].

H. Schubert [32], in his research, also mentioned the dependence of tensile strengths and liquid distribution on the system, which can be characterized by saturation. It can be said this is the comprehensive research, adding more information for the mentioned above. Different liquid distribution influences the strength of moist agglomerate in different ways. The diagram in Figure 13 shows the idea about these relationships. The upper chart is the relationship between tensile stress and saturation. Corresponding to the degree of saturation, the lower chart shows the capillary pressure in the particle system.

With a certain assumption, Rumpf [33] has given the tensile stress in the pendular state:

$$\sigma_t = \frac{1 - \varepsilon}{\varepsilon} \cdot \frac{F^*}{x^2} \quad (35)$$

Where  $\varepsilon$  is the porosity,  $F^*$  is the mean adhesion force transmitted at a contact point and  $x$  the mean particle size. For liquid bridge:

$$F^* = F_H \cdot \gamma_{lg} \cdot x \quad (36)$$

Where  $\gamma_{lg}$  is the surface tension;  $F_H$  is the average adhesion force per contact point.

According to Heinrich Schubert [34], the meaningful value for the dimensionless contact spacing is assumed 0.035 (distance particles/particle size), the equation (36) can be written:

$$F^* \cong 1,9 \cdot \gamma_{lg} \cdot x \quad (37)$$

Equation (35) is rewritten:

$$\sigma_z \cong 1,9 \cdot \frac{1 - \varepsilon}{\varepsilon} \cdot \frac{\gamma_{lg}}{x} \quad (38)$$

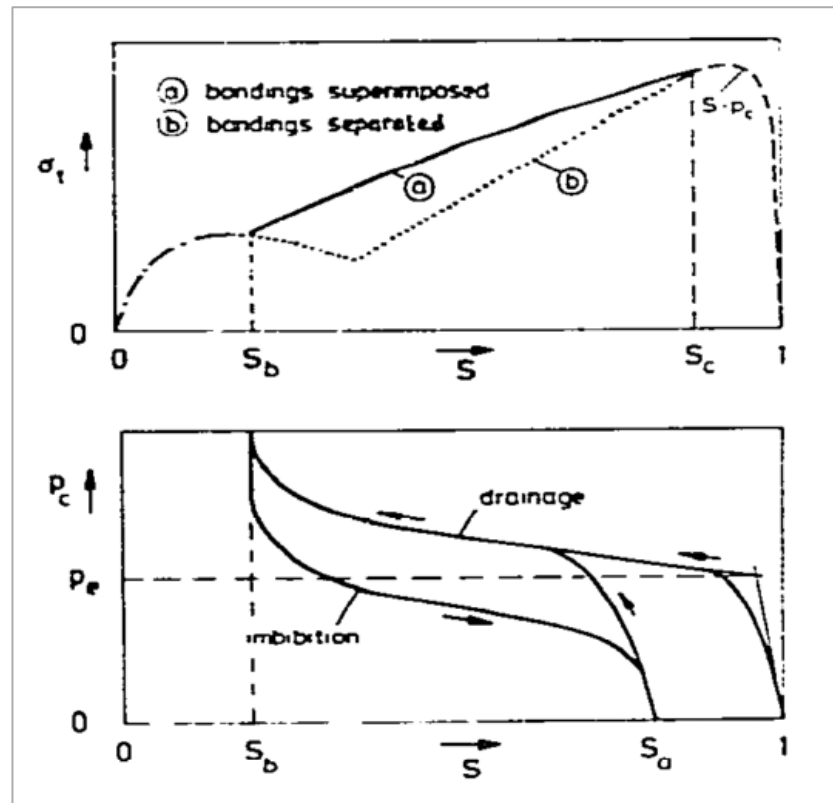


Figure 13. Tensile stress and capillary pressure as a function of saturation [32].

In the capillary state, tensile stress can be calculated following the equation:

$$\sigma_t = S \cdot p_c \quad (39)$$

For the funicular state, the tensile stress is the result of both bondings caused by liquid bridge and bonding caused by region filled by liquid. The assumption is if either bonding bridge or bonding capillary dominated, tensile stress is indicated by plot b (Figure 13 top). If both bonding mechanisms are superimposed, tensile stress is shown in the plot a (Figure 13 top). The extent to which the bridge model contributes cannot be predicted with certainty. Helmar Schubert [35] discussed the tensile stress caused by two mechanisms following equation:

For liquid bridge mechanism:

$$\sigma'_B = \sigma_B \cdot (S_k - S)/(S_k - S_B) \quad (40)$$

For capillary mechanism:

$$\sigma'_k = p_k \cdot S_k \cdot (S - S_B)/(S_k - S_B) \quad (41)$$

Tensile stress in case of both superimposed mechanism is suggested:

$$\sigma_z = \sigma_B (\text{pendular}) \cdot \frac{S_k - S}{S_k - S_B} + p_k \cdot S_k \cdot \frac{(S - S_B)}{S_k - S_B} \quad (42)$$

#### 1.6. Coal processing/ washing

Coal is a fossil fuel. It is a combustible, sedimentary, organic rock, which is composed of carbon, hydrogen, and oxygen. It is formed from vegetation that has been consolidated between other rock strata and altered by the combined effect of pressure and heat over millions of years to form coal seam.

The degree of change undergone by a coal as it matures from peat to anthracite, known as coalification – has an important bearing on its physical and chemical properties and as referred to the rank of the coal. Lower rank coal such as lignite and sub-bituminous coals are typically softer, friable materials with a dull, earthy appearance. They are characterized by high moisture levels, low carbon content, and therefore a low energy content. High-rank coal is generally harder and stronger, often has a black, vitreous luster. They have more carbon, lower moisture content, and produce more energy.

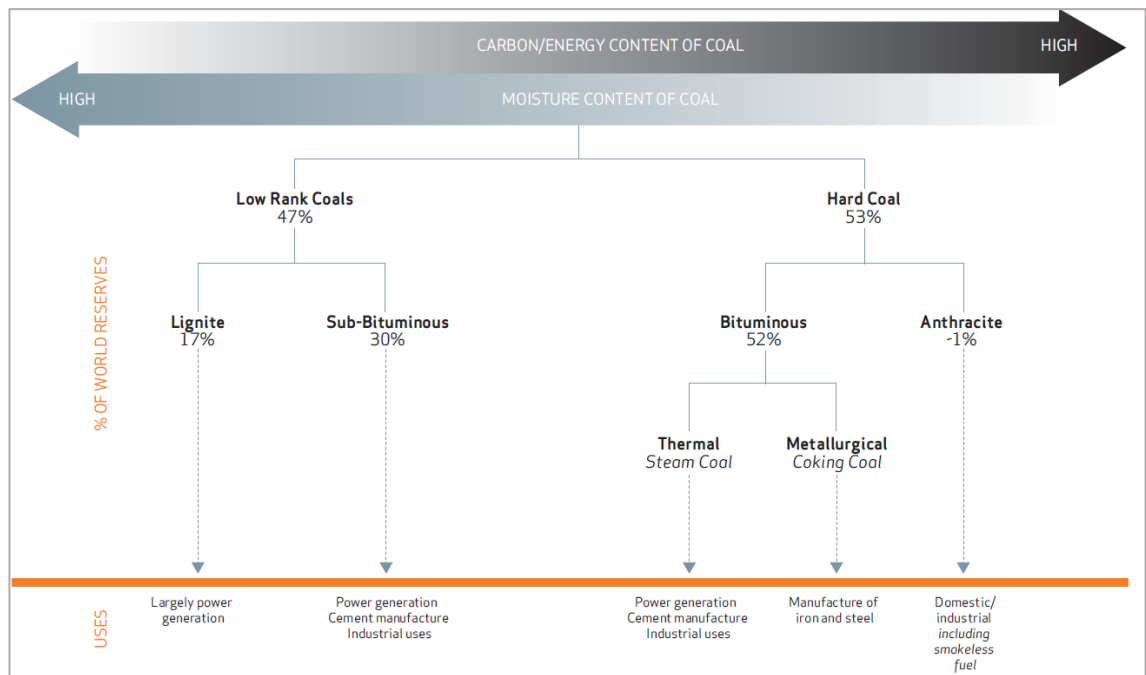


Figure 14. Types of coal [36].

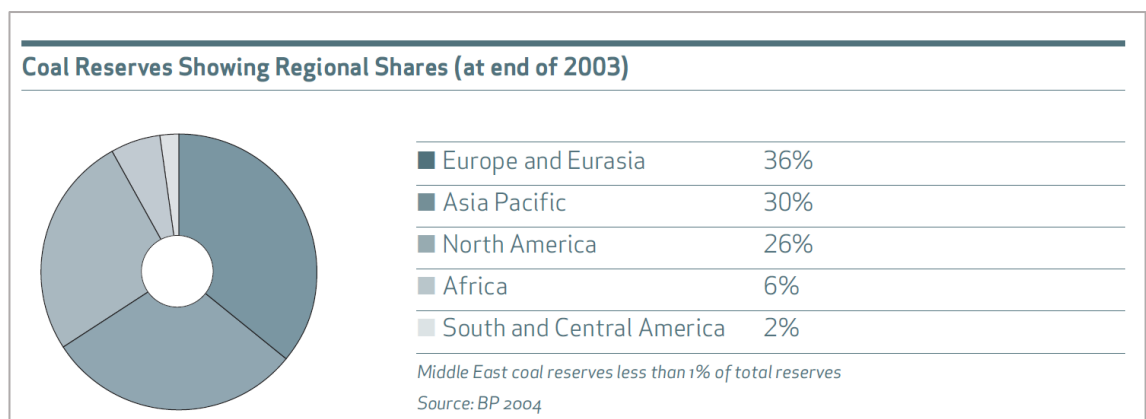


Figure 15. Coal reserves in regions [36].

Anthracite is at the top of the rank scale and has a corresponding higher carbon and energy content and lower levels of moisture. The ranking of types of coal is shown in Figure 14. It has been estimated that there are over 984 billion tonnes of proven coal reserved worldwide. Coal can be found on every continent in over 70 countries, with the most significant reserves in the USA, China, Russia, and India. Figure 15 shows the coal reserves in each region [36].

Vietnam is one of the most important producers of anthracite. Currency available data show that the coal reserves in Vietnam are about 49.8 billion tons. Coals reserve are classified into a few categories (according to the Vietnam standard): measured and indicated reserves (categories A, B, and C1) is 33%, inferred 39%, and prognostic



resource (B) is 28%. Vietnam has almost types of coal such as anthracite (already mined), bituminous, sub-bituminous coal, lignite coal, and peat coal. Coal is located along Vietnam such as Quangninh, Red River delta, Mekong river delta, etc. (Figure 16).

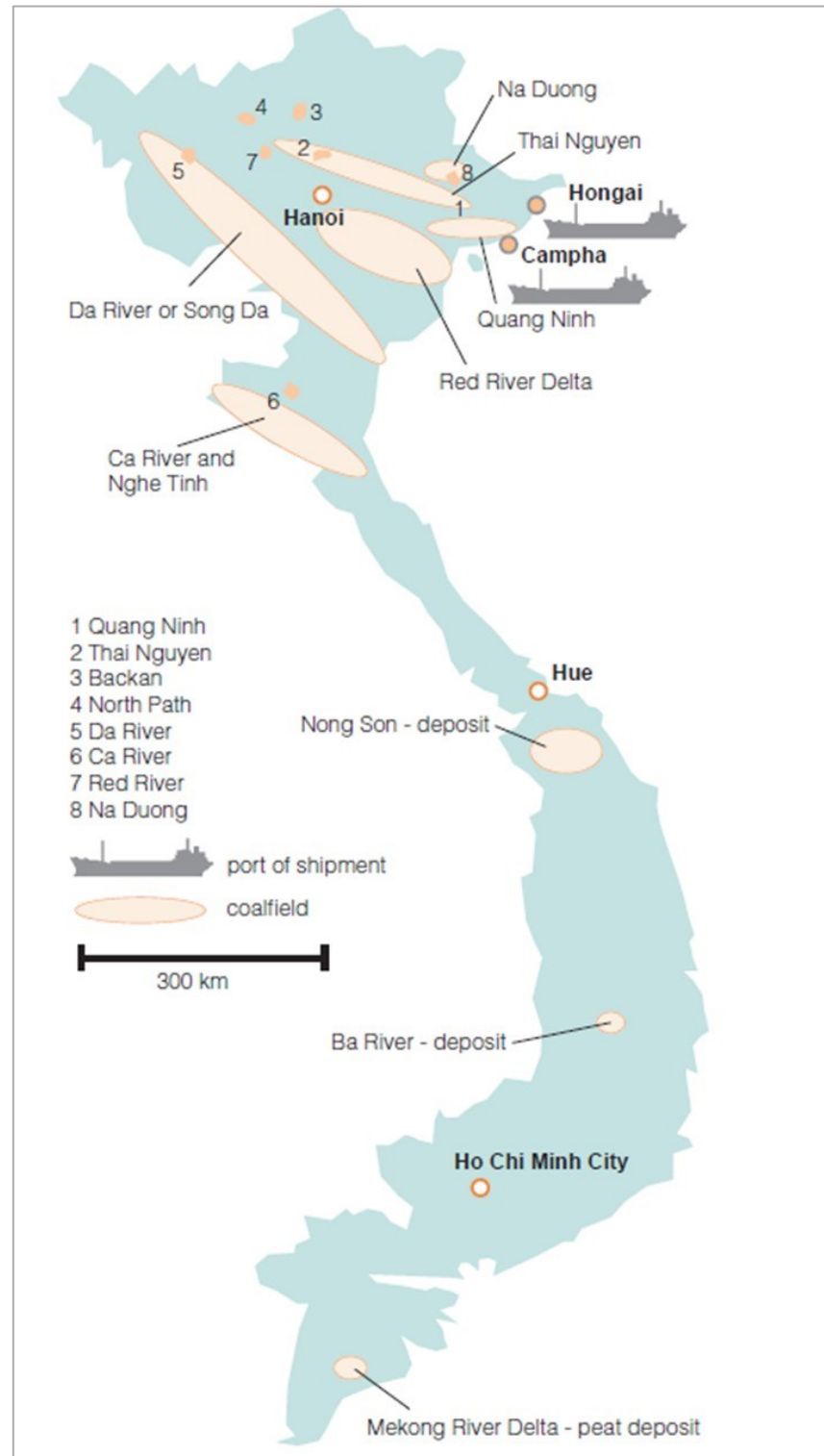


Figure 16. The distribution of coal reserves in Vietnam [37-40].

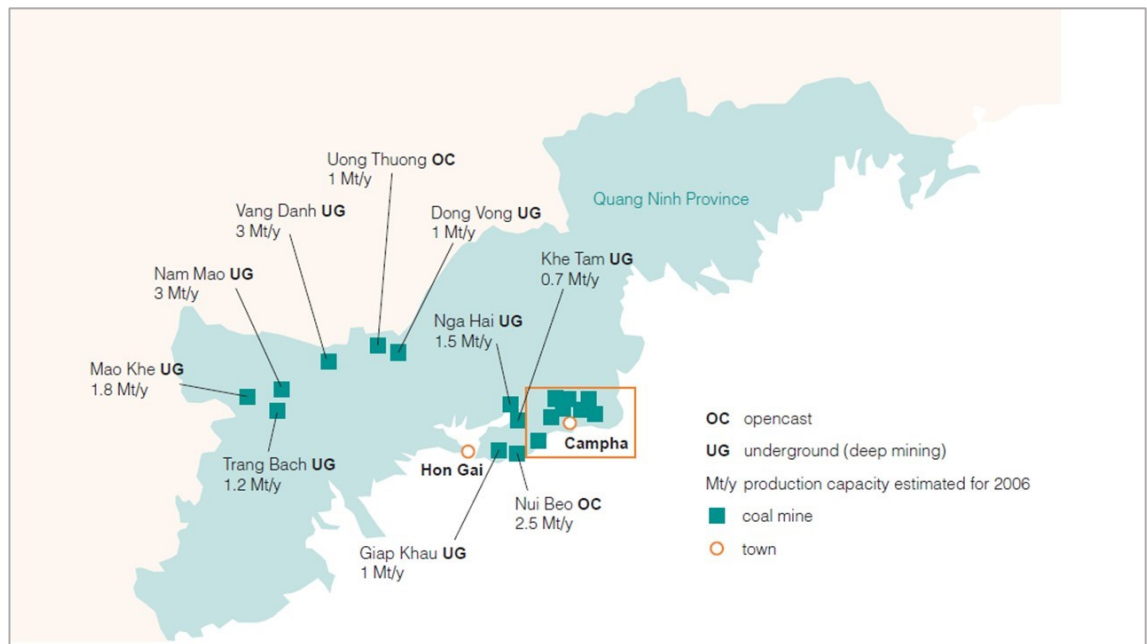


Figure 17. The distribution of coal reserves in Quang Ninh [37-40].

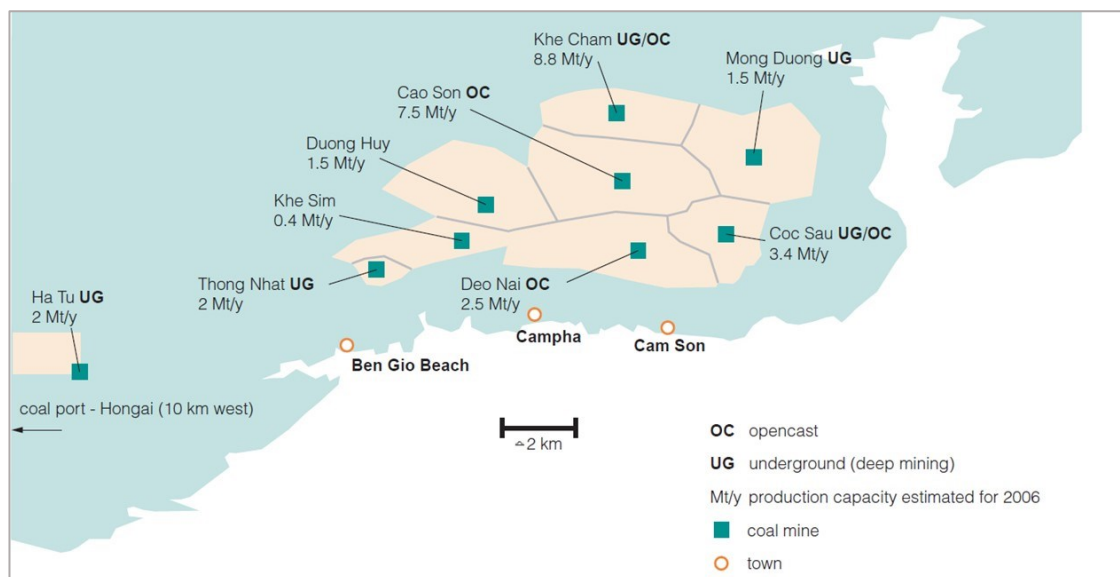


Figure 18. Major coal mines around the Cam Pha - Quang Ninh region [37, 38].

The most important coal basin in Viet Nam is Quang Ninh. Quang Ninh is in North East part of the country with an area of about 5900 km<sup>2</sup>. Coalfields are located near the coast, so it is convenient for transportation. Coal is exploited from 1839 to today. Figure 17 shows the main coal deposit in the Quang Ninh basin. Otherwise, the major coal mines around Cam Pha, where supply run-of-mine coal (ROM coal) for Cua Ong Coal Washing Plant, is also shown in Figure 18.

Coal plays an important role in the economy and the development of Vietnam. The demand of coal for the domestic market has increased steadily every year. In five years, domestic coal demand has risen from 18 million tons (in 2007) to 24.8 million tons (in 2012). According to the master plan of coal industry development in Vietnam 2020, with perspective 2030, the total coal will get up to 60 million tons in 2020, 65 -70 million tons in 2025, and 65-75 million tons in 2030. According to the balance of supply and demand, if the power plants put into operation on schedule under the master plan VII (National Master Plan For Power Development – Vietnam Government), Vietnam will need 62 -72 million tons of coal, in which coal for power need 42-72 million tons, coal for other industries need 20-22 million tons. Vietnam has to import energy coal with the amount from 10 -12 million tons in 2020 [41]. The supply and demand of coal are predicted to 2030, shown in Figure 19.

In past years, Vietnam exported coal to many countries and territories such as the EU, Japan, Korea, India, Taiwan, China, etc. Nevertheless, for the future, when the domestic demand arises, the export plan will reduce and reduce more in the coming years to ensure coal supply to the economy. Vinacomin, in the role of an economic corporation with 100% owned by the state, has promoted technological research, apply advanced coal processing technology toward to diversification of products, create clean and environment-friendly products [41].

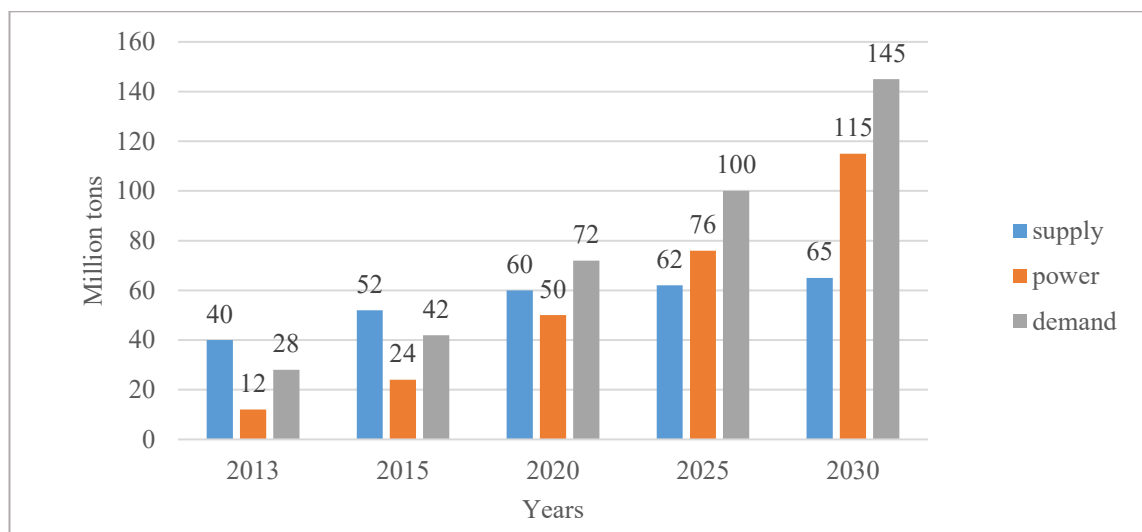


Figure 19. The data and prediction of supply and demand of coal [41].

In the Vietnam coal industry, coal is usually prepared before consuming. There are two stages of preparation. The first one is that two implements the ROM coal pre-

treatment system by hand-picking, screening, grinding, or blending. In the second stage, coal is upgraded in the preparation plant. In Quang Ninh, there are three big plants, including Cua Ong Coal Washing plant, Nam Cau Trang Coal Washing plant, and Vang Danh Coal Washing plant. The former is the greatest plant, with more than 10 million tons per year. The Cua Ong plants include two modules (factory 1 and 2) with many methods for enrichment like Jig, spiral separator, cyclones, dense medium separator. The flowsheet is shown in Figure 20 and Figure 21.

The products are diverse in types and quality such as clean coal below 6mm, 6 - 15 mm; 15-35 mm; 35 – 50 mm with the ash content 5 – 6 %, moisture content 6%; for fines coal products, the ash content can reach 8 – 45%, the moisture content is from 8 to 11.5 %. The quality of coal is achieved by separation technologies in factories 1 and 2. The residual moisture content of coarse coal products can be reduced easily by the screen. Fine coal from two factories is collected to the Dewatering plant. The flowsheet for this factory is shown in Figure 22. The Dewatering plant (also called the Environment plant) was built by the Chinese in 2010. The annual capacity up to 1 million tons per year with the designed residual moisture content of products 20-22% after filtration and continue reducing to 10% after thermal drying. The plant has three hyperbaric filters 90 tons/hour, three air compressor 2.52 m<sup>3</sup>/ minute, nine air compressors 40 m<sup>3</sup>/minute, three disk feeders with conveyor belt, and other transportation equipment. Before coming to the dewatering, below 1 mm fine coal is pumped to thickening with flocculant aid. A significant amount of water is separated. The remaining water with fines coal is pumped to filter. After filtration, fines coal is transported to the thermal rotary drum dryer. The residual moisture content of fine coal is expected, reducing to 10%. However, the actual production shows the residual moisture content after filtration and drying are 25% and 15%, respectively. This issue affects the quality of products, difficult for transportation, increasing production cost (due to remaining water in products cannot re-production), environmental pollution.

It can be said that coal has an important role in energy security and general economic development. This role is especially crucial in the context of a developing country like Vietnam.

This Ph.D. thesis focuses on crack formation mechanism - one of the detrimental factors affecting the filtration efficiency, assessing the moisture content of materials and using new methods to prevent adverse factors, improve the efficiency of filtration and

dewatering. Pure limestone, which is a kind of material object, was used. Otherwise, in order to have a link to a commercial relevant application, especially for Vietnam, fine-grained coal (after washing) is used. The coal belongs to the Cua Ong Coal Washing Company, which is currently being filtered by hyperbaric filter technology. Still, the filtration results are not like the expected, as mentioned above as well as in Figure 22. There was some research about coal dewatering, but there is not for fines coal in Vietnam. The result of research about Vietnam fine coal is not only meaning in academic but also in practical production. More details of coal properties, as well as limestone, are described in the "the materials used" section (section 3.1 - pages 51).









## 2. Literature review

### 2.1. Cracking on filter cake and the dewatering process with and without cracking

Cracking is an undesired phenomenon that is encountered frequently during the deliquoring phase (mechanical displacement phase) of the filtration process. When the crack occurs, the air preferentially flows through the great channels, which are much bigger than the tortuous pathway of pores. The local pressure difference is not enough to push the liquid out of the filter cake. This phenomenon leads to a significant disadvantage about the economy, such as the gas consumption (in some cases is the washing water consumption) is mostly increased by order of magnitude. Otherwise, the process has negative results like higher residual moisture content, lower purity. Even to satisfy the requirement of consumers or to achieve the technical criteria, the disadvantage mentioned compelling the choice of more expensive dewatering processes such as higher thermal energy drying stage.

In the case of the gas differential dewatering process, when the gas gets in contact with the wet surface of the filter cake, the cracks may occur. There are two kinds of cracking mechanisms that can be seen in Figure 23.

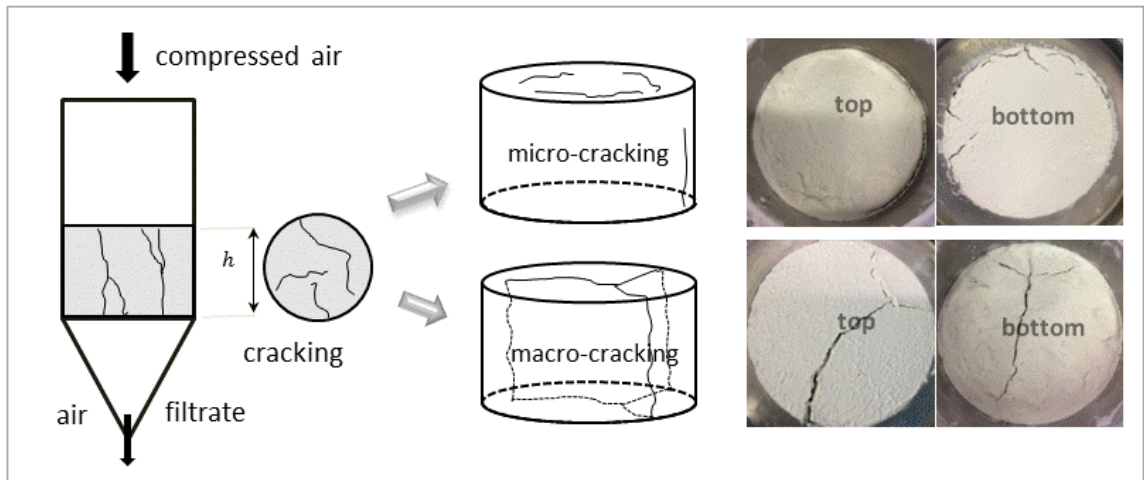


Figure 23. Diagram and picture for micro-cracking and macro-cracking on filter cake during the mechanical displacement phase.

Micro-cracking is a kind of phenomenon that cracking happens on top or at the bottom or the edge of the filter cake. However, they do not contact together and are usually small, randomly shaped. This cracking does not or less affect the dewatering as well as the washing process.

The second one is macro-cracking. This one occurs on top of the filter cake and propagates through the filter cake to the bottom of the filter cake. They are characterized by large size, link from top to bottom, similar shape. They have a tremendous negative effect to further deliquoring and most disadvantage mentioned above.

Also, there should be another mentioned disadvantage that also occurs from the cake formation and remain during the deliquoring phase. The delamination planes divide the filter cake into two or more sections horizontally, as illustrated in Figure 24. This phenomenon is caused by stratification particles with different degrees. It can also affect the amount of liquid inside the filter cake as well as the results of the post-process (like washing, extraction, etc.).

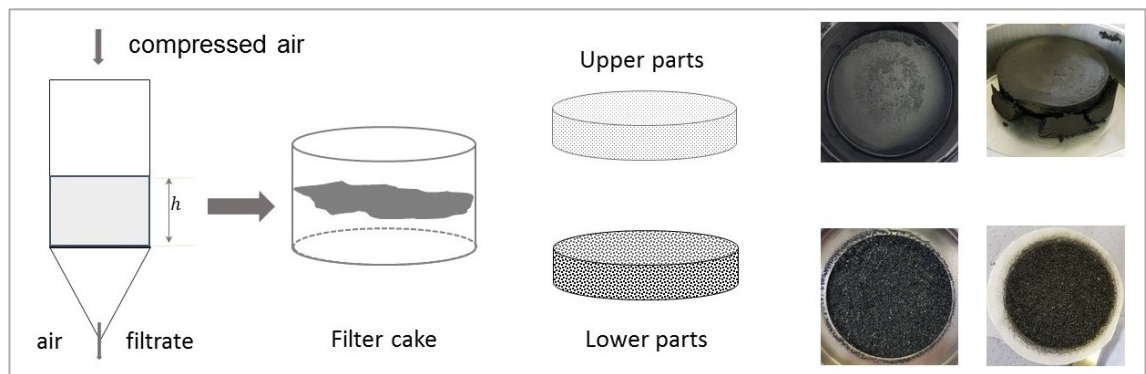


Figure 24. Diagram and images for cracking horizontally due to sedimentation.

For almost understanding, shrinkage cracking is considered to be a random phenomenon. Due to the lack of knowledge of physical reasons for crack formation and the hugely detrimental effects, shrinkage cracking has been tolerated in industrial filtration. However, according to Anlauf et al. [42], several methods have been applied to prevent cracking effects using additional constructive measures. Figure 25 shows a few of them.

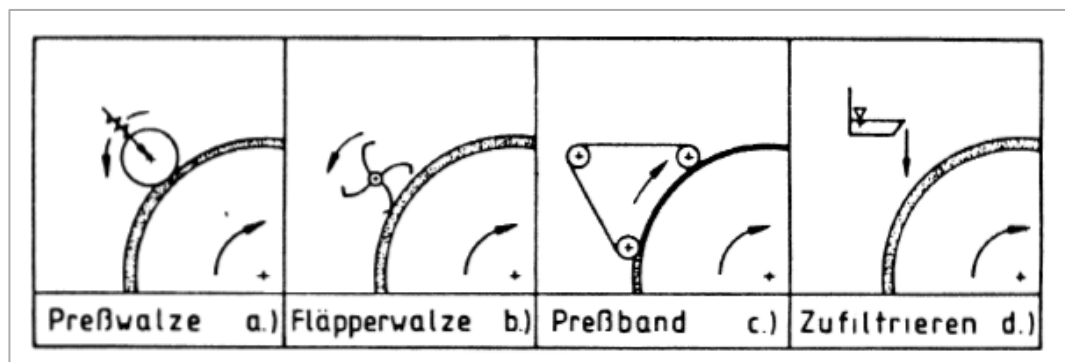


Figure 25. Constructive measure for suppression of crack formation [42].

With the assistance of the roller, specially designed spindles incorporating flattening elements and pressure belt, the crack can be pressed or smeared together and, indeed, partly suppressed. The first two ways are presented, as in the case of smooth spreading of the cracks formed in batch pressure filter with stirrers. These methods are indeed a superficial solution because either crack is still inside the filter cake or split again. The prevent cracks by pressure belt are the most expensive measures and decrease the dewatering area of the rotary filter. The later problem in this method can be solved by using the belt of a porous woven material, in which case a supplementary construction is necessary in order to remove clogging particles. One of the last measures to close the crack in filter cake is the addition of feed suspension. This issue is in-effect because one hand, the part of the filter cake is moistened again that. On the other hand, such “double-filtered” includes the zone of inhomogeneous permeability caused by crack formation reappear again. The best methods to eliminate the harmful effects of crack as well as to avoid the crack formation on filter cake is, of course, clarify the physical of process.

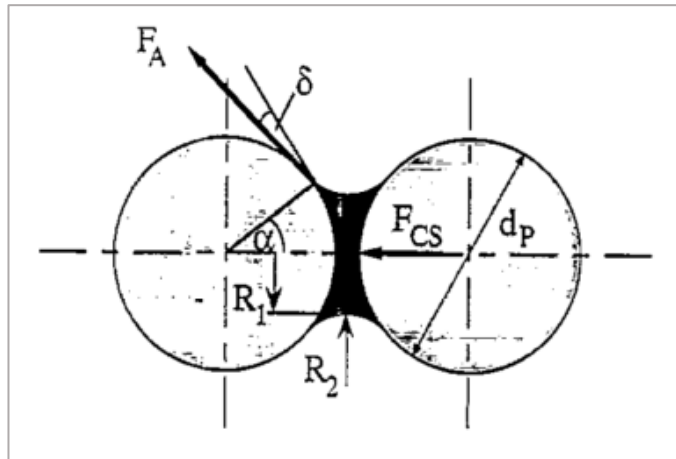


Figure 26. Schematic illustration of the liquid bridge between two particles and the corresponding effective capillary forces (adhesion  $F_A$  and capillary suction  $F_{CS}$ ) [5].

Wiedemann and Stahl [5] studied the shrinkage behavior, which can be determined for all products. The formation of cracking is generally caused by the shrinkage of the filter cake, which is the result of the action of capillary forces or the change of particle interaction forces. In the case of the gas differential dewatering process, the capillary forces (including adhesion force and capillary suction forces in Figure 26) are driving the potential for the shrinkage. They arise at the moment when the gas phase gets in contact with the wet filter cake surface. If the stresses generated by the capillary forces exceed the tensile strength of the filter cake, the formation of crack begins [32].

The tensile strength is given by stress, which is transferable until the weakest bridges break.

The results of the investigation indicated that all measured shrinkage curves could be divided into three parts: normal, residual, and zero shrinkage, as can be seen in Figure 27. In the normal section, the shrinkage of the filter cake achieves with the keeping initial saturated state (saturation = 1). Residual shrinkage witnessed the decreasing of both saturation (S) and void ratio (e), which the later is characterized by the ratio between pore volume and solid volume. In the zero shrinkage section, the void ratio shows the constant value, while the saturation continuously reduced, leading to the further desaturation of the filter cake.

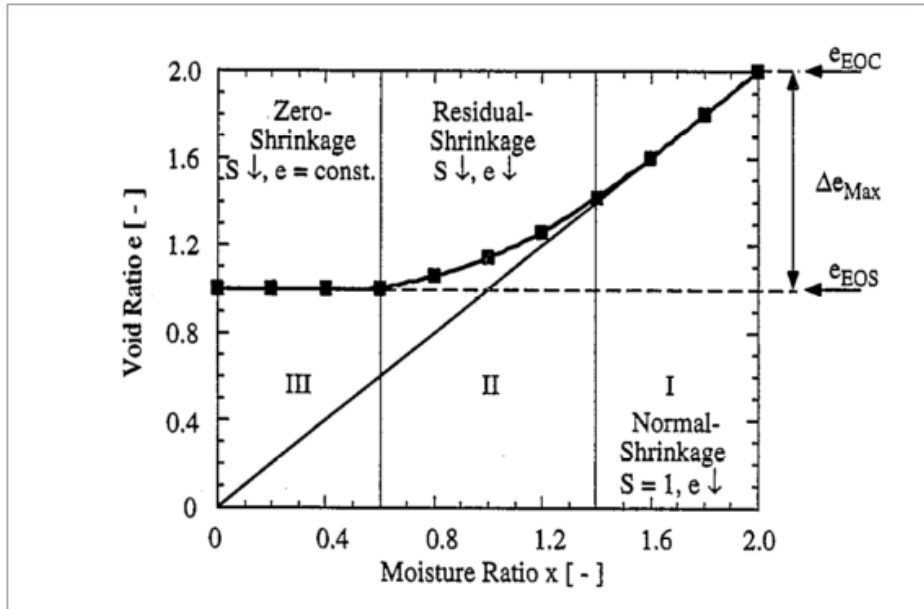


Figure 27. Characteristic shrinkage curve with three sections [5].

The maximum dimension of the filter cake, as can be called shrinkage potential  $\Delta e_{\max}$ , is positively affected by a decrease of the surface tension (Figure 28). By observation, the change of shrinkage potential can be directly correlated with the change of cracking behavior. When the shrinkage potential does not exceed the critical shrinkage potential (the value is different with different material), no formation of cracking (Figure 29). Otherwise, by reducing surface tension as a means of thermal energy input in the phase interface. In that case, surface tension in the function of temperature at the phase boundary. One of the most economical methods of supplying high temperature is, using saturated or superheated steam instead of the gas during the mechanical displacement phase.

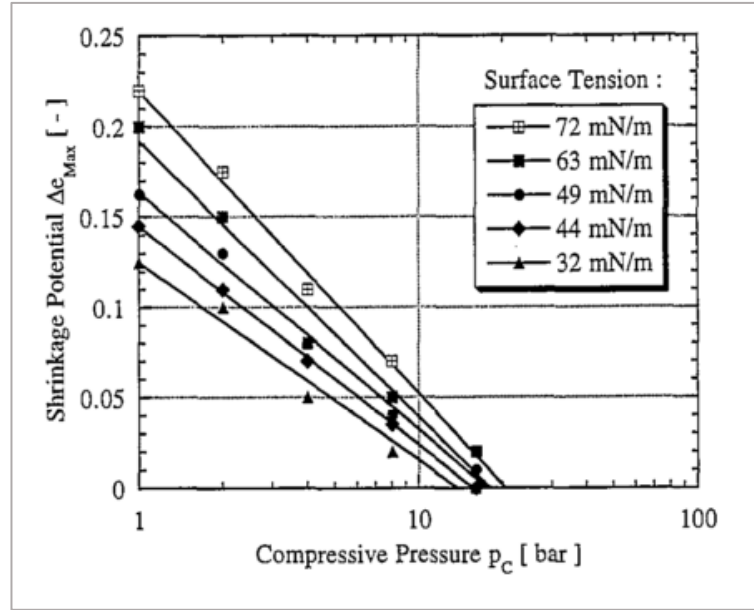


Figure 28. The shrinkage potential of filter cake against the compressive pressure at variety of surface tension [5].

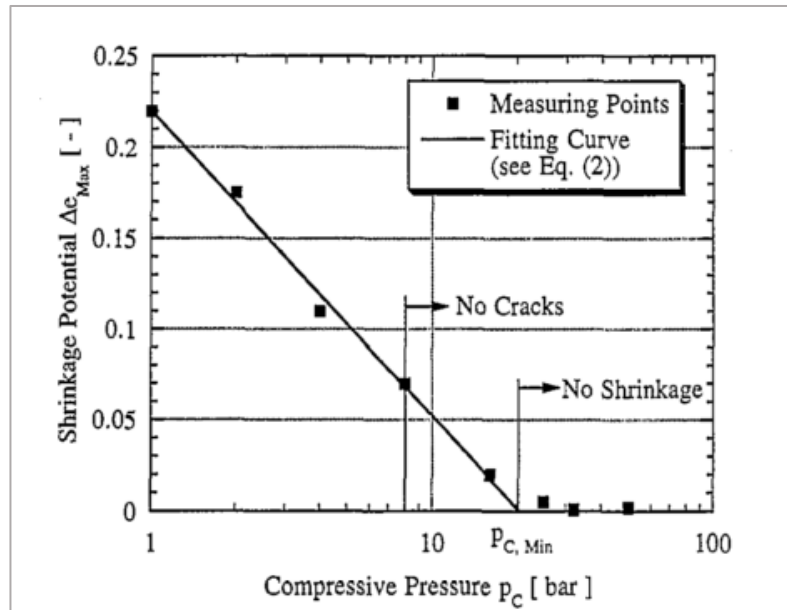


Figure 29. No crack and no shrinkage at the higher pressure minimum compressive pressure [5].

Otherwise, the variety of organic and inorganic materials with the different particle size distribution (Figure 30) for tests showed the effects on shrinkage potential. It can be seen that smaller material need higher minimum compressive pressure. The

shrinkage potential at each pressure is higher for smaller size products, as can be seen in Figure 31.

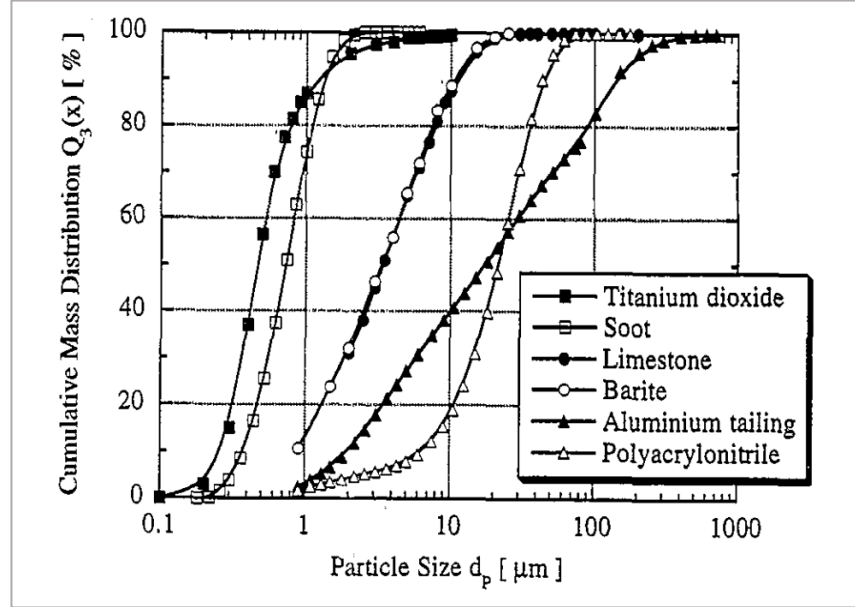


Figure 30. The particle size distribution of some test materials [5].

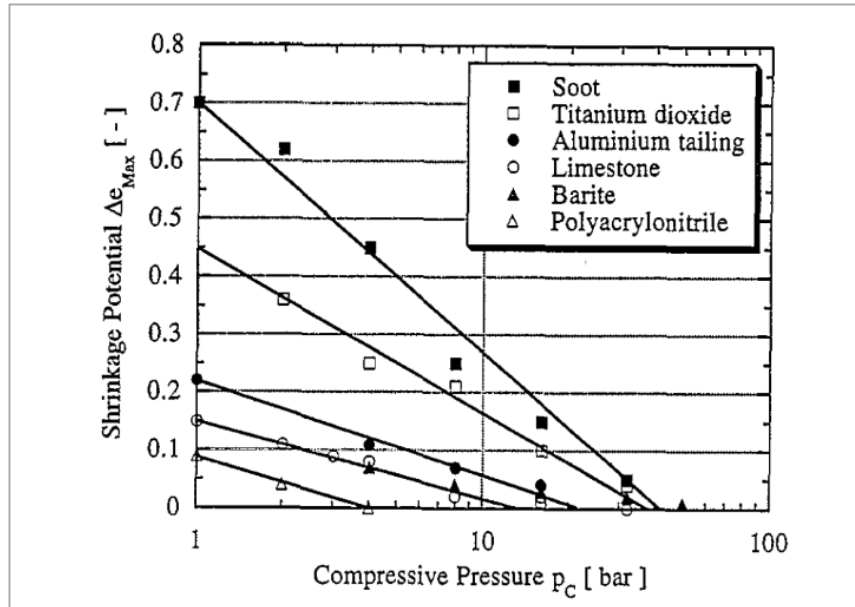


Figure 31. Comparison of the shrinkage behaviour of different organic and inorganic test products [5].

Anlauf et al. [16, 42] investigated that the appropriate choice in cake formation and dewatering conditions or the accurate dimension of the filter area influences the shrinkage crack formation and may prevent its formation. The tensile stresses between the particles caused by the displacement of liquid in the deliquoring phase can be partly

compensated by cake shrinkage. However, because of the cake/cloth interface, the movement of particles is restricted. The shrinkage degree of the filter cake is not the same in all directions. The two existing possibilities are demonstrated in Figure 32. The tensile stresses, which can be withstood before it cracks, increase with the increase of pre-stress caused by the filtration pressure difference. Thus, *Anlauf* concluded that the higher applied pressure, the lesser is the tendency for the cake to crack. There is a relationship between the filter cake height and filtration pressure difference. For each the amount of filtration pressure, there exists a maximal cake height independent of the filter area, where the pre-stress is enough to stabilize particle structure.

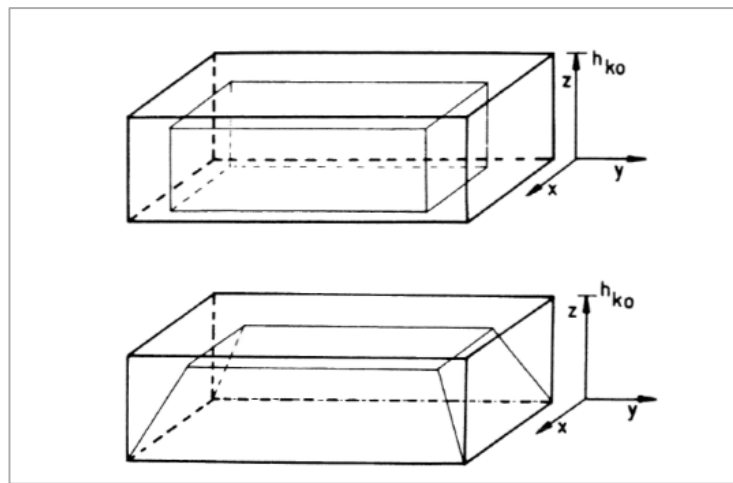


Figure 32. Confined and non-confined shrinkage of a filter cake [16, 42].

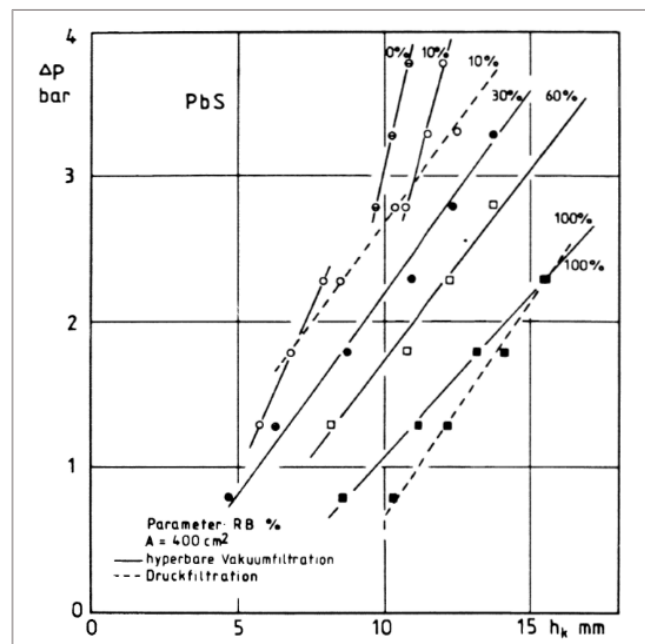


Figure 33. Cake cracking during pressure and hyperbaric vacuum filtration of PbS ore [42].



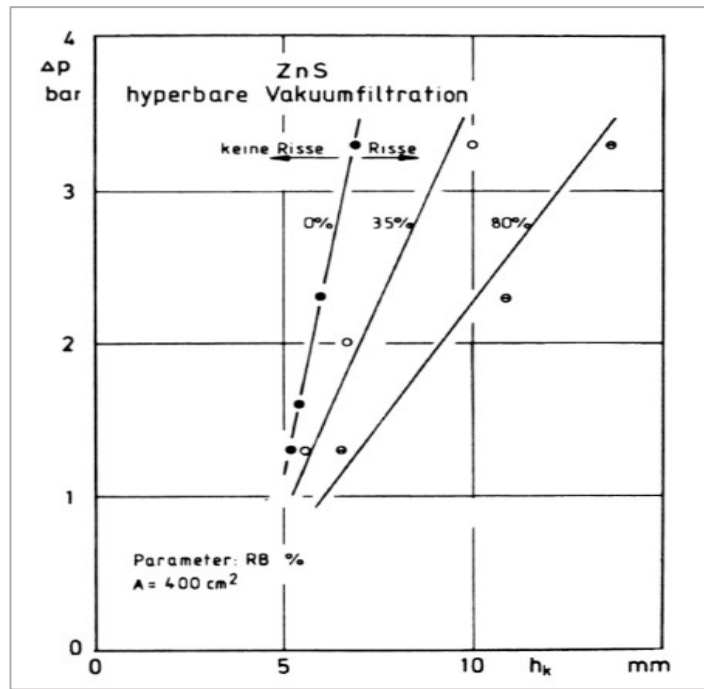


Figure 34. Cake cracking during pressure and hyperbaric vacuum filtration of ZnS ore [42].

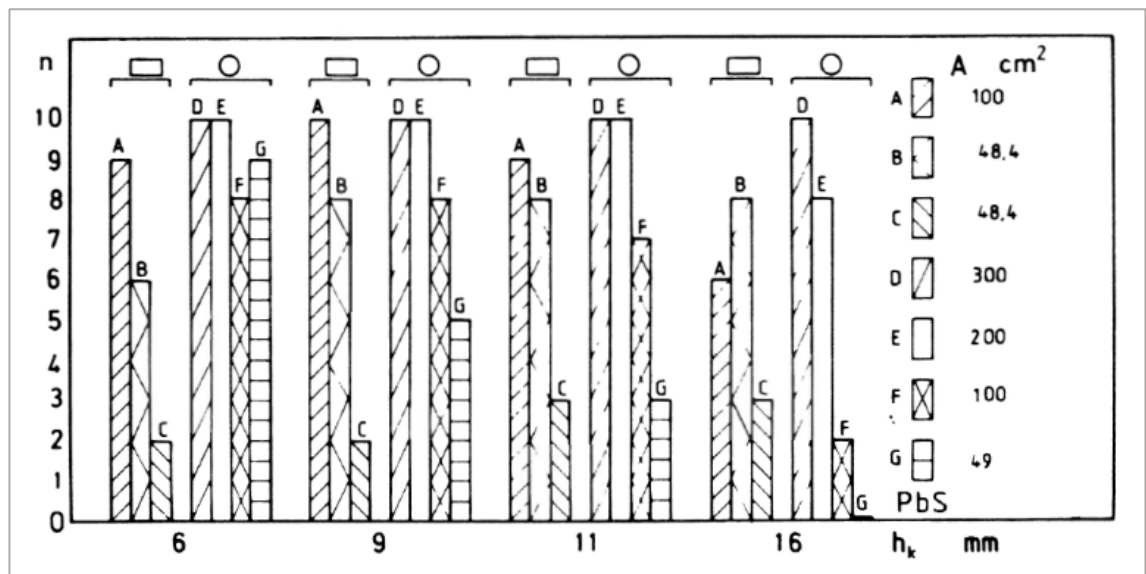


Figure 35. The probability of cake cracking in the difference of filter cake area and cake thickness for circular and rectangular filter plate [42].

Anlauf's experiments were conducted in circular and rectangular hand filter plates. For rectangular filter plates with  $A = 48.4 \text{ cm}^2$ , the probability of cracks rises slightly with higher cakes. The result was the same with the area of  $400 \text{ cm}^2$ , as can be shown in Figure 33 and Figure 34. Otherwise, two figures also show the combination of suitable filter cake height and pressure, which had 0 % of cracking formation probability.



For circular filter plates with  $A = 300 \text{ cm}^2$ , 100% cracking occurred for all cake height. While with  $A = 49 \text{ cm}^2$ , the experimental result shows a contrary tendency, the higher cake, the lesser cracking formation during dewatering, as shown in Figure 35 (G).

However, the effect of the height of filter cake on crack formation was conducted in a large area and low filter cake. It means the ratio between filter cake height and area ( $h/A$ ) is much smaller than 1. The result for cracking formation probability in  $h/A = 1$  or much higher than 1 need to research.

Wakeman mentioned the role of internal stresses in filter cake cracking in case of vacuum filtration[43]. There are three typical shapes of saturation distribution curves, as can be seen in Figure 36.

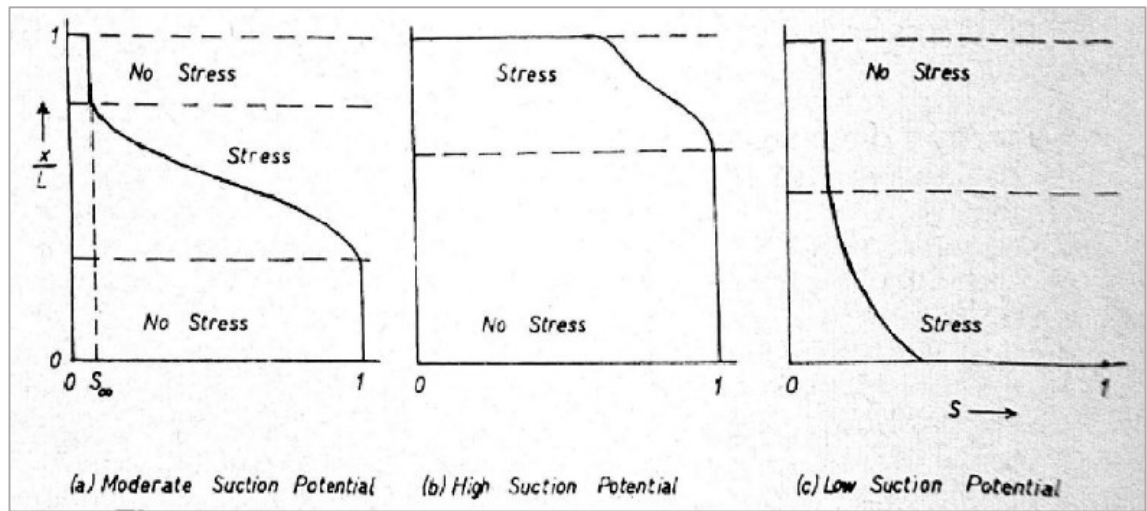


Figure 36. Illustration saturation distribution curves [43].

Schematic (a) on the left obtained by the drainage a cake with moderate suction potential. In the region near the cake surface, close filter cloth, the saturation is independent with its position on the filter cake. There is no dewatering in this region. The stress is focused on the central core of the cake, where saturation has a gradient. Schematic (b) in the middle shows the obtained from filter cake with high suction potential, where only the layer on top of the filter cake, close to the air inlet surface, withstand stress and draining the cake. A big part of the filter cake is at a constant saturation level. Schematic (c) on the right is typically for low suction potential cakes, which can be drained to almost their permanent residual saturation level. The stress for this situation can be found in the lower part of the filter cake, close the filter cloth. The cracking phenomenon is usually observed in high suction potential filter cake, where the

stress concentrated on the top surface, exposed to the gas, as can be seen in Figure 37. For the moderate suction potential cake, by increasing the desaturation force will prevent the cracking cake. The pressure drop is increased, and the stress boundary moves deeper into the cake. Greater deep at the surface becomes unstressed. Stress is indicated between the dashed line in Figure 38.

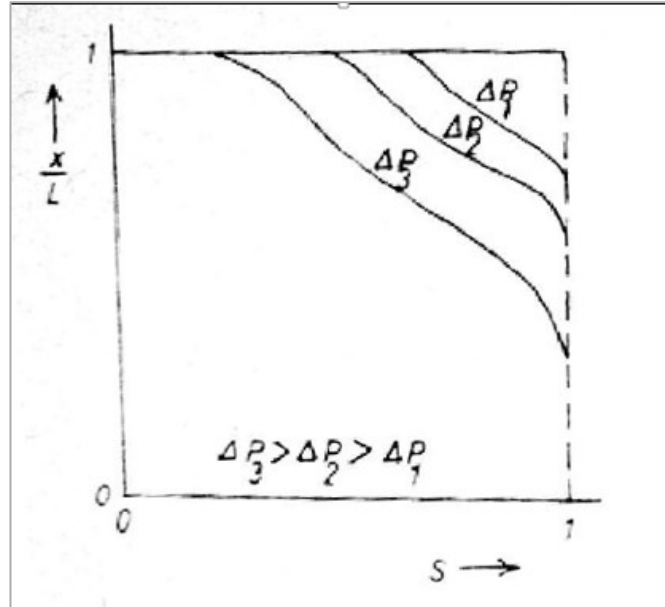


Figure 37. For high suction potential filter cake [43].

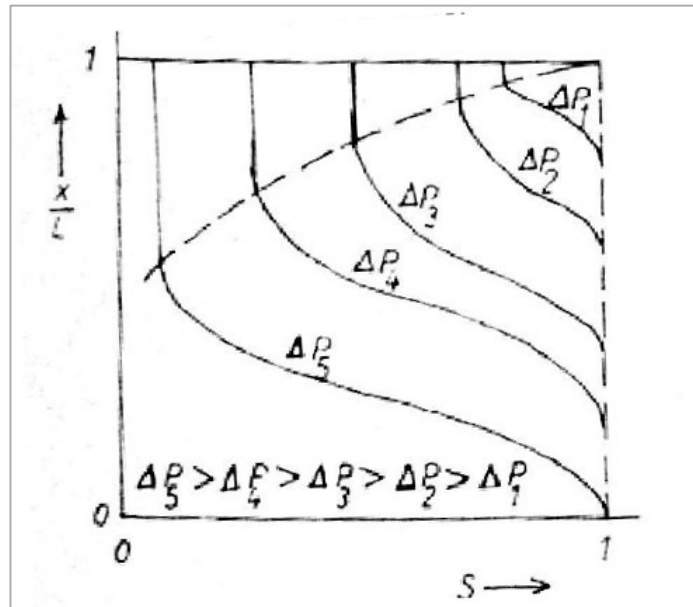


Figure 38. For moderate suction potential filter cake [43].

Rushton et al. mentioned some attention of researchers about the cake cracking in their book “Solid-liquid filtration and separation technology” [1]. Cake cracking may

occur in the rotary vacuum drum filter, in which case the effective vacuum pick up may be reduced. A list of methods is suggested to prevent the cracks. They are firstly the formation of filter cake from diluted feeds suspension rather than concentrated ones. Thus, in the formation of pre-coats from filter aid, 1 or 2 mm layers are usual, from feed slurry is 3 – 6 wt%. The secondary is the avoidance of the uncontrolled filter cake dewatering. The successive method is the formation of thin filter cake rather than thick filter cake; the deep of filter cake can be easily controlled by the speed of the rotary drum. Finally, cake cracking can be avoided when the precoat is formed under the lower vacuum rather than that used in the filtration process.

They also discussed the cracking are the results of the sudden change in porosity during the cake washing operation. Both cake porosity and specific resistance are strong functions of solids concentration. In the washing phase, there is no solid content input of the flowing liquor. This may lead to a change in the structure of filter cake. In some conditions, the difference in solids content leads to the change of structure filter cake. Further work suggested that filter cake cracking may be controlled by appreciating filter media, which are divided into sets of the small permeable zone. The filter cake is formed on those elements and spread out in honeycomb formation.

Barua, in his Doctor of philosophy (PhD) Thesis “Experimental study of filter cake cracking during deliquoring” [4] shows the detailed research about cracking formation. It can be considered as the most comprehensive study of filter cake cracking up to now. His investigation shows that the occurrence of cracking can be influenced and prevented through careful control of the critical input parameters. They are initial slurry concentration, settling time, filter cake aspect ratio, the number of fine particles, filtration pressure difference, surfactant addition, surface tension, and viscosity of suspending solvent. The study shows that cracking is the result of a specific repeatable mechanism. Trends of cracking can be seen, although some anomalies also have seen. The materials were high purity calcium carbonate ( $\text{CaCO}_3$ ) batch codes Superlon L15 & L200, produced from high purity carboniferous limestone. The L15 is fine material while the L200 is the wider particle size distribution, consist the coarse material. The mean particle size of the material is shown in Table 2. The L15 was used to mix with L200 at 20% increment in order to investigate particle size influence. The first result is the effect of the mass fraction of fines on filter cake craking. The trend can be observed by incremental the amount of lower  $15\mu\text{m}$  particles, the higher probability and degree of cracking. Two

kinds of prefiltration time are applied: no settling and full settling. No settling time is mean the suspension was filtered immediately in Nutsche. Meanwhile, the full settling is mean the suspension is charged in the Nutsche and left standing overnight before actual filtration is started.

Table 2. The mean particle size of batches of Calcium carbonate is used [4].

	L15 in $\mu\text{m}$	L200 in $\mu\text{m}$
Batch 2	6.38	27.76
Batch 3	6.12	15.55
Batch 4	5.77	12.97

From the result of experiments, concentration and settling time also play an important role in filter cracking. A higher concentration of initial suspension and a long settling time lead to greater probability and degree of cracking. Barua suggested the careful control of the segregation and flocs in filter cake may lead to the reduction trend of cracking formation.

The next test is the influence of the height of filter cake on crack formation. By changing the mass of the solid, the height of the filter cake increases. The investigated result shows that the filter cake thickness is also influenced to the cracking occurrence. The reason is mainly the wall side friction. This issue can be solved by increasing the filtration pressure difference. Thus, there are a maximum packing density and more significant tensile strengths on filter cake. Otherwise, a pre-deformation of flocs while still in the fully saturated state and reduction lateral shrinkage potential make the filter cake deliquoring without fissures [4].

Filtration temperature is affected to crack formation through the surface charge density, which affects flocculation tendency. Therefore, the room temperature produces the lowest zeta potential, which agglomeration most likely. The weak bond associated with flocs breaks lead to the collapse of the structure of the particles. The result is the formation of crack. The effect of temperature on cracking is non-linear but its change leads to the shift of agglomeration, one reason for cracking.

The utilization of solvent with a lower surface tension reduces the cracking probability, which reconciles with a reduction in capillary pressure. The solvent with higher surface tension can make a more significant capillary force, and the resulting stresses can lead to cracking. A solvent of increased viscosity in the formation of a liquid bridge that retains the viscous component. This issue may reduce, even prevent the crack formation. However, even the liquid bridge rupture, the solvent still stays on the particle surface, lead to the high residual moisture content. In the study of surfactant addition effect, the chemical was used anionic (sodium dodecyl sulfate, SDS); (ii) cationic (Cetyltrimethylammonium Bromide, CTAB); (iii) non-ionic (Polyoxyethylene sorbitan monooleate, Tween 80). Surface tension influence is mentioned again to reinforce the assertion of the reduction degree of cracking.

Barua had concluded that cracking is not a stochastic process, and its trend can be observed. He also found a newly defined parameter “permeability ratio”, which is the ratio between liquid permeability during cake formation and gas permeability during de-saturation, as seen in Equation (43). The term permeability ratio is an excellent relevance parameter to indicate the occurrence (or non-occurrence) filter cake cracking as well as estimate the degree of cracking.

$$\text{permeability ratio} = \frac{B_g}{B_l} \quad (43)$$

Where  $B_g$ ,  $B_l$  are the gas permeability and liquid permeability, respectively.

The liquid permeability was calculated from:

$$B_l = \frac{V_l \cdot l \cdot \mu_l}{\Delta p \cdot A} \quad (44)$$

Similarly, the gas permeability was calculated from:

$$B_g = \frac{V_g \cdot l \cdot \mu_g}{\Delta p \cdot A} \quad (45)$$

Where  $V_l$ ,  $V_g$  is the volumetric flow rate of liquid, gas;  $\mu_l$ ,  $\mu_g$  are the viscosity of liquid, gas;  $A$  is filtration area;  $\Delta p$  is a filtration pressure difference.

Barua concludes that determine the degree of cracking is difficult to elucidate because of the degree of branches and the fragmentary nature of the crack that form, but

it seems two parameters that dominate the extent. They are the maximum potential for outward lateral motion (lateral shrinkage potential) and the maximum collapsibility of the large flocs in a dispersion.

Base on the finding in Barua's research, he suggested some further research that should be focused. They are repulsive behavior between particles, the formation of skin at the filter medium when using high compressibility materials, using the difference of filter media, and especially the crack formation using other solid materials.

## 2.2. Summary and focus of research

Although the disadvantage phenomenon that occurs during the filtration process, the research about cracking is not enough. The mechanism of cracking is indistinctive, and it is considered as a stochastic phenomenon in some cases. Critical practical input parameters (directly influences, familiar parameters during solid-liquid filtration) as well as effectively countermeasure and avoidance cracking need to be studied more. By literature review, it can be summarised what has been published in the research of shrinkage cracking on filter cake, as can be seen in Table 3.

Table 3. Summarize influence elements from literature.

Parameters/ influence elements	Finding from publications
Particle size (including the number of fine particles)	<ul style="list-style-type: none"> <li>- Larger the particle size, the lower the shrinkage potential and the higher the minimum compressive difference [5].</li> <li>- The probability of crack formation as well as the degree of cracking increase by increment the fines fraction [4].</li> </ul>
Feed slurry concentration	<ul style="list-style-type: none"> <li>- Cracking occurs more at concentrated suspension [4]. The trend of cracking may be caused by the formation of the flocs in high solid volume concentration of the suspension.</li> <li>- In order to prevent the cracking, the formation of pre-coat from filter aid in diluted feeds rather than concentrated ones [1].</li> </ul>

Compressive pressure	<ul style="list-style-type: none"> <li>- Generally, the rising of applied pressure leads to lower crack probability. The reasons are: <ul style="list-style-type: none"> <li>+ higher packing density [4]</li> <li>+ pre-deformation flocs [4]</li> <li>+ lower shrinkage potential [5]</li> <li>+ increase the tensile strengths due to increase pre-stress during filtration[42].</li> </ul> </li> </ul>
Height and area of the filter cake.	<ul style="list-style-type: none"> <li>- Small and large rectangular are higher filter cake lead to higher cracks probability [42].</li> <li>- Large circular area, cracking occur at every surveyed filter cake deeps. In contrast, the small circular is, filter cake height increase leads to the reduction of cracking degrees [42].</li> <li>- With the area of filter cake stable in 20 cm<sup>2</sup>, the increased height of filter cake leads to a high degree of cracking (the reason is the wall friction effect) [4].</li> </ul>
Filtration temperature	<ul style="list-style-type: none"> <li>- High temperatures lead to lower surface tension. Resulting in lower shrinkage potential [5].</li> <li>- High temperatures can be produced by another energy source such as saturated or superheated steam [5].</li> <li>- Temperature affects the zeta potential, which decided the particle agglomeration. Without flocs connecting with the particles system, there is no collapsing at the weak bond of filter cake [4].</li> </ul>
Internal stress	<ul style="list-style-type: none"> <li>- Cracking likely occurs at high suction potential filter cake, where the stresses focus on the surface of filter cake, exposed to the gas. Moderate and low suction potential filter cake experimented the dewatering without crack due to stress concentrated in the middle and bottom of the filter cake, respectively [43].</li> </ul>
Solvent, viscosity, and surfactant addition.	<ul style="list-style-type: none"> <li>- Both three parameters related to the surface tension, which lower surface tension or higher viscosity, can avoid the crack [4].</li> </ul>

Settling time	<ul style="list-style-type: none"> <li>- The higher settling time, the greater the possibility of crack formation and degree of crack [4]. This issue related to the degree of the fine particle on top of the filter cake. The formation of the fine layer leads to the higher capillary pressure entry as well as more shrinkage cracking.</li> </ul>
---------------	---

From some literature, there are some ideas about the critical input parameters, which are “familiar” and directly affect to crack formation is suggested.

The first one is the temperature of the filtration process. Temperature can be created from another energy source. One of the ways is using steam pressure filtration. This method is the combination of pressure filtration and thermal (is produced by steam and superheated steam). This process can avoid cracking formation by its mechanism, and the likely reduce surface tension, which affects tensile stress on filter cake.

The secondary is the effect of particle size on crack formation. Materials have a similar particle shape and particle size distribution (same span  $(x_{90} - x_{10})/x_{50}$  ) but having a distinct difference particle size (even very fines and very coarse materials). The cack formation leads to the knowledge about the internal stress effect on various sizes of the material.

The next input parameter is a solid volume concentration of suspension. Tests with various concentration of suspension are conducted in lower pressure difference to see the sedimentation effect on shrinkage cracking during filtration as well as the change of tensile stresses.

A pressure difference is one of the operating parameters by the filtration, and the dewatering step can be controlled. According to the literature, the change in the amount of applied pressure, the cracking can be avoided. In this research limitation, the compression air is used during the filtration process as well as the countermeasure to shrinkage cracking.

Finally, the height of the filter cake is also an interesting parameter, which can be used to scale-up. While Anlauf [42] mentioned the effect of filter cake height on cracking formation with the ratio  $h/A$  much smaller than 1, Barua, in his test, focus on the impact with the ratio more significant than 1. The filter area is  $0.002 \text{ m}^2$  while the solid weight is up to 100 grams limestone, leading to a rather "high" filter cake. For any aspect ratio



higher than 1 assumes a very small filter area, the result in a side effect is inevitable. The tests for the aspect ratio around 1 are conducted to see the trend of cracking.

The result for cracking was recorded in many ways, such as “cracking”, “no cracking,” or the probability of cracks. Barua also suggested the permeability ratio, which compares gas permeability after air breakthrough at the filter medium (when equilibrium is reached) and liquid permeability immediately before air breakthrough. Through his research, this newly defined parameter is an excellent indicator of the occurrence and estimates the degree of cracking[4].

Due to the research in the narrow range of a disadvantage phenomenon during filtration, the overlap of working is evitable. When a different result occurs, it will be explained. Base on interpretation, those would be new theories or mechanisms. In order to recognize the occurrence as well as to quantify the degree of cracks, the term permeability ratio is used as a relevance parameter. However, the approach is different and could be explained in the next part.

The most outstanding in this research is, researching the effect of some critical input parameters on crack formation using conventional filtration and steam pressure filtration. The material for preliminary-testing is limestone; after that, Vietnam coal (coal sampling is carried out at Cuaong Coal Washing Plant) is used as another material. By comparing two kinds of materials, there would be an insight into the mechanism of shrinkage cracking and its impact on dewatering.

The objective of this research is to continue contributing to the understanding of the cracking mechanism, offering the new method to avoid shrinkage cracking as well as improve dewatering efficiency, especially for Vietnam coal after processing.

### 3. Material, methods and the result of capillary pressure curve and tensile stress versus saturation

#### 3.1. Material used

##### 3.1.1. Limestone

Two kinds of materials (KS12 and KS100) with the same density of  $2710 \text{ kg/m}^3$ , median particle size  $x_{50,3}$  of  $2.46 \text{ }\mu\text{m}$ , and  $20.68 \text{ }\mu\text{m}$  respectively were used. The particle size distribution of materials have span  $(x_{90}-x_{10})/x_{50}$  of 2.98 for KS12 and of 3.88 for KS100 and is shown in Figure 39.

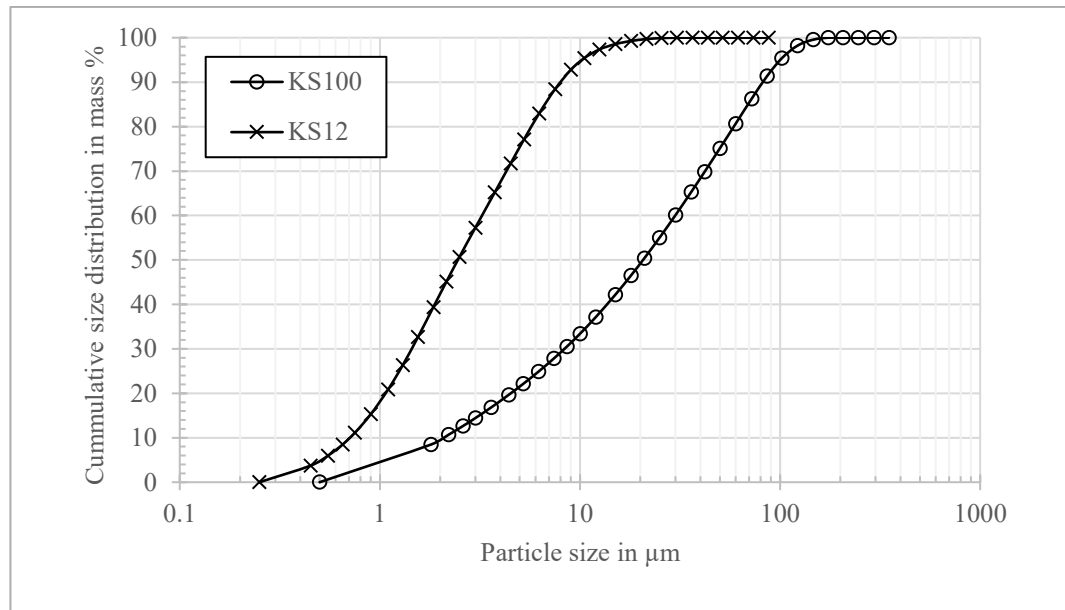
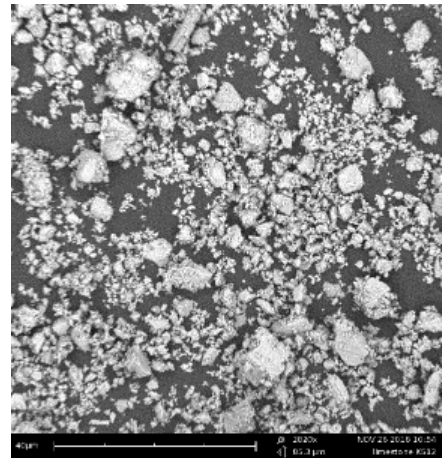
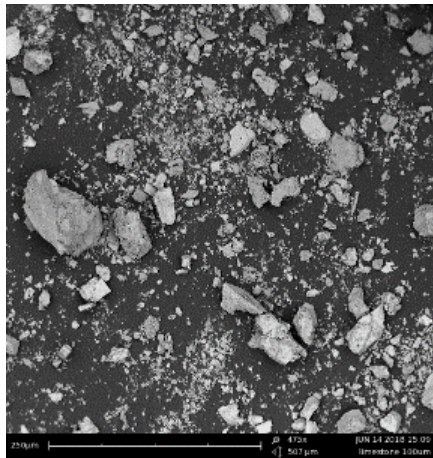


Figure 39. The particle size distribution of KS12 and KS100.



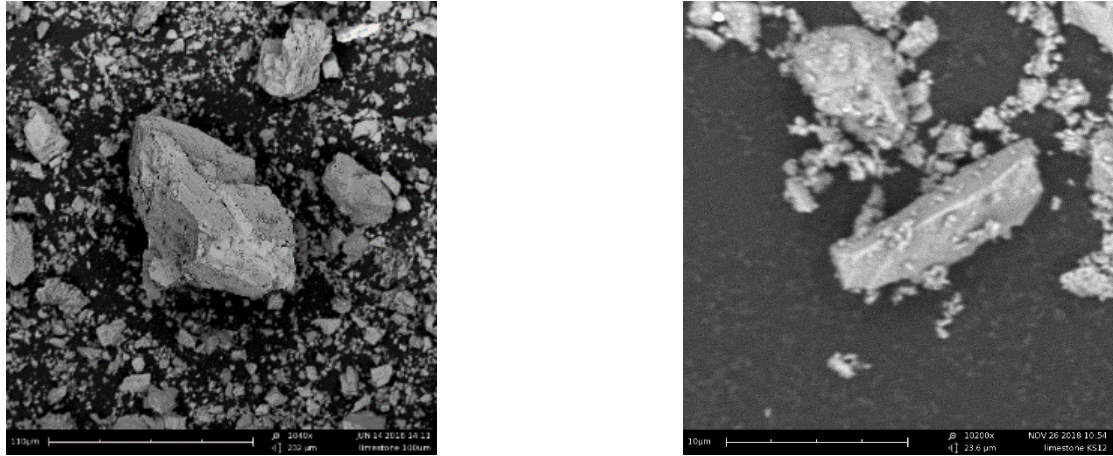


Figure 40. SEM pictures for KS100 (left) and KS12 (right).

The proportion of particles below 10  $\mu\text{m}$  of KS12 and KS100 is significantly different, with 94.51% and 33.39%, respectively. Scanning electron microscope (SEM) images, as can be seen in Figure 40, demonstrate irregular – shaped of both coarse and fine materials.

For all experiments, the solid was dispersed in deionized water and stirred to guarantee a maximum of slurry homogeneity and particle dispersion. The temperature of suspension is the room temperature (approximately 20 degrees Celsius) for all tests. In some exceptional cases, to avoid particle agglomeration in storage, ultrasonic was used to keep particles dispersion on feed slurry. The sample size to be prepared is 50 grams, which is corresponded to 18 mm of filter cake height for experiments on the effect of solid volume fraction, particle size, and applied pressure difference. The amount of distilled water changed depend on various volume concentrations (0.05 to 0.4). The gas pressure difference for filtration experiments (in case of test on the influence of volume fraction, filter cake height and particle size) are “1-1 bar” (1 bar for cake formation – 1 bar for mechanical displacement phase), “1-3 bar” (1 bar for cake formation – 3 bar for mechanical displacement phase) and “3-3 bar” (3 bar for cake formation – 3 bar for mechanical displacement phase). For all tests, polypropylene filter cloth with the satin weave pattern and pore size of 6  $\mu\text{m}$  (05-1010-SK 006, Sefar AG, Heiden, Switzerland) was used. These filter media has an air permeability of 18  $\text{m}^3/\text{m}^2/\text{h}$  at 20 mm water column.

### 3.1.2. Vietnam Coal

In order to get the link to a commercial relevant application in the case of Vietnam, fine coal slurry comes from the Cua Ong Coal Washing plant before the thickening was chosen as one of the material. This material is collected from feed suspension before thickening and drying afterward. Suspension for all test laboratory is coal powder, which was collected from Vietnam, and distilled water to re-slurry. Coal is insoluble in the water at all temperatures. Anthracite is not explosive; the amount of sulfur (S) content and the amount of volatile matter are small. The burning temperature is 350 - 400°C. In the outdoor temperature, under the sunlight, coal can not burn on its own. The amount of clay in fines coal is small, around 0.5 – 1%. The speed of sedimentation of almost particles as well as the sedimentation curve, are illustrated in Table 4 and Figure 41.

Table 4. Sedimentation of coal corresponding to the concentration of the suspension.

The solid volume concentration of suspension in %	5	10	15	20	25	30	35	40
Sedimentation rate (m/h)	0.1860	0.1062	0.0542	0.0360	0.0254	0.0067	0.0056	0.0052

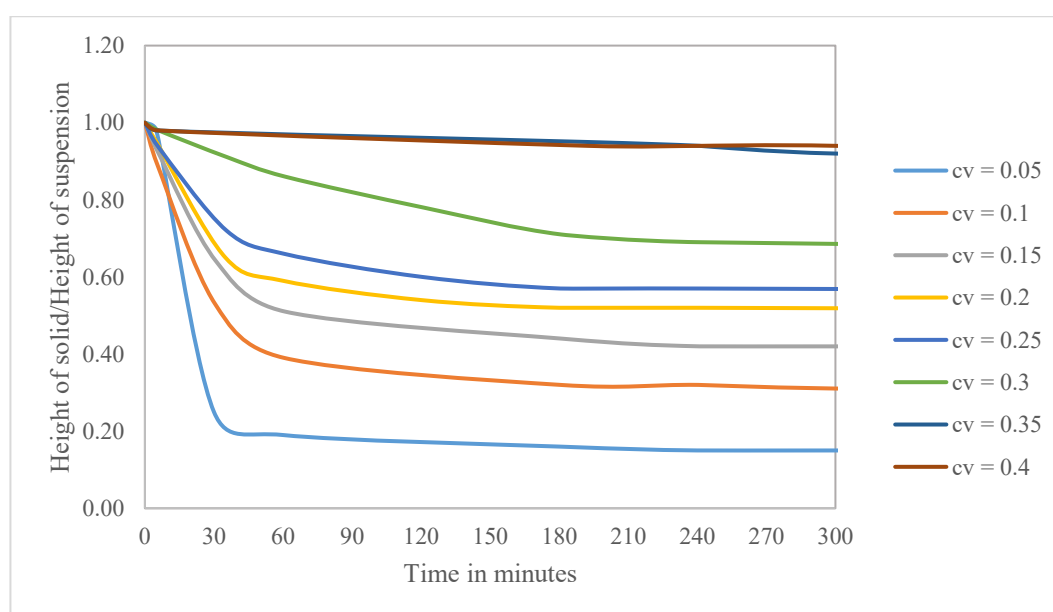


Figure 41. The sedimentation curve of coal in different solid volume concentration of the suspension (cv).

The density of coal is typically around 1400 –1550 kg/m<sup>3</sup>. This value can be changed to 1250 kg/m<sup>3</sup> and 1200 kg/m<sup>3</sup> in the moisture content of 20% and 40 - 50%,

respectively. The coal sample using for research is low-quality coal with the ash content around 35%, and the density (dry state) is measured 1497 kg/m<sup>3</sup>. The measured density in the laboratory is used for all calculations in this research. The particle size distribution of coal powder is shown in Table 5 and Figure 42.

Table 5. Coal particles properties.

$x_{10}$ in $\mu\text{m}$	$x_{16}$ in $\mu\text{m}$	$x_{50}$ in $\mu\text{m}$	$x_{80}$ in $\mu\text{m}$	$x_{90}$ in $\mu\text{m}$	$x_{97}$ in $\mu\text{m}$
2.03	2.94	11.78	62.85	119.84	210.52

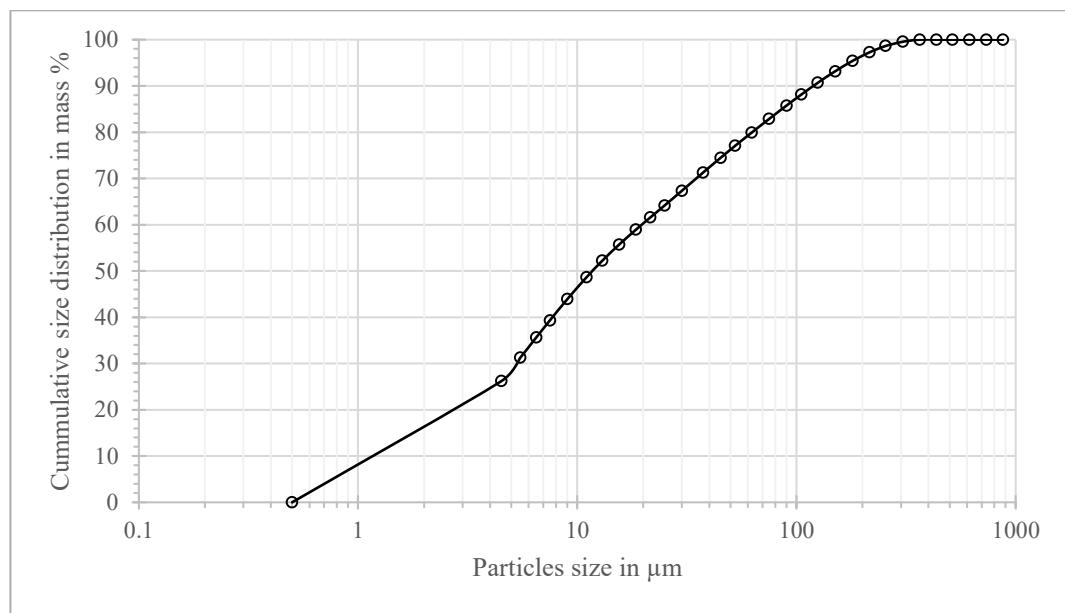


Figure 42. The particle size distribution of fine coal.

The result is defined by laser diffraction equipment. The median particle size  $x_{50,3}$  is 11.78  $\mu\text{m}$ , which is higher than that of fine limestone KS12 and lower than that of coarse limestone KS100. The particle size distribution of materials has span  $(x_{90}-x_{10})/x_{50}$  of 10. This value is higher than those of both kinds of limestone. The coal sample shows a broader distribution. The below 10  $\mu\text{m}$  particle size account for 45 % and 90% of particles is below 0.125 mm. This amount of very fine particles in coal samples are significant. This issue may lead to the crack formation and negative efficiency of dewatering.

By the SEM technique, the images for the irregular-shape of big coal particles and the flake –shape for fine and ultra-fine particles also show in Figure 43.

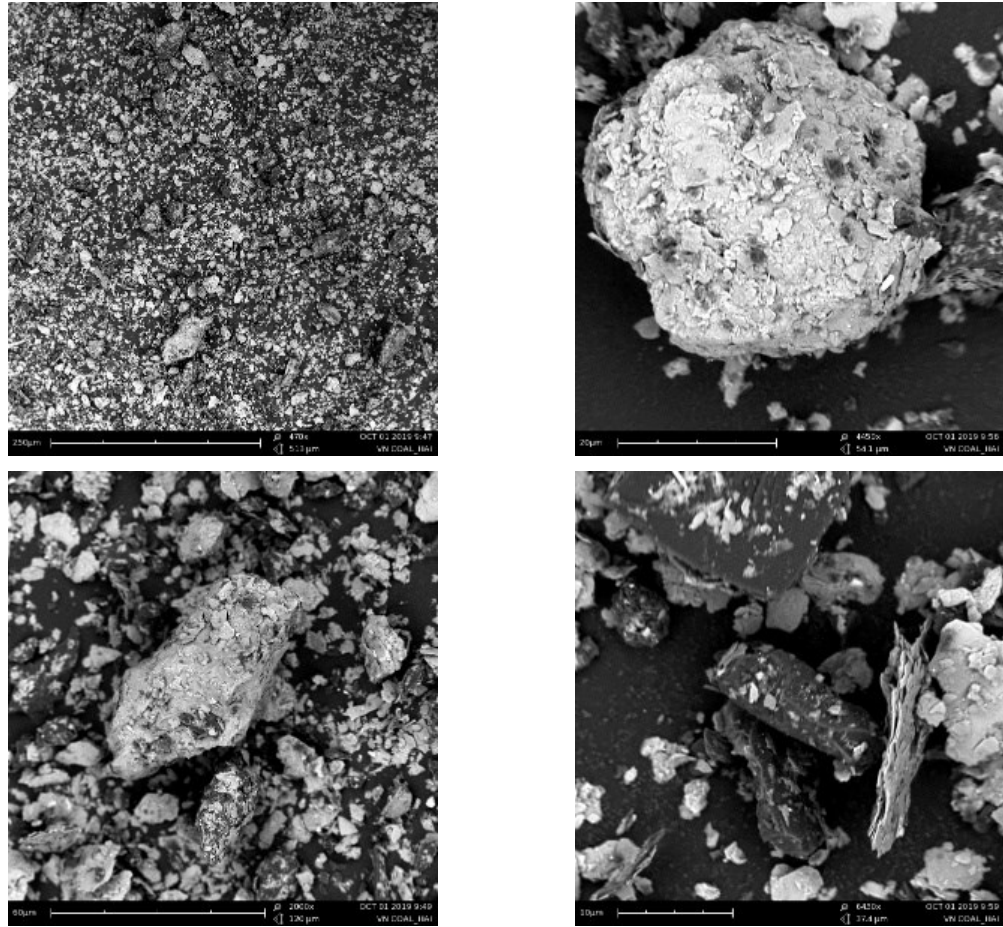


Figure 43. SEM images for coal particles.

Tests procedure with coal is similar to the procedure with limestone, as mentioned above. Only the difference related to the mass of the solid is that it altered down to 30 grams, equivalent approximately 15 mm of filter cake height.

### 3.2. Conventional filtration rig and steam pressure filtration rig

#### 3.2.1. Conventional filtration rig

The filtration rig is built according to VDI 2762-2 [18]. Gas-driven filtration experiments were conducted in a stainless steel pressure filter Nutsche with an area of  $19.64 \text{ cm}^2$ , as shown in Figure 44 and Figure 45. The filter medium has support from a perforated medium sheet with a large open cross-section area. There is a cake formation unit connected Nutsche long tube and filter medium support unit. By disassemble this unit, the filter cake can remove easily. Otherwise, the device possesses a quick connection for the lid and be equipped with the valve to regulate the pressure and with a pressure gauge. The lid has a sight glass to look inside and attached light. The quantity of filtrate is measured by using a scale connected to a computer [18]. At the end of the filtration



process, when there is no water flow through the filter cake, a plastic tube was used to connect between Nutsche and Rotameter to measure the air volume flow rate.



Figure 44. Images for the Nutsche apparatus (according to VDI 2762-2) [18].

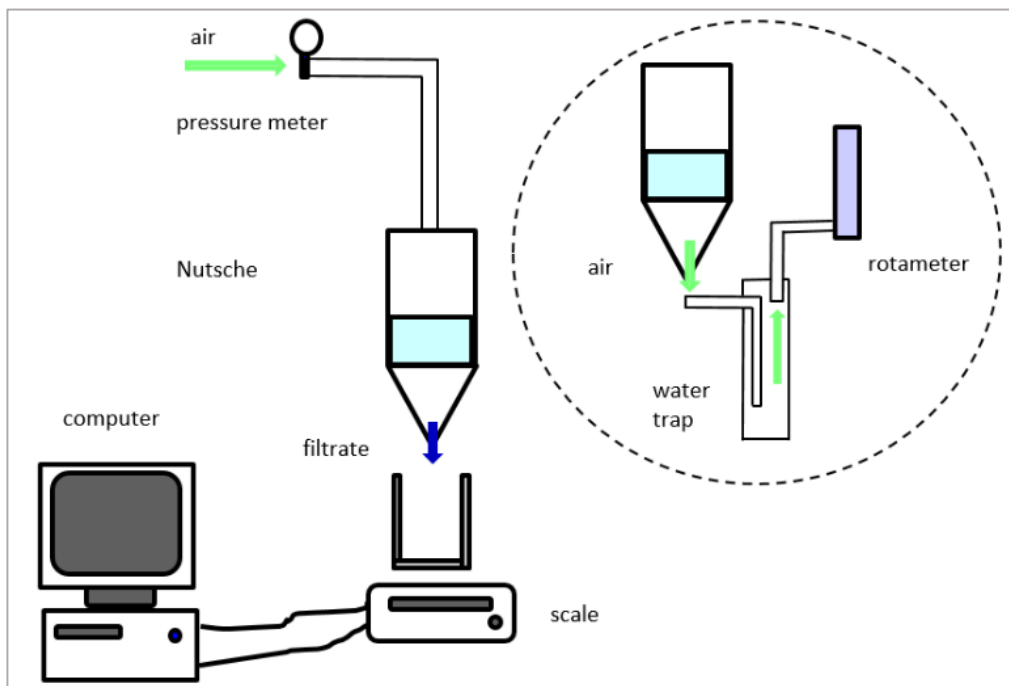


Figure 45. Schematic diagram of the experimental setup.

### 3.2.2. Steam pressure filtration rig

The steam pressure filtration rig (Figure 47) was built based on the standard Nutsche with the totally same length tube and cake formation unit, which has been described above [18]. The different things are the compressed air and compressed saturated steam from steam source to supply to Nutsche.

The steam is provided by the evaporator. This steam and the entrained water from the evaporator are separated. The steam can be a little superheated if the temperature of pipes is higher than the steam temperature.

The tube, the cake formation unit and almost pipes are covered by Styrofoam to avoid the heat transfer into the ambient environment. Nutsche and cake formation unit are heated by an oil heater to approximately 160° Celcius. There is a thermocouple that is installed to control and maintain the temperature stable. Four thermocouples are remaining in the cake formation unit, which is built to measure each layer temperature profile of filter cake during filtration. The thermocouple contact with the cake formation unit to measure the filter medium's temperature and filtrate's temperature[13].

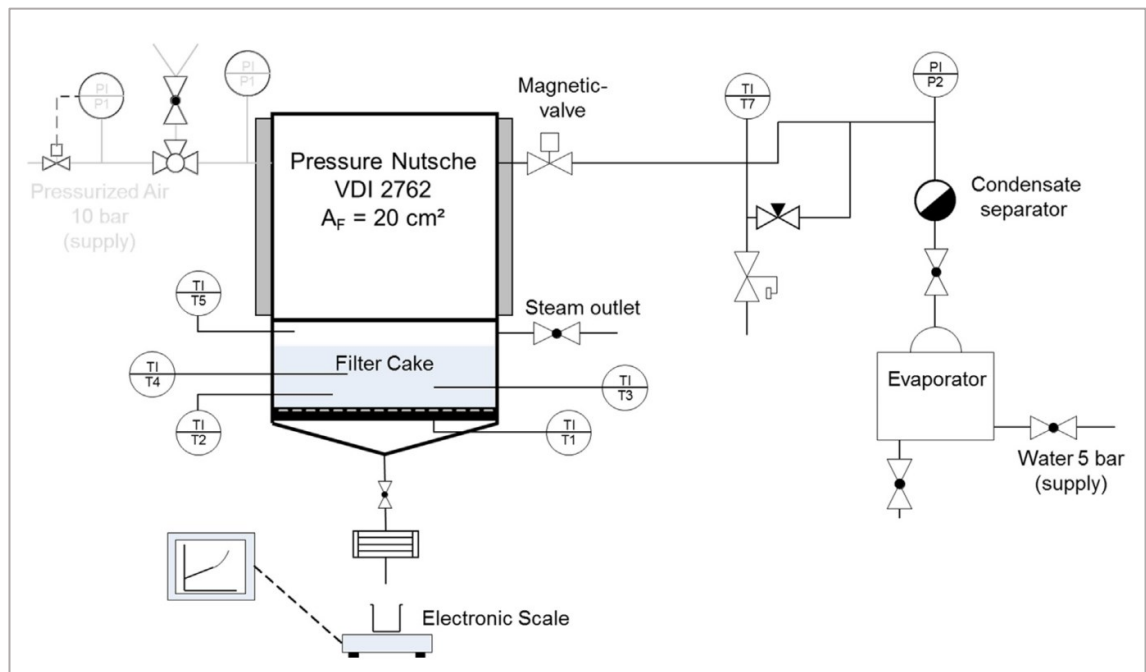


Figure 46. Diagram of steam pressure filtration according to VDI 2762/2, [12, 13, 18].





Figure 47. Steam pressure filtration apparatus [12, 13].

### 3.3. Filtration experimental

The preparation of the feed suspensions was conducted as follows: solid is dispersed in the amount of distilled water at the room temperature (approximately 20°C) and is stirred until well mixed. The amount of water depends on the mass of the solid and the amount of solid volume fraction for tests. After that, the slurry is poured in the Nutsche, and the top cover is closed. In the investigation of crack formation during filtration, there are two stages. The first stage is the cake formation. The compressed air is applied. The filtrate flows through, and particles also are built on filter cloth (SK 006). This step will be finished when the saturation of filter cake reaches to 1. It is observed through the light glass until no water surface on the filter cake. As soon as the saturation reaches 1, the air is vented. The filtrate mass was recorded by the electronic scale during filtration. The collected filtrate is recorded by Diadem software. This result is used to calculate specific resistance cake (according to VDI 2762-2) and liquid permeability before breaking through the filter medium of air.

The second stage is the mechanical displacement phase. Depend on the kind of filtration, the compressed air or the saturated steam is applied.

For conventional pressure filtration, compressed air, which is regulated by valve and pressure gauge, is applied to push water flow out from pores. When there was no water flow through the filter cake, the Rotameter was connected to Nutsche to measure the air volume flow rate during deliquoring with or without cracking. The air volume flow rate, which is measured by Rotameter, is used for calculating the air permeability.

For steam pressure filtration, the steam outlet and magnetite valve are opened to allow the steam entering the Nutsche. After the instant time (1 or 2 seconds), the steam outlet is closed, steam starts to displace water from the pores. Tests were conducted until the steam break through the filter cake, which is observed as well as by the temperature of the filter cloth thermocouple. In order to prevent the cracking, which may be caused by the thermocouples, the only thermocouple (TC3) under the filter cloth is used. Then, the condenser unit is connected to collect the amount of steam breakthrough under the liquid form. The balance scale is used for measuring the amount of condensation water to the time. From that to calculate the volume steam flowrate and the steam permeability. After recording the mass of condensed steam, the steam flux is stopped by closing the magnetic valve. The Nutsche is then to vented slowly in order to avoid the filter cake broken. The destruction of filter cake can occur when the venting is open fast. The temperature of the remaining liquid is still higher than the boiling temperature of ambient pressure. The liquid inside can be forced to evaporate and break the filter cake. Otherwise, slowly venting can avoid the evaporation of water, which is the main error for the wrong moisture content of filter cake after deliquoring.

The filter cake then is taken photos to observe the shrinkage cracking. Finally, it quickly removes out of the cake formation unit to dry.

After removing, the filter cake is dried at 50°C ( $\pm 5^\circ\text{C}$ ) until the constant weigh. By measuring the height of filter cake as well as the mass of wet and dry filter cake, saturation, which is the relation between the pore volume occupied by liquid and total pore volume of the filter cake, is calculated.

### 3.4. Relevant parameter

The pressure difference is to keep constant during the cake formation and dewatering phase. By measuring filter cake height as well as the mass of filter cake before

and after drying, *saturation*, which is the relation between the pore volume occupied by liquid and total pore volume of the filter cake, is calculated according to Equation 27. Otherwise, the amount of water remaining in filter cake is also expressed by the *residual moisture content* in mass % (which is denoted M). This parameter is defined:

$$M = \frac{\text{the mass of wet filter cake} - \text{the mass of dry filter cake}}{\text{the mass of wet filter cake}} \cdot 100\% \quad (46)$$

The applied pressure difference in the dewatering process must be large enough to overcome the entry capillary pressure of the filter cake. Shortly after the cake formation phase, the cake splits into a number of the fragment, and the numerous cracks propagate from cake surface into the cake itself. Cake cracking means that the gas flow rate necessary for sustaining the dewatering pressure difference rises considerably due to the increase of free flow area in the filter cake [42]. Accordingly, permeability for gas will increase significantly when the crack occurs compare with permeability for liquid during the cake formation phase. The permeability ratio is applied to quantify the number of cracks and the degree of cracks. This term is the ratio of liquid permeability in cake formation phase and air permeability after filtration and is indicated by  $\beta^*$  symbol.

$$\text{Permeability ratio } \beta_{CPF}^* = \frac{\text{gas permeability}}{\text{liquid permeability}} = \frac{K_G}{K_L} \quad (47)$$

This equation is used in the case of conventional pressure filtration, and it can be written again for steam pressure filtration.

$$\text{Permeability ratio } \beta_{SPF}^* = \frac{\text{steam permeability}}{\text{liquid permeability}} = \frac{K_{ST}}{K_L} \quad (48)$$

#### *Liquid permeability $K_L$*

From Darcy equation for incompressible flow in laminar regime, liquid permeability ( $K_L$ ) is reciprocal of specific filter resistance cake, which is mentioned and calculated according to VDI 2762-2 [18].

$$K_L = \frac{1}{r_c} \quad (49)$$

Tests for crack formation on filter cake were done in Nutsche. During filtration, the filtrate was collected and shown in the diagram “t/V versus V” Figure 6. The specific

resistance filter cake was then calculated from pressure difference  $\Delta p$ , filter cake area  $A$ , dynamic viscosity  $\mu_L$ , the slope of interpolating straight line ( $t/V$  versus  $V$ ) diagram.

$$r_c = \frac{a \cdot 2 \cdot \Delta p \cdot A^2}{\mu_L \cdot \kappa} \quad (50)$$

Where  $A$  is filter area ( $0.001964 \text{ m}^2$ );  $\Delta p$  is pressure difference; coefficient  $\kappa$  was calculated from porosity and volume fraction as can be seen in Equation (25).

The value of liquid viscosity is the strong function of temperature. For the conventional pressure filtration, the temperature for cake formation as well as deliquoring is room temperature (approximately  $20^\circ\text{C}$ ). In the case of steam pressure filtration, in order to reduce the condensation phenomenon on the top of filter cake in the deliquoring stage, Nutsche, cake formation unit are heated up to more than  $100^\circ\text{C}$ . This issue affects the temperature of filter cake during filtration. Therefore, depending on the value of temperature (which is collected by a thermocouple), the viscosity of a liquid can be changed according to Table 6.

Table 6. The viscosity of water corresponding to the temperature.

Source: [https://www.engineersedge.com/physics/water\\_\\_density\\_viscosity\\_specific\\_weight\\_13146.htm](https://www.engineersedge.com/physics/water__density_viscosity_specific_weight_13146.htm)

Temperature ( $^\circ\text{C}$ )	Viscosity (mPa.s)
10	1.308
20	1.002
30	0.7978
40	0.6531
50	0.5471
60	0.4658
70	0.4044
80	0.3550
90	0.3150
100	0.2822

#### *Gas permeability $K_G$*

On the other hand, Wyckoff et al. [44] also show Darcy equation for compressible flow in the laminar regime, where square pressure drop,  $dp^2/dx$ , is constant along the flow

channel rather than  $dp/dx$  itself. Hence gas permeability is computed from the laboratory measurements in the following equation:

$$K_{G \text{ measurement}} = \frac{2 \cdot p_2 \cdot \dot{V} \cdot \mu_G \cdot L}{A \cdot (p_1^2 - p_2^2)} \quad (51)$$

Where  $\dot{V}$  is the air volume flow rate;  $\mu_G$  is the viscosity of gas;  $L$  is the height of filter cake;  $p_1$ ,  $p_2$  are the input and output air pressure.

For two immiscible fluids flow through a porous medium, when the filter cake approach to irreducible wetting fluid saturation, gas flow through the filter cake. Applied pressure difference during the filtration phase and deliquoring phase is kept constant. Liquid and airflow simultaneously through porous media. Therefore, air permeability ( $K_G$ ) is calculated from air relative permeability ( $K_{GrI}$ ) and air permeability measurement ( $K_{G \text{ measurement}}$ ):

$$K_G = \frac{K_{G \text{ measurement}}}{K_{GrI}} \quad (52)$$

Where the relative permeability  $K_{GrI}$  is calculated according to Equation (34):

$$K_{GrI} = (1 - S_R)^2 (1 - S_R^{(2+\lambda)/\lambda})$$

$\lambda$  is a value, depending on the size range of the particle in the distribution is suggested 5 to be reasonable value for practical purposes.  $S_R$  is average reduced saturation and is defined as [22]:

$$S_R = \frac{S - S_\infty}{1 - S_\infty} \quad (53)$$

According to Wakeman, the term of irreducible saturation of pressure deliquored cake,  $S_\infty$ , has been correlated as:

$$S_\infty = 0,155 \cdot (1 + 0,031 \cdot N_{cap}^{-0,49}) \quad (54)$$

It can be seen that the value of irreducible saturation is also a function of capillary number  $N_{cap}$ . This value expresses the ratio of the dewatering force to the surface tension force retaining fluid in the cake, which is defined by:

$$N_{cap} = \frac{\varepsilon^3 \cdot x^2 \cdot (\rho_l \cdot g \cdot L + \Delta p)}{(1 - \varepsilon)^2 \cdot L \cdot \sigma} \quad (55)$$

Gas permeability, according to Equation (52), is used for dewatering without cracks and micro-shrinkage cracking.

When the macro-cracks occur, the airflow preferentially through big channels of filter cake without liquid leads to the significantly increasing air volume flowing rate. In this situation, absolute air permeability ( $K_{G \text{ measurement}}$ ) is suggested.

### Steam permeability $K_{ST}$

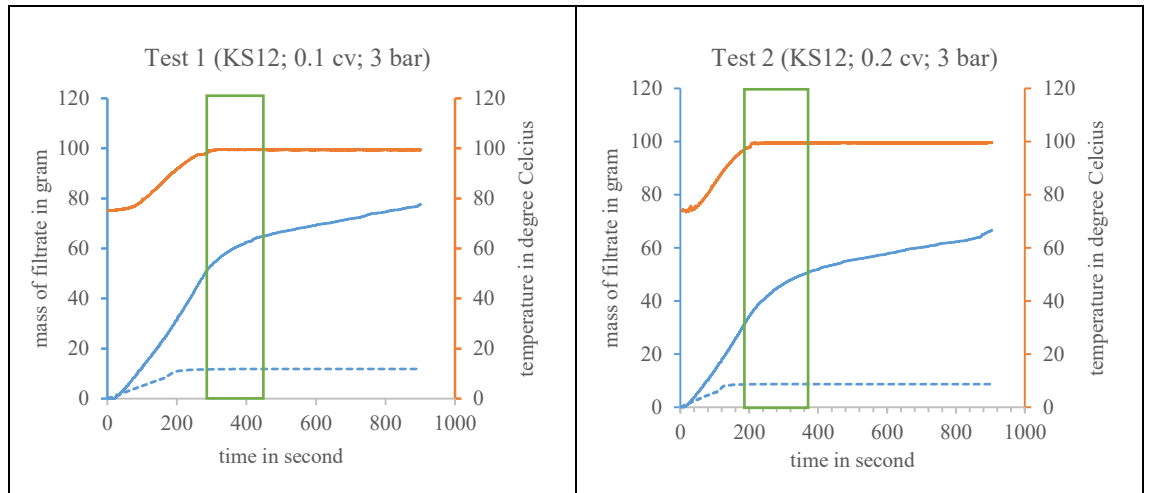
Similarly the gas permeability, steam permeability is defined as the following:

$$K_{ST} = \frac{2 \cdot p_2 \cdot \dot{V}_{ST} \cdot \mu_{ST} \cdot L}{A \cdot (p_1^2 - p_2^2)} \quad (56)$$

Where  $\mu_{ST}$  is the viscosity of steam;  $\dot{V}_{ST}$  is the steam volume flow rate.

The steam volume flow rate is calculated by the measure of the mass of condensate water ( $m_{cw}$ ) in a unit of time and is shown in the equation:

$$\dot{V}_{ST} = \frac{m_{cw}}{t \cdot \rho_{ST}} \quad (57)$$



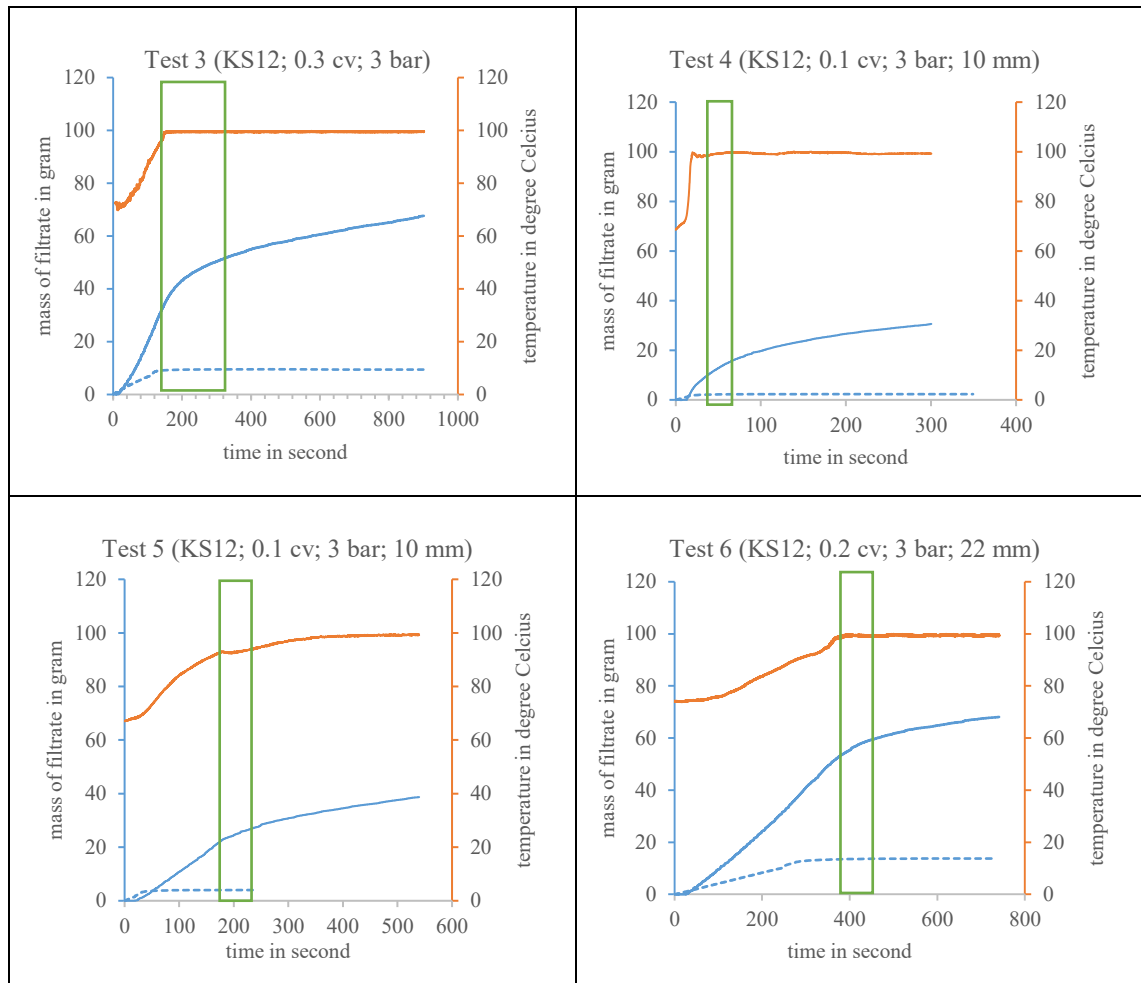


Figure 48. The mass of filtrate from the moment the gas breaking through for SPF (blue line) and CPF (blue dash line) and the temperature profile of filter cloth when using SPF (orange line).

One of the notes when measuring the mass of condensate water is the measuring time. Some tests with limestone have been shown that there is a transition area (green area) between the mechanical displacement phase (which finishes at the moment of steam beginning breakthrough) and steam breakthrough totally through the filter cake. Figure 48 indicated this area when using the steam pressure filtration.

This transition time has occurred during the steam pressure filtration, not in conventional filtration. The reason is that the displacement front needs more time to flow out of the filter cake. In the transition area, there is not only condensed water but also water from the front. A measurement for the water mass flow rate leads to incorrect steam permeability. Therefore, the mass of condensed water from steam should be measure after a period of transition. For almost cases, it would be suggested that the steam volume flow

rate should measure after steam breakthrough a period, for example, 200 seconds in the case of KS12.

### 3.5. Analyze technique

Besides the output parameter above, the analysis of samples also supports the intensive understanding of the core characteristic of the filter cake. The analytical techniques and the equipment used are described in detail.

The laser diffraction is used to analyze the particle size properties. This method relies on the theory that the light passing through the suspension, the diffraction angle is inversely proportional to the particle size. They include the laser source with a suitable wavelength (typically 0.63  $\mu\text{m}$ ) and the suitable detector (usually is the slice of photosensitive with the number of discrete detectors. Relating the diffraction angle with particle size, Mie theory is used for the interaction of light with matter. It allows particle size in the range 0.1 – 2000  $\mu\text{m}$ , provided that the refractive indices of the particle material and suspending medium are known. This method gives a volume distribution and a diameter known as the laser diameter. The associated software permits displaying a variety of size distributions and means derived from the original measured distribution [29]. This technique shows the particle size distribution as well as the frequency distribution, useful for interpretation particle size effect on test results.

The Scanning electron microscope (SEM) is a kind of electron microscope that produces the image of the sample by scanning the surface with a focused beam of the electron. The electrons interact with atoms in the sample, producing various signals that contain information about the surface topography and composition of the sample. Due to the narrow electron beam, the SEM micrograph has great deep of field, yielding a characteristic three dimensional useful for the understanding of the surface structure. A wide range of magnifications is possible, from about ten times to more than 500000 times. By using SEM, the shape of the particle, as well as the surface roughness, can be seen to explain the phenomenon, which appears during the filtration process.

The appearance of cracks phenomenon in the filter cake is recorded by the camera as well as visually observed. In order to assess the extent of cracks, the permeability ratio parameter combining obtained images is used. In addition, the dewatering efficiency in the filtration process is assessed through parameters of saturation and residual moisture content of filter cake.



### 3.6. Tensile stresses depend on saturation during deliquoring

According to Wiedemann [5], the stress generated by the capillary force exceeds the tensile strength of filter cake, the cracks begin. Tensile strength is given by stress, which is transferable until to weakest bridge break. The difference in tensile stress could be a primary reason for shrinkage crack formation. H. Schubert [32], in his research, also mentioned the dependence of tensile strengths and liquid distribution on the system, which can be characterized by saturation. These approaches can be used for both – the quantification of the tensile strength as well as the tensile stress. Depend on the amount of water on the filter cake, it can be divided into three parts, corresponding to the value of tensile stress, as seen in Figure 49.

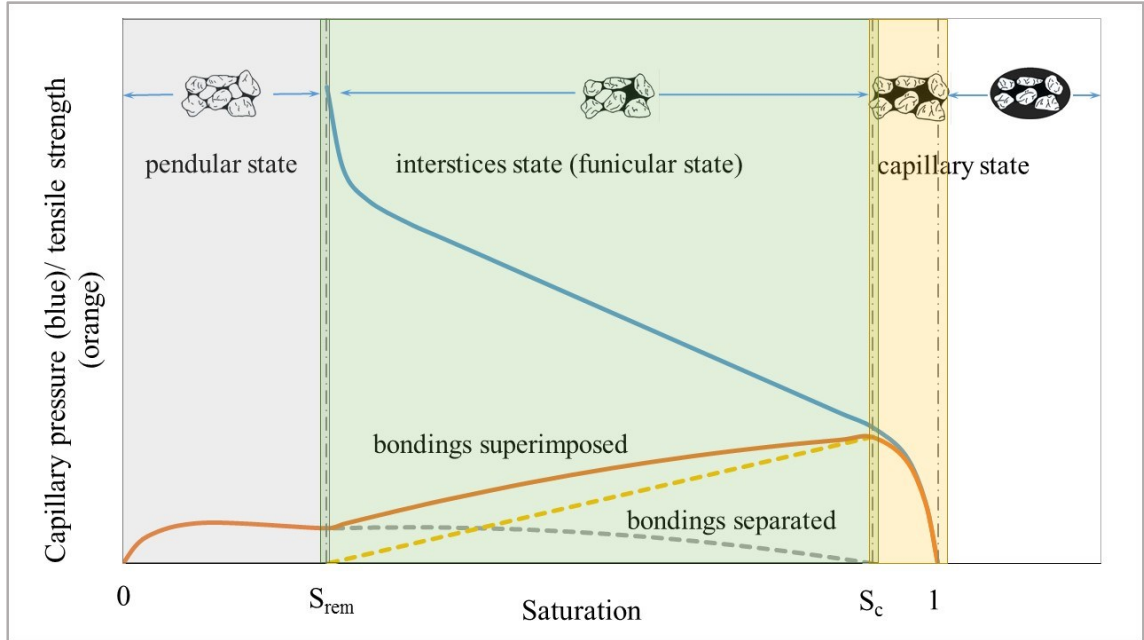


Figure 49. Schematic of capillary and tensile strength against saturation.

The first region (a grey area) is pendular, where a small quantity of liquid saturation causes the liquid bridge between individual particles. Tensile strengths are defined according to Equation (39).

The capillary state (yellow area) is presented where pores are entirely filled with corresponding saturation approach 1. At later state, tensile stresses are calculated according to Equation (39). The interstices state (green area) corresponds to the degree of saturation from  $S_{rem}$  to  $S_c$ , where both liquid bridge and pore filled with liquid affected on tensile stress. The calculation is taken account the effect of both mechanisms. Therefore, the tensile stress is defined according to Equation (42).

Tensile stress, which is the main reason that causes shrinkage cracking, depending on the degree of saturation. At saturation is 1, the maximal capillary pressure acts. By increasing applied pressure, the liquid is pushed out of the pores, reducing the moisture. Typically, the liquid in large pores is more easily drained than that of small ones. The empty pores generated weaker regions in the filter cake compare with around areas. The cracks occur as soon as the reduction of the degree of saturation (below 1), where tensile stress also shows the high value (Figure 49).

This model can be used to explain reasonably the occurrence shrinkage cracking on filter cake, especially in capillary state and intersticious state. The relationship between capillary pressure and saturation during filtration are measured by pressure filter cell, as is described next paragraph. The value of tensile stresses is assumed, calculated, and drawn by Equation (38), (39) and (42).

For the measurement of the capillary pressure curve, the method is available and is described in the VDI 2762-3 [45]. Firstly, the cake is formed according to VDI 2762-2[18]. Very shortly before the filter cake emerges from the suspension, the pressure difference must be regulated to 0. The thin layer of liquid should remain on the filter cake no more than 1 mm. In this way, the deliquoring does not begin too soon. Very quickly, the filter cake with the cake formation unit is connected to the press unit and install in the lab-scale compression permeable cell. In order to stabilization and ensure the filter cake in the saturated status ( $S=1$ ), the filter cake is compressed by a piston with the pressure up to 4.5 bar in 30 minutes. The equipment is shown in Figure 50. And then, by increasing the pressure slightly using the regulator, the residual water on the filter cake is drained to reach the saturation of 1.

The value of air compressed is still below the capillary entry pressure of the formed filter cake. In this way, a little remaining water on top of the filter cake is drained. In order to collect the filtrate during the capillary pressure measurement without evaporation, a beaker with a narrow throat is used. An electronic scale is tared to 0 in order to record the quantity of filtrate accurately. With the completed all procedure, the pressure is increased step by step by 10 kPa and measure some points overcoming the pressure difference. Once the pressure increase sufficiently, it can be grown in a range of 50 kPa. When there is no filtrate flowing through the Nutsche in 10 minutes at the given pressure setting, pressure can be raised next level. The displaced filtrate at each pressure

is registered by scale. The increment until the upper limit of the measuring range is reached or further increase pressure lead to no more filtrate.

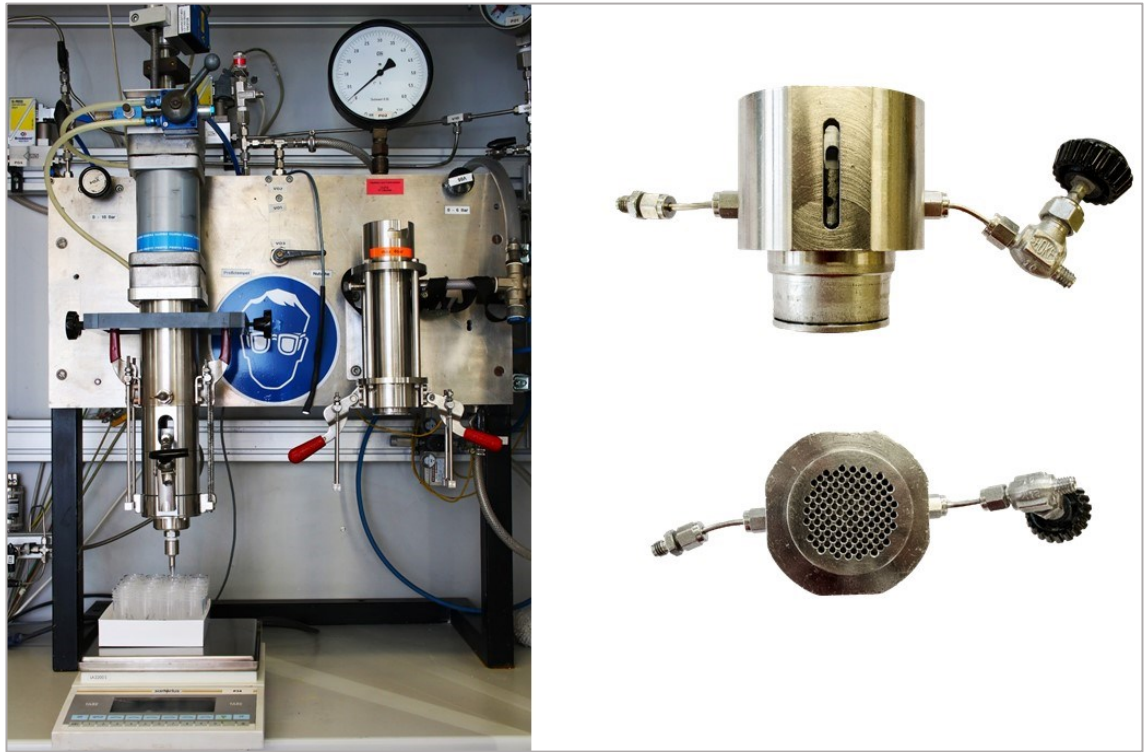


Figure 50. Images for lab-scale compression permeable cell.

Saturation correspondent the pressure level is calculated. A semi-permeable membrane is used to lead to no airflow through filter cake, which its name is the Durapore membrane filter. It is made from hydrophilic polyvinylidene fluoride (PVDF) with  $0.1 \mu\text{m}$  of pore size. The bubble point at 23 degrees Celcius is higher than 5 bar. The water flow rate is higher than  $0.33 \text{ ml/min} \times \text{cm}^2$ . Thus, the results are not affected by the drying effect. The collected filtrate is caused by mechanical deliquoring. From the saturation at each pressure, the capillary curve is drawn. Base on the capillary pressure result, the relationship between tensile stress and saturation is also calculated and showed in the chart, as can be indicated in the next chapter.

#### **4. The influence of operating parameters on cracks formation in case of limestone**

##### **4.1. Capillary pressure curve and tensile stress during the filtration in the case of limestone**

The result for Limestone KS12 is shown in Figure 51. The filter cake is formed by 1bar (0.1 MPa) of air pressure difference. Because of the equipment safety limit as well as the technical properties of the experimental membrane, the capillary pressure is only increased from 0.01 MPa to a maximum value of 0.425 MPa (highest the capillary pressure - due to the limitation of safety in CP cell). The capillary pressure increases to 0.425 MPa in expectation of the change system's status from capillary to the funicular. Although the pretty high capillary pressure is applied, the saturation of filter cake is reduced very little and slowly. The reason for this phenomenon is the very fine particle size of the material. For most surveyed solid concentration, the saturation decrease stops around 0.9. The status of the filter cake is in the capillary state, where pores are almost filled by water. In this state, tensile stress between particles usually gets the highest value. The cracking formation is predicted would appear quickly when a few weak points in a system occur. Based on the capillary pressure curves, tensile stresses are calculated by Equation (38), (39) and (42), which are also shown in Figure 51. For values of 0.1 and 0.3 MPa of capillary pressure, the stresses caused in filter cakes have a similar magnitude. They explain the phenomenon of large cracks as well as poor dewatering efficiency when filtering this fine material. Otherwise, Figure 51 also shows that the solid volume fraction of suspension, for fine material, does not affect as much the capillary pressure as well as tensile stress, especially at lower pressure difference.

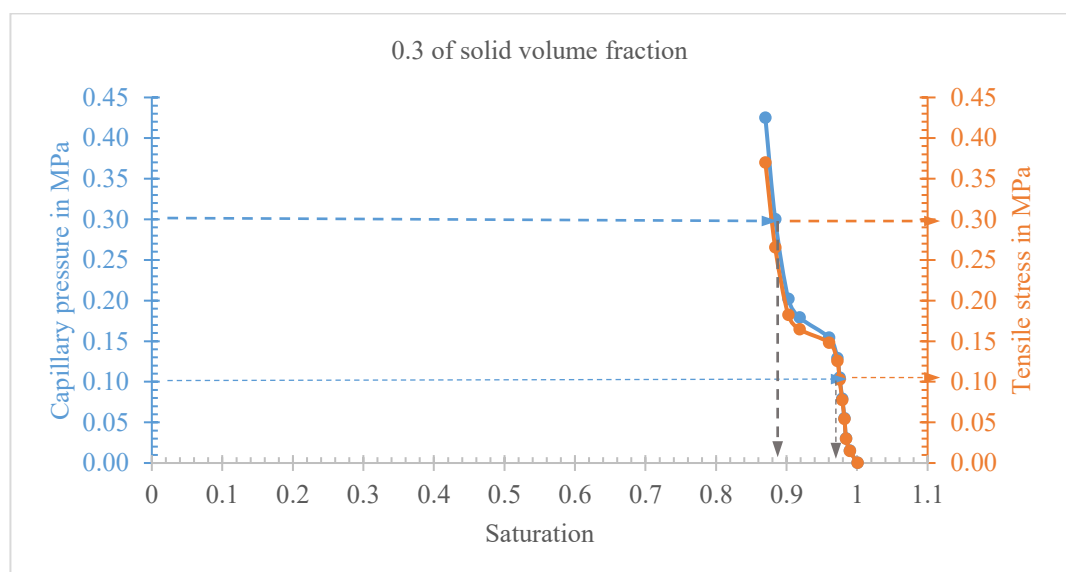
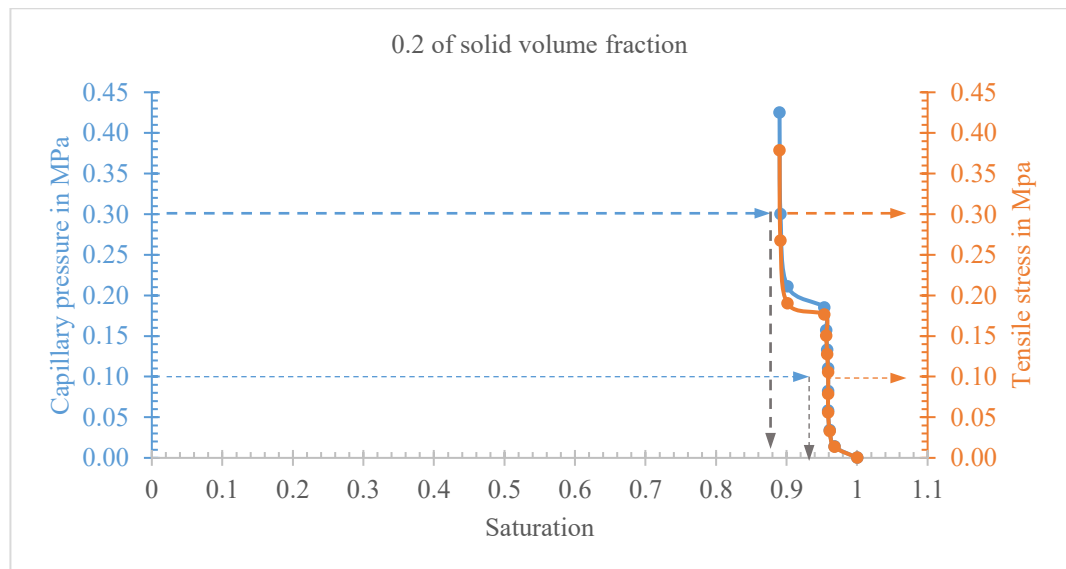
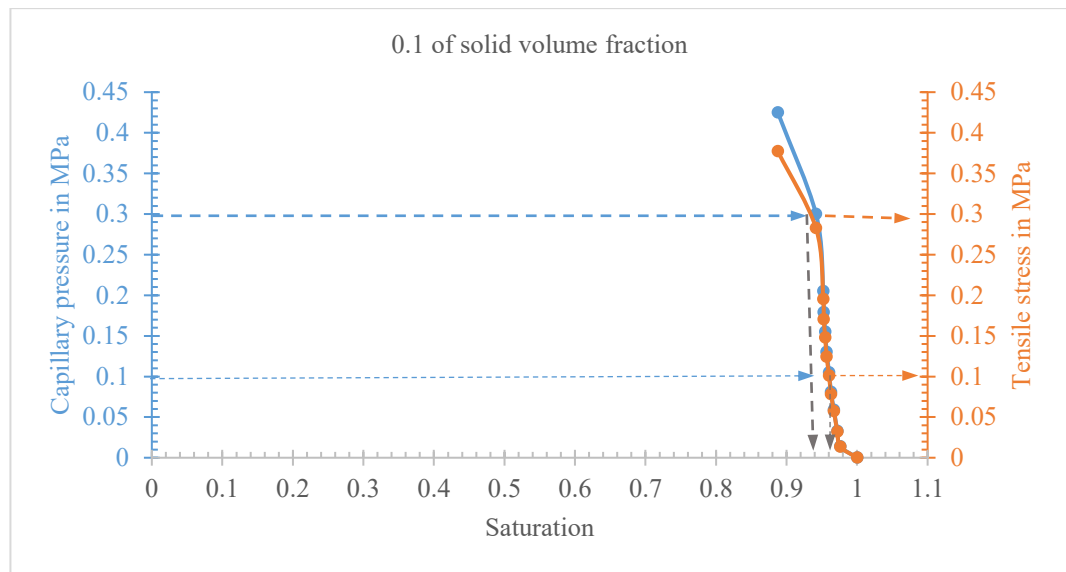


Figure 51. Capillary pressure and tensile stresses against saturation for KS12.

Figure 52 shows the relationship between the saturation, residual moisture content of filter cake at 3 bar of pressure difference and the volume fraction. It can be seen that, although the pretty high applied pressure, the amount of water reduce very slowly with the different volume fraction. Otherwise, the chart for the relationship between capillary pressure and the residual moisture content, as can be seen in Appendix D2, indicate a similar trend.

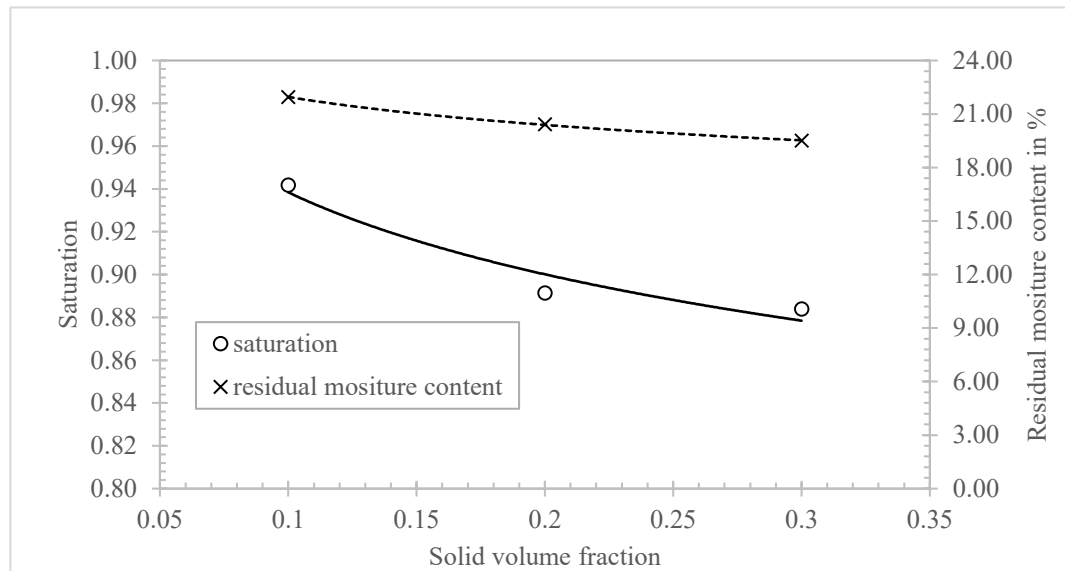
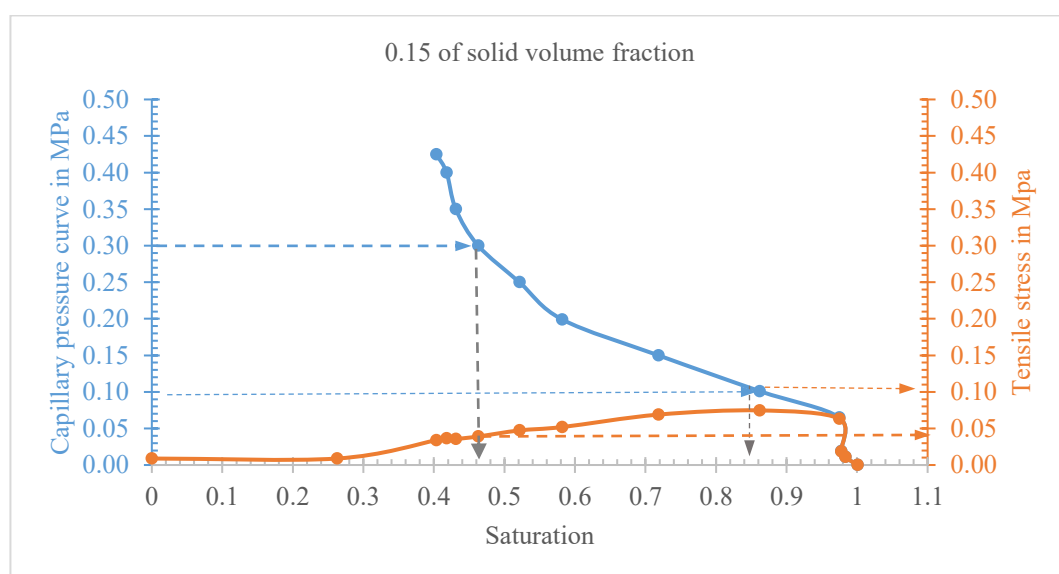
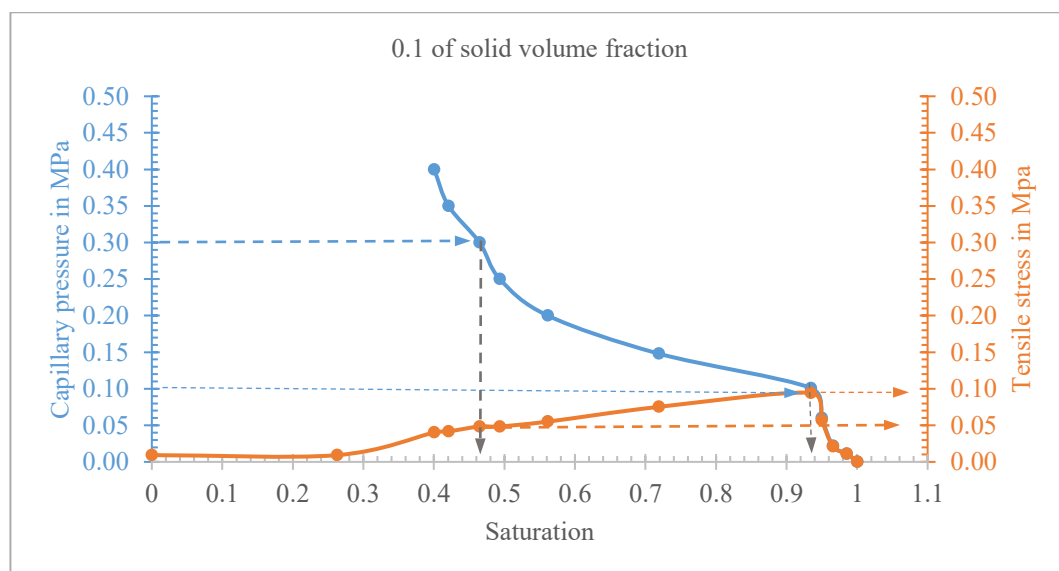
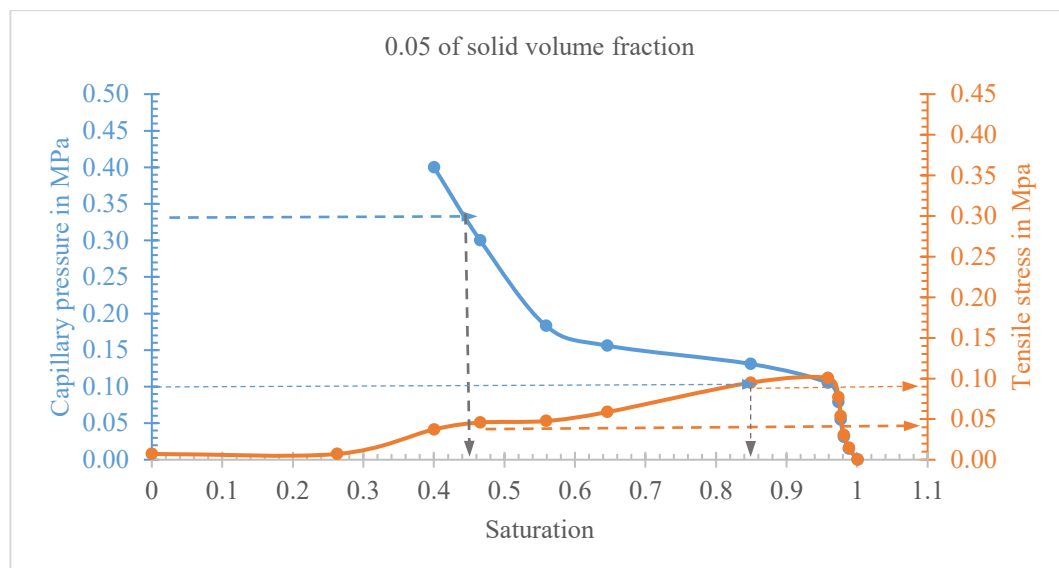
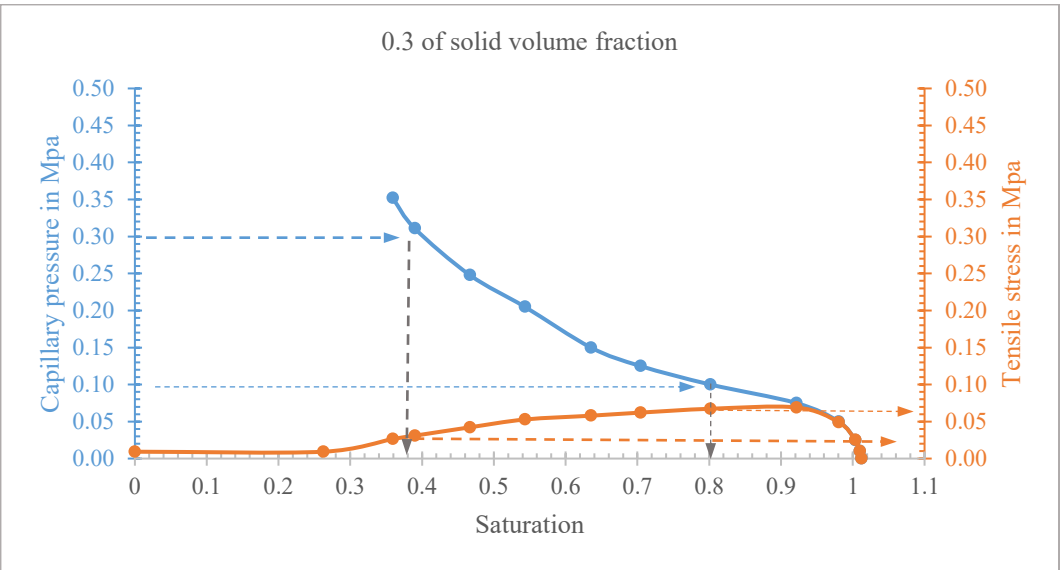
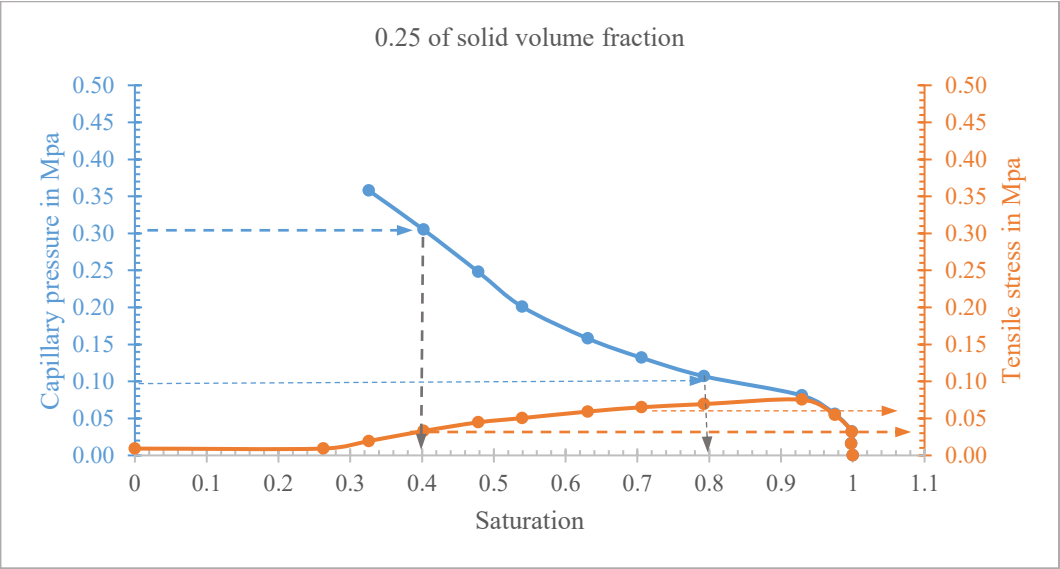
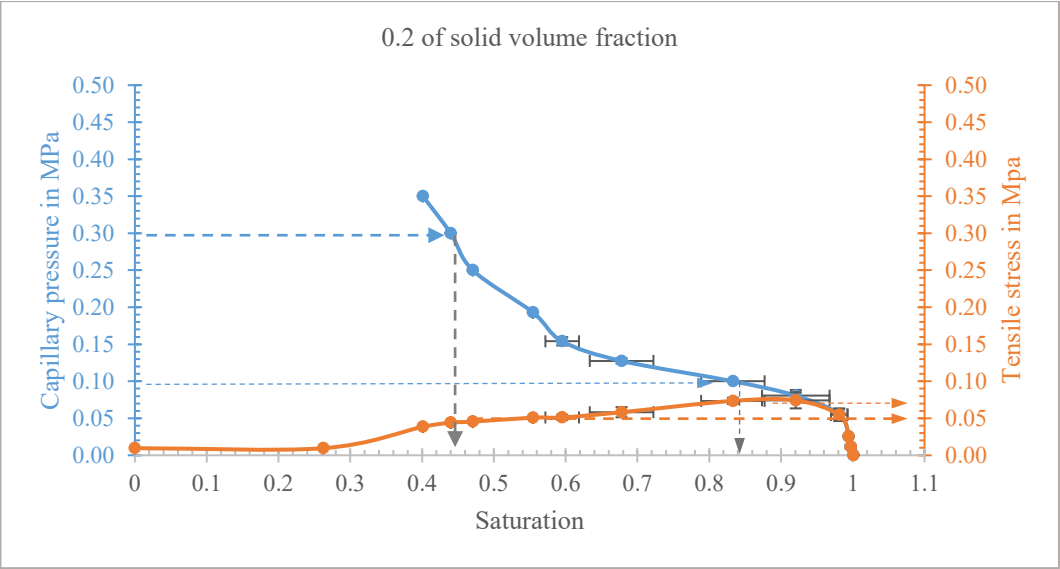


Figure 52. The saturation and residual moisture content of KS12 filter cake at 3 bar capillary pressure as the function of the volume fraction.

Turning to the KS100 coarse material, the results of the capillary pressure measurement and the tensile stress calculation are shown in Figure 53. Measurements are executed with solid concentration ranging from 0.05 to 0.4. The applied pressure difference for the filter cake formation process is 0.1 MPa. It can be divided into three areas according to the degree of volume fraction.







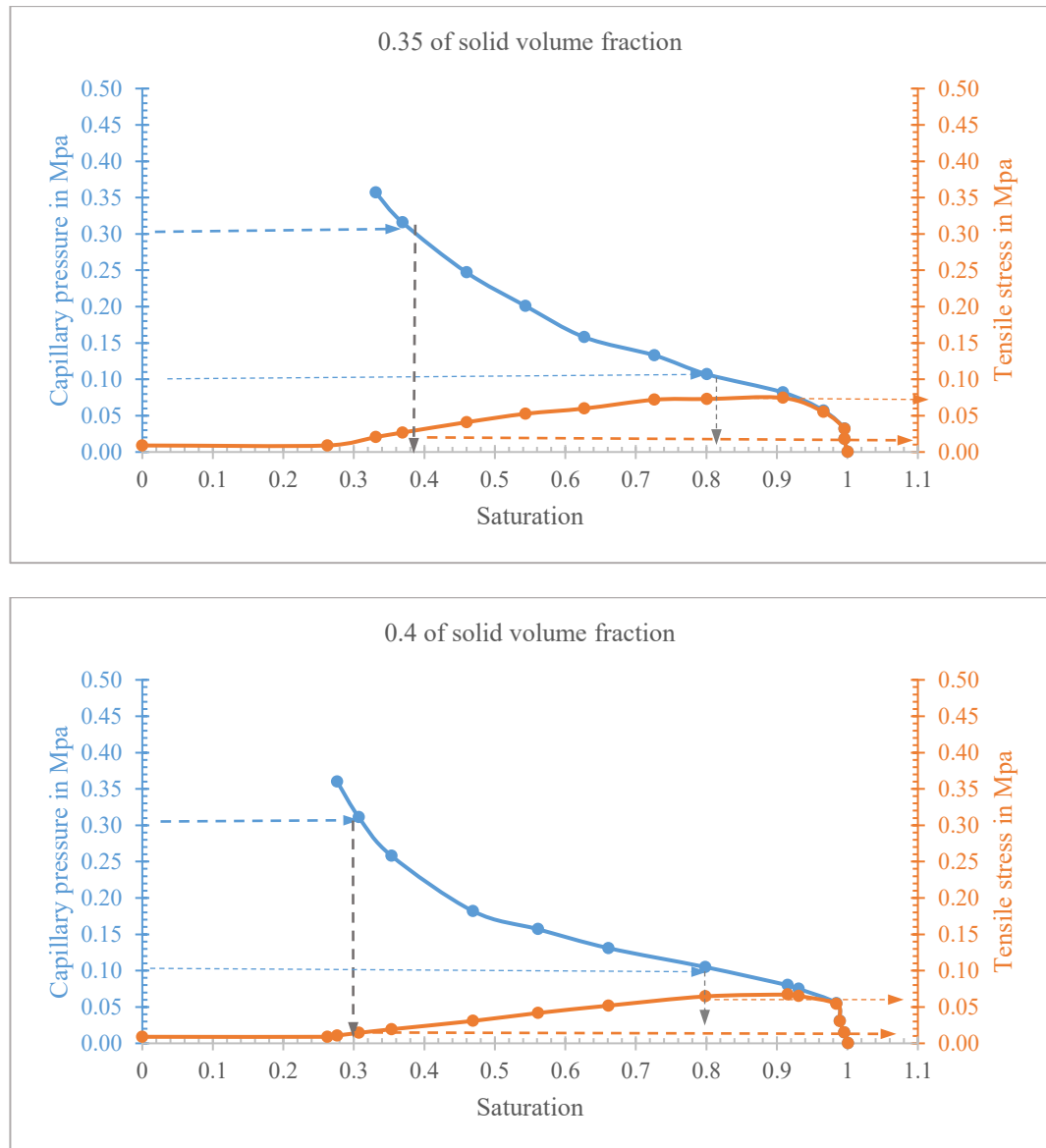


Figure 53. Capillary pressure and tensile stresses against saturation for KS100.

The first area, as can be called “dilute suspension area”, includes the 0.05 and 0.1 of solid volume fraction of suspension. This dilute suspension zone is characterized by a high value of entry capillary pressure and high tensile stress value. For 0.1 MPa of applied capillary pressure, the tensile stress has a corresponding value (0.1 MPa). The saturation is also high with 0.96 and 0.94 for 0.05 and 0.1 of volume fraction, respectively. The filter cake is in the capillary state, where a little water is drained out of filter cake. Shrinkage cracking may occur in filter cake in this zone. For 0.3 MPa of applied capillary pressure, tensile stress reduces to approximately 0.05 MPa for both 0.05 and 0.1. The filter cake reached the interstices state, one of good status to dewatering as well as prevent the appearance of shrinkage cracking.

The second area includes the 0.15 and 0.2 of volume fraction, called the “transfer area”. For both 0.1 and 0.3 MPa of applied capillary pressure, the filter cake is in the interstices state. However, because the degree of homogeneity of the filter cake is still low, these values are still relatively high.

The third area includes the solid volume fraction of suspension from 0.25 to 0.4, as can be called the “concentrate suspension area” of the filter cake. The saturation, as well as the tensile stress, are pretty low, with can achieve good filtration without shrinkage cracking.

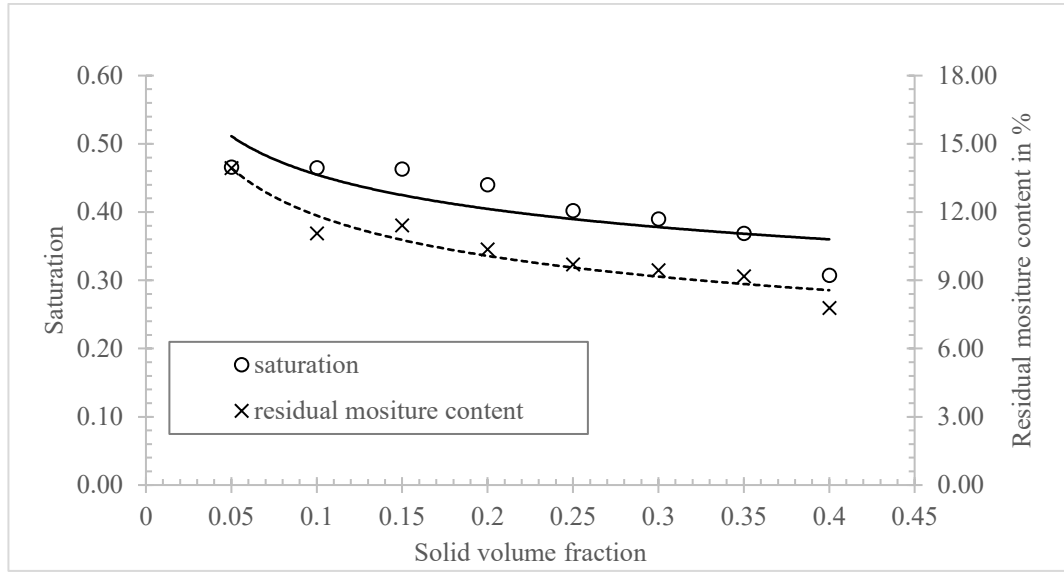


Figure 54. The saturation and residual moisture content of KS100 filter cake at 3 bar capillary pressure as the function of the volume fraction.

Figure 54 also supports for the discussion above. Generally, there is a reduction trend of the amount of water inside the filter cake when the volume fraction increase from 0.05 to 0.4 (at 3 bar of capillary pressure). This issue shows the dependent on the saturation and residual moisture content on the volume fraction. This data also can be used to explain the test result for KS100, as shown next chapter. The measurement also shows the relationship between the capillary pressure and the residual moisture content, as indicated in Appendix D3.

Generally, the homogeneity of filter cake according to volume fraction depends on the structure of the material as well as the manner of filtration. KS100 material using 0.1 MPa of pressure difference for cake formation show three areas: sedimentation (below 0.1 of volume fraction), transfer area (0.15 to 0.2 of volume fraction), and homogeneous area (over 0.25 of volume fraction). Besides, the increasing applied capillary pressure in

the mechanical displacement phase both reduces the amount of water remaining in the filter cake and reduces tensile stress. It will increase the possibility of preventing crack formation. This assumption will be tested in the experiments, which are presented in the next session.

4.2. Test were conducted using conventional pressure filtration

4.2.1. Particle size distribution effect

In Barua's research [4], he also mentioned the effect of particle size, especially the mass fraction of fine particles on cracking. The result shows that the increasing proportion of fine particles (below 15  $\mu\text{m}$ ) in the slurry increases the likelihood of cracking. Wiedemann also gave the comparison of shrinkage behavior of different organic and inorganic test products. The result was, generally, finer materials have higher shrinkage potential than coarser ones [5].

For smaller particles system, capillary pressure gets a higher value and produce higher tensile stress. Similarly, the presence of a significant number of fine particles in coarse material leads to a wide distribution of particle size. In this filter cake system, there is the formation of capillaries of various sizes. At the positions where we have big pores, capillary would be empty and are being weaker points. Tensile stress has an intense effect on these weak points, and cracks occur as can be expressed in Figure 55.

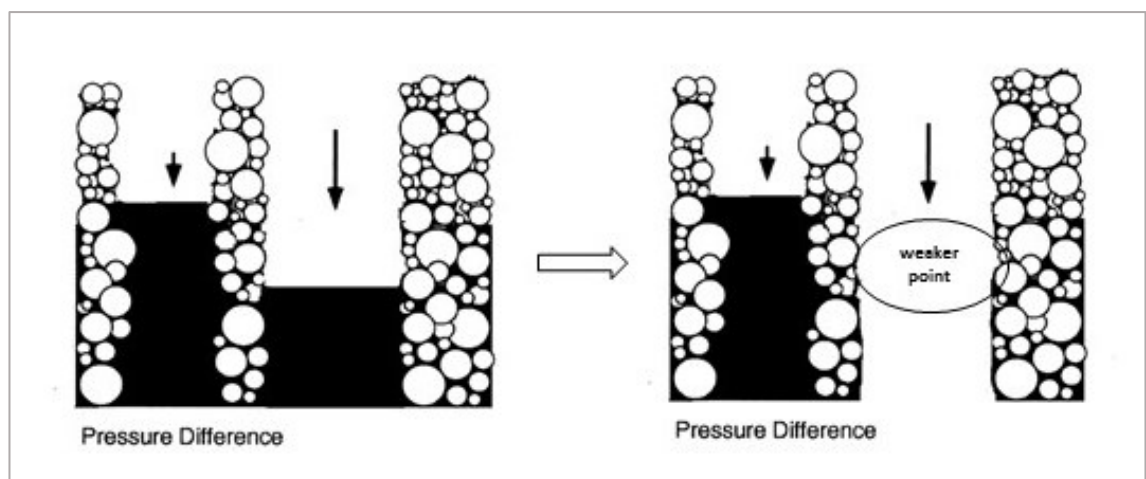


Figure 55. Water is pushed out of the large and small capillaries.

For two kinds of significantly different particle size materials, tests were conducted similarly to see the difference of cracking behavior. The compression pressure

is 1 bar, the thickness of the filter cake of 18 mm, and various concentrations of slurry to see the effect of particle size distribution on cracking.

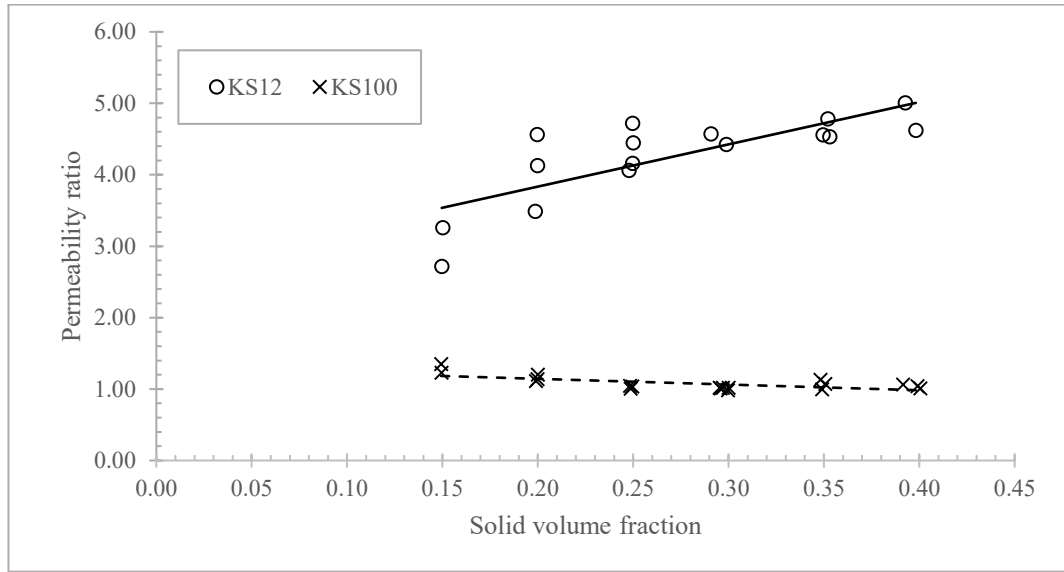


Figure 56. Permeability ratio of fine limestone KS 12 and coarse limestone KS 100 filter cakes at some volume fraction values; “1-1 bar” of pressure difference; 50 grams of solid content.

As can be seen in Figure 56, the permeability ratio has different values. For coarse particle, those values are around 1.5-1 when the solid volume fraction increase from 0.15 to 0.4. By visual observation of the filter cake, as is shown in Figure 60, there is less macro- cracking as well as shrinkage micro-cracking at the almost solid concentration for the coarse material.

Meanwhile, there is the contrast phenomenon for fine material. For most surveyed concentration, macro-cracking, as well as shrinkage micro-cracking, occur with different degrees. This issue also consistent with the value of the permeability ratio, which is shown in Figure 56. From 0.15 to 0.4 of solid volume fraction, the permeability ratio is relatively high, around 4. They are approximately four times more than those values of coarse material. The result gets the agreement with the investigation in some literature as mentioned below [4, 5]. However, the behavior of cracking according to the volume fraction is seemed quite different, which can be discussed clearly next part.

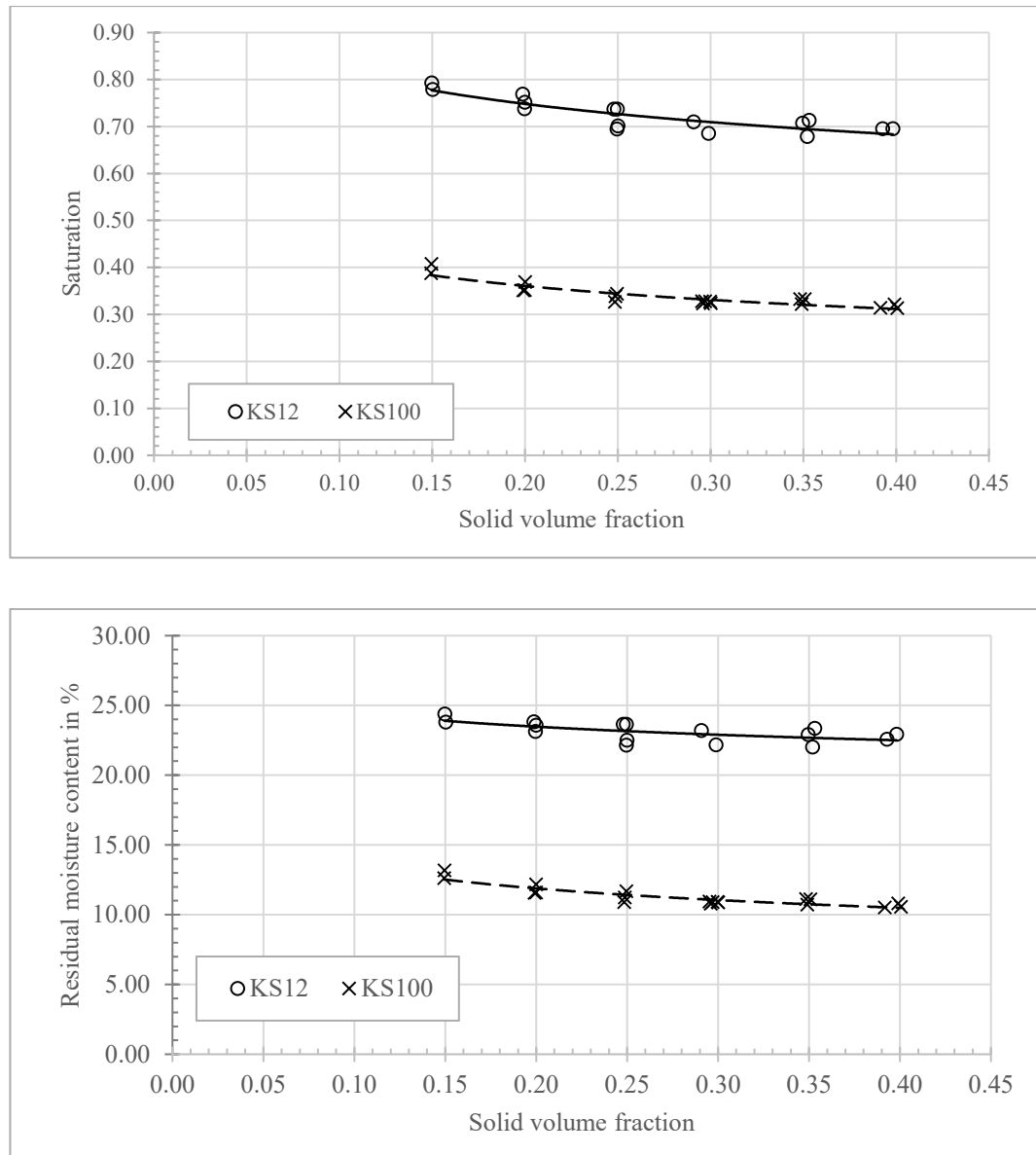


Figure 57. Saturation and residual moisture content of KS 12 and KS 100 filter cakes at some volume fraction values; “1-1 bar” of pressure difference; 50 gram of solid content.

The increase in cracks in the filter cake (which is indicated by the permeability ratio) has a negative effect on the amount of water pushing out of the filter cake. For coarse material, the degree of saturation, as well as residual moisture content, according to Figure 57, are low (0.3 - 0.4 of saturation or approximately 13% to 10% of residual moisture content). Micro-cracking, in these cases, does not significantly affect to dewatering. About saturation as well as the amount of water in mass retaining on fine filter cake, are also much higher. The saturation is around 0.7- 0.8, corresponding to 22% - 24% of residual moisture content. The great amount of water remaining in the filter cake is perhaps caused by the filtration of fine material.

It can be noticed that the coarse material filter cake has high efficiency in dewatering, and fewer cracks appear. The capillaries are large enough to push the liquid out of filter cake simultaneously with the low required dewatering force. This is in agreement with what was observed in specific resistance value, which is shown in Figure 58. The significantly low value is around  $2 \times 10^{10}$  m/kg, and there is no significant distinction in the surveyed range. Porosity (as shown in Figure 59) also shows the homogeneous status with values around 0.502 and 0.506. Those values are much lower compared to the porosity of fine material KS12. Easy drainage and quick removal from filter cake are the basis for the assumption that few weaker locations. Moreover, the tensile stress in Figure 53 is also lower (0.06 - 0.07 MPa), resulting in cracks that can be prevented. Overall, the filtering of coarse materials is quite effective in concerns about crack formation as well as moisture.

Meanwhile, there are tiny capillaries, which are formed by filtering fine-grained material. It requires a stronger dewatering force. The specific resistance also shows very high values, from  $2 \times 10^{11}$  m/kg to  $3 \times 10^{11}$  m/kg, ten times more than the values of the coarse filter cake. However, 1 bar of pressure difference is not enough to overcome the capillary forces. The result is that the water is only pushed out of the few large capillaries and still retained in the almost small capillaries; the weaker position in filter cake occurs. The high capillary force between particles in small capillaries, which including the adhesion force and capillary suction forces, pull particles towards its side, forming up hollow channels. Figure 51 shows the tensile stress is much higher (0.1MPa) than that of the coarse material. The result is the formation of cracking.

When cracking occurs, air preferentially flows through the big channels, the pressure profile in the cake changes, and no water is drained anymore. It can be said that the crack occurs because of the amount of water remaining in the small capillaries. There is a back effect that the cracks are the main reason to prevent further dewatering during filtration.

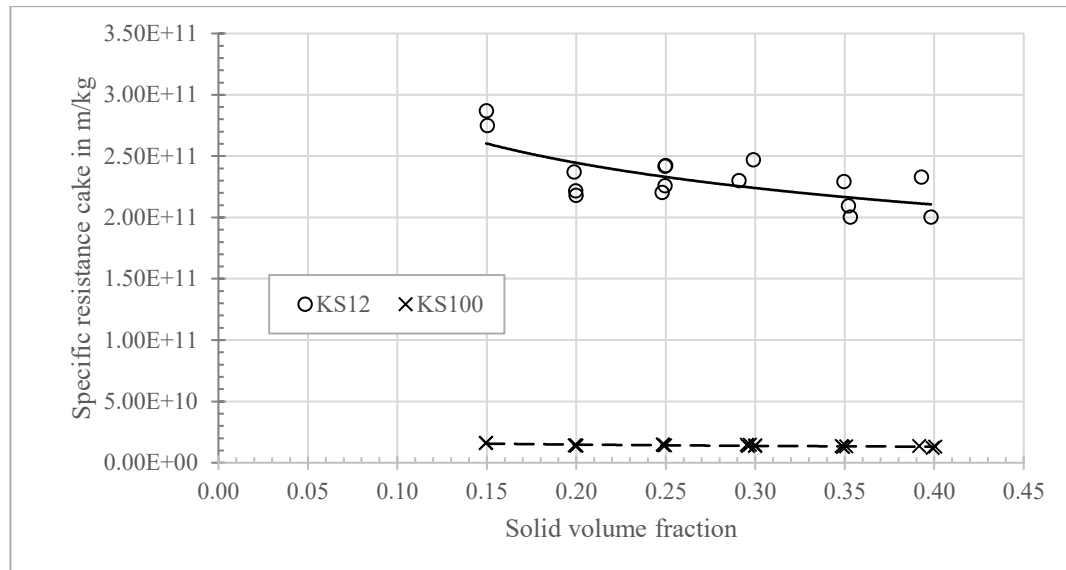


Figure 58. The specific resistance of KS 12 and KS 100 filter cakes at some volume fraction values; 1 bar of pressure difference in the cake formation phase; 50 gram of solid content.

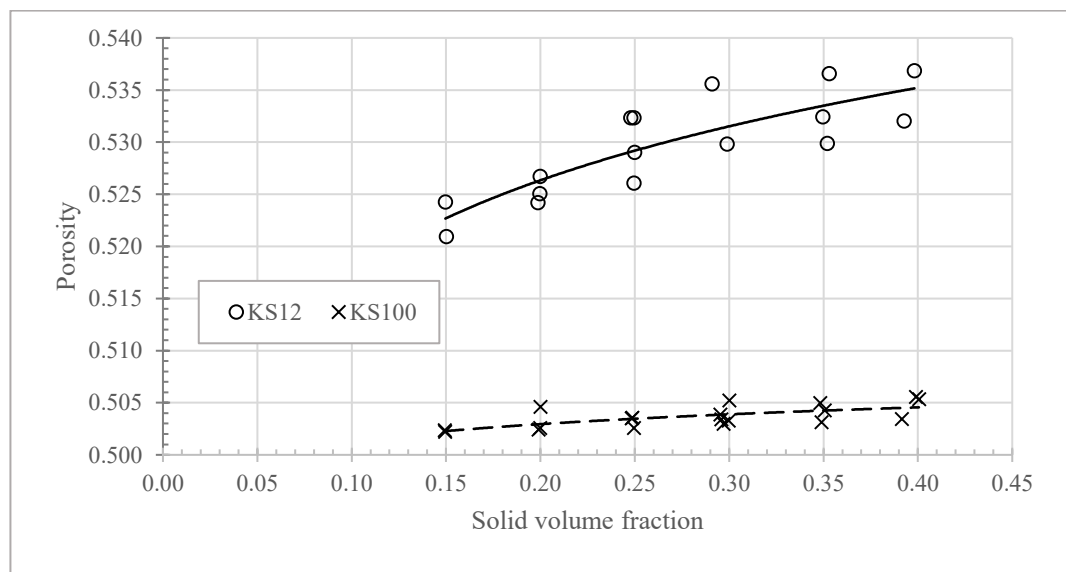


Figure 59. The porosity of KS 12 and KS 100 filter cakes at some volume fraction values; 1 bar of pressure difference in the cake formation phase; 50 gram of solid content.

Figure 58 and Figure 59 show the interesting points. For fine material KS12, there is an opposite trend in specific resistance cake and porosity. While the specific resistance cake decrease from approximately  $3 \times 10^{11}$  to  $2 \times 10^{11}$  m/kg, the porosity increase from 0.52 to 0.535. This issue can be explained base on the capillary model. The lower void volume leads to small capillaries, where the water is difficult to flow through the porous media and vice versus. This phenomenon also occurs in the case of coarse material KS100.

However, the change in trend is smaller. The specific resistance cake reduces from  $1.6 \times 10^{10}$  down to  $1.3 \times 10^{10}$  m/kg. The porosity also increases slightly from 0.503 to 0.506. The increase of resistance with the reduction of porosity confirms the finding of Rumpf - Gupte [46], Carman – Kozeny [15, 47]. Whereby, the permeability of filter cake  $k$  is directly proportioned to the porosity  $\varepsilon$ , in the case of the other two parameters (the grain size and tortuosity) are usually kept constant [48].

$$k = \frac{\varepsilon^3}{K \cdot (1 - \varepsilon)^2 \cdot S_v^2}$$

Where  $S_v$  is the specific surface area per unit volume of the particle and  $K$  is Kozeny constant [1, 15]

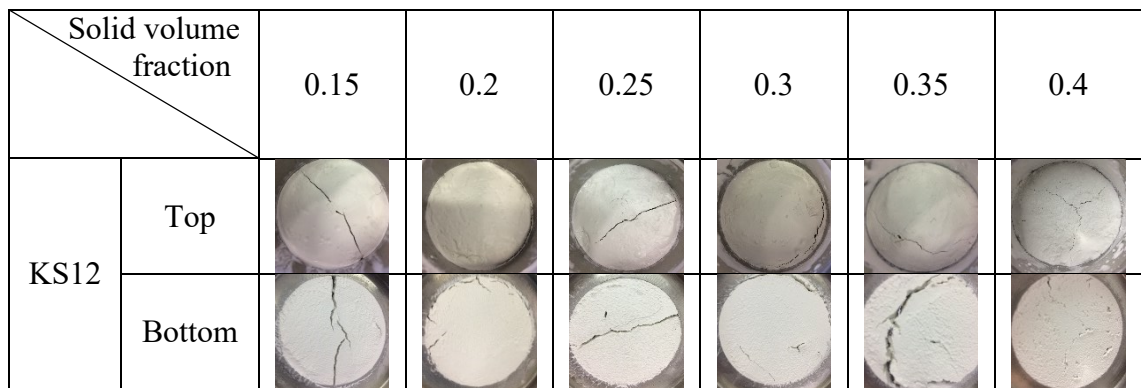
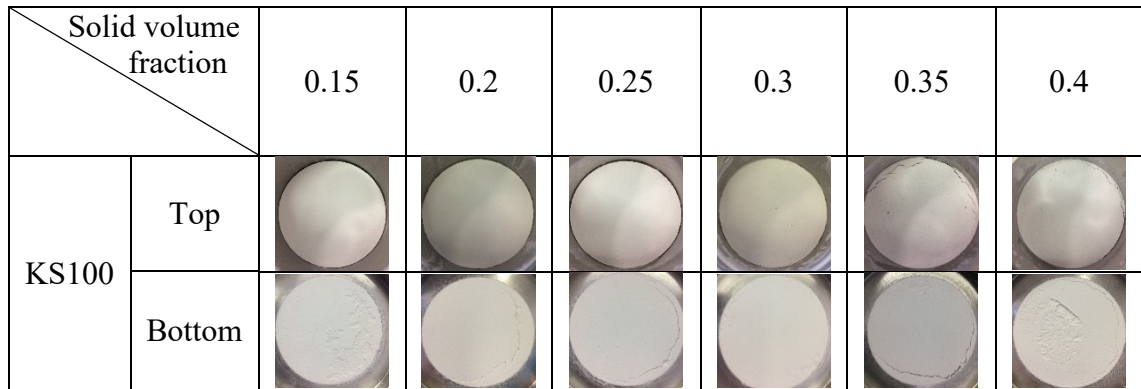


Figure 60. Images for the top and bottom of coarse material (KS100) and fine material (KS12) filter cake; “1-1 bar” of the pressure difference ( $\Delta p$ ); 18 mm of filter cake thickness.

Figure 60 shows the images of the top and bottom layer of filter cake in the case of limestone. All images are taken as soon as the cake formation unit is removed out of the Nutsche. Overall, the probability and degree of cracking are consistent with the result



of the permeability ratio. For coarse material KS100, images indicated slight shrinkage on top and micro-cracking at the bottom layer, around the filter cake. The difference in the shape of micro-crackings as well as the shrinkage, showed no propagation of cracks from the upper part to the lower. They are certain cracks at the special positions of the filter cake. Therefore, the deliquoring process was executed normally. The filter cake can easily remove a considerable amount of water inside.

Meanwhile, fine material KS12 in almost cases of solid volume fraction shows the opposite phenomenon. The very large shape similarity between cracks in the upper and lower layers of the filter cake indicated that these cracks form and develop from top to bottom, forming large continuous channels. In addition, these cracks have a large size by visual observation. This issue leads to a negative effect on the deliquoring phase because the gas flow prefers to pass through the macroscopic cracks rather than the pores.

#### 4.2.2. The solid volume fraction of suspension effect

##### *For coarse material KS100*

Tests were conducted in the change of volume fraction of solid. By changing the amount of distilled water, the concentration of suspension change from 0.05 to 0.4. The height of the filter cake (approximately 18 mm) is kept constant. The applied pressure difference has changed: “1-1 bar”, “1-3 bar”. The purpose of these tests to know which type of cracks occur when they occur as well as clarify the mechanism of crack formation. Otherwise, the result of the tests leads to the knowledge of the negative effect of cracking on dewatering.

Figure 61 showed a permeability ratio for KS100 filter cake has a decreased trend to approximately 1 when volume fraction growth up to 0.2 before keep constant until 0.4 of solid volume fraction. The chart can be divided into three parts as a discussion above: “dilute suspension area,” “transfer area,” and “concentrate suspension area.”

The dilute suspension area (or inhomogeneous zone) occurs when filtering the low slurry concentration. The solid volume fraction of suspension in this case, below 0.1. According to Figure 61 and Figure 71 (upper), filter cake in this region phenomenon of shrinkage and micro-cracking. Values of permeability ratio, residual moisture content, saturation, as well as specific resistance, which is defined according to the VDI 2762 -2 [18], are higher compared to those of the rest parts. These phenomena can be explained because of the demixing phenomenon on filter cake. Coarse particles have settled first,

packed on the filter cloth. Fine particles are filtered out through a new bed, including coarse particles and filter cloth. Fine particles on top of the filter cake generate more small capillaries, where water can be retained. The tensile stress is higher in comparison to homogeneous filter cake, which is formed from the concentrate suspension, as can be seen in Figure 53.

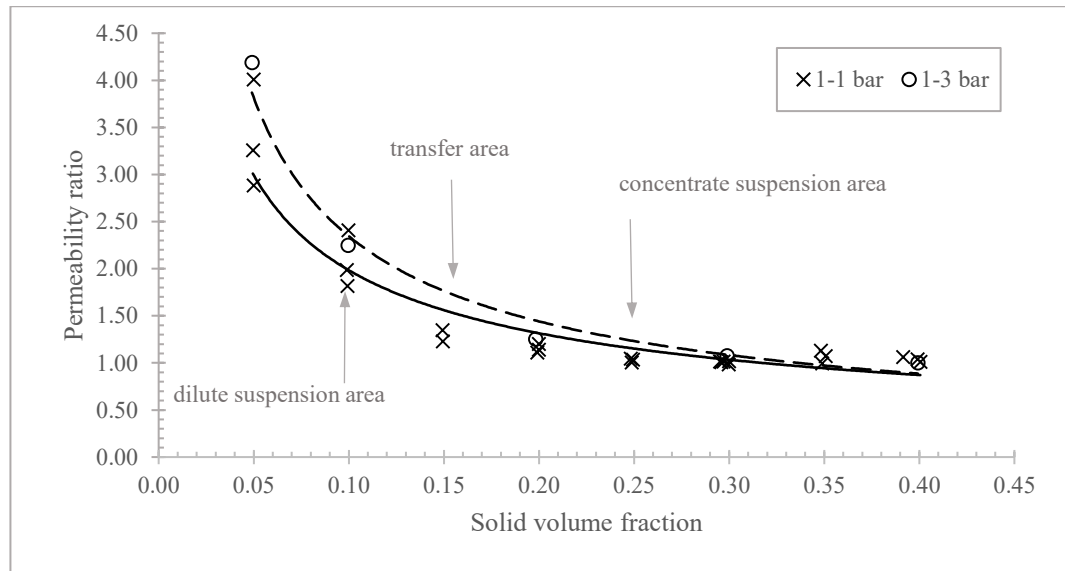


Figure 61. Permeability ratio of KS100 filter cake in variety of solid volume fraction of suspension; 18 mm of filter cake thickness; “1-1 bar” and “1-3 bar” of pressure difference.

The second part belonged to a range from 0.15 to 0.2 of solid volume fraction. The filter cake becomes more homogeneous than in the first area. The result is the probability and degree of cracking decrease and the corresponding permeability ratio drops from around 1.5 to approximately 1. Images for filter cake in Figure 71 also supported this evaluation.

From 0.25 to 0.4 of volume fraction, the filter cake is dewatered without cracking. It can be called “the concentrate suspension area” in the chart. The value of the permeability ratio keeps stable around 1 (except some cases at 0.3 and 0.4 of volume fraction is going to be discussed next graph). It is clearly explained by the large and homogeneity of the capillaries, and as a result, the dewatering efficiency is increased.

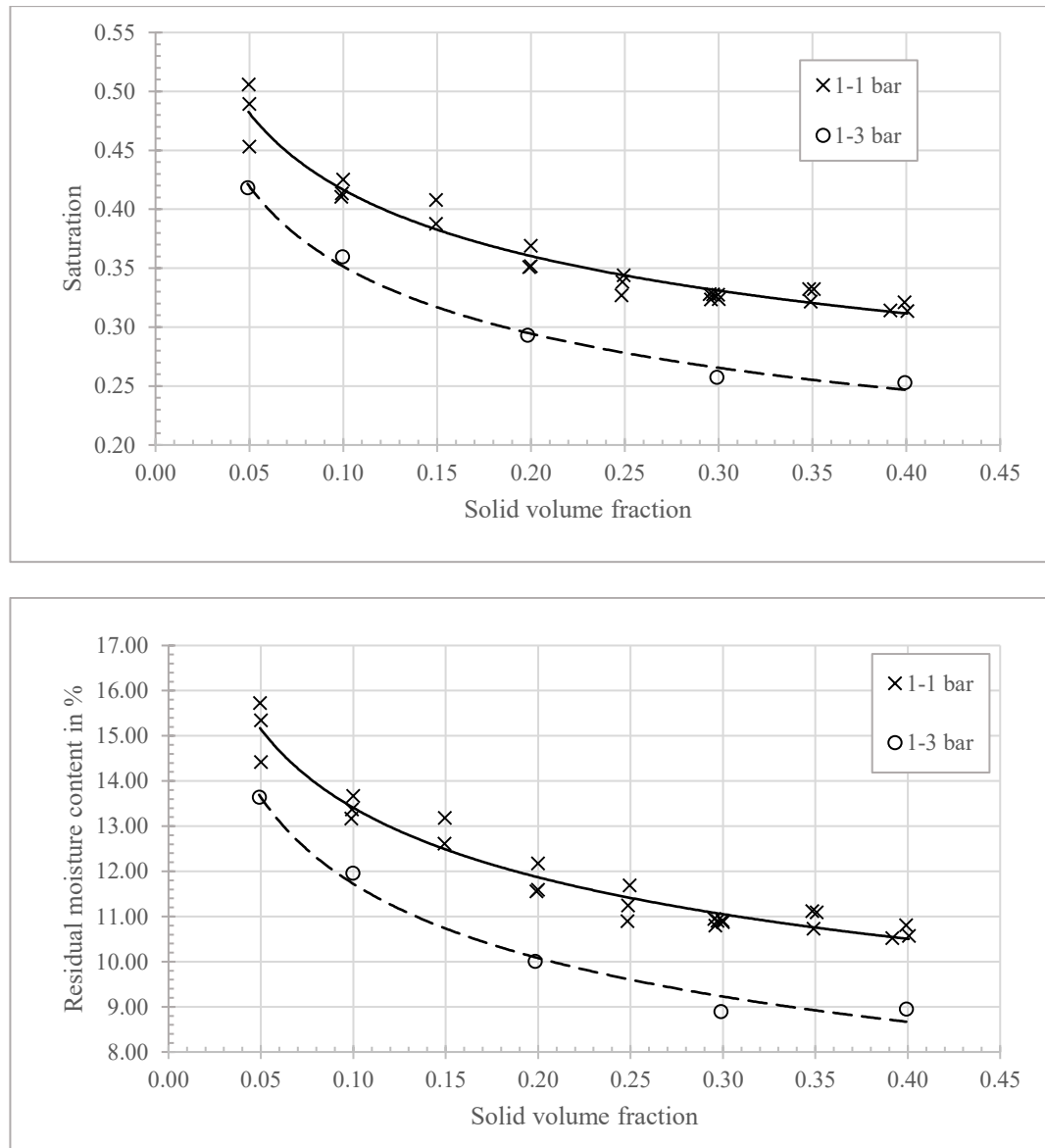


Figure 62. Saturation and residual moisture content of KS100 filter cake in variety of solid volume fraction of suspension; 18 mm of filter cake thickness; “1-1 bar” and “1-3 bar” of pressure difference.

Figure 62 shows the efficiency of dewatering during filtration. As can be seen, the water-retaining within the filter cake reduces when the volume fraction increases from 0.05 to 0.25. This amount of water cannot reduce any more in range 0.25 to 0.4 of solid volume fraction at the constant pressure difference. This stability obtains because the filter cake has reached the highest homogeneous state. The moisture values obtained is the equilibrium between the dewatering forces to the surface tension force retaining fluid in the filter cake.

One disadvantage of filtering coarse material is the sedimentation phenomenon. At lower volume fraction, the significant amount of coarse particles quickly settle down, lying on the filter cloth. Then comes the fine particles. Because of this de-mixing phenomenon, the general porosity of filter cake is low. It can be noticed that porosity is minimal in the upper layer of the filter cake, and it is quite large at the bottom layer of the filter cake.

Moreover, the fine-grained particles in the top layer cause the high-value specific resistance in the upper layer effecting the whole filter cake, as shown in Figure 63. The de-mixing results in a higher requirement of applied pressure to push water out of the upper pore of the filter cake, while this value is entirely redundant for large pores at the bottom layer of the filter cake. This obviously increases the production cost as well as more compressed air consumed in the highest dewatering requirements.

The de-mixing phenomenon only ends when the sludge is filtered at high concentrations (from 0.25 or higher).

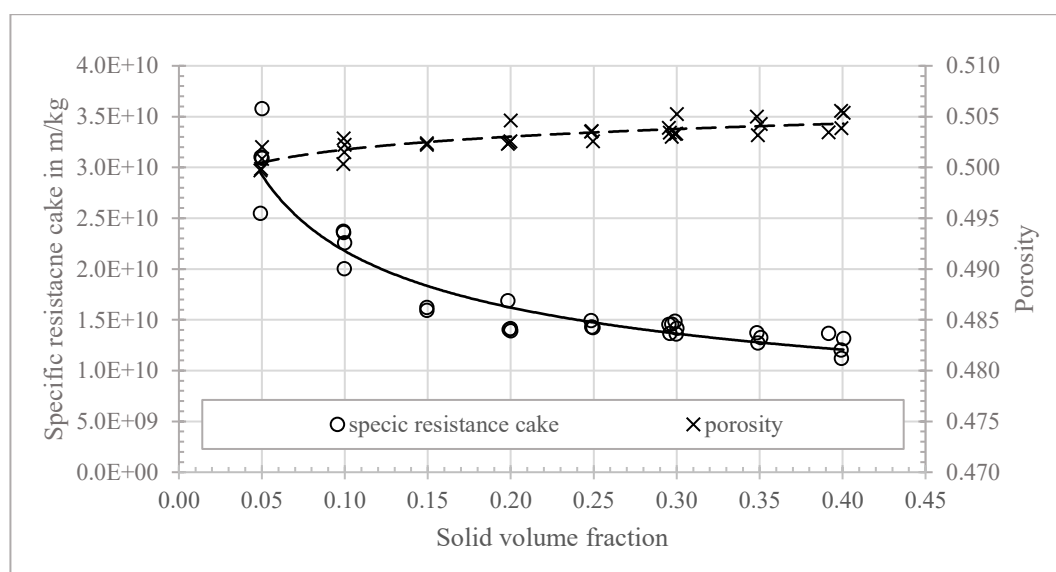


Figure 63. Specific resistance and porosity of KS100 filter cake in variety of solid volume fraction of suspension; 18 mm of filter cake thickness; 1 bar of pressure difference in the cake formation phase.

About the sedimentation phenomenon during filtration at low solid volume fraction, chart of the ratio of filtration time and filtrate volume ( $t/V$ ) versus filtrate volume ( $V$ ) for KS100 in various volume fraction which is shown in Figure 64 (in case of “1-1 bar” condition – the other conditions are similar) indicated the manner of each filtration process. From 0.25 to 0.4, the classic straight lines are seen. Nevertheless, from 0.05 to

0.2, it is seen that lines are not entirely straight, but they curve in places. These curves indicated that the domination of sedimentation [17]. Median particle size on top and at the bottom of the thin layer filter cake, as can be seen in Figure 65, showed this dissimilarity (in case of “1-1 bar” condition – the other conditions are similar). These value on top is much smaller than that at the bottom in volume concentration 0.05 and 0.1 while the rest part of volume fraction witnessed the similarity of parameters.

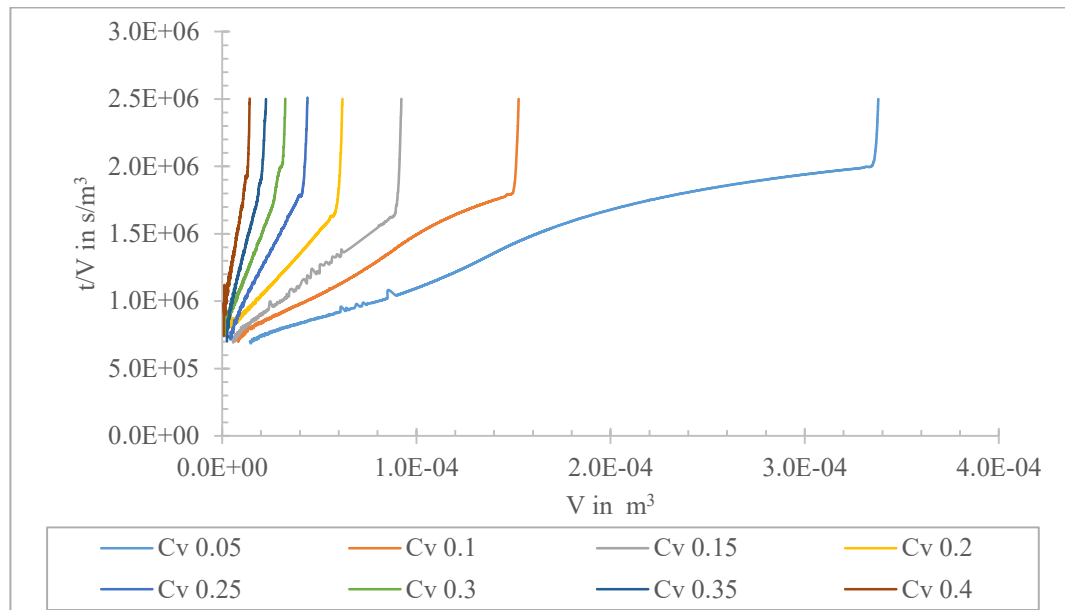


Figure 64. The ratio of filtration time and filtrate volume ( $t/V$ ) as a function of filtrate volume for KS100 in various volume fraction; 18 mm of filter cake thickness; 1 bar of pressure difference in the cake formation phase.

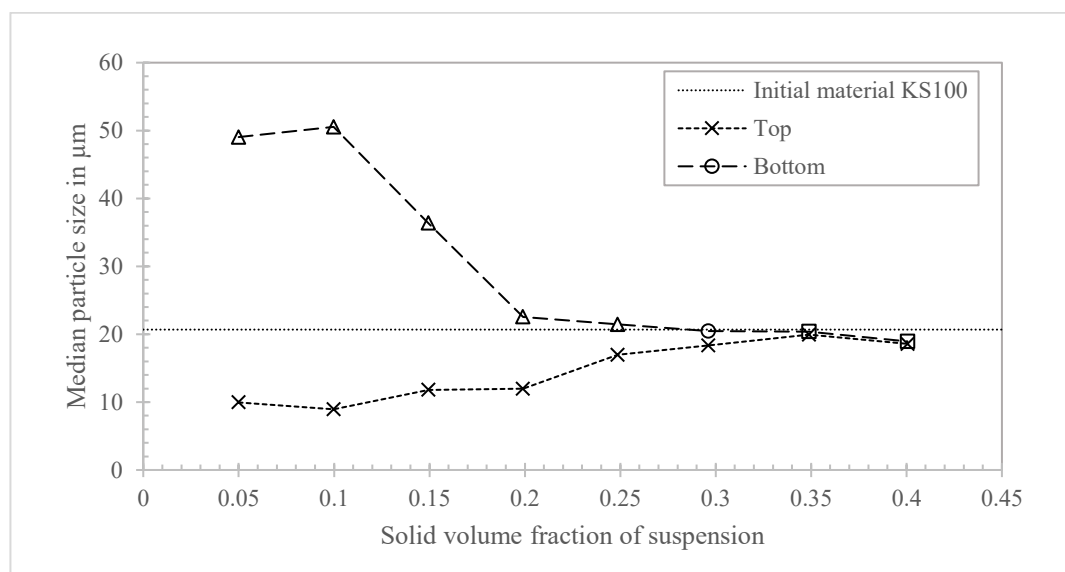


Figure 65. Median particle size on top and bottom layers of KS100 filter cake; 1 bar of pressure difference in the cake formation phase; 18 mm of filter cake thickness.

By visual observation, as shown in Figure 71, filter cakes have micro-cracking at high volume fraction. The value of the permeability ratio then becomes a little higher than 1. One of the assumptions is used to interpret the result as a closer particle's proximity in higher concentrated suspension leads to the agglomeration of fine particles the same as the description in Barua's research with 0.5 of volume fraction [4]. The agglomerated fine particles mixed other particles and contacted with particles network. Because of the weak bond of flocs, they have deformation and initiation of the crack network. Finally, the collapse of the whole structure occurs lead to micro-cracking occurs. This assumption is also used to explain for macro-cracking on fine filter cake KS12 mentioned below. The result of the zeta potential measurement (Appendix D6) also supports this interpretation. The value is relatively low at room temperature of -15 mV and -10 mV for KS100 and KS12, respectively. Besides the change of tensile stress during deliquoring, agglomeration of fine particles is one of the critical mechanisms of shrinkage cracking filter cake. *One of the ideas for this situation is the carefully controlling of agglomeration by pH value or the presence of dispersant lead to the reduction of settling and clump.* The result would be no shrinkage cracking at 0.35, and 0.4 of volume fraction and permeability ratio would keep constant at around 1.

The tests are executed using a “1-1 bar” and “1-3 bar” of pressure difference. The result of the two conditions shown in Figure 61 and Figure 62. The permeability ratio has a similar trend, but the value is smaller for a “1-3 bar” of compressed air. The image of filter cake with shrinkage cracking does not also occur, as shown in Figure 71 (upper). This result suitable for the measurement capillary pressure curve and tensile stress, as presented above. Otherwise, the efficiency of dewatering gets remarkably high at every solid volume fraction of suspension.

Generally, when the volume fraction increases, the probability and the degree of shrinkage cracking reduce. The reason for this trend is the homogeneity in the filter cake. Finally, the dewatering efficiency is improved. Besides that, a note at the high solid concentration of feed suspension that there is another reason that can cause cracks is the agglomeration breakage of the fine particles flocs. In the case of KS100, only micro-cracking occurs and has less effect on the dewatering effect. One of the ideas to reduce cracking and improve the efficiency of dewatering is using the higher capillary pressure for the mechanical displacement phase (the change of operation during filtration).

*For fine material KS12*

Tests were conducted similar for coarse material: “1-1 bar”, “1-3 bar” of compressed air, 18 mm of the height of filter cake, corresponds to 50 grams of the mass limestone.

The results in Figure 66 and Figure 71 (lower) show large cracks at all values of solid concentration. However, their degree is different. Generally, when the volume fraction increases, the probability and degree of macro-cracking reduce. This trend is similar to coarse material. At the dilute suspension, the permeability ratio has high values (35), and this value decreases to 25 for a “1-3 bar”. Saturation also has the same trend. For a “1-1 bar”, macro-cracking also occurs from 0.15 to 0.4. This issue seems not to change the degree as the value in Figure 66 (around 4 of permeability ratio).

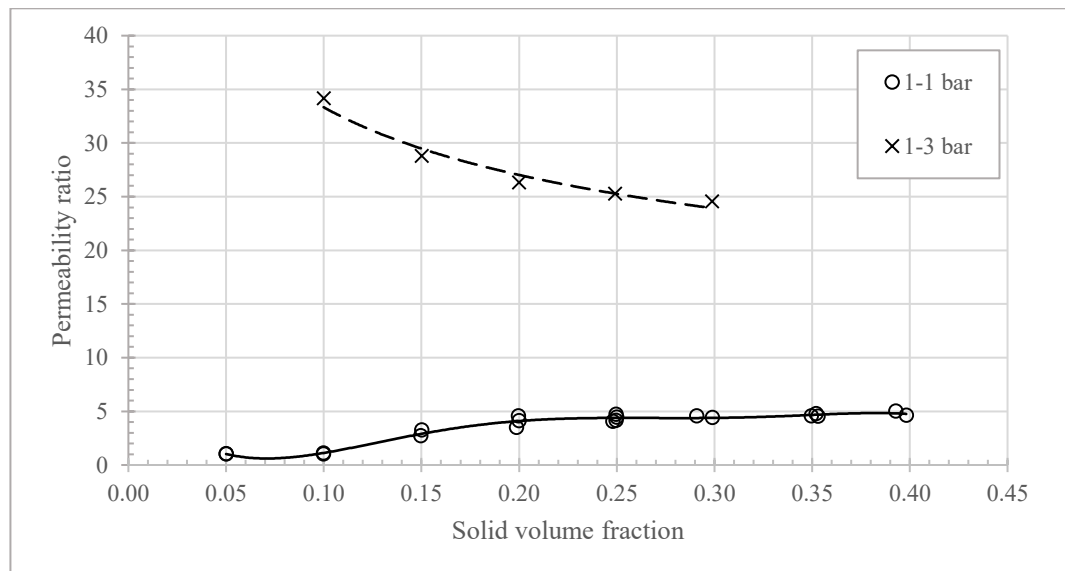
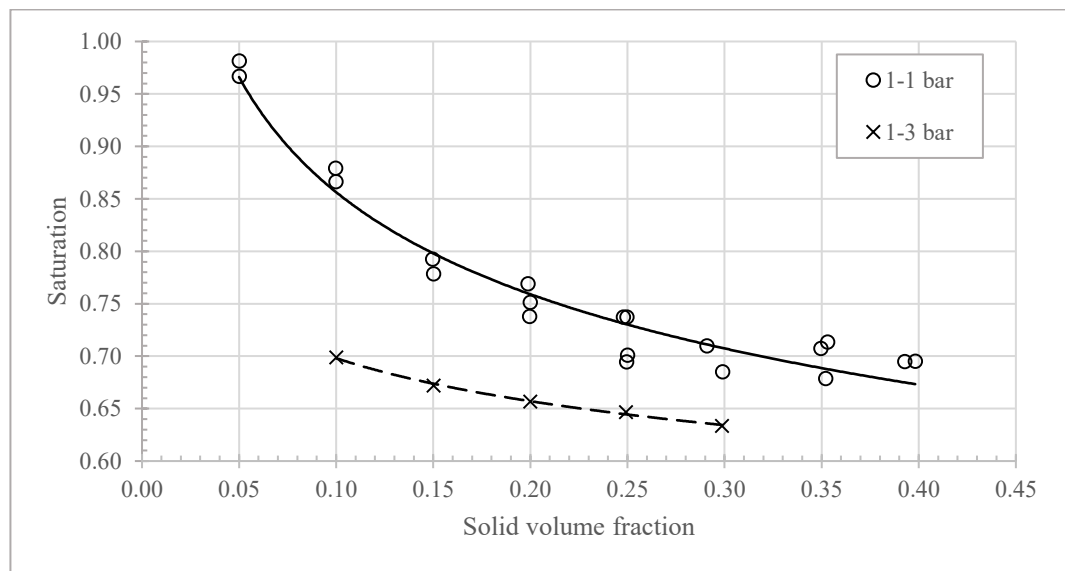


Figure 66. Permeability ratio for KS12 filter cake in various solid volume fraction; 18 mm of filter cake thickness; “1-1 bar” and “1-3 bar” of pressure difference.

There are two reasons to explain the formation of cracking in fine filter cake. The first one is the weak positions, which are formed in large capillaries after the water is pushed out. The adhesive force and the capillary suction force caused by water retained in the small capillaries pulls them. Tensile stress, in this case, is pretty high, as can be seen in Figure 51. The second one is the breaking of fine particle agglomeration under stress during filtration, as mentioned above. While the main reason for macro-cracking, in the case of using “1-3 bar” of compressed air, can be explained by the weaker points occurring in filter cake. The cracking on the filter cake, filtered using “1-1 bar” pressure difference, caused by the second reason in mostly. The sedimentation phenomenon can also explain the reduced trend at the “1-3 bar” of pressure difference. At 0.05 and 0.1 of

volume fraction, the mechanical displacement phase does not appear on filter cake, as seen the low permeability ratio in Figure 66. The compressed air is less enough for the mechanical displacement phase.

The saturation and residual moisture content in Figure 67 show the reduction trend when the volume fraction increase. This issue is suitable for the result, as is shown in Figure 52. Otherwise, although the permeability ratio, as well as the images for filter cakes, which is filtered under “1-3 bar”, shows the high degree of macro-cracking, the amount of water remaining on filter cake is still lowered compare with that of “1-1 bar”. The residual moisture and saturation of filter cake in the case of the “1-3 bar” are lower than those of 1-1 bar. The complete difference of the mechanical of the two phenomena is the reason, as discussed above. Otherwise, the compressed air 1 bar is less enough to push water out of both large and small capillaries. There is less water that can go out. The result in saturation still higher (0.7 - ~1). Meanwhile, for 3 bar in the mechanical displacement phase, more water in larger capillaries is pushed out. The macro-crack occurs, airflow preferentially through the big channels than pores. As a result, dewatering does not take place further, and the saturation only gets to 0.65. Figure 52 as well as Appendix D2, also has the same trend.





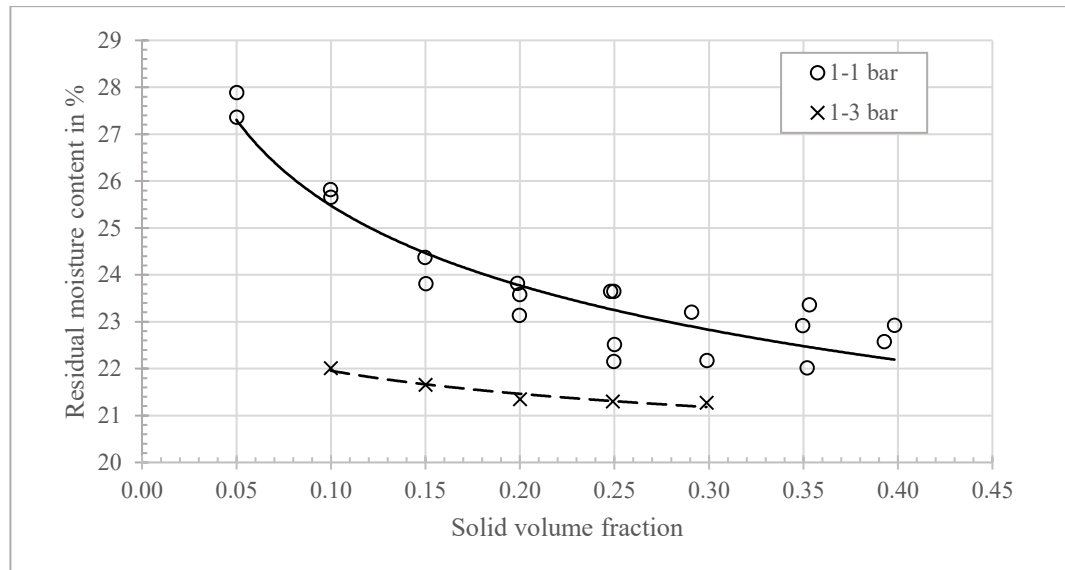


Figure 67. Saturation and residual moisture content for KS12 filter cake; 18 mm of filter cake thickness; “1-1 bar” and “1-3 bar” of pressure difference.

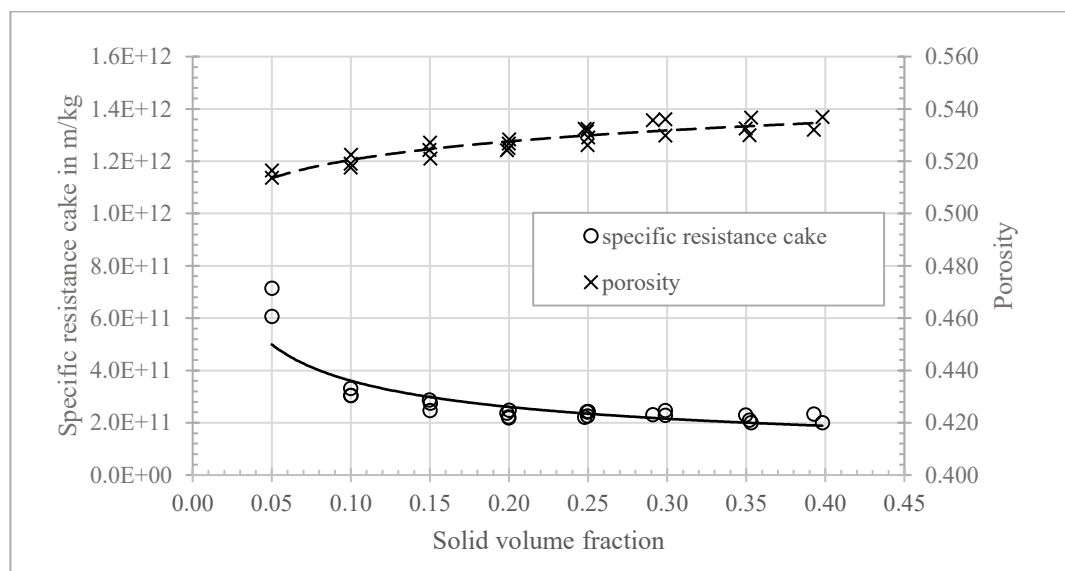


Figure 68. Specific resistance and porosity of KS12 filter cake; 18 mm of filter cake thickness, 1 bar of pressure difference in the cake formation phase.

As with the filtration of coarse-grained material, when increasing the concentration of solids, the result for fine-grained material witnesses a slight increase in porosity from 0.513 to 0.537 and a decrease in specific resistance from  $7 \times 10^{11}$  m/kg to  $2.3 \times 10^{11}$  m/kg. This specific resistance value is achieved at 0.2 of solid concentration, maintained until 0.4 of solid concentration. There seems to be an effect of sedimentation here. Although the data in Figure 69 do not clearly show this difference as well as does not really prove the de-mixing. Actually, the particles are too small to quantify the de-

mixing used PSD-measurements with Laser diffraction. If the result takes into account the potential error-bars, de-mixing may occur at 0.1 of volume fraction. Moreover, Figure 70 shows the graph of the ( $t/V$  versus  $V$ ) curve is bent at 0.05 and 0.1 of volume fraction while the remaining ones are the straight lines. The sedimentation phenomenon dominated these processes [17, 18]. This is the main reason which exacerbates for poor dewatering performance of fine-grained material and the appearance of larger cracks.

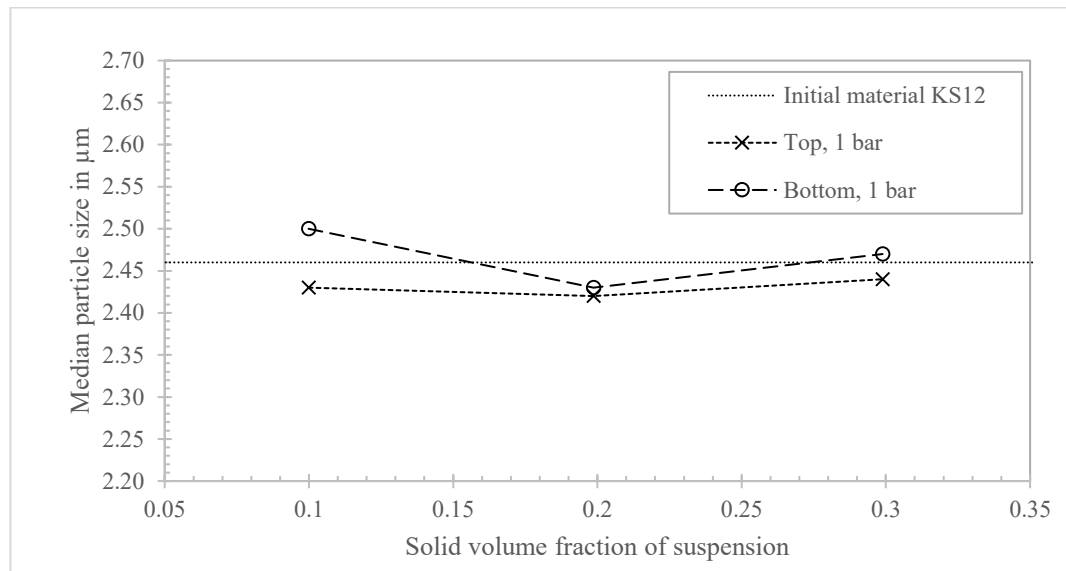


Figure 69. Median particle size on top and bottom layers of KS12 filter cake; 1 bar of pressure difference in the cake formation phase; 18 mm of filter cake thickness.

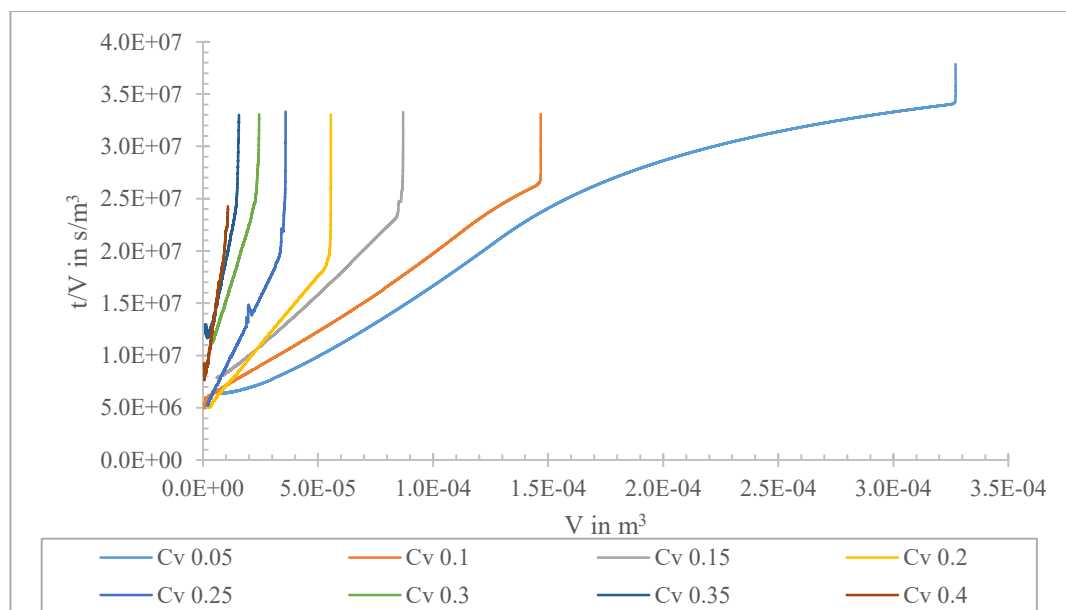


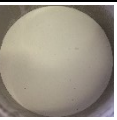









Figure 70. The ratio of filtration time and filtrate volume ( $t/V$ ) as a function of filtrate volume for KS12 in various volume fraction; 18 mm of filter cake thickness; 1 bar of pressure difference in the cake formation phase.

Solid volume fraction		0.05	0.1	0.2	0.3	0.4
KS100	Top					
	Bottom					


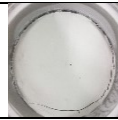

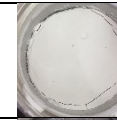





Solid volume fraction		0.1	0.15	0.2	0.25	0.3
KS12	Top					
	Bottom					

Figure 71. Images for KS100 (upper) and KS12 (lower) top and bottom filter cakes with the different volume concentrations of the suspension; the height of filter cake 18 mm; “1-1 bar” of pressure difference.

By visual observation, it can be seen that the coarse-grained filter cake shows a good filtration result. Most of the filter cakes do not have the formation of macro-cracking. There are only a few cases of slight shrinkage when filter low solid volume fraction suspension, and some micro-cracks when filtering the high concentration sludge. However, these micro-cracks do not affect the deliquoring process. The filter cake is stable in shape and has a low residual moisture content.

In the case of filtering the suspension with the difference of the volume fraction, fine material KS100 filter cakes have cracks. The shape of the cracks is a combination of branches, surrounding cracks, and even large cuts cross the filter cake, similar in shape on the upper and lower layer. These are typical signs of macroscopic cracks. The result is the filter cakes are still pretty wet.

#### 4.2.3. Height of filter cake (filter cake deep/ filter cake thickness) effect

Some input parameters are fixed to survey the effect of the height of filter cake on cracks formation. Because of the limitation of the filtration rig, the maximal height of

filter cake of 30 mm and volume fraction are chosen. The different applied pressure cake is “1-1 bar” and “1-3 bar” of pressure difference.

*For coarse material KS100*

Tests are carried out with coarse material (KS100) at 0.3 of volume fraction. It can be seen in Figure 75, the probability of cracking formation as well as the degree of cracking increase when the height of the filter cake goes up. In the survey range of height, the filter cake is mainly dewatered effectively without cracks. In some cases, the micro-shrinkage and cracking appear. However, they do not affect the filtration efficiency. Similar to the image obtained by the filter cake, the permeability ratio in Figure 72 indicates value stability of approximately 1 when the filter cake height reaches 18 mm. The permeability ratio value begins to increase as the filter cake height increases.

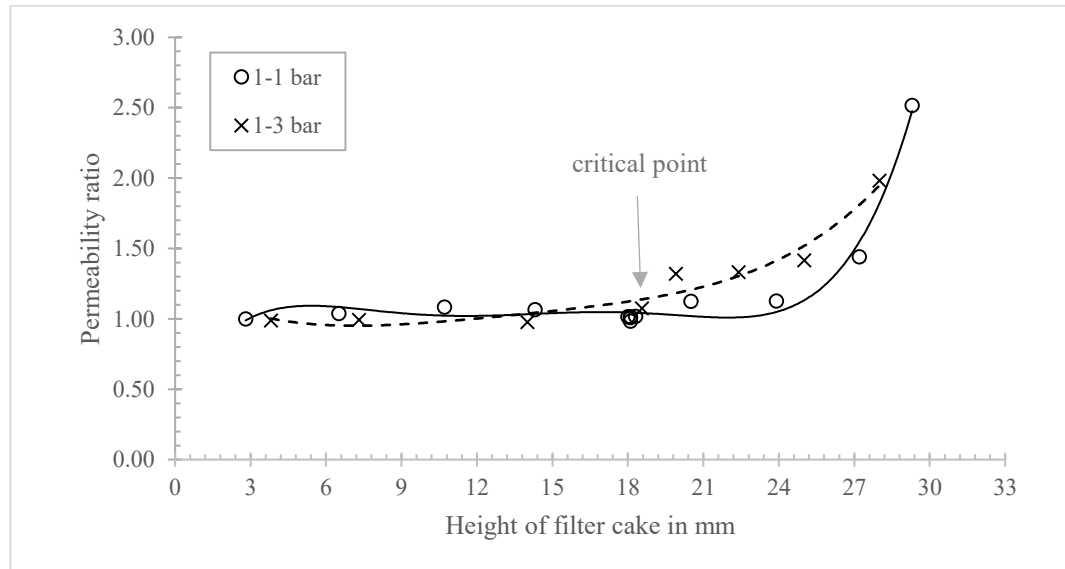


Figure 72. Permeability ratio of KS100 filter cake using “1-1 bar” and “1-3 bar” of pressure difference; 0.3 of solid volume fraction.

The result for cracking in KS100 efficiency of dewatering did not affect as much (the saturation is around 0.2 and 0.4). By increasing the height of filter cake from 15 mm to 23 mm, macro-cracking occurs with the value of permeability ratio more than 20. This issue may explain that the filter cake has been reduced slightly by the filter cake height due to the high pressure applied in the dewatering phase (mechanical displacement phase).

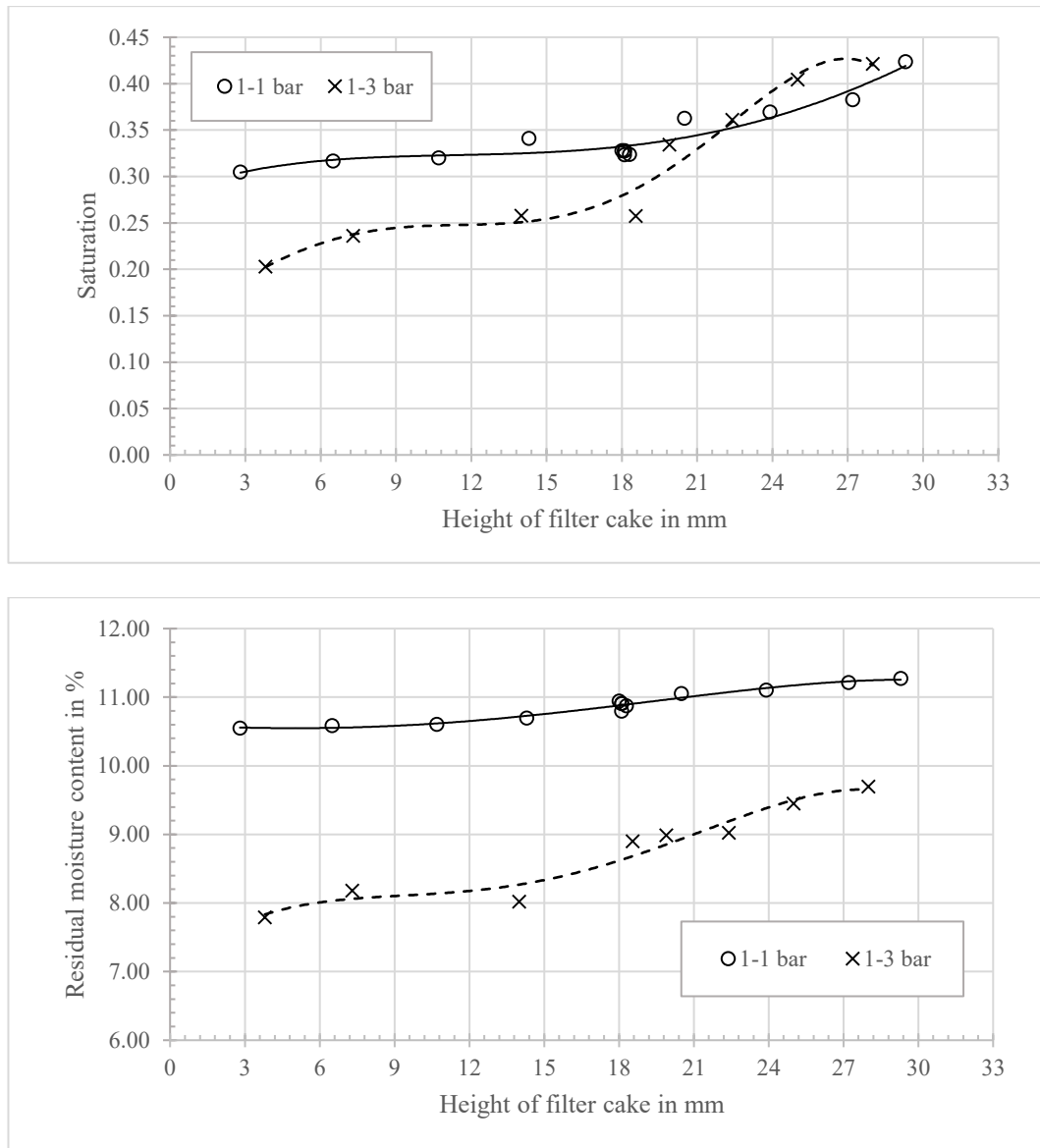


Figure 73. Saturation and residual moisture content of KS100 filter cake using “1-1 bar” and “1-3 bar” of pressure difference; 0.3 of solid volume fraction.

Figure 74 adds to the disadvantage of filtration that the filter cake has a high height, especially for dewatering purposes. The surveyed range of the filter cake deep can be divided into two parts. The first part is the constant area. Although the height increases from 3 to 20 mm, the specific resistance cake remains constant with the value around  $1.4 \times 10^{10}$  m/kg. In the second area: specific resistance shows a rapid and significant increase, almost twice as high as the value in a constant zone when the height reaches 30 mm. The value of porosity, in general, is reduced, and in keeping with the increasing trend of specific resistance.

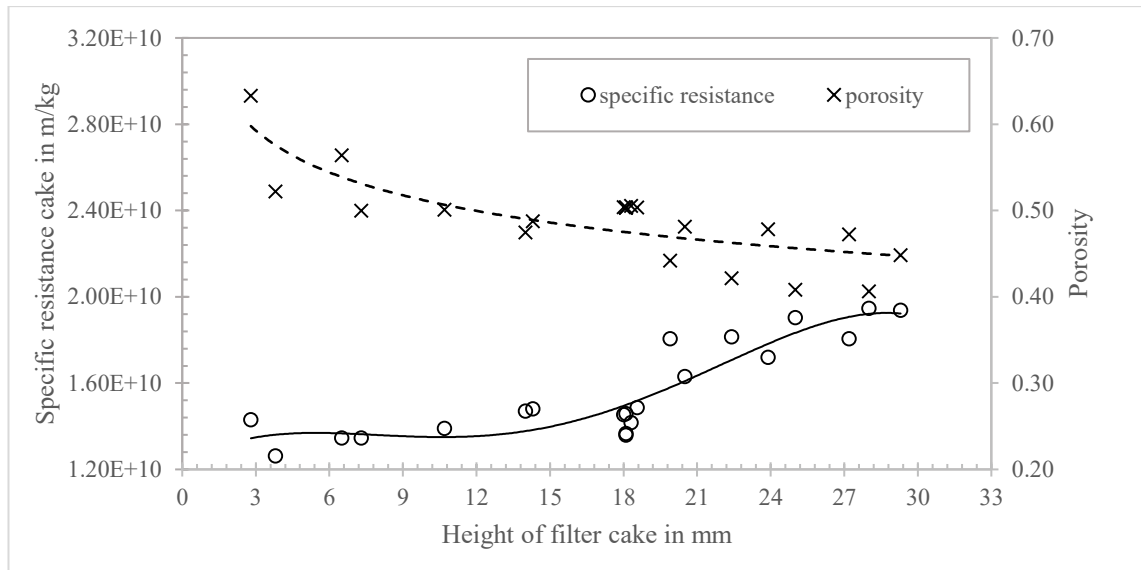


Figure 74. Specific resistance and porosity of KS100 filter cake using “1-1 bar” and “1-3 bar” of pressure difference; 0.3 of solid volume fraction.

The phenomenon of the increasing degree of cracking can be explained by some hypothesis. Firstly is the interpretation of Barua [4] related to the wall effect. The secondary is the mechanism of cracking, as above discussed, which is related to the weak position in the filter cake. One of the mechanisms related to the small filter cake is that it has an intense contact with the filter cloth. Therefore, the filter cake structure can be stabilized [42]. Otherwise, the agglomeration of particles' reason is not to be missed.

The results in his research get a good agreement with Barua's research about the trend probably and the degree of cracking [4]. The more significant losses because of wall friction during filtration are the main reason. The low filter cake has a small contact area with the containment wall. Therefore the compressed force can be applied to the whole filter cake without any significant effect at any particular location. The filter cake is homogeneous. However, with high filter cake, the wall friction is greater due to the large contact area. The compressive force is different at locations on filter cake. It is intense in the middle of the filter cake and reduces gradually to the edge, especially where contacting with the containment wall. This results in a lower packing density on the edge of the filter cake. Gray, in his book [49], pointed out that “the cyclic variation in voidage extends to a distance of about 4.5 to 5 particle diameters before it is dissipated”. The weaker points appear at the interface of particles and containment walls. The different distribution of density and stress lead to the cracks formed around the filter cake edge.

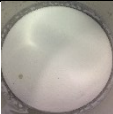
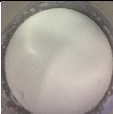








This explanation is valid for the small filter Nutsche and is less or no significance meaningful on a large scale or in practice.

On the other hand, due to the thick filter cake (high wall friction), the ability of stress transition from top to the bottom of the filter cake under compressed air is low. The upper part of the filter cake becomes stark with high packing density. Due to lost stress, the particles in the lower part have loose connections. The elastic strain is recovered. The un-uniform in packing density and filter cakes are easily divided into two parts horizontally (which is horizontal cracks), or cracks at the bottom.

One more assumption related to the agglomeration occurs in high filter cake thickness. The increasing of the height filter cake means the mass of material increases in the fixed space. The density of fine particles rise. It is an excellent condition to increase the chance of encountering and agglomeration of fine-grained particles in the material.

One final assumption that can be mentioned is the effect of sedimentation. The increase in filter cake height is due to the corresponding increase in the amount of material mixed with distilled water. Due to the constant filtration area, the distance of the settling of particles increases. Coarse particles have enough time to settle on the filter cloth, while fine particles take longer. Stratification may occur during filtration. However, it has not been observed clearly in the case of coarse material (Appendix B8 and B9). This situation is encountered more when filtering fine-grained materials, which will be discussed further in the next section (in the case of limestone KS12).

Overall, the probability and degree of shrinkage cracking just only occur in the high filter cake. The permeability ratio increases rapidly after the critical point of filter cake deep. For filter cake height smaller than this critical point, the material is well dewatered without cracks. The value of the permeability ratio as well as other output parameters (saturation, residual moisture content, porosity, and specific resistance), has no change. The shrinkage cracking occurs almost around the filter cake, near the interface with the containment wall. This proves that the mechanism of forming cracks is mainly due to the wall effect. It is the systematic effect, which derives from the lab-scale equipment. This negative effect will be improved further in pilot-scale and industrial – scale. From the result of residual moisture content, the use of the high-pressure difference in the mechanical displacement process (also called the deliquoring/dewatering phase) provides high efficiency for the filtration process, especially in the water draining of products.

Filter cake height in mm		6.5	10.7	14.3	23.9	29.3
"1-1 bar"	Top					
	Bottom					











Filter cake height in mm		18.6	19.9	22.4	25.0	28.0
"1-3 bar"	Top					
	Bottom					

Figure 75. Images for KS100 filter cake with difference height; 0.3 of solid volume fraction.

The image of the filter cakes reinforces the results of the permeability ratio. The higher the height of the filter cake, the greater the probability and extent of cracking. Micro-cracks as well as shrinkage appear more when the filter cake thickness reaches 24 mm or more. The trend is suitable for both filtration processes that use the "1-1" bar of pressure difference as well as the "1-3" bar of pressure difference.

#### *For fine particle KS12*

The same result also gets with the tests for coarse particles. Tests were conducted with 0.1 of the volume fraction. Figure 76 shows the increasing trend of the permeability ratio when the filter cake thickness increase. The value for the "1-1 bar" condition is from 1 to 5, with the height from 18 - 34 mm. Those values for the "1-3 bar" condition is 10 to 60 with the height of the filter cake rise from 8 to 30 mm. By the visual observation, macro-cracking occurs at almost cases in the filter cake. The shape of these cracks is quite diverse. Some cracks cut across the filter cake and spread to the bottom of the filter cake. In other cases, the cracks appear around the circumference of the filter cake, close to the interface of particles to the containment wall. There are some cracks shaped like branches.



The diversity in the shape and degree of cracks are caused not only by the filter cake height effect but also by the different crack formation mechanism.

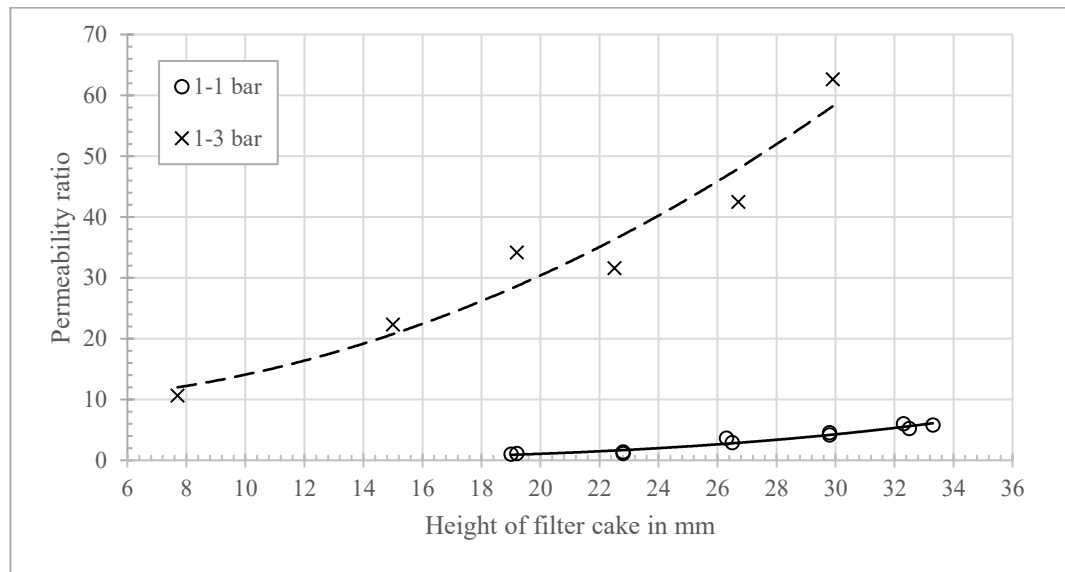


Figure 76. Permeability ratio of KS12 filter cake using “1-1 bar” and “1-3 bar” of pressure difference; 0.1 of solid volume fraction.

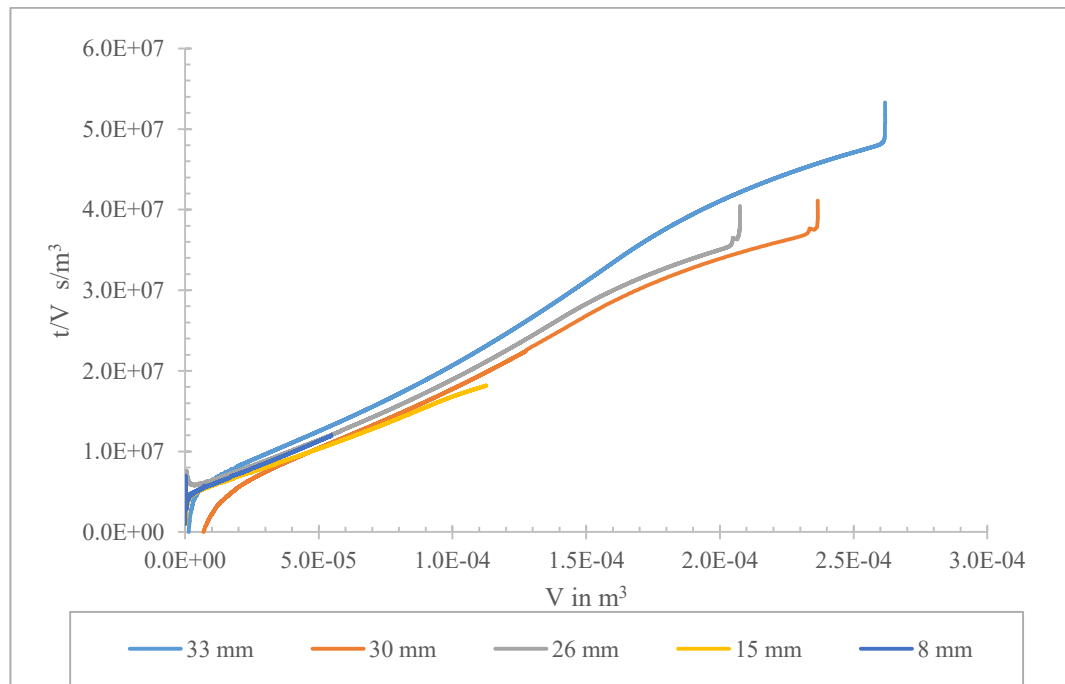
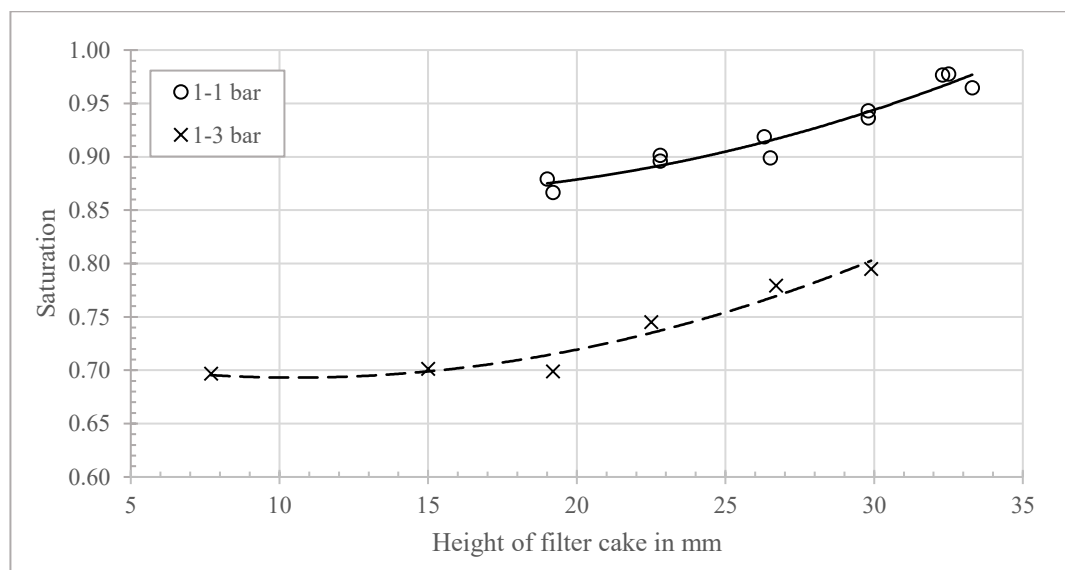


Figure 77. Diagram  $t/V$  versus  $V$  of filter cake with the various filter cake deep; 0.1 of solid volume fraction; 1 bar of pressure difference in the cake formation phase.

The reason for crack formation can be the high tensile stress on the filter cake, the wall effect, agglomeration, and the sedimentation. The high tensile stress usually creates

the crack which cut across the filter cake, propagate through to the bottom. The wall effect makes the crack around the filter cake. The agglomeration and sedimentation can create the shrinkage, micro-cracking. There have been indications that the sedimentation in the filter cake at a high filter cake is not observed for coarse materials. This statement is shown in Figure 77. The ( $t/V$  versus  $V$ ) curve in case of high filter cake (from 26 mm and more) are bent at some positions. Meanwhile, the curves for 8 and 15 mm filter cake height are straight lines. Some filter cakes are subject to an individual mechanism; many cracks on filter cake are caused by the combination of all mechanisms.

The different phenomenon also leads to a difference in the degree of disadvantage. Overall, filter cake has a high permeability ratio (high degree of cracking) and has a high saturation as well as great residual moisture content. As can be seen in Figure 78, the saturation increase slightly from 0.9 to approximately 1 when filter cake deep up to 33 mm ("1-1 bar" condition). The moisture content is pretty high, with approximately 27 %. The filter cake is still wet. It can be said that the efficiency of solid-liquid separation is low. While the value of saturation and moisture content is still high with 0.7 - 0.8 (corresponding the 22 - 23% of residual moisture content), the result is quite excited for the cake, which is filtered using the "1-3 bar" condition. Although the degree of cracking is higher than that using a "1-1 bar" condition, the efficiency of dewatering is a little better.



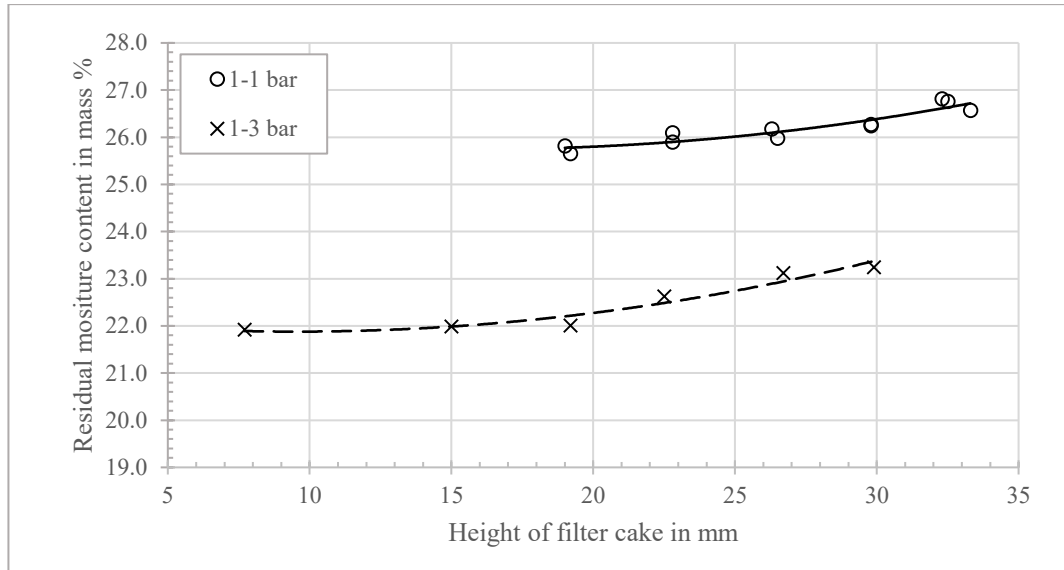


Figure 78. Saturation and residual moisture content of KS12 filter cake using “1-1 bar” and “1-3 bar” of pressure difference; 0.1 of solid volume fraction.

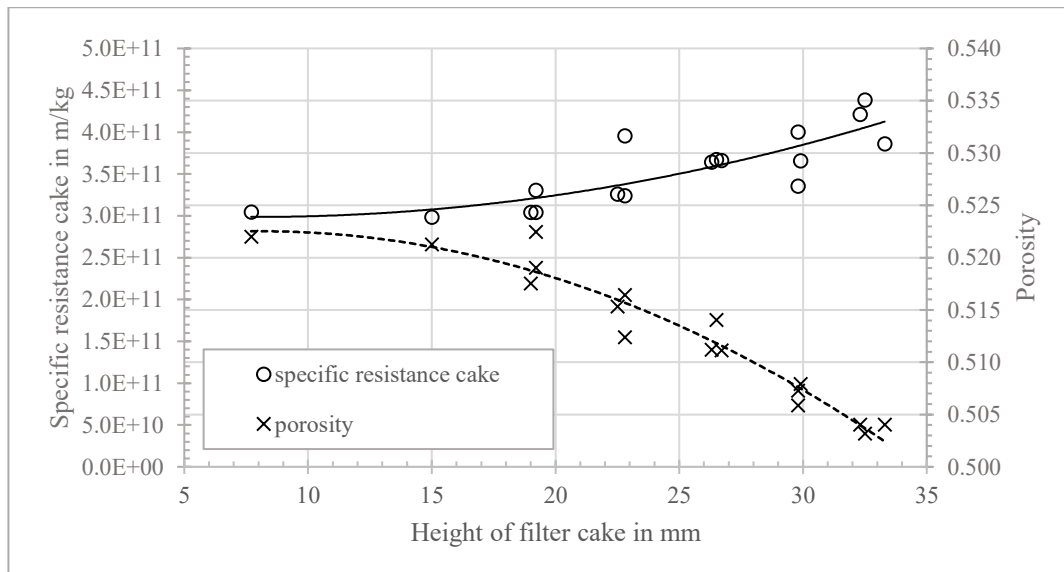












Figure 79. Specific resistance and porosity of KS12 filter cake; 1 bar of pressure difference in the cake formation phase; 0.1 of solid volume fraction.

The specific resistance cake and porosity show an opposite trend. While the specific increase gradually from  $3 \times 10^{11}$  m/kg to  $4 \times 10^{11}$  m/kg, the porosity reduces very slightly from 0.525 to 0.505. Two opposite trends of specific resistance and porosity get the agreement with the test result above as well as the investigation of Rumpf - Gupte [46], Carman – Kozeny [15, 47]. The reason for the increase in specific resistance as well as the lower porosity is the sedimentation phenomenon. The fine particles settled on the coarse particles lead to high resistance (come with the much lower porosity) on top of the

filter cake. The result is that the total values of the whole cake also change according to the trend above, compared with the homogeneous filter cake.

Filter cake height in mm		19.2	22.8	24.3	29.8	32.3
“1-1 bar”	Top					
	Bottom					



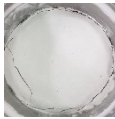



Filter cake height in mm		7.7	15.0	22.5
“1-3 bar”	Top			
	Bottom			

Figure 80. Images for KS12 filter cake with different height; 0.1 of volume fraction.

In general, the filter cakes have the appearance of shrinkage and macro-cracking. This is completely reasonable because the test material is a super-fine material KS12. However, it can be observed that, at a low filter cake height, the degree of cracking is less, even not occur (filter cake in case of 1-1 bar pressure difference, 19.2 mm height). In addition, when filtering the filter cake at the application pressure of 1-3 bar, the level of cracking is greatly reduced, the residual moisture content is also improved significantly.

#### 4.2.4. Pressure difference effect

Air pressure difference is one of the critical parameters, which affect cracking formation. This operation parameter can be regulated to achieve the most efficiency for many purposes (prevent the cracking, good dewatering, economy, etc.). Tests were conducted with a variety of pressure differences. The air pressure difference kept stable

during the cake formation phase and deliquoring phase. The height of the filter cake approximately 18 mm. Suspension with different solid volume fractions is chosen in order to discover the crack formation as well as the efficiency of filtration.

For the coarse material (as can be seen in Figure 81 and Figure 82), the tendency of cracking when at various pressure difference get the good agreement with Barua's research [4], Wiedemann's research [5] and Anlauf's research [42]. The probability of cracking formation as well as the degree of cracking are likely reduced or keep stable. As summarised in Table 3, the reasons for these good results are higher packing density, pre-deformation flocs; lower shrinkage potential; increase tensile strengths due to increase pre-stress during filtration.

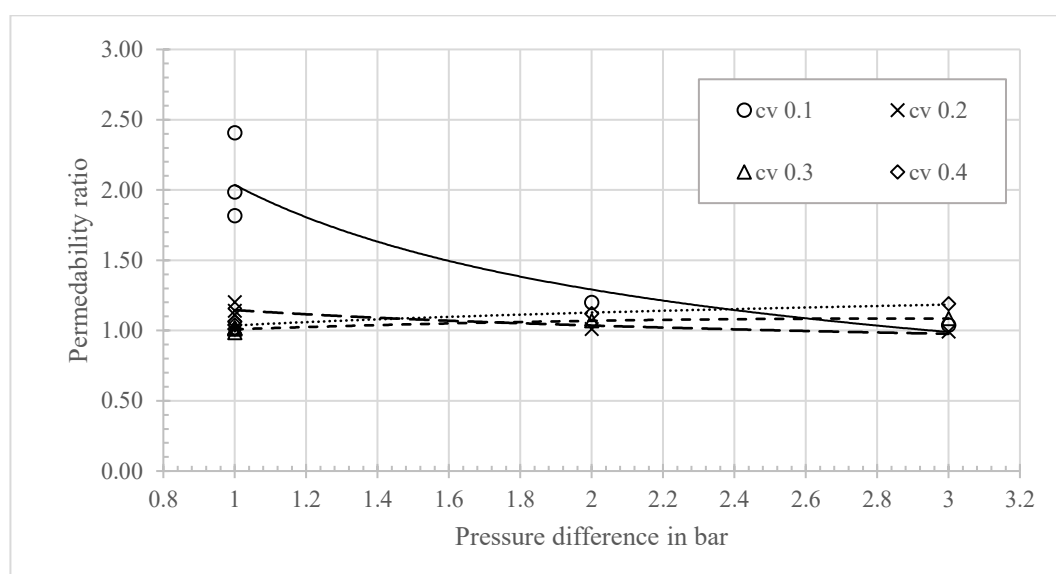


Figure 81. Permeability ratio of KS100 (coarse material) filter cake using the variety of pressure difference; 18 mm of filter cake thickness.

Also, the increase in applied pressure difference reduces the wall effect as well as the sedimentation phenomenon during the formation of the filter cake. With a higher pressure difference, more water is pushed out of the capillaries; the filter cake reaches the irreducible state as can be known as the state in which the amount of water in filter cake can not reduce anymore, although the high applied pressure difference and long time. Additionally, with high pressure, water is drained simultaneously at large and small capillaries. The number of weak positions, which is formed in filter cake, is also small. The main and also the initial cause of crack formation is prevented. For coarse materials, the permeability ratio is constant at 0.3, 0.4 of the solid volume concentration, around 1 of magnitude. The result proves that the filter cake can completely dewater without crack

formation from 1 bar pressure. This excellent filtration process remains unchanged when the pressure increase. However, for 0.1 of solid-phase volume concentrations, there is a significant improvement in filtration efficiency as the crack degree goes down gradually to 1 when the applied pressure is increased. The image in Figure 81 also clearly indicates these.

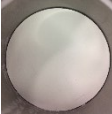

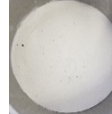

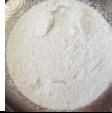













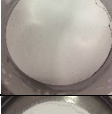





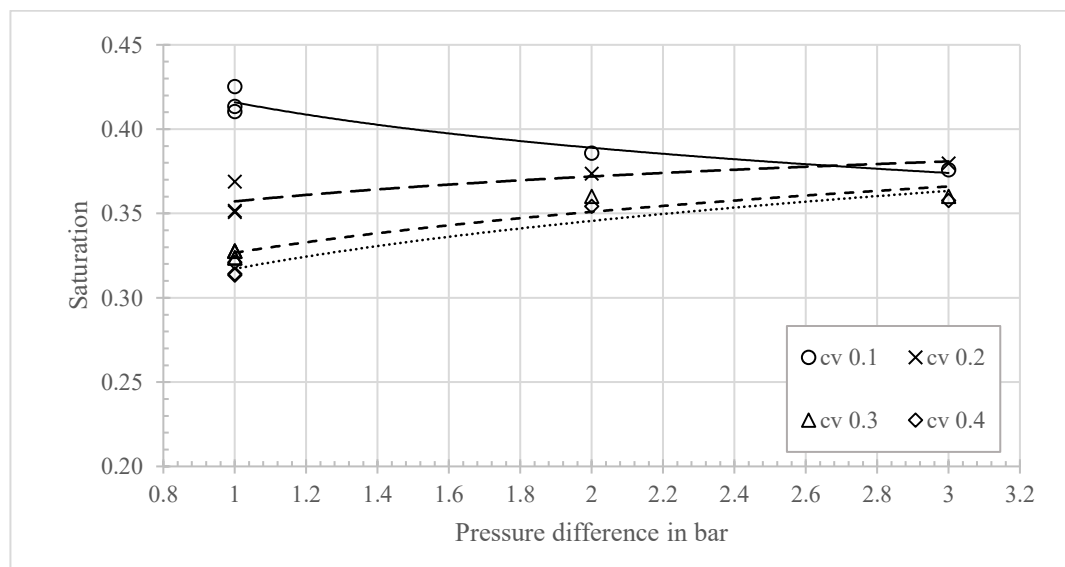
The pressure difference in bar							
Volume fraction cv		“1-1 bar”		“2-2 bar”		“3-3 bar”	
0.1	Top						
	Bottom						
0.2	Top						
	Bottom						
0.3	Top						
	Bottom						
0.4	Top						
	Bottom						

Figure 82. Images for KS100 filter cake in the variety of pressure difference; 18 mm of filter cake thickness.

Along with the improvement of crack formation in filter cake, saturation and residual moisture also change positively. In most cases, as to be shown in Figure 83, indicate a slight or unchanged decrease. This saturation level generally reaches a value of around 0.35, while the residual moisture content decreases gradually to minimum as 10%. The reason for the decrease in moisture, while the saturation remained the same trend because of the higher packing density at high applied pressure difference. The comment is also expressed in Figure 84. The specific resistance generally increases slightly while

the porosity reduces moderately. The exception occurs when filtration of the feed suspension with a solid volume fraction of 0.1. It can be seen that specific resistance and porosity both decreases with the increasing applied pressure difference. Specific resistance tends to decrease to a similar value of  $1.5 \times 10^{10}$  m/kg, like to the result with other volume fraction of feed slurry. This result achieves because the filter cake at high applied pressure has become as homogeneous as possible. Porosity witnessed a sharp decrease due to the transition from the sedimentation area to a homogeneity area and achieving a constant value of 0.49. Overall, this is an interesting compressibility effect when the pressure difference increase. It can be seen that the residual moisture content decrease or stay constant while the saturation grows up. The saturation seems not fit to the capillary pressure curve, measured in Figure 53. The saturation is in the range of (0.3-0.8) in the range of 1 to 3 bar capillary pressure. Some points can explain this issue:

- The data in Figure 53 is measure in operational parameters (1 bar pressure difference for cake formation – 0.1 to 3 bar capillary pressure for dewatering). The data for those tests are conducted in same pressure difference for cake formation and deliquoring (1-1 bar; 2-2 bar; 3-3 bar)
- In capillary pressure measurement, the filter cake is compressed by a piston with the pressure up to 4.5 bar. The filter cake is much more compressed, results in the water inside the filter cake can flow out easily.
- The filter cloth for all tests is standard SK006, in which the water and air can flow simultaneously. While the semi-permeable membrane, which only liquid can flow through, is used for capillary pressure measurement



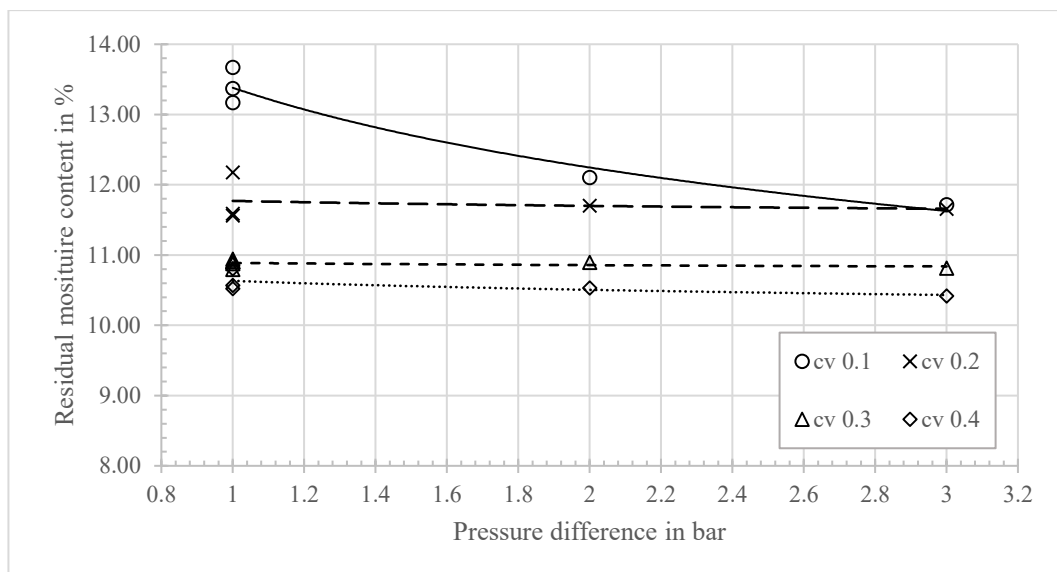
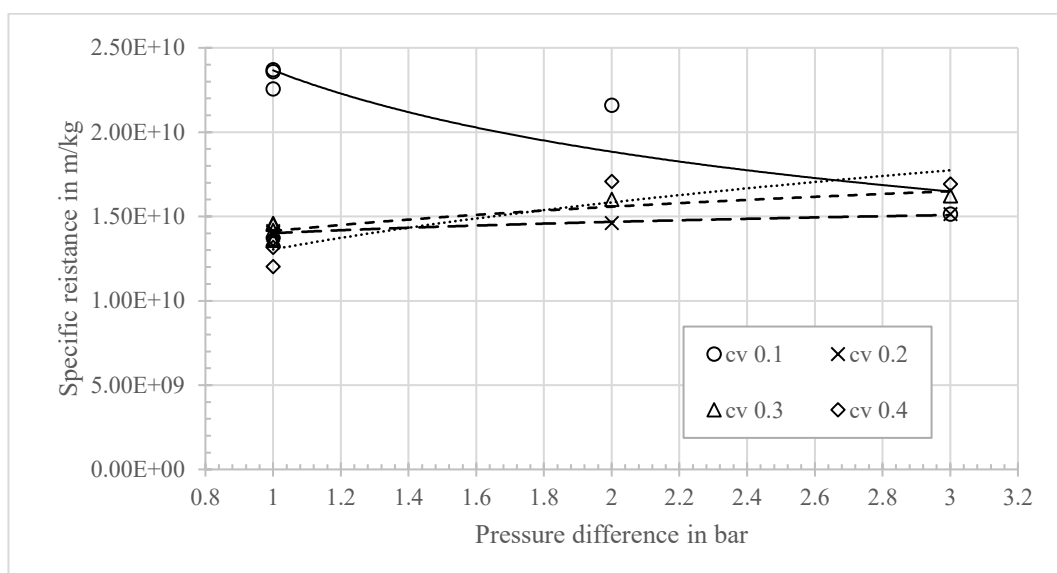


Figure 83. Saturation and residual moisture content of KS100 (coarse material) filter cake using the variety of pressure difference; 18 mm of filter cake thickness.





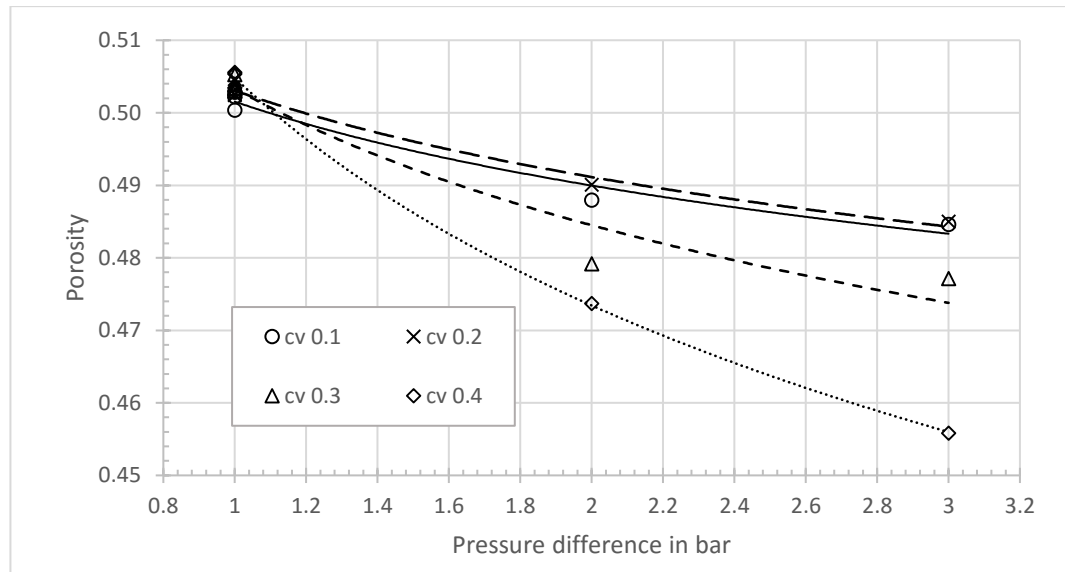


Figure 84. Specific resistance and porosity of KS100 (coarse material) filter cake using the variety of pressure difference; 18 mm of filter cake thickness.

For fine particles KS12 (Figure 85), the applied pressure difference is increased from 1 and just reach 3 bar due to the limitation of the experimental equipment. Tests were conducted in 18 mm of the filter cake. The volume fraction is 0.1, 0.2, 0.25 and 0.3. Figure 85 shows the increasing trend of the permeability ratio. This trend is consistent with the images observed in Figure 86. The probability and extent of cracks increase rapidly as the increase of the applied pressure difference. The value of the permeability ratio increased from 5 to approximately 25. There was no significant difference in the filter cakes with different initial suspension concentrations.

The increasing trend of cracks shows a difference from the coarse materials as well as the conclusions of previous studies. The reason for this phenomenon is the formation of weaknesses during the displacement of water out of the capillary. Because the size of the capillaries is too small, the applied pressure difference is not significant enough to push water out of the capillaries simultaneously. Also, the filter cake is in a "capillary state," which is a state of high stress, which is mentioned in Figure 49 and Figure 51. The particles subjected the influence of capillary forces, pulling particles in the weaker positions towards its side. As a result, large channels are formed. Air flows preferably through the cracks. The deliquoring process is seriously affected. A stronger dewater force is proposed, which can be drained water from the tiny and ultra-tiny capillaries. Then the filtration efficiency will be improved with no cracks. Moreover, the

expected results could reach an agreement with the previous studies as well as the trend of coarse particles.

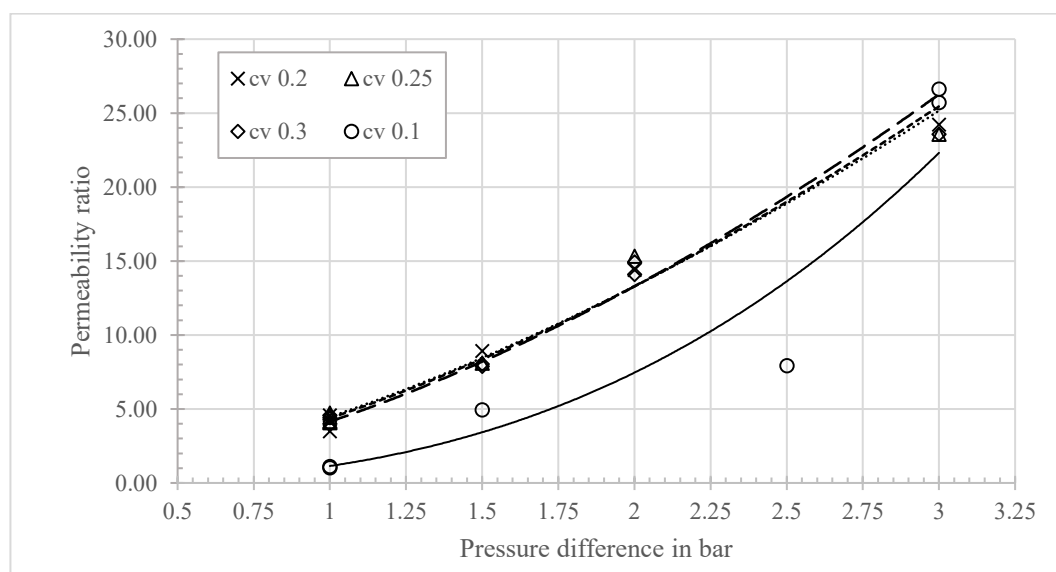


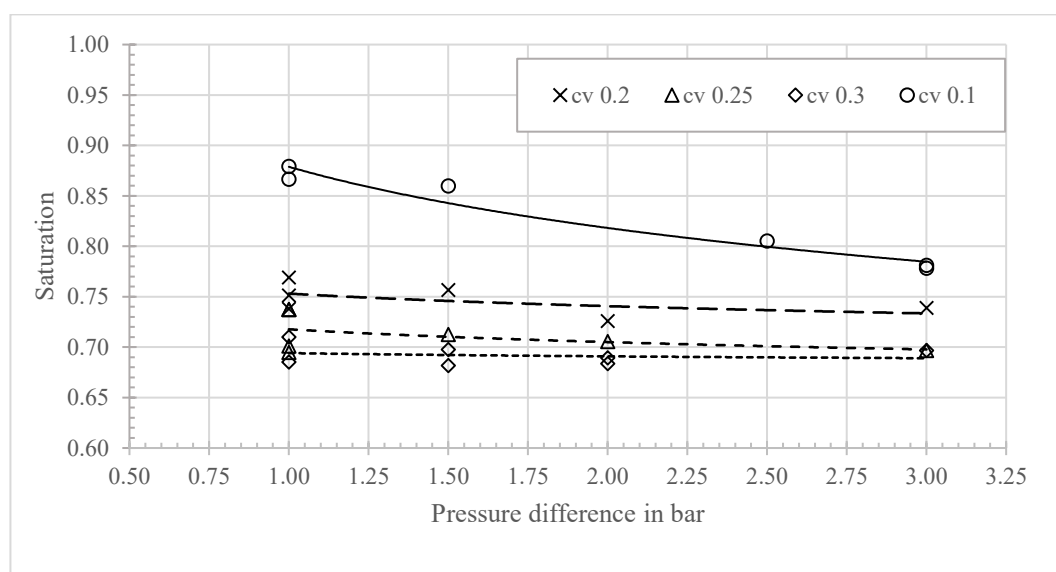
Figure 85. Permeability ratio of KS12 (fine material) filter cake using the variety of pressure difference; 18 mm of filter cake thickness.

Volume fraction cv		Pressure difference in bar			
		"1-1 bar"	"1.5-1.5 bar"	"2-2 bar" ("2.5-2.5 bar" in case of cv 0.1)	"3-3 bar"
0.1	Top				
	Bottom				
0.2	Top				
	Bottom				
0.25	Top				
	Bottom				
0.3	Top				



Figure 86. Images for KS12 filter cake in the variety of applied pressure difference; 18 mm of filter cake thickness.

Otherwise, cracking may be caused by the agglomeration of very fine particles, as mentioned above. The mechanism of cracking is also referred to by Barua [4]. The agglomerated fine particles mixed other particles and contacted with particles network. Because of the weak bond of flocs, they have deformation and initiation of the crack network. The collapse of the whole structure occurs. At higher pressure, where filter cake is formed and reaches to the high packing density stage (as can be seen in Figure 88 – the trend of specific resistance cake and porosity), the flocs are broken before capillary pressure entry. The cracking should be prevented as the KS100. However, because of the considerable amount of fine particles in the material and the lack of magnitude of applied pressure, the flocs are not broken totally. Finally, macro cracking formation as the mechanism mentioned above.



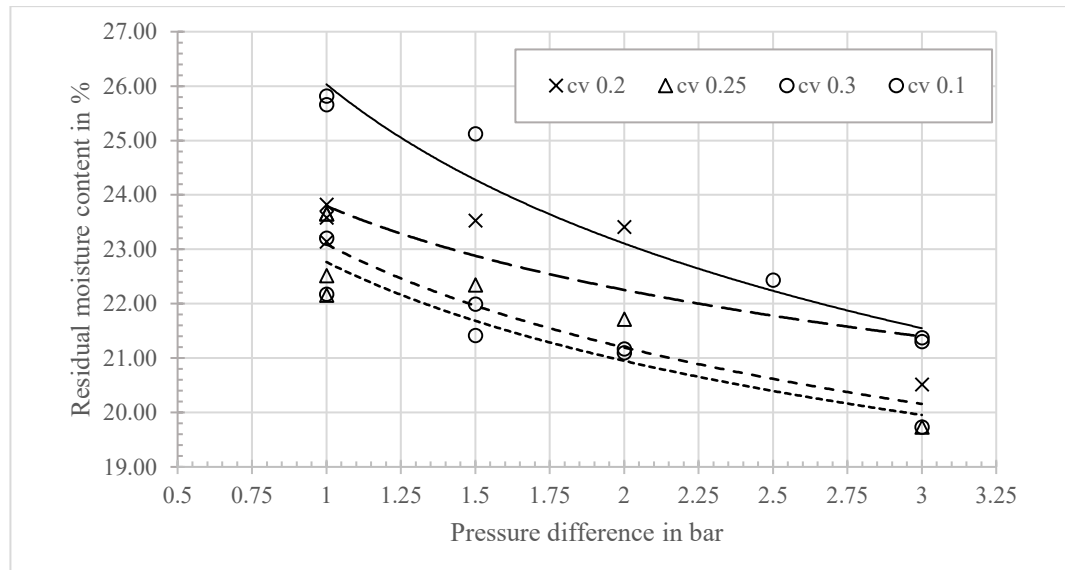


Figure 87. Saturation and residual moisture content of KS12 (fine material) filter cake using the variety of pressure difference; 18 mm of filter cake thickness.

In general, despite the significant increase in crack degree, there was no significant difference in saturation and residual moisture content, except the case of 0.1 of volume fraction. Saturation is in the range of 0.69 to 0.77. Corresponds to it is the moisture around from 20% to 25%. These values for 0.1 of volume fraction are from 0.88 to 0.78, correspond 26% to 21.5 % of residual moisture content. The result of saturation as well as the residual moisture content are lower compare with the data of capillary pressure measurement, as can be seen in Figure 51. Those results are similar to the filtering KS100 result, as mentioned above. The reason can be explained base on the difference of filter media, the applied air pressure during filtration and the compressive filter cake by the piston (in case of capillary pressure measurement). Overall, these values are still high because much water exists in the filter cake. The formation of cracks prevents the dewatering process furthermore.

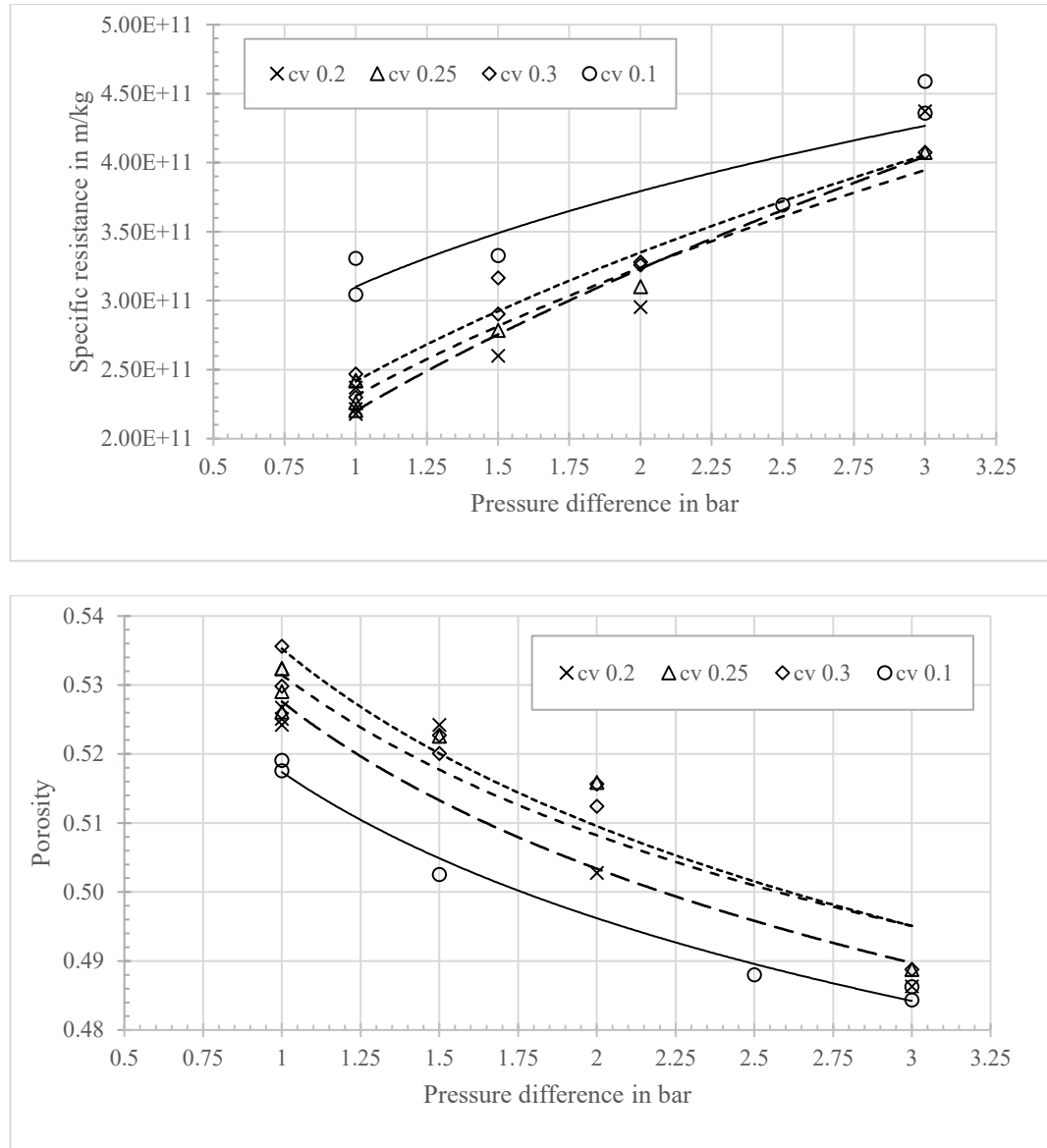


Figure 88. Specific resistance and porosity of KS12 (fine material) filter cake using the variety of pressure difference; 18 mm of filter cake thickness.

Figure 88 shows the relationship of specific resistance and porosity with an increasing applied pressure differential. While the specific resistance increased from  $2.2 \times 10^{11}$  to  $4.5 \times 10^{11}$  m/kg, porosity decreased from about 0.53 down to approximately 0.485. This result reached an agreement with the findings of Rumpf-Grupte [46], Carman–Kozeny [15, 47], as mentioned above. In addition, the results also show that the material is seem compressed at the high applied pressure difference. The proof of this comment derives from the result of the decrease of overall porosity, along with an increase in specific resistance filter cake. Otherwise, as shown in Figure 87, while the residual moisture content tends to decrease drastically, the saturation is almost unchanged. This phenomenon indicates that the void volume has been reduced in the filter cake at the high

applied pressure. A reasonable explanation can be made regarding an increase in the packing density. At low applied pressure difference, the low and loose packing density is caused by the effect of fine grain size, wall effect. When the applied pressure increases, the compressive force becomes stronger, exceed the influence of the above factors. Filter cakes have a higher and tight packing density.

Moreover, one of the assumptions related to the compression of the filter cake is the agglomeration of ultrafine particles. When the high-pressure difference is applied, there is a pre-deformation of flocs during a fully saturated state. The result is the reduction of void volume in filter cake. However, this is still the hypothesis, needs more proof in future work.

#### 4.3. The difference in the crack formation by using steam pressure filtration

As mentioned above by Widermann and Stahl [5], the reduction of surface tension lead to the decrease of shrinkage potential as well as minimum compressive pressure. One of the most economical ways of providing the high temperature is, using saturated or superheated steam instead of the gas during the mechanical displacement phase. By using steam pressure filtration, which is the combination of the mechanical and thermal process, is not only the reduction of probability of the cracking formation but also the improvement of dewatering efficiency. Otherwise, its mechanism, which has the simultaneous displacement of water, can lead to the reduction of the tensile stress as well as avoid the weak points on the filter cake system.

The results for both fine-grained limestone and coarse grain limestone were not as expected. The general trend shows that the probability and extent of crack formation still occur when using steam pressure filtration. However, the probability and the degree of cracking for both materials are different compared to conventional pressure filtration. The saturation and residual moisture content are also improved partly.

Tests were firstly conducted using steam pressure filtration for fine material KS12. The filter cake is formed in Nutsche, according to VDI 2762-2[18]. In the next step, the steam enters the Nutsche by the opening magnetic valve. The thermocouple TC3 is in contact with the filter cloth to measure the temperature of the filtrate. Otherwise, it is also to investigate the moment of steam breakthrough (the temperature reaches approximately 100 degrees Celcius). The information about the temperature profile of tests is shown in Appendix C3. After entering the Nutsche, the steam penetrates the filter cake. The test is

ended when the steam pressure breakthrough the filter cake (mechanical displacement phase end). The venting valve is opened slowly[12, 13]. However, due to the pressure difference between the inside of the Nutsche and the ambient environment, the hot water in the filter cake becomes superheated and evaporates. The mechanical force caused by this evaporation leads to the filter cake destruction, as is described by Peuker and Stahl [8]. Thus, the images of the filter cake after the deliquoring phase using steam pressure filtration, which is captured by the camera, cannot properly reflect the cracking probability and degree. Most of the filter cakes have a very low tendency to crack when observed through the Nutsche's sight glass during the mechanical displacement phase. Although there is no filter cake image is recorded, the result of tests which are shown in Figure 89, Figure 90 (at the variety of volume fraction) and Figure 91, Figure 92 (at the variety of filter cake thickness) also indicated the efficiency of steam pressure filtration as well as the different cracking probability between two kinds of filtration.

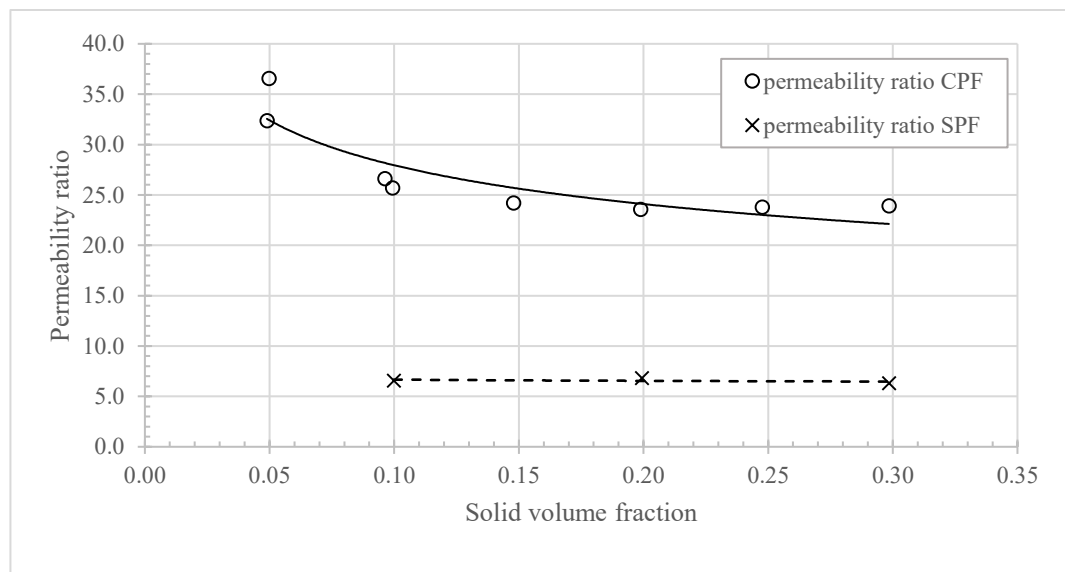


Figure 89. Permeability ratio of KS12 filter cake using conventional pressure filtration (CPF) and steam pressure filtration (SPF) in various volume fraction; “3 -3 bar” of pressure difference; 18 mm of filter cake height.

At the variety of solid volume fraction of suspension, it can be seen while macro-cracking occurs at every volume fraction using conventional pressure filtration, there are only shrinkage micro-cracking filter cakes after filtering by steam. The corresponding permeability ratio for the two types is around 6 and 25, respectively. Although the permeability ratio of filter cake after steam pressure filtration is still high, it is much smaller in comparison to those caused by conventional. By using the steam pressure

filtration, the amount of water after deliquoring is also better ( $S_{SPF} \sim 0.7-0.8$  (no drying phase)) <<  $S_{CPF} \sim 0.95$  (no drying phase)).

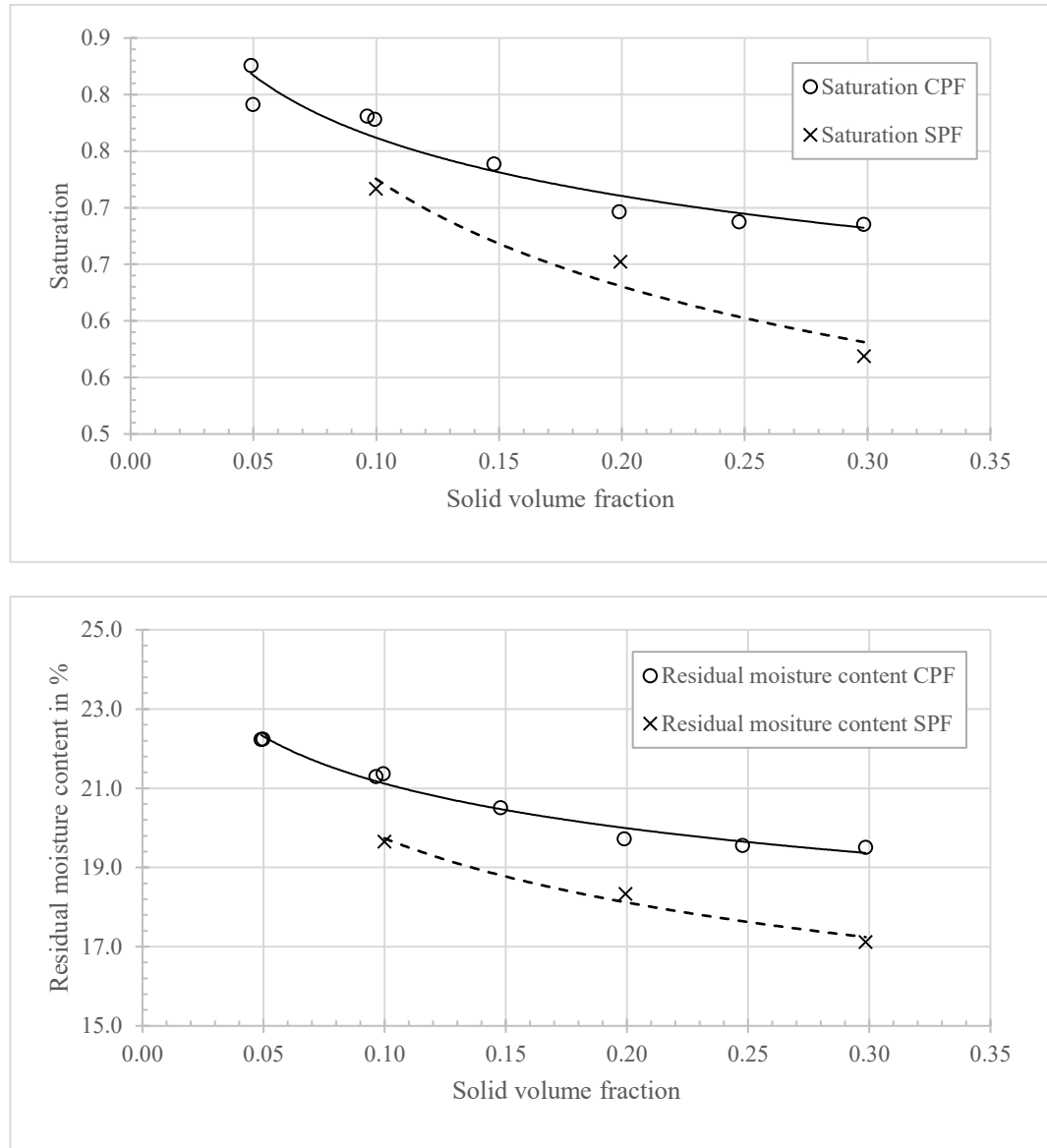


Figure 90. Saturation and residual moisture content of KS12 filter cake in various volume fraction; ; using SPF and CPF ; “3-3 bar” of pressure difference; 18 mm of filter cake height.

The phenomenon of filter cake using steam pressure filtration with limestone continue to repeat when observing the effect of filter cake height on the filtration result and crack formation. For fine material, the results are quite positive when both the permeability ratio, saturation, and moisture content of filter cake show a better degree compared to traditional filtration. The permeability ratio increase from 3 to 10 when the filter cake reaches to 22 mm. They are much smaller than 30 of permeability ratios at the



same height when using conventional pressure filtration. The degree of shrinkage cracking decrease leads to the water inside the filter cake also lower. For thin filter cake (4 mm), the residual moisture content is approximately 14%. At the highest surveyed filter cake (22 mm), this value is also 20%. Generally, the amount of water using steam pressure filtration is lower than that of conventional pressure filtration. However, the difference is not significant, as can be seen in Figure 92. The results support that continuous condensation may occur during the process. The longer the de-watering time becomes the closer the lines get (too much time for un-controlled condensation).

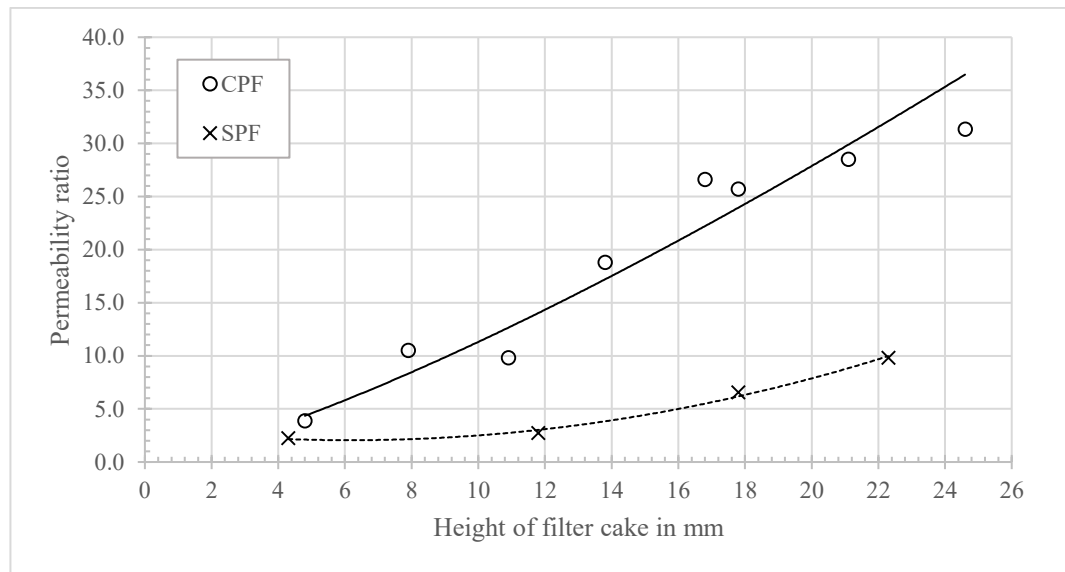
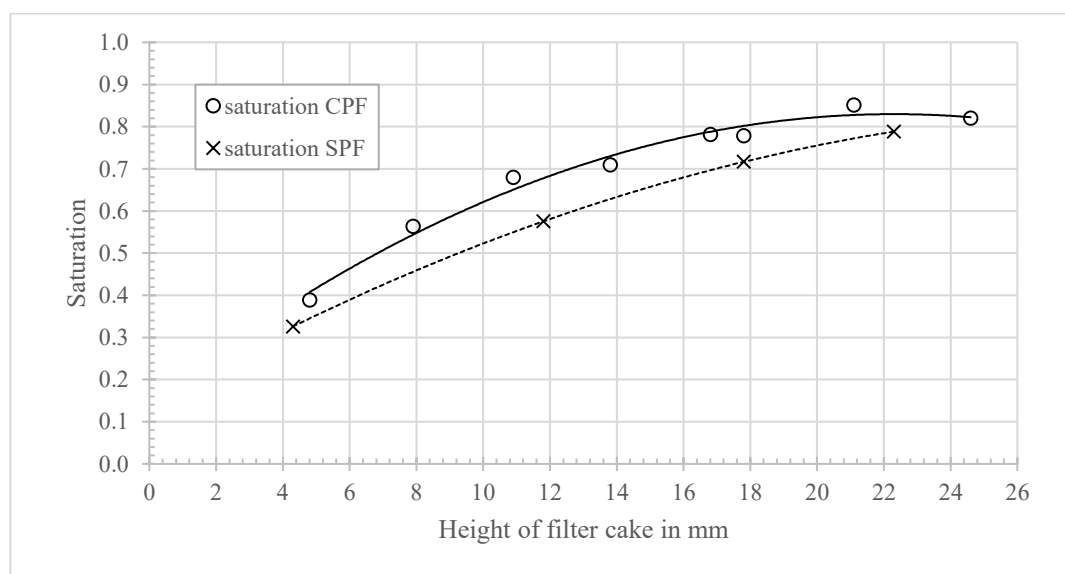


Figure 91. Permeability ratio of KS12 filter cake in various filter cake height; using SPF and CPF; “3-3 bar” of pressure difference; 0.1 of volume fraction.



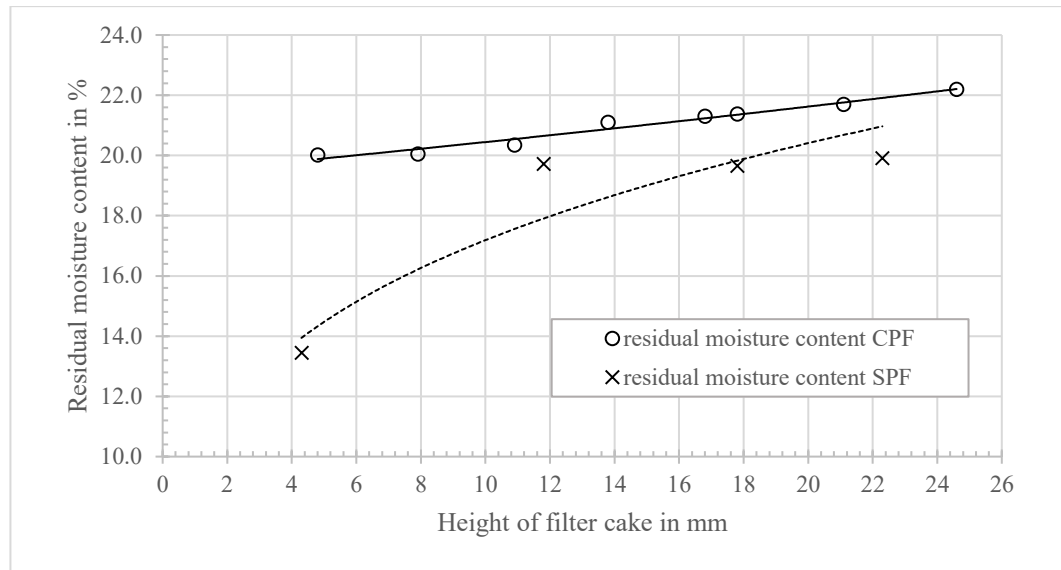


Figure 92. Saturation and residual moisture content of KS12 filter cake in the variety of filter cake height; using SPF and CPF; “3-3 bar” of pressure difference; 0.1 of volume fraction.

For the coarse material KS100, in the requirement to stabilize the filter cake after the mechanical displacement phase. The procedure to remove the filter cake is changed. After the steam break through the filter cake, the magnetic valve is closed. The filter cake is left in Nutsche until there is then the equilibrium of pressure inside the Nutsche and ambient environment. However, this test procedure leads to a big problem in systematic errors. The condensed water from some tubes is flowed back to the Nutsche, increase the saturation as well as the residual moisture content in filter cake. The test again with KS100, as shown in Appendix C3, indicated that systematic errors reach to 16%. Otherwise, because of the lack of comprehensive understanding of the change of material properties during the steam pressure filtration as well as the poor control of the negative effect due to long filtration time, almost experimental results (in the case of KS100) are just only indicated in Appendix C1, C2. The use of steam filters also somewhat improves the dewatering efficiency and reduces the probability and degree of cracks. For fine materials, this efficiency is remarkably high when compared to traditional filtration. The results for coarse grain size are acceptable (taking account of the systematic errors). Other reasons for KS100's problem may be the appearance of negative effects and material characteristics when limestone is at high-temperature conditions. Overall, in the case of limestone, it is recommended to use steam filtration for fine particle size with the improving filtration efficiency, maybe using both types of filtration with coarse particle size material.

#### 4.4. General conclusion

The permeability ratio is an appropriate output parameter to quantify cracks. The high permeability ratio is consistent with the large number of cracks observed on the filter cake and vice versa.

Cracks in filter cake can be divided into two types: shrinkage micro-cracking and macro-shrinkage. The micro-shrinkage cracks are small in size, difficult to observe, occur locally in certain locations (above the surface, on the bottom or around the side of the filter cake), and there is no contact together. This phenomenon affects the dewatering efficiency less. Macro-cracking is usually large, propagating from the surface of the filter cake to the bottom of the filter cake. The shape of the cracks also varies. Sometimes significant cuts divide the filter cake into sections. Sometimes there are cracks around the filter cake. In addition, there is another type of cracking, which is harder to observe, dividing the filter cake into two parts in horizontal. The extent of its influence depends on each specific case.

Through the experimental results of the effect of solid volume concentration in the suspension, filter cake height, and the applied pressure difference to crack formation, the mechanism cause shrinkage cracking in the filter cake can be list as follows:

- *The tensile stress* in the filter cake, which occurs during the mechanical displacement phase. Its magnitude depends on the degree of saturation and capillary pressure. Due to the heterogeneity of the pore structure and the liquid distribution inside the filter cake, there are always forming the weakest points. If the magnitude of tensile stress exceeds the tensile strength, cracks will appear.
- *Sedimentation* is one cause of crack formation in filter cake. When this phenomenon occurs, the filter cake is divided into two parts with small grains located on the upper layer; the coarse grain size is in the lower layer. If the stratification becomes considerable, cracks not only appear in the top layer of the filter cake, but there are also cracks dividing the filter cake into two parts horizontally.
- *The wall effect* during lab-scale experiments causes wall friction at the interface of outward particles with the containment wall. The phenomenon causes particles to have a lower packing density than that of at the center of the filter cake. It is also related to pressure loss in the lower layer of the filter cake, especially for thick filter cake. Low packing density at the bottom of the filter cake also occurs. As a result, shrinkage cracking is formed around the circumference of the filter cake and at the

bottom of the filter cake. From the filter cake observation, the mechanism is assumed. The proof of this issue needs to be defined in future work.

- Last but not least is *the agglomeration* of fine particles. The agglomerated fine particles mixed to other particles and contacted the particles network. Because of the weak bond of flocs, they have deformation and initiation of the crack network in the mechanical phase, under the compressed air. Finally, the collapse of the whole structure occurs.

The results of the application pressure increase in the mechanical displacement phase or both phases of filter cake formation and mechanical displacement show a good effect in improving the filtration process as well as preventing cracks.

Steam filtration show to be a suitable way to reduce crack formation in the filter cake and to increase dewatering efficiency. The high-pressure steam flows into contact with the cold surface of the filter cake, condensation, and forming the even displacement front. This steam continuously condenses within the large capillaries with the reducing local pressure. Simultaneously, the less steam condensate in the small capillaries and the local pressure is still high. As a result, the mother liquid is pushed out simultaneously in both large and small capillaries. This issue will reduce tensile stress by the reduction of saturation as well as the formation of weak positions in the filter cake. High temperatures also lead to the reduced surface tension of the water (which is causing the high tensile stress). In addition, convection and conduction of heat caused the filter cake to heat up, lead to further moisture reduction. The result is a marked improvement for fine-grained limestone. The amount of water inside the filter cake is expected much lower after deliquoring, but it was not achieved because of the continuous condensation of steam. One of the suggestions that carefully control the steam flow into the system, especially water condensation. The condensation time should not too long.

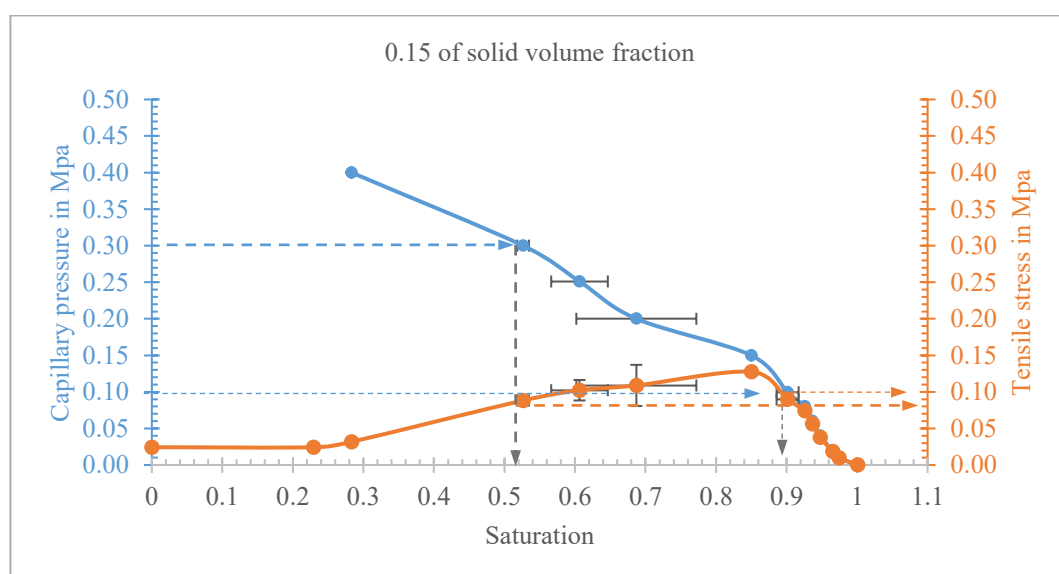
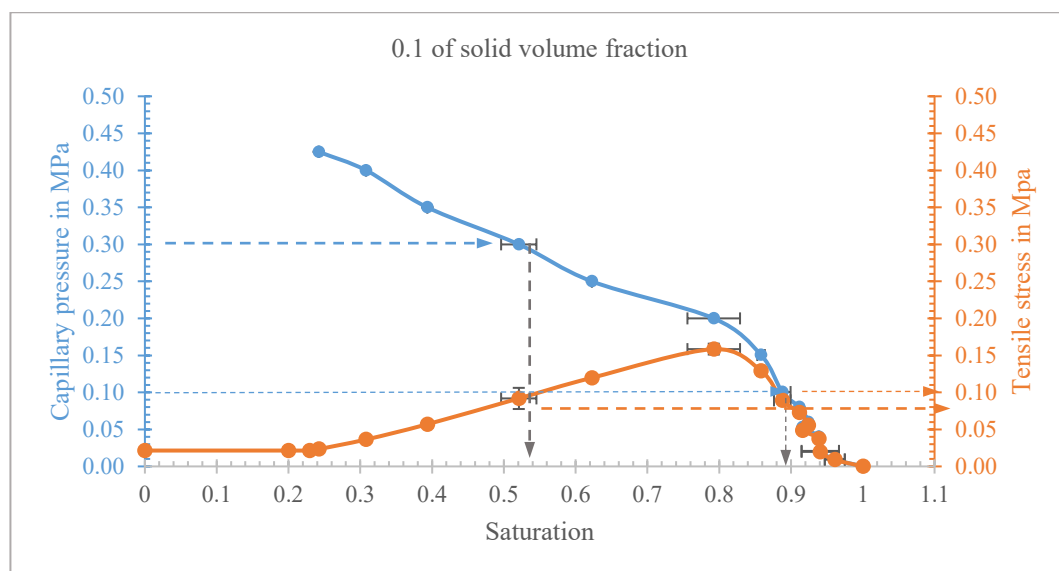
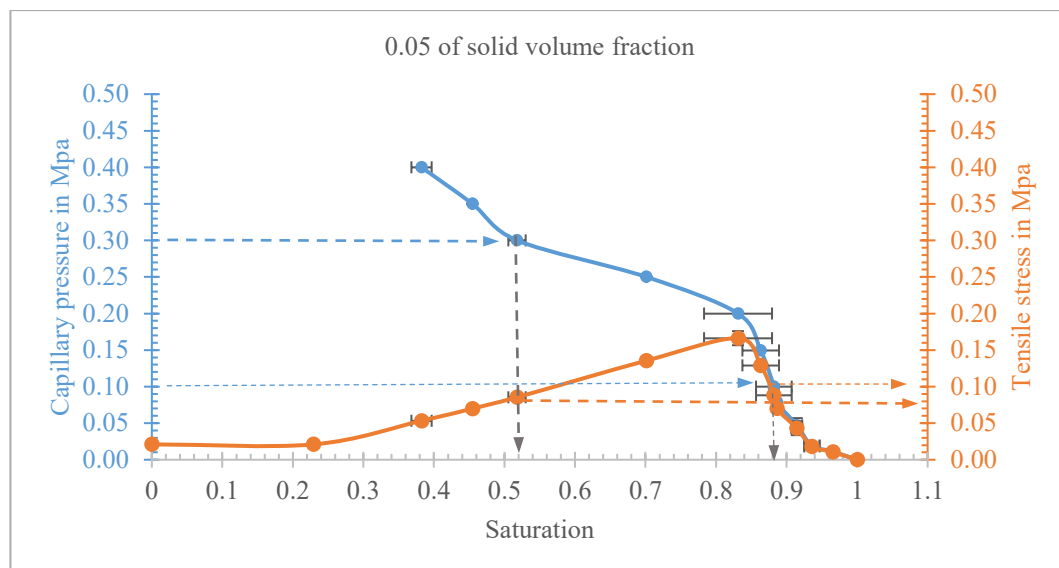
## **5. The influence of operating parameters on cracks formation in the case of Vietnam coal**

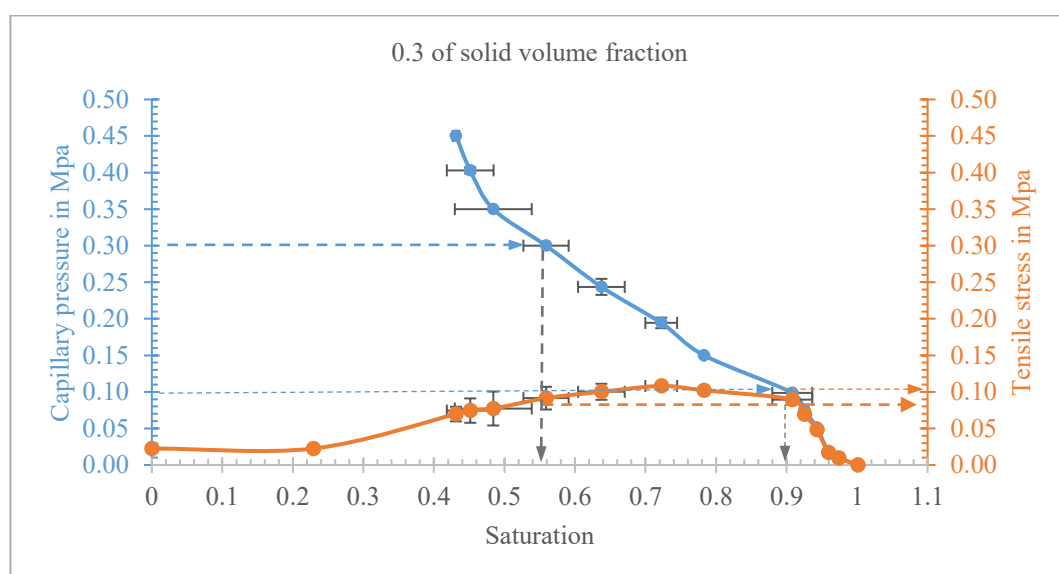
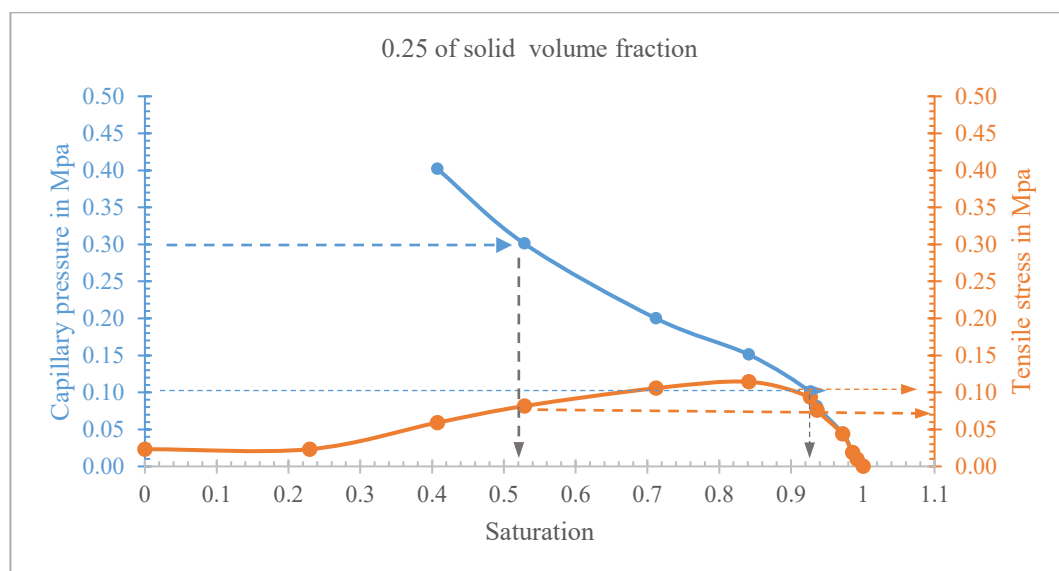
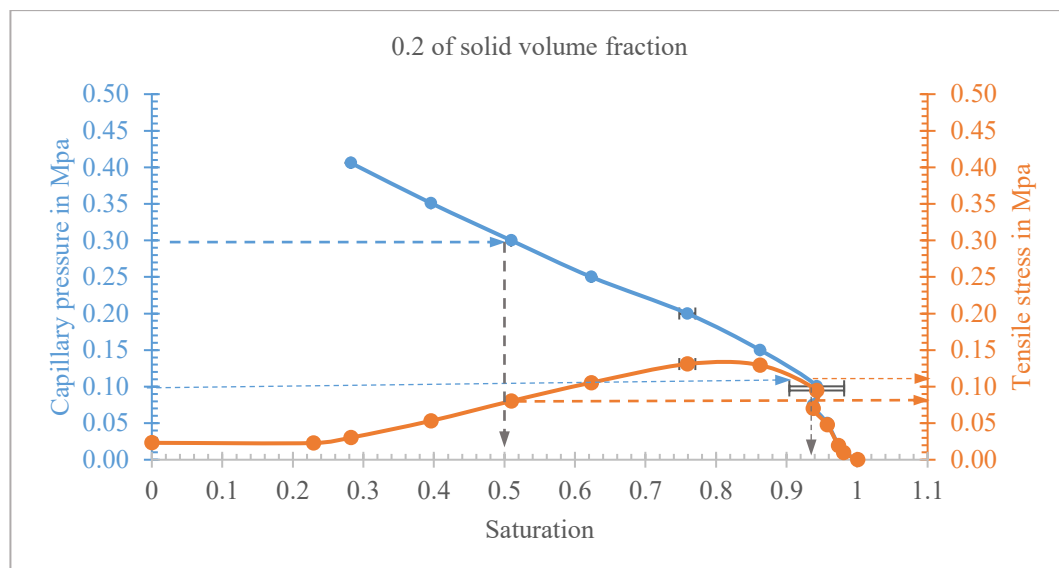
### **5.1. Capillary pressure curve and tensile stress during filtration in case of Vietnam coal**

Measurement is continued to a similar method and the same input parameters for Vietnamese coal. The results are shown in the graphs in Figure 93. While almost filter cakes are in the capillary state at 0.1 MPa of applied pressure capillary (except 0.35 and 0.4 of volume fraction), all filter cake is on interstices state (funicular state) at 0.3 MPa. The saturation and tensile stress at the former one are around 0.9 and 0.1 MPa, respectively. This value is quite large and affects the shrinkage cracking inside the filter cake as well as the dewatering efficiency. For 0.3 MPa of pressure difference, although the saturation is around 0.5, in some cases are 0.4, the tensile stress is pretty high (0.08 MPa to 0.09 MPa). They are not different as much compare with the result at 0.1 MPa of capillary pressure. It can be predicted that although dewatering may be better, the degree of the shrinkage cracking phenomenon will not decrease much when the high-pressure difference is applied. It can be commented that because of high fine particles in the material, the sedimentation dominated the cake formation. A significant amount of very fine particles are on top of the filter cake while the coarse particles are at the bottom, above the filter cloth. This issue causes un-uniform capillaries inside filter cake, where the diameter changes between top and bottom.

One highlight of the measurement results is that at high sludge uniformity (0.35 and 0.4), for both 0.1 and 0.3 MPa of capillary pressure, the filter cake is in a funicular state. This is a good state for effective dewatering and cracks prevention. The filter cake is entirely homogeneous; the capillaries are sufficiently large as well as uniform in size.

Overall, the process of VN coal filtration, following the difference of volume fraction of feed suspension, can be divided into two main areas: sedimentation area (until 0.1 of volume fraction) and homogeneous area (over 0.2 of volume fraction). The transfer area is not clear (maybe occur at 0.15 of volume fraction), according to the result of this measurement. The increasing pressure difference in the mechanical displacement phase is still one of the ideas to reduce the degree of saturation and the tensile stress.





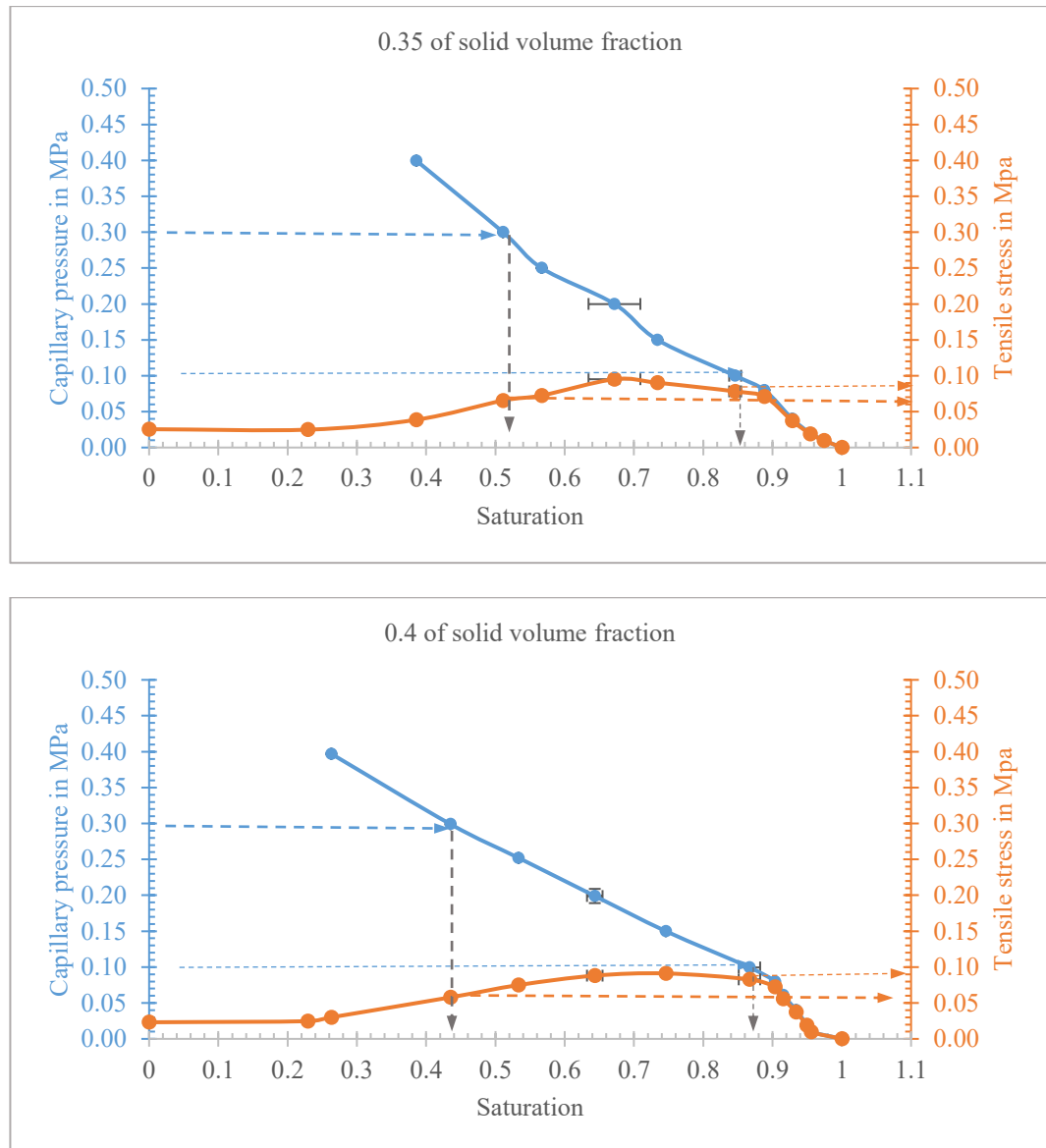


Figure 93. Capillary pressure and tensile stresses against saturation for VN Coal.

Figure 94 also shows the trend of saturation and residual moisture content at 3 bar of pressure capillary in the variety of volume fraction. Overall, the increase the solid concentration, the lower the amount of water inside the filter cake. However, the degree of reduction is quite slightly and there is an abnormal value at 0.3 of the volume fraction (a little higher than the remaining parts). The increase, in this case, is not significant and can be taken into account for the systematic errors. In conclusion, the trend of the result is suitable and gets an agreement with the result of limestone, which is shown in Figure 52 and Figure 54. Otherwise, from the capillary pressure curve measurement, the relationship between the residual moisture content and capillary pressure is also indicated in Appendix D4.



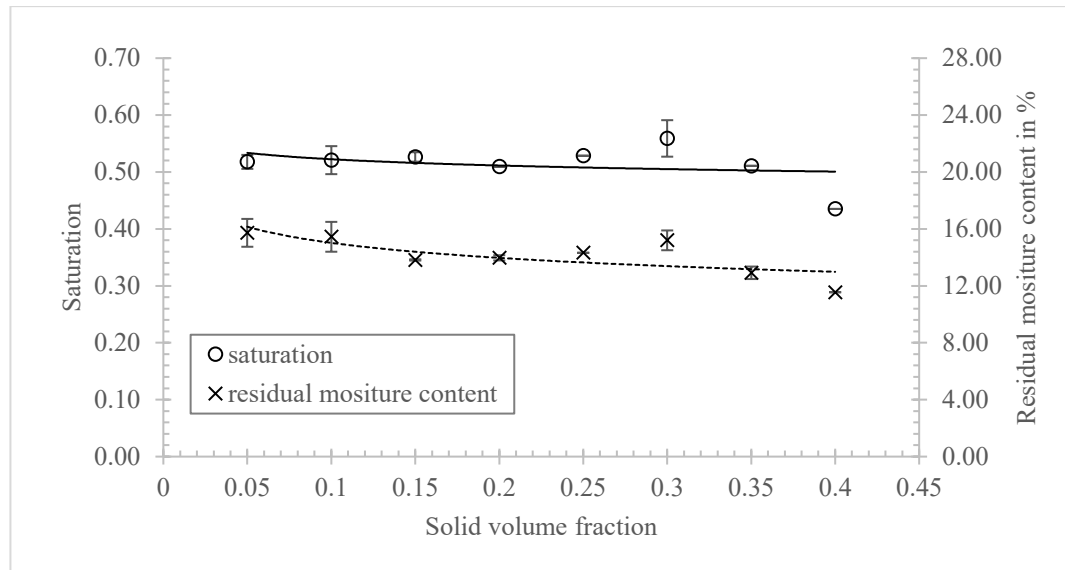


Figure 94. The saturation and residual moisture content of VN coal filter cake at 3 bar capillary pressure as the function of the volume fraction.

## 5.2. Test were conducted using conventional pressure filtration

### 5.2.1. The influence of the solid volume fraction on crack formation and saturation

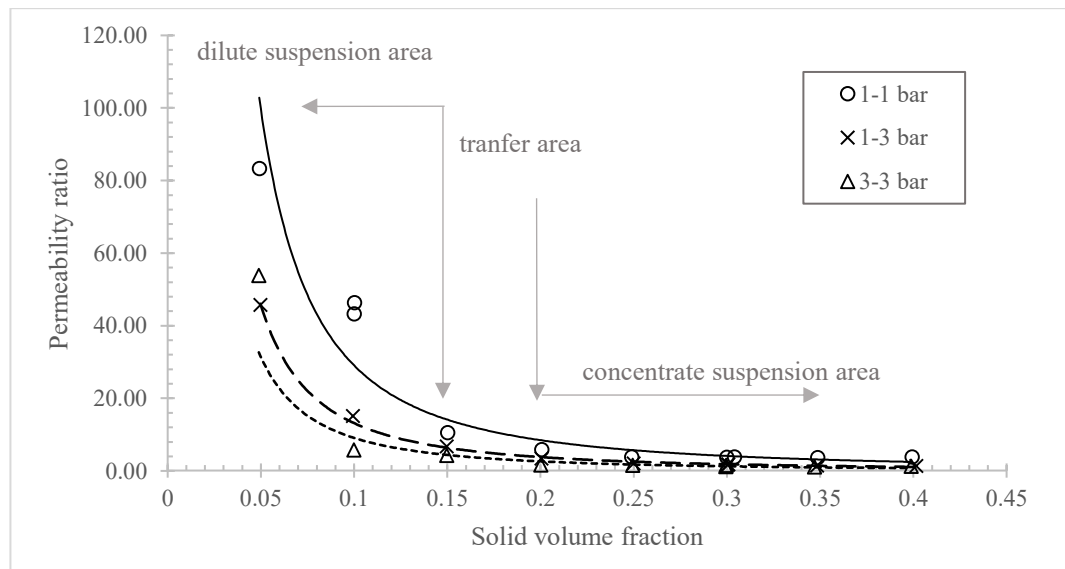


Figure 95. Permeability ratio of VN coal filter cake in the variety of volume fraction; 15 mm of filter cake height.

The experiment was conducted to investigate the effect of the solid volume concentration on the crack formation and the dewatering efficiency of filtration. The initial suspension is re-slurry by mixing dry coal powder with distilled water. The weight of coal per experiment is 30 grams equivalent to approximately 15 mm of filter cake height. Depending on the concentration of the suspension for each test, the mass of water

is used accordingly. The applied pressures difference is “1-1 bar”, “1-3 bar”, and “3-3 bar”.

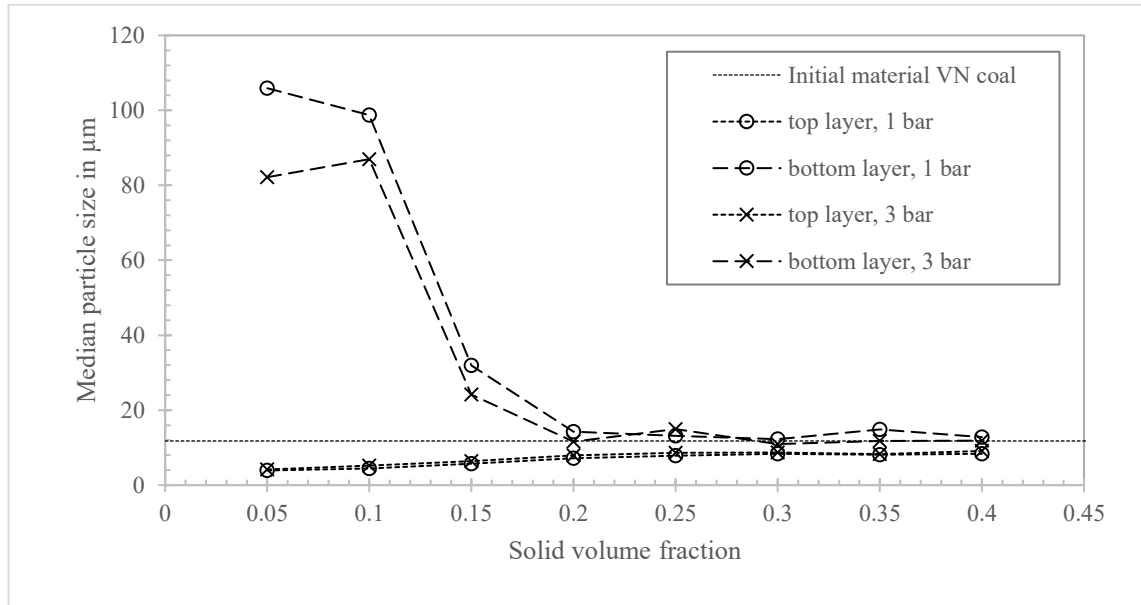


Figure 96. The median particle size of the upper and bottom layer filter cake; 15 mm of filter cake height; 1 bar and 3 bar of pressure difference in the cake formation phase.

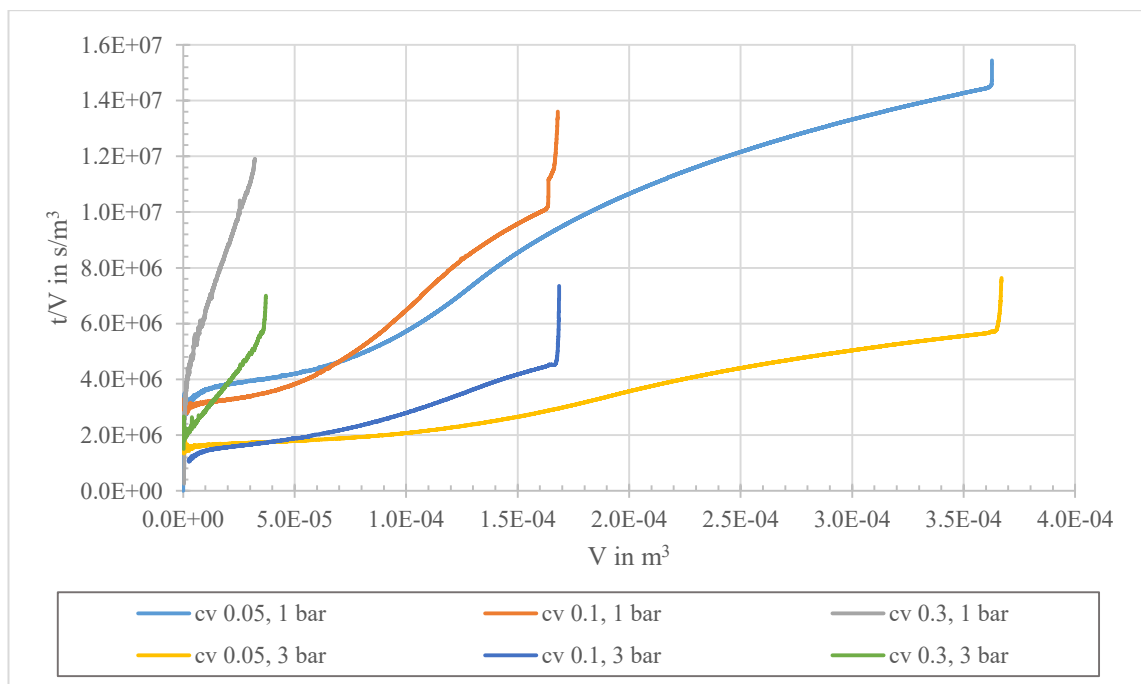
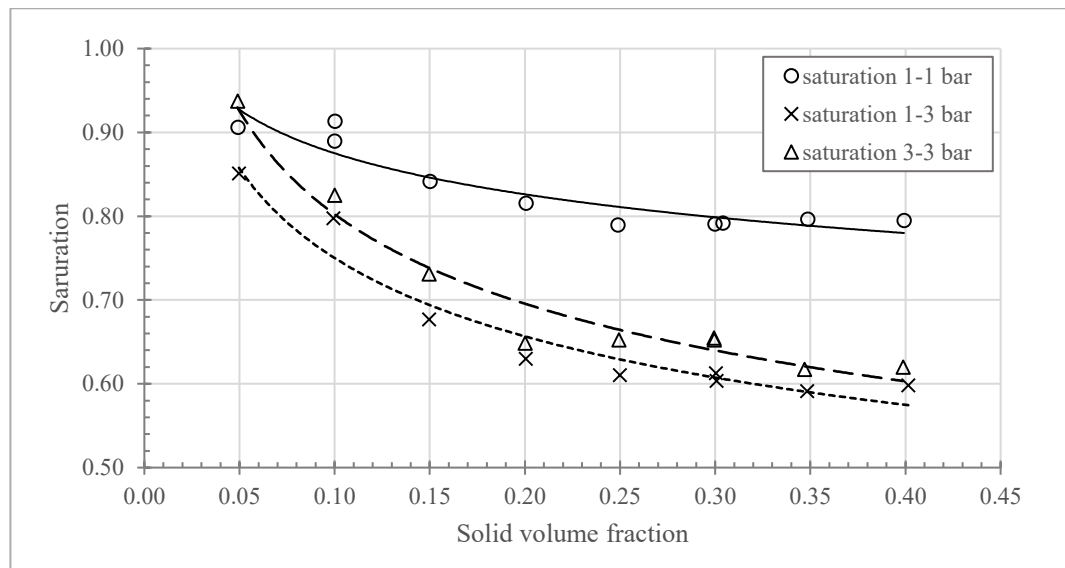


Figure 97. Diagram of  $t/V$  versus  $V$ ; in the variety of volume fraction; 15 mm of filter cake height; 1 bar and 3 bar of pressure difference in the cake formation phase.

As shown in Figure 95, the permeability ratio shows a decreasing trend when the solid volume fraction of suspension increases from 0.05 to 0.4. This issue occurs at both

three applied pressure difference. It also gets an agreement with the coarse and fine limestone, as mentioned above. Data on the permeability ratio with the variety of solid volume fraction show the dilute suspension area (sedimentation area) and concentrate suspension area (homogeneous area). The transfer area is pretty narrow, ranging from 0.15 to 0.2 of the solid volume fraction of initial suspension. There is a difference in filtration result in the lower volume fraction (0.05 to 0.15). While shrinkage, micro-cracking as well as macro cracking is observed on top and at the bottom of limestone filter cake, the result for this situation is the separation into two distinct layers in horizontal (cracking in horizontal), as is described in Figure 24. The cracking on the top and bottom surface of coal filter cake does not exist. This phenomenon is the strong sedimentation of particles fine coal material in case of dilute suspension filtration. The particle size distribution of coal in Figure 42 shows a broad distribution with the largest particle size up to 300  $\mu\text{m}$ , and a significant amount of particle material below 10  $\mu\text{m}$  (accounted for 40%). The long filtration time and dilute feed slurry create conditions for free settling particles. Also, because this is an industrial material, the composition contains many minerals with different densities. All of the above factors create strong sedimentation of particles. The data on the median size of particles which packed at the top and bottom layers on the filter cake (Figure 96) and the bent of the graphs ( $t/V$  versus  $V$ ) (Figure 97) support this explanation.



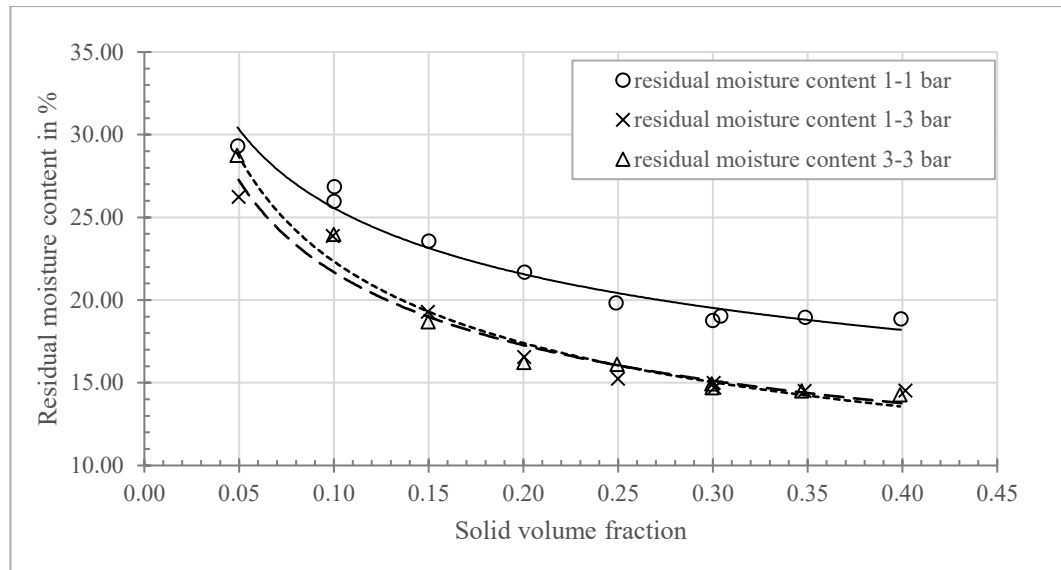


Figure 98. Saturation and residual moisture content of VN coal filter cake in the variety of volume fraction; 15 mm of filter cake height.

From 0.2 to 0.25 of the volumetric concentration in the feed slurry, the particles in coal settle hinder during filtration. This one makes the filter cake more homogeneous. The permeability ratio reduces significantly to around the value of 1 to 3. The filter cake is dewatered without the appearance of cracks. The amount of saturation and residual moisture content decreased sharply compared to the previous sedimentation area. However, these values are still different, depending on the applied pressure difference. Specifically, for the “1-1 bar” of compressed air, the saturation value is around 0.8, equivalent to about 20% moisture. These values are almost unchanged when increasing the volume fraction to 0.4. It can discuss that the dewatering process reaches the limitation of residual moisture content, in which the amount of water cannot reduce more at this pressure difference. The saturation and residual moisture content in the balance area are lower at “1-3 bar” and “3-3 bar” of pressure difference, shown in Figure 98. Because this type of coal is the industrial material, the requirement for the remaining water in the material after filtration must be low as much as possible. *The recommendation is that suspension should only be filtered with solid volumes fraction of 0.2 or more. The pressure difference should be “1-3 bar” or “3 -3 bar”.*

The trend of crack formation, degree of cracking, and saturation of filter cake are adequate with the previous discussion. It can be confirmed that the increases in sedimentation degree related to the high tensile stress in filter cake. The weaker positions between particles inside the filter cake will be dragged, forming large channels. For fine

coal, cracking is observed on the side of the filter cake and follow the horizontal of the filter cake. The crack formation mechanism is not only the high tensile stresses in the filter cake but also the wall effect and the different degrees of packing density.

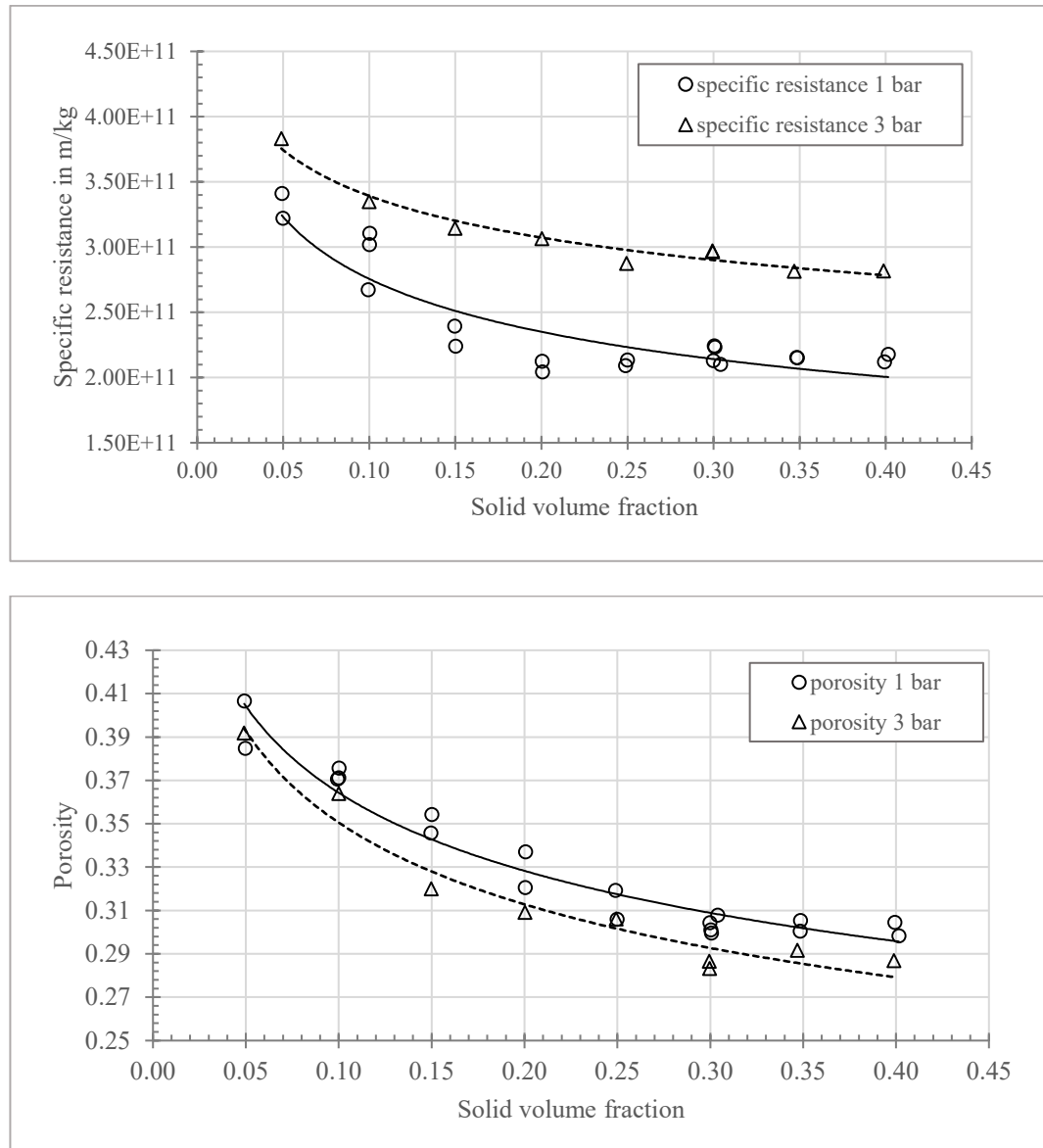


Figure 99. Specific resistance and porosity of VN coal filter cake in the variety of volume fraction; 15 mm of filter cake height; 1 bar and 3 bar of pressure difference in the cake formation phase.

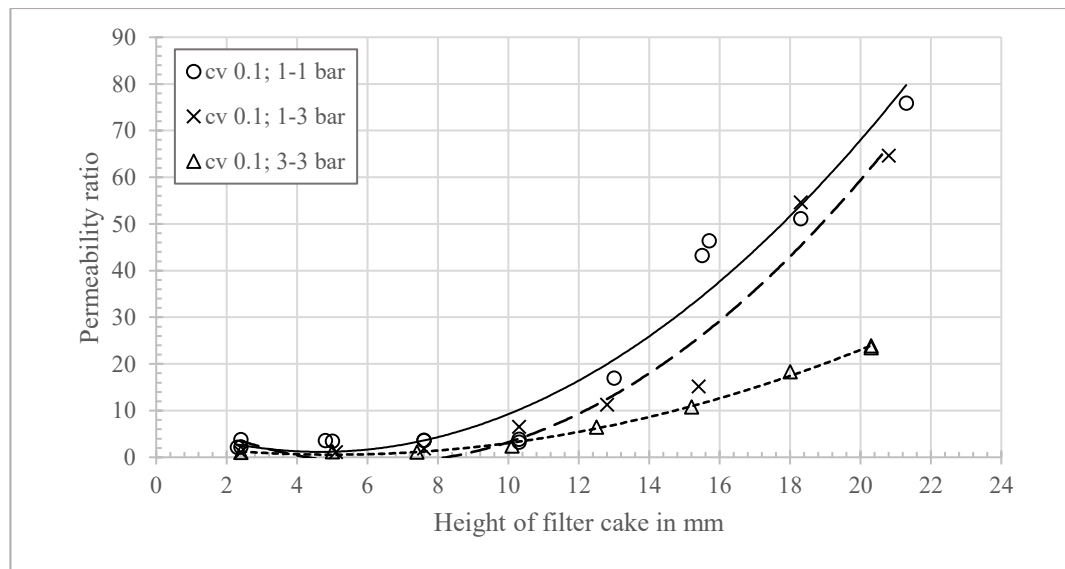
The specific resistance of filter cake, generally, shows the decreasing trend when the solid volume fraction of suspension grows up from 0.05 to 0.4. This value reduces significantly in the sedimentation area before keep stable from 0.2 of solid volume fraction. This trend is suitable for both fine and coarse limestone, as mentioned above. On the other hand, porosity expresses an opposite trend. While the porosity of limestone

increases slightly, that of coal decrease like the specific resistance trend. The phenomenon is pretty unique and unpopular. The reason can be a significant amount of fine particles in coal. For the sedimentation zone, they form a very thick layer on top of the filter cake. While the coarse particles at the bottom filter cake are in a thin layer, they account for a minor proportion of the total filter cake. The result is the sum of specific resistance as well as the porosity, generally is high. By increasing the volume fraction, filter cake becomes more homogeneous, and those values are also decreasing.

### 5.2.2. The influence of the height of filter cake on crack formation and saturation

In investigating the crack formation and studying its effect on filter cake moisture, filter cake height is a parameter not to be missed. This parameter is essential for scale-up and is directly related to the ability of the performance of the filter equipment. Choosing the right filter cake height has not only technical meaning but also brings higher economic efficiency and higher productivity.

The experiment was conducted using conventional pressure filtration, using Nutsche, as described above. The applied pressure differences are “1-1 bar”, “1-3 bar”, and “3-3 bar”. The height of the filter cake is changed by changing the mass of the coal mixing with distilled water in feed suspension. Concentration of solid-phase volume is fixed at 0.1 (sedimentation area) and 0.3 (homogeneous area).



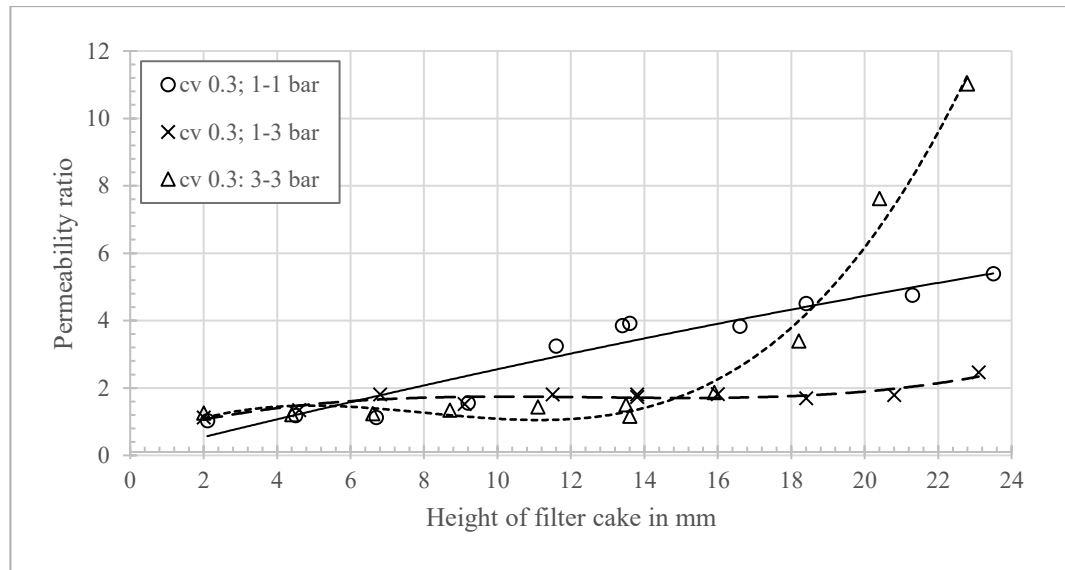












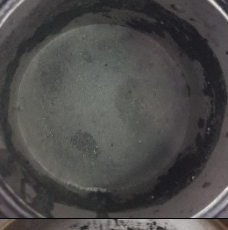










Figure 100. Permeability ratio of VN coal filter cake in the variety of filter cake height; 0.1 and 0.3 of volume fraction.

Figure 101 shows the upper and lower layers of the coal filter cake under parameters of the solid volume fraction of the suspension, the pressure difference, and the filter cake height. As for solids content, a clear difference can be seen between the filter cake in 0.1 and 0.3 of the volume fraction. For the low solid concentration of suspension, the filter cake has apparent delamination. The coarse particles deposits at the bottom part of the filter cake. Even this layer tends to be separated from the filter cake in some cases (when removing the filter cake out of the cake formation unit, this layer is separated from the main part of filter cake). Meanwhile, fine particles are located on the upper layer, increasing specific resistance as well as the value of capillary pressure entry. The results are pretty wet filter cakes. For the 0.3 of volume fraction, the filter cakes are observed to be homogeneous from top to bottom, the filter cake dewatering better in those cases. From the images, it can be seen that the height of the filter cake increased, cracks appear (in some cases), especially at the height of 21 mm or more. For the effect of application pressure, filter cake images are shown in all three conditions “1-1 bar”, “1-3 bar”, and “3-3 bar”. The coal filter cake is difficult to observe visually, so the difference is not as evident as for limestone.



		2 mm	10 mm	21 mm
“1-1 bar”	Top			
	Bottom			
“1-3 bar”	Top			
	Bottom			
“3-3 bar”	Top			
	Bottom			

		9 mm	11 mm	21 mm
“1-1 bar”	Top			



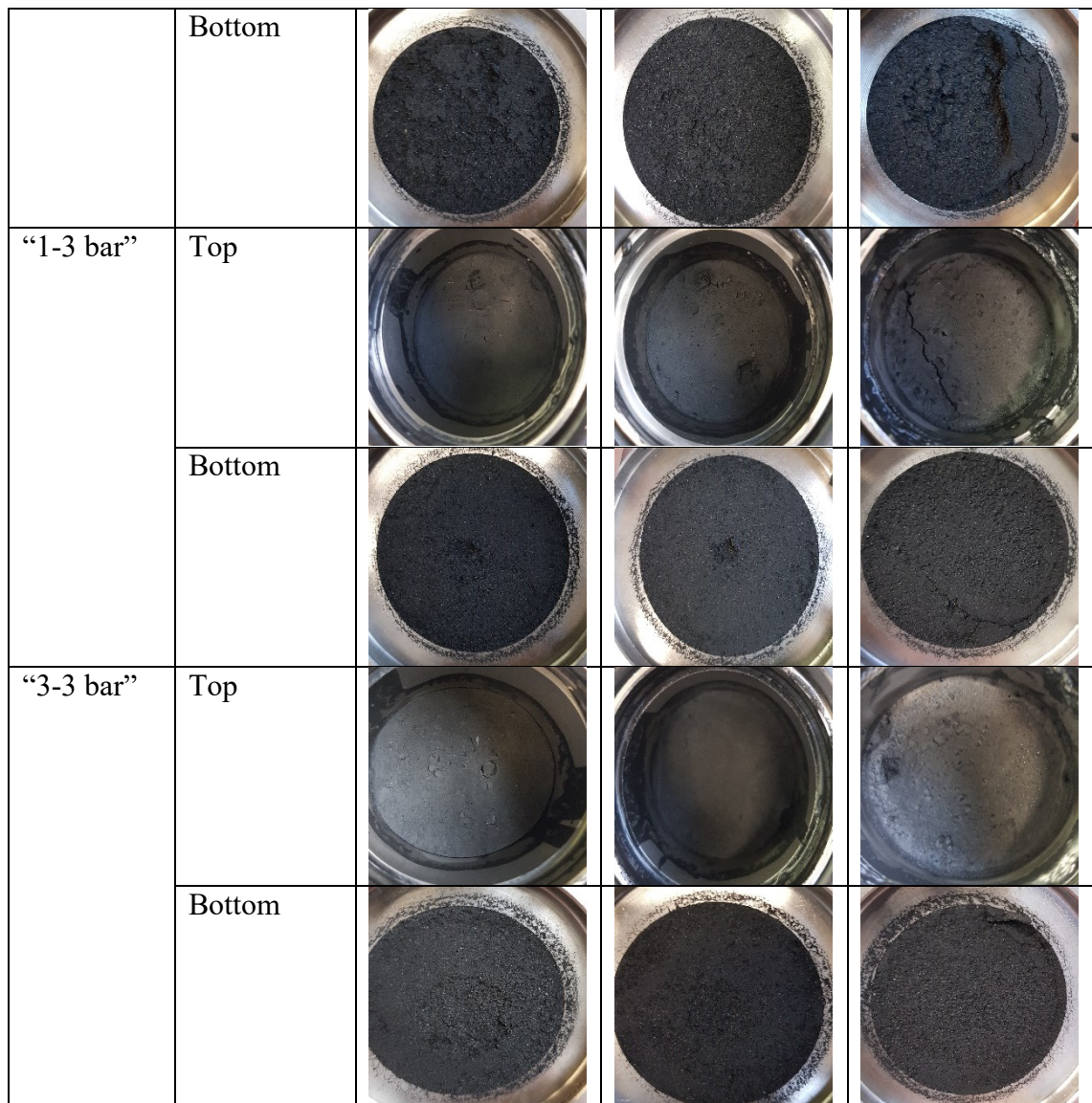


Figure 101. Images for coal filter cake in various filter cake height, 0.1 and 0.3 of volume fraction.

Overall, there was an increase in the permeability value as the height of the filter cake increased. However, the extent of their increase, which is shown in Figure 100, is different. For the sedimentation area (0.1 of volume fraction), the permeability value does not increase when the filter cake height is less than 10 mm. These values increased very quickly after that. The increased wall effect leads to an increase in wall friction (the reason for the loss of compressed force as well as loosening in the packing of the coal particles). Besides, due to the increase in the mass of distilled water and coal (in order to increase filter cake height and fix solid volume fraction in suspension) leads to higher filtration times. As a result, the degree of stratification also increases. All of those standpoints are supported by the results of the permeability ratio using the higher pressure difference (“3-

3 bar”) is lower than the rest ones. For homogeneous areas (0.3 of the solid volume fraction), there is generally a slight increase in the permeability ratio. This result is particularly good when the permeability ratio is almost constant with a pressure of “1-3 bar” when the height increases from 2 mm to 23 mm. This significant improvement is caused by the homogenized filter cake, the similar size of capillaries. Water is displaced simultaneously. The result is that the lower tensile stresses and fewer weak positions are formed between particles.

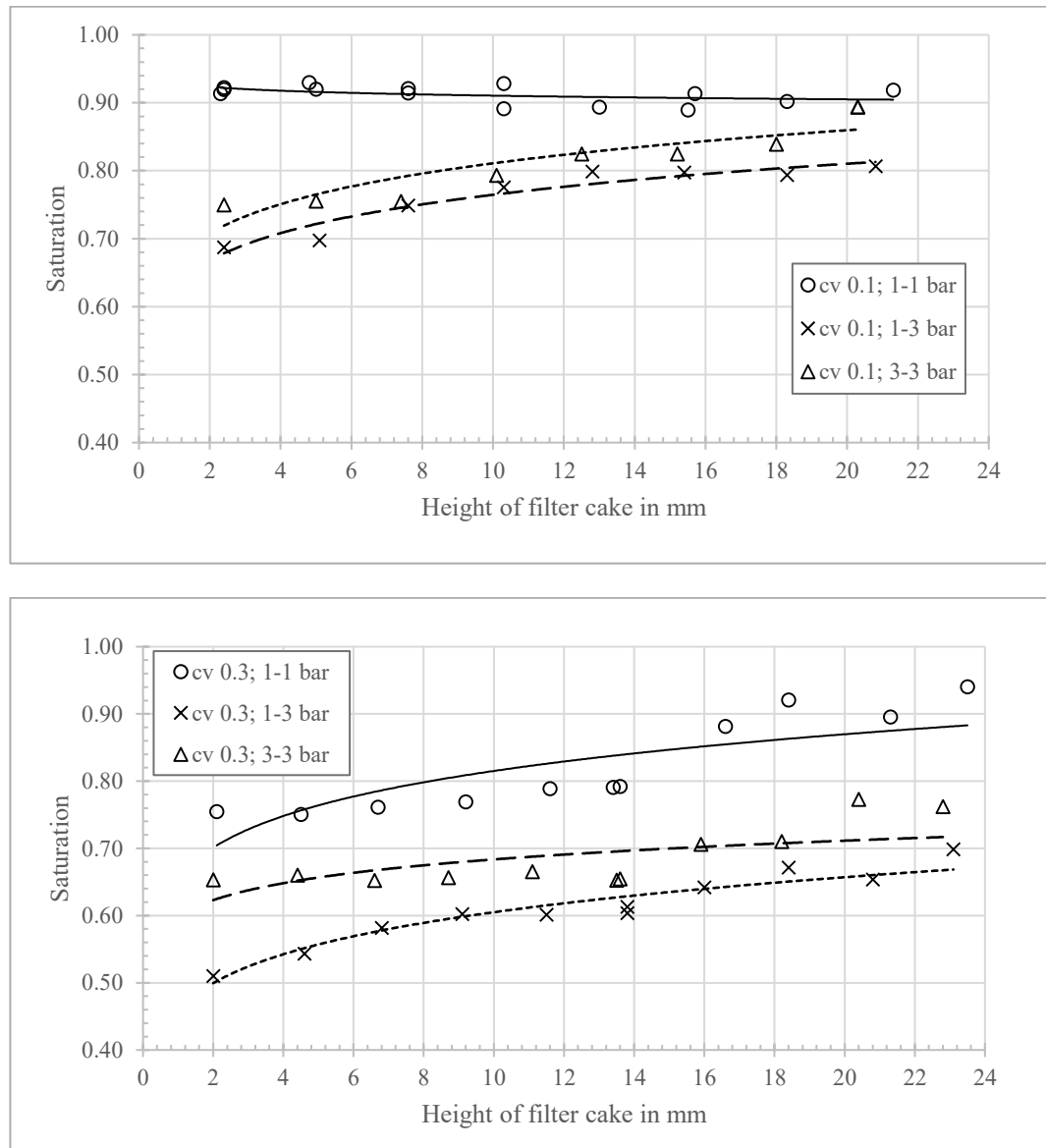


Figure 102. Saturation of VN coal filter cake in the variety of filter cake height; 0.1 and 0.3 of volume fraction.

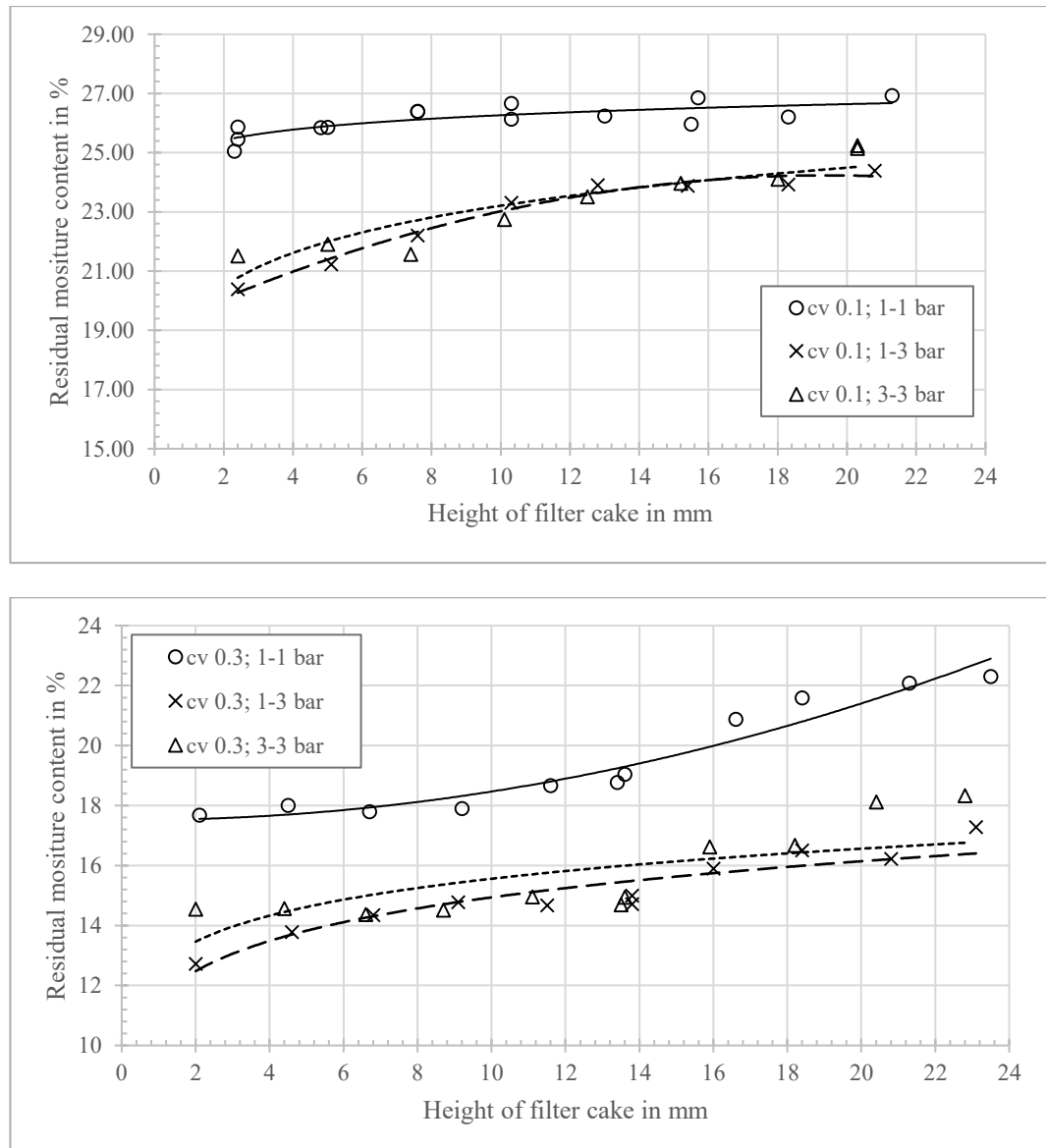


Figure 103. The residual moisture content of VN coal filter cake in the variety of filter cake height; 0.1 and 0.3 of volume fraction.

The amount of water in the filter cake tends to increase as the height of the filter cake increases. The trend is even quite similar to the direction of the permeability ratio. Values increase slowly or remain constant when the filter cake height is less than 10 mm and 14 mm for sedimentation zone and homogenization zone. In general, the amount of water in the filter cake is still high for dilute slurry filtration and is improved for concentrated sludge filtration. The reason is clearly explained above. This trend is reached in agreement with both fine and coarse limestone. The best dewatering effect is achieved in the range of 0.5 - 0.6 of saturation, equivalent to 12 -16% of the remaining moisture. The recommended parameter for coal filtration is a solid phase volume concentration of 0.3, the applied pressure difference of “1-3 bar”. *Because there is no distinct in residual*

moisture content, the selected filter cake deep can be 14 mm, even in the range of 18 - 24 mm, in order to maximize productivity. In dilute slurry filtration, the recommended filter cake height should be less than 10 mm.

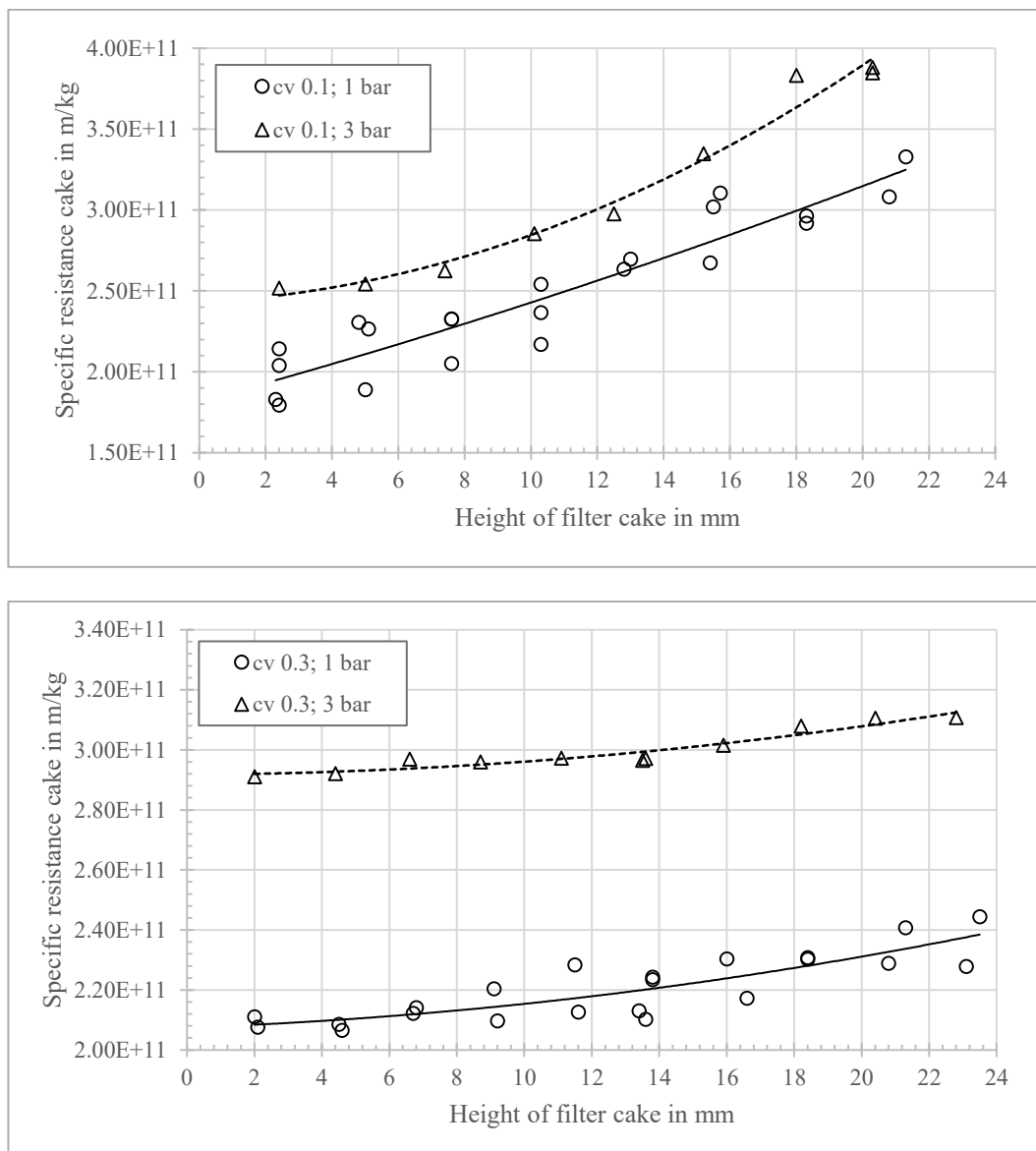


Figure 104. The specific resistance of VN coal filter cake in the variety of filter cake height; 0.1 and 0.3 of volume fraction; 1 bar and 3 bar of pressure difference in the cake formation phase.

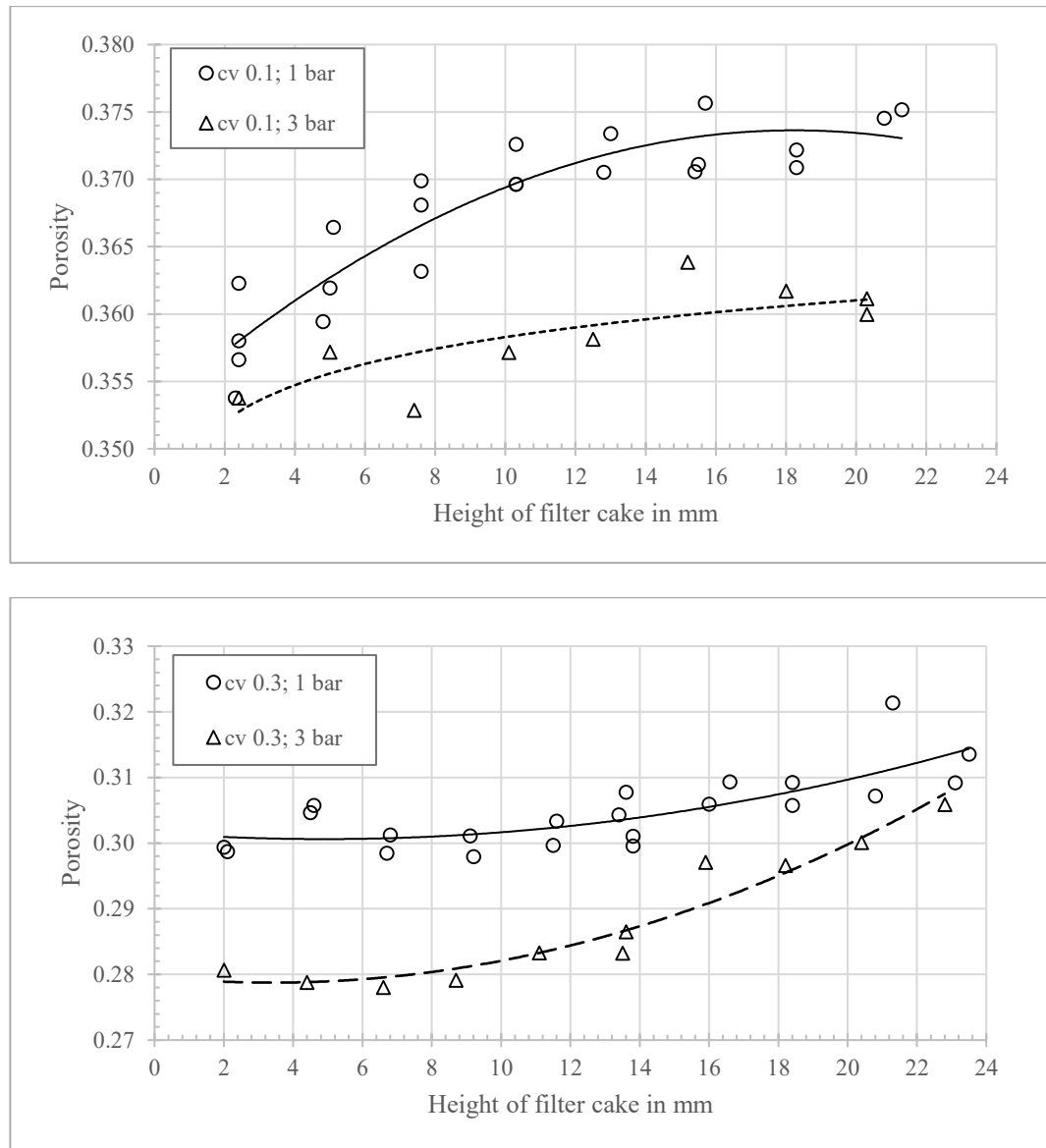


Figure 105. The porosity of VN coal filter cake in the variety of filter cake height; 0.1 and 0.3 of volume fraction; 1 bar and 3 bar of pressure difference in the cake formation phase.

In general, specific resistance and porosity were reached in agreement with coarse and fine size limestone. The uptrend is mainly due to the high degree of stratification and the low packing density of the particles. This trend substantially impacts the filter cake when filtering in the sedimentation area and has less effect on the filter cake in the homogeneous regions. One of the new findings is the stability of filter parameters until a certain height (as can be called “critical point”) of filter cake before increasing rapidly with the increase of filter cake deep. The data in Figure 104 and Figure 105 also suitable for this detection.

### 5.2.3. The influence of pressure difference on crack formation and saturation

The experiment was conducted with a change parameter of pressure difference. The pressure difference will be kept constant throughout the cake formation and deliquoring phase. The solid concentration of surveyed suspension was 0.1 and 0.3. The filter cake height is fixed at approximately 15 mm (30 grams of the solid mass). The purpose of the experiment is to evaluate the dewatering efficiency and observe the degree of crack formation of the coal filter cake under the effect of a flexible parameter, which can be easily adjusted in the operation of the filtration device.

The results of measurement and calculation of the permeability ratio, as shown by the graph in Figure 106, show a downward trend at both the concentrate and dilute suspension. However, the degree of reduction is different. The permeability ratio decreased significantly from 45 to 3 for a solid volume fraction of 0.1. Meanwhile, these values decreased slightly from 5 to 2 for a sludge concentration of 0.3. As seen in the filter cake images (Figure 107), most cracks do not occur at the top and bottom like limestone or may appear micro-cracking as be difficult to investigate by visual observation. One apparent observation is that there exist cracks that divide the filter cake into two sections horizontally. They appear in most filter cakes when diluting aqueous suspension using low-pressure differences, which correspond to high permeability ratio values.

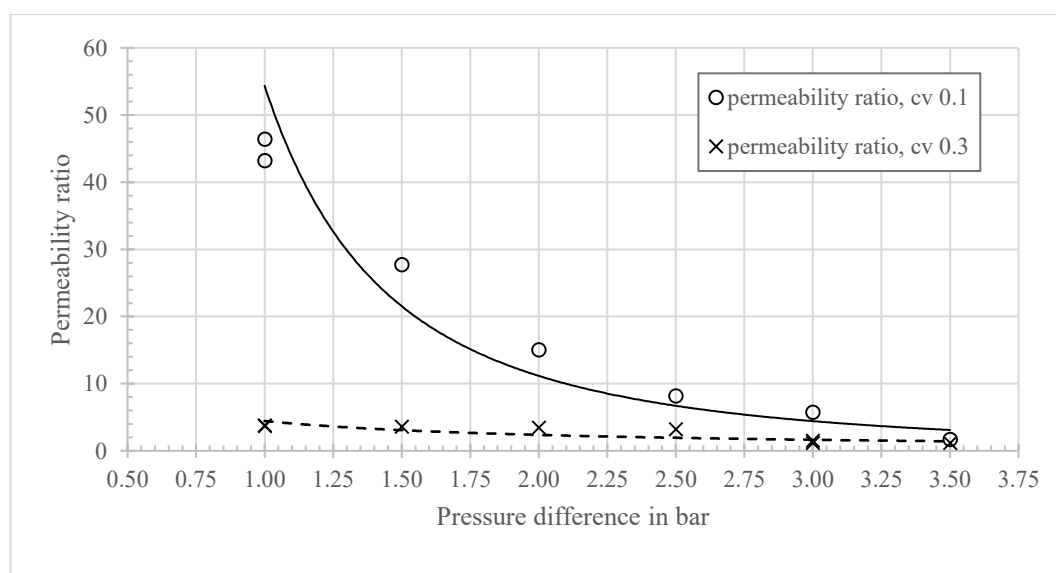


Figure 106. Permeability ratio of filter cake in the variety of pressure difference; 15 mm of filter cake thickness; using CPF.



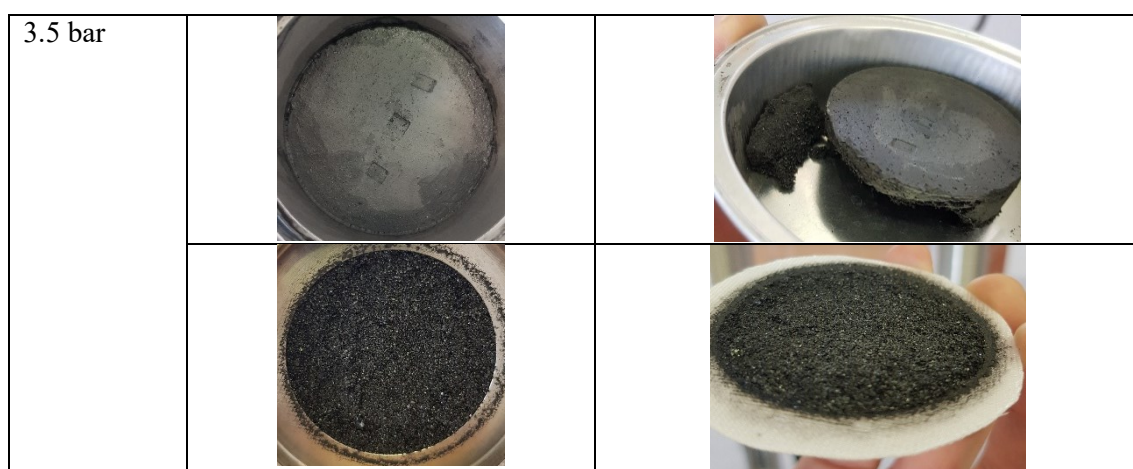
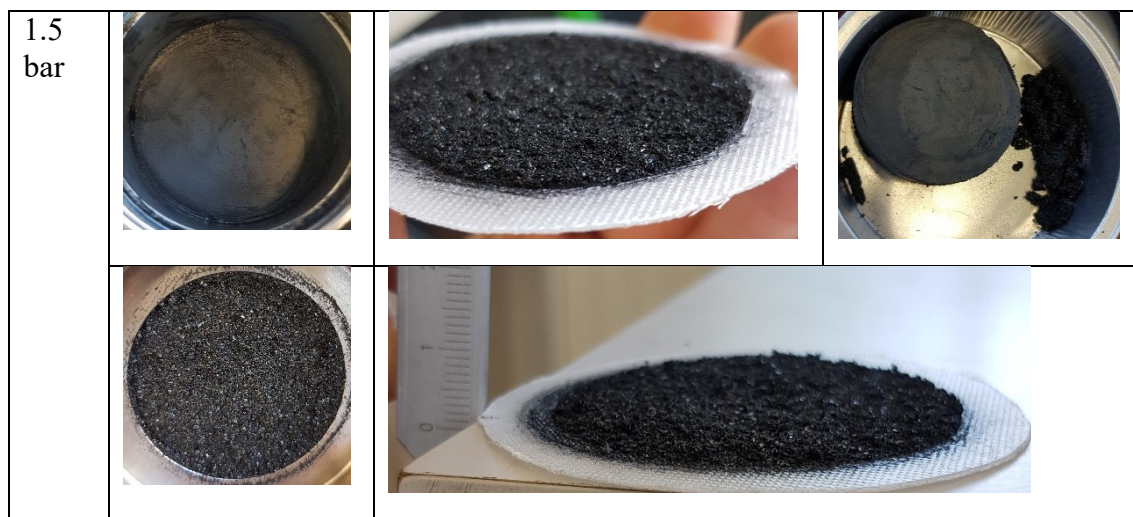
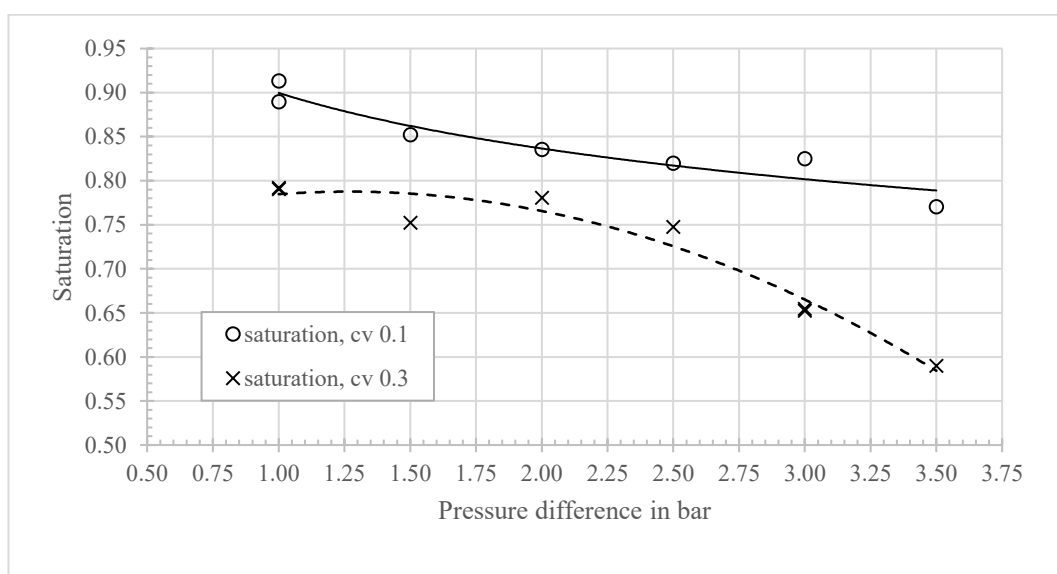


Figure 107. Images for filter cake in the 1.5 and 3.5 bar of pressure difference; 0.1 of solid volume fraction; 15 mm of filter cake thickness.



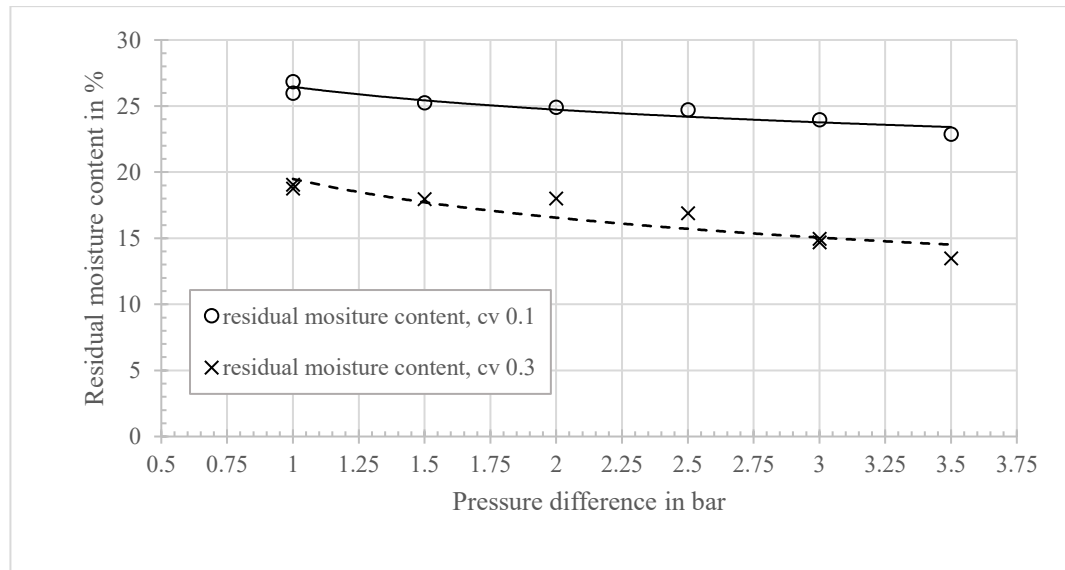


Figure 108. Saturation and residual moisture content of filter cake in the variety of pressure difference; 15 mm of filter cake thickness.

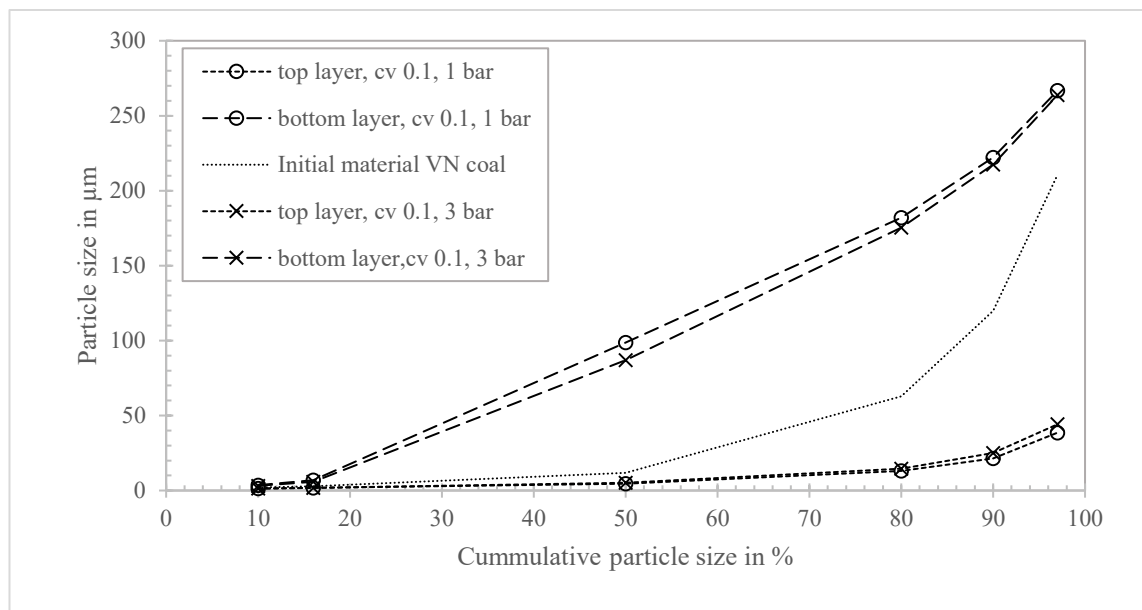
Along with improving the permeability ratio when increasing the pressure difference, the amount of water in the filter cake also decreases. However, the level of reduction is not too high for both values of the solid phase concentration, as can be seen in Figure 108. This degree of reduction shows a low efficiency in dewatering by increasing the application pressure, although crack formation has been avoided. Besides, due to the filtration device's durability and operating costs, the pressure cannot be increased further. This promotes the need for another filtration method to improve the efficiency of this fine-grained coal, and steam pressure filtration is one of the suggested methods, as can be shown next parts.

Back to the crack formation in the filter cake and the permeability ratio value, we can see the results reached an agreement with some previous studies. Barua [4] has shown that as the applied pressure increases, the probability and degree of crack formation decrease. This phenomenon is explained based on changes in tensile strength, capillary force, packing density, and pre-deformation flocs. Wiedemann and Stahl, in their research[5], have shown that increasing compressed air leads to a reduction in shrinkage potential. This trend is similar to the previous research results of coarse-sized limestone. The result for the fine particle size is quite different because the entry capillary pressure requires to be more significant for the deliquoring phase taking place. In other words, with the maximal applied pressure difference of 3 bar, the filter cake is still completely



in the capillary state (as is mentioned in Figure 49 and Figure 51), where there is high tensile stress, causing a great degree of cracking.

The decrease in the crack's degree and the permeability ratio value for coal is similar to the description of Barua and previous discussions on coarse-grained limestone. However, in the filter cake, there appears a significant horizontal crack, which is described in Figure 24. This phenomenon is due to the strong sedimentation of the coarse particles during the filtration process. As a result, the fine particles concentrated in the upper part, which requires even higher pressure to dewatering. Moreover, because the amount of water in the upper layer is not pushed out of the filter cake, water in the lower layer does not suffer any dewater force. The moisture of filter cake is kept high. In laboratory equipment, shrinkage may occur around the filter cake, preferably air passes through the feces adjacent to the filter cake to the containment wall. As a result, the filter cake cannot further be dewatering.



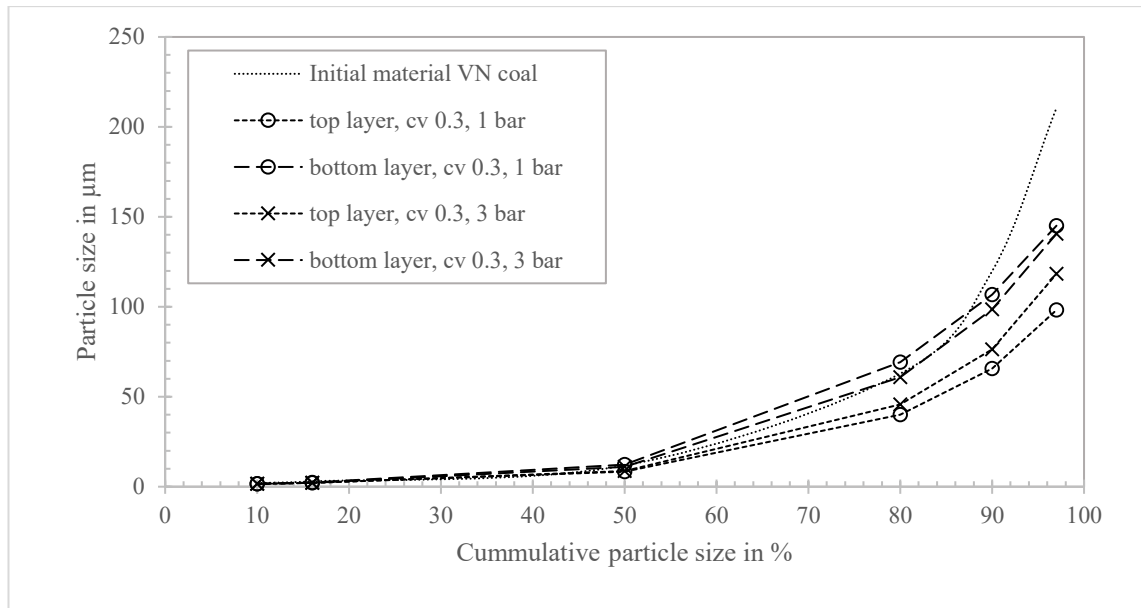


Figure 109. Particle size distribution on the top and bottom layer of the filter cake; 1 bar and 3 bar of pressure difference in the cake formation phase.

Figure 109 shows the differences in the particle size distribution of the upper and lower layers of the filter cake. It can be observed that although the pressure increases from 1 to 3 bar, the difference in particle distribution is significant with a solid phase content of 0.1. This issue shows that the degree of sedimentation is still high, and the residual moisture does not decrease too much. For solid-phase content of 0.3, the filter cake is inherently homogeneous at 1 bar, and there is no difference at 3 bar. The filter cake is in equilibrium status and cannot be dewatered even though the pressure has increased. In summary, the increase in applied pressure limits cracking formation reduces filtration time but does not improve too much for dewatering purposes.

### 5.3. Estimate the efficiency dewatering as well as the crack formation using steam pressure filtration

Steam pressure filtration can be regarded as the further development of hyperbaric filtration or vacuum filtration using the saturated steam or superheated steam. It is the combination of thermal and mechanical in order to attain the lowest residual moisture content. This process is characterized by the even macroscopic sharply distinctive displacement front. The application of steam pressure for displacement dewatering is relevant in branches of the chemical, mineral processing, and recycling industry [50].

With the coal material, Burton is first to apply steam to reduce the residual moisture content using a vacuum filter. The result shows significant efficiency in order

to reduce the water in the filter cake[51]. S. Gerl and W Stahl, in his research, also show that the steam pressure filtration can provide an economical and effective technique whereas conventional solid-liquid separation processes do not lead to a marketable residual moisture content of the product [52]. They conclude that the condensates front remove the capillary water. After the steam breakthrough, the filter cake is heat up to saturated steam temperature. By using pressurized air, the remaining water continuing evaporation due to the stored latent heat of filter cake.

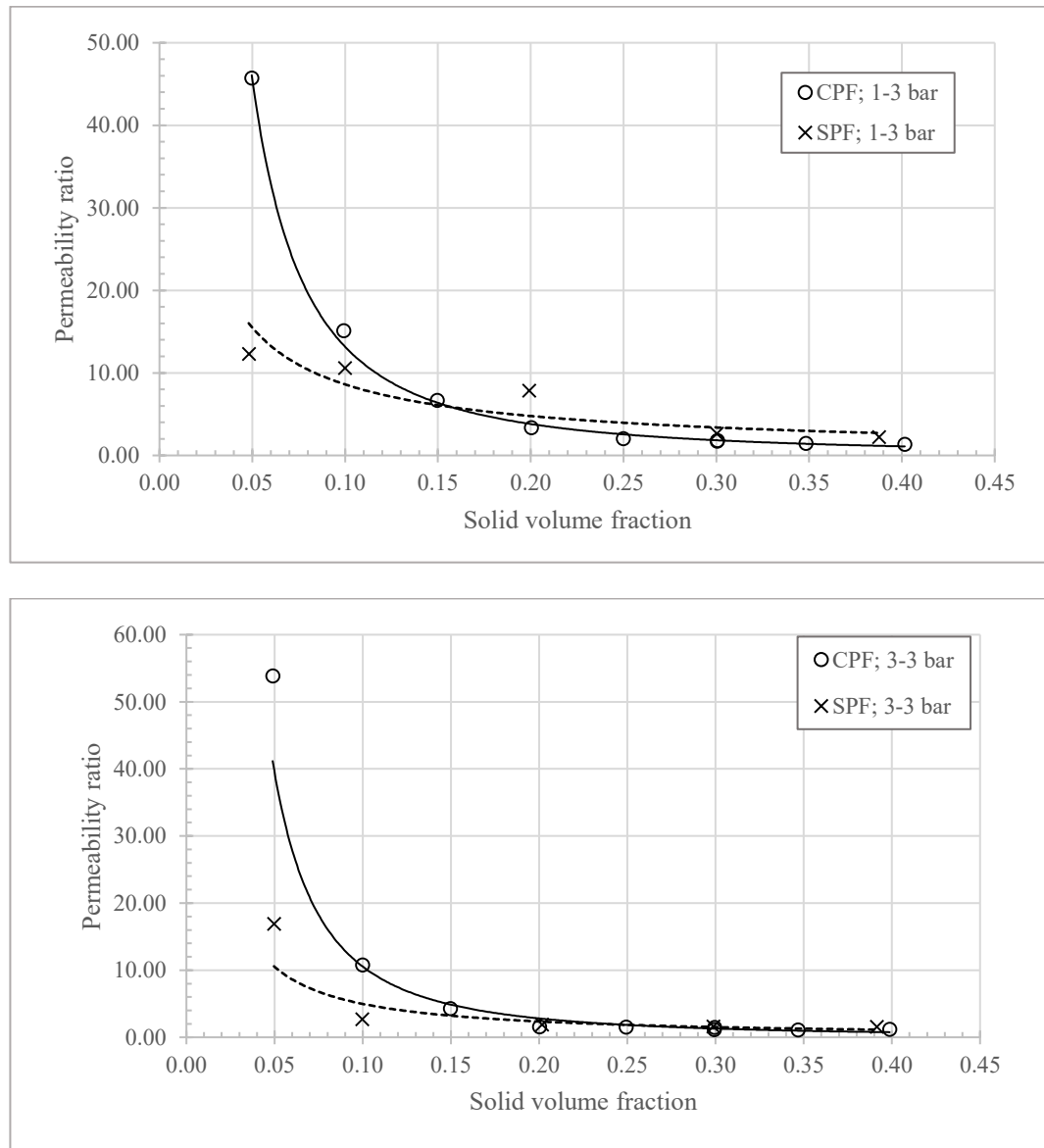


Figure 110. Permeability ratio of VN coal filter cake in the variety of volume fraction; 15 mm of filter cake height; using steam pressure filtration (SPF) and conventional pressure filtration (CPF).

Like with limestone, tests were conducted firstly with the variety of solid volume fraction of suspension. The height of the filter cake is approximately 15 mm, corresponding to 30 grams of the mass of coal. The applied pressure differences are “1-3 bar” and “3-3 bar”.

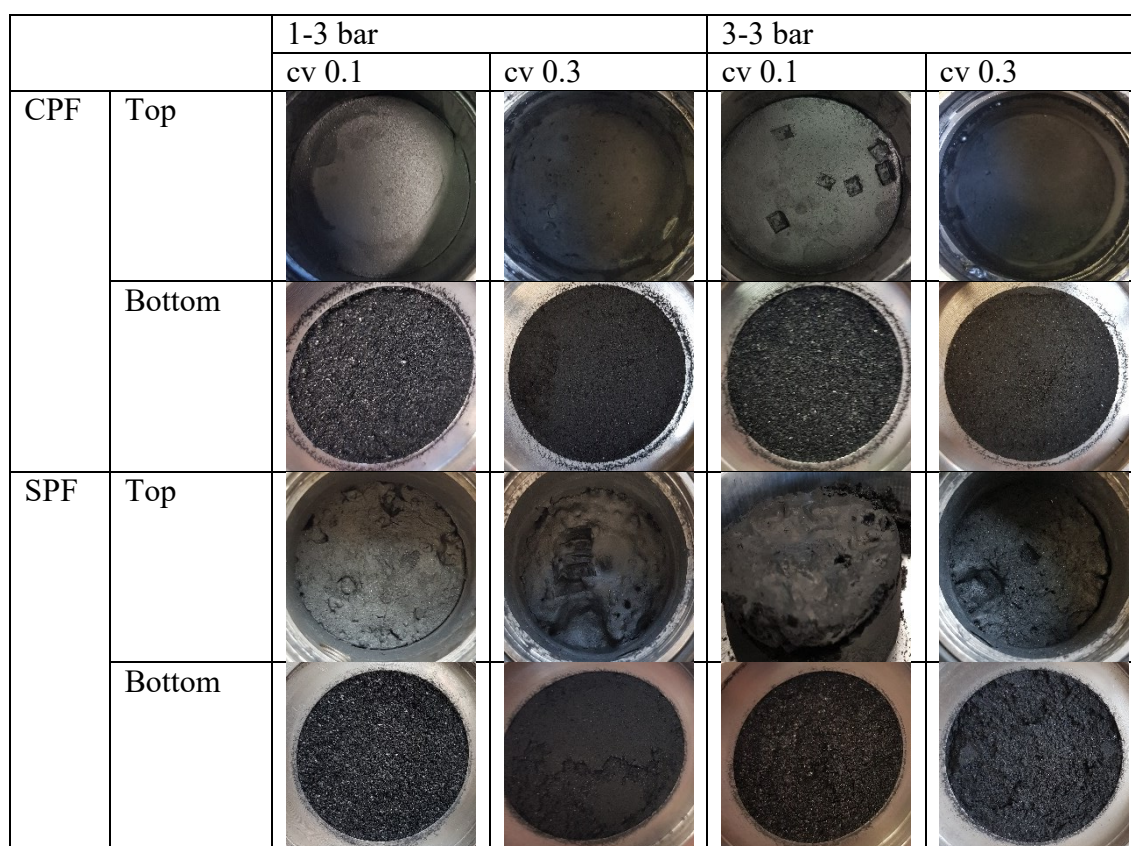


Figure 111. Images for coal filter cake using steam pressure filtration (SPF) and conventional pressure filtration (CPF).

The permeability ratio, as seen in Figure 110, tends to decrease as the filter cake becomes more than homogeneous. In general, at “1-3 bar” and “3-3 bar” of applied pressure, the degree of cracks is improved significantly in the sedimentation area, and quite similar in the homogeneous area compared to conventional pressure filtration. This issue can be explained with the assumption of reducing tensile stress, as concluded above with limestone. At lower volume fraction, the permeability ratio is still higher due to sedimentation, as cannot overcome in this way.

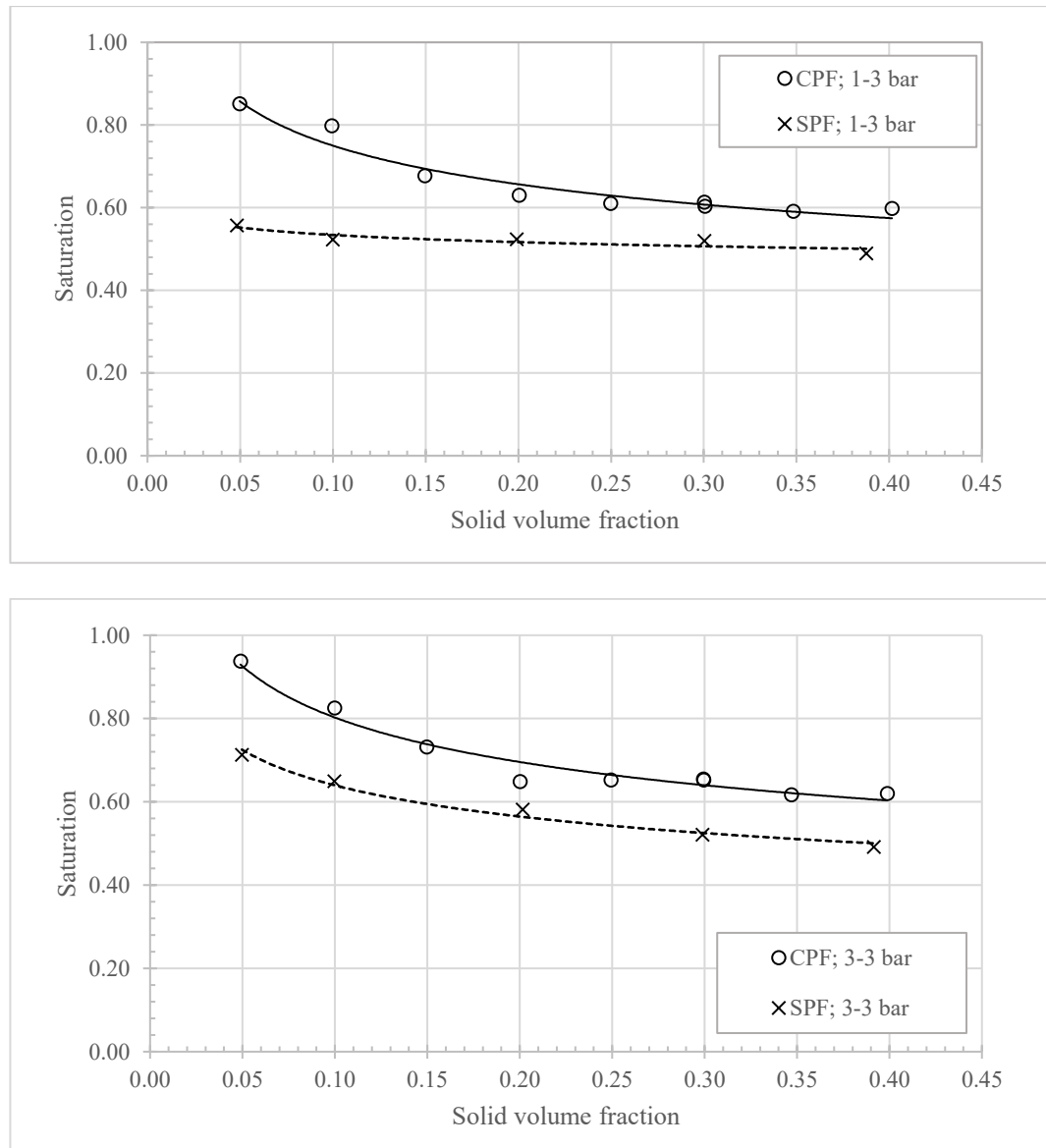


Figure 112. Saturation of VN coal filter cake in the variety of volume fraction; 15 mm of filter cake height; using SPF and CPF.

Although the difference in permeability, as well as the degree of cracking, is not too much, filter cake using steam filter still shows outstanding efficiency in deliquoring. As seen in Figure 112 and Figure 113, the saturation ranges from 0.5 to 0.7, equivalent to 14-26% moisture. This amount of water is much lower than traditional filtration from 1% to 8%, depending on the solid volume fraction in the feed suspension.

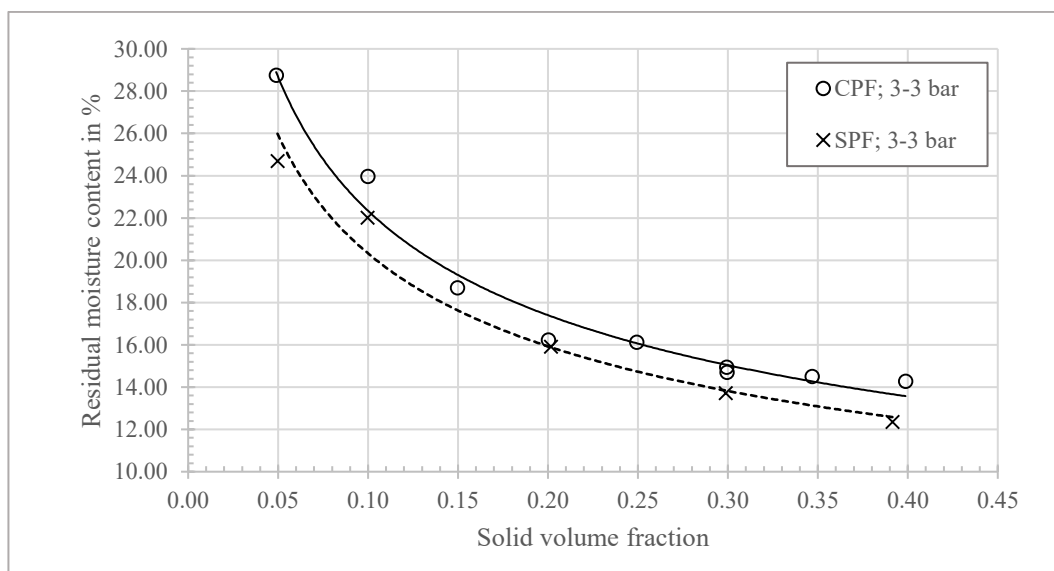
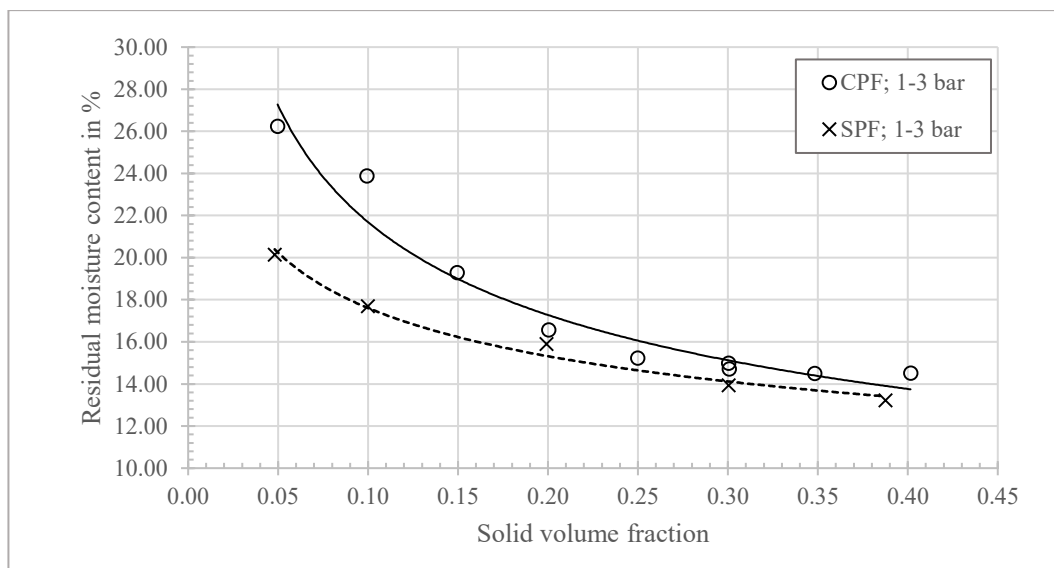


Figure 113. The residual moisture content of VN coal filter cake in the variety of volume fraction; 15 mm of filter cake height; using SPF and CPF.

Since there is no significant difference, even it is also more prominent in the dewatering efficiency and the ability of crack prevention, *the recommended applied pressure for subsequent experiments is “1-3 bar”. The volume concentration in the feed suspension should be 0.3.*

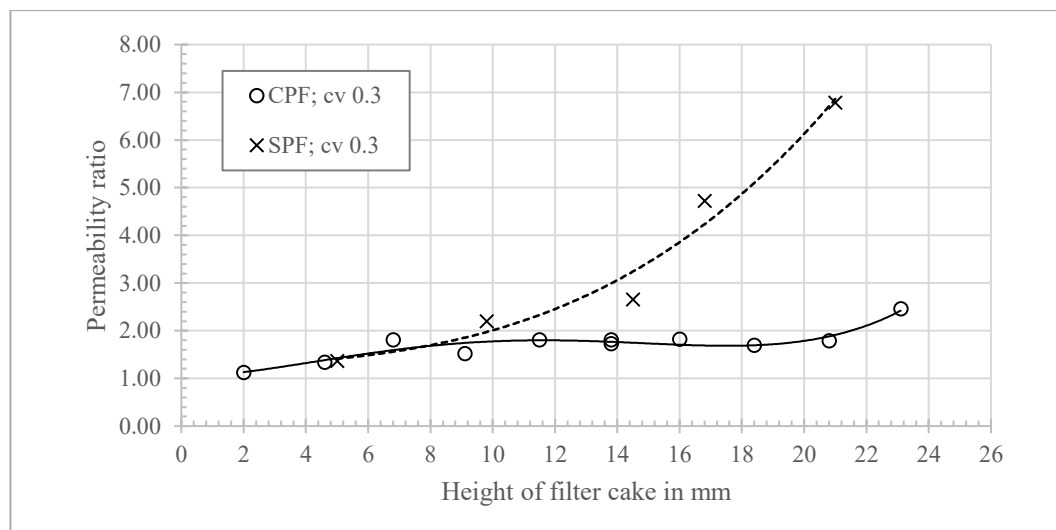


Figure 114. Permeability ratio of VN coal filter cake in the variety of height; using SPF and CPF; 0.3 of volume fraction, “1-3 bar” of pressure difference.

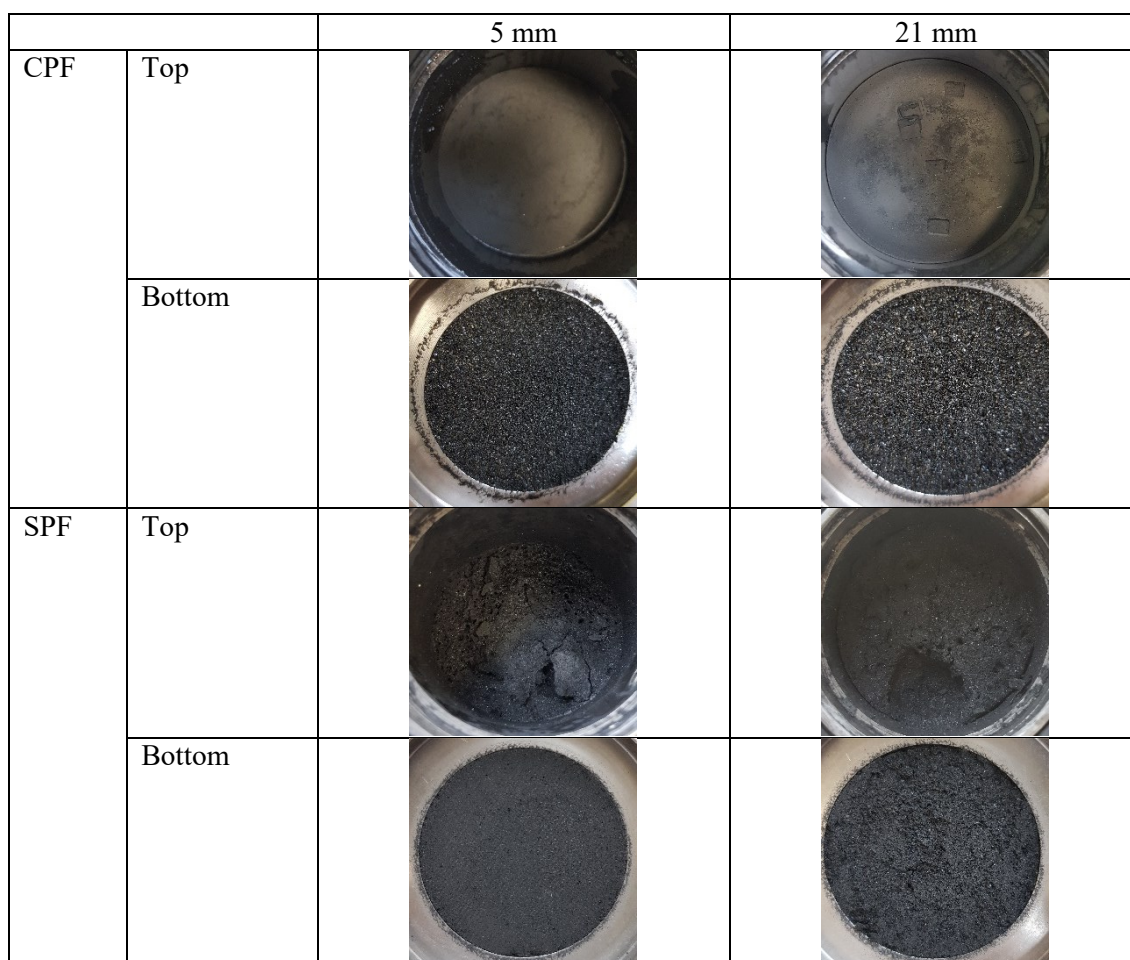
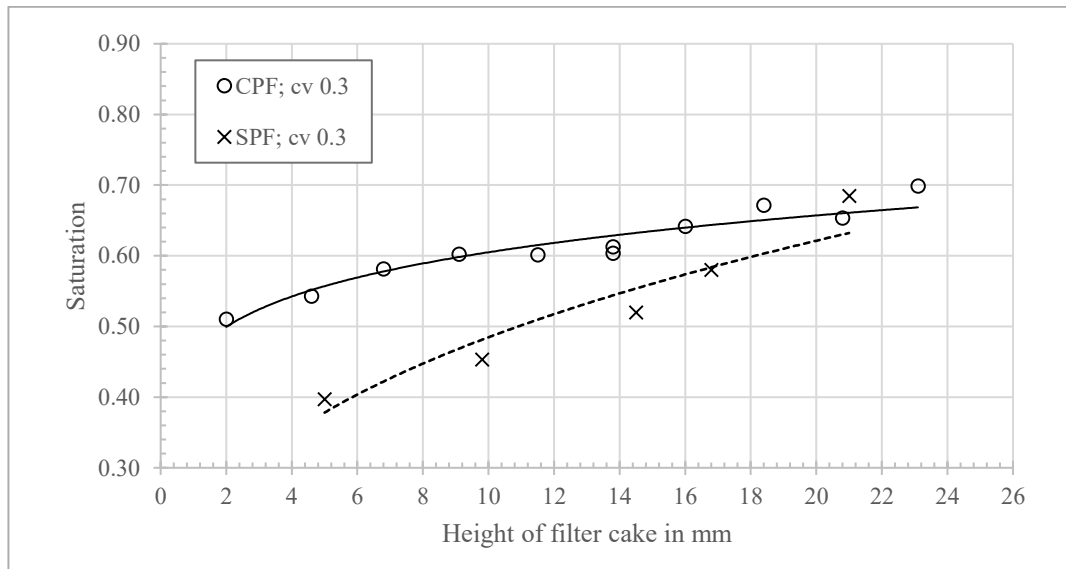


Figure 115. Images for VN coal filter cake in various height; using SPF and CPF; 0.3 of volume fraction; “1-3 bar” of pressure difference.

The next experiment was to observe the effect of filter cake height on the dewatering efficiency and crack prevention. The test was conducted at the above-suggested pressure difference and solid volume fraction. The result is shown in Figure 114. In general, the probability and the degree of crack increases as the filter cake height increases. Its causes are mainly due to the wall effect, the break of agglomerated fine particles in particle network as well as the compression pressure loss. These mechanisms are difficult to overcome when using steam pressure filtration. At the height of filter cake less than 10 mm, the permeability ratio is almost constant and has a similar magnitude as traditional filtration. This value then increased faster than traditional filtration, reaching a value of 7 at the height of 21 mm, compared with the value of 2 of the ratio of permeability to traditional filtration. This issue because of the more prolonged mechanical displacement phase. The filter cake is heated up because of conduction and convection heat before the steam breakthrough. The result is the appearance of the drying effect. S.Gerl and W.Stahl [52], in their publication, also show the dependence of time steam breakthrough to the height of filter cake  $t_{stb} = h_c^2$ . Peuker also show the detailed formular in calculation the steam breakthrough time base on the concentration parameter  $\kappa$ , the angle of cake formation  $\beta_{cf}$ , the pressure difference, and the capillary pressure [8].

$$t_{stb} = \frac{\Delta_p \cdot \kappa \cdot \beta_{cf}}{2 \cdot \pi \cdot n \cdot (\Delta_p - p_{ke})}$$





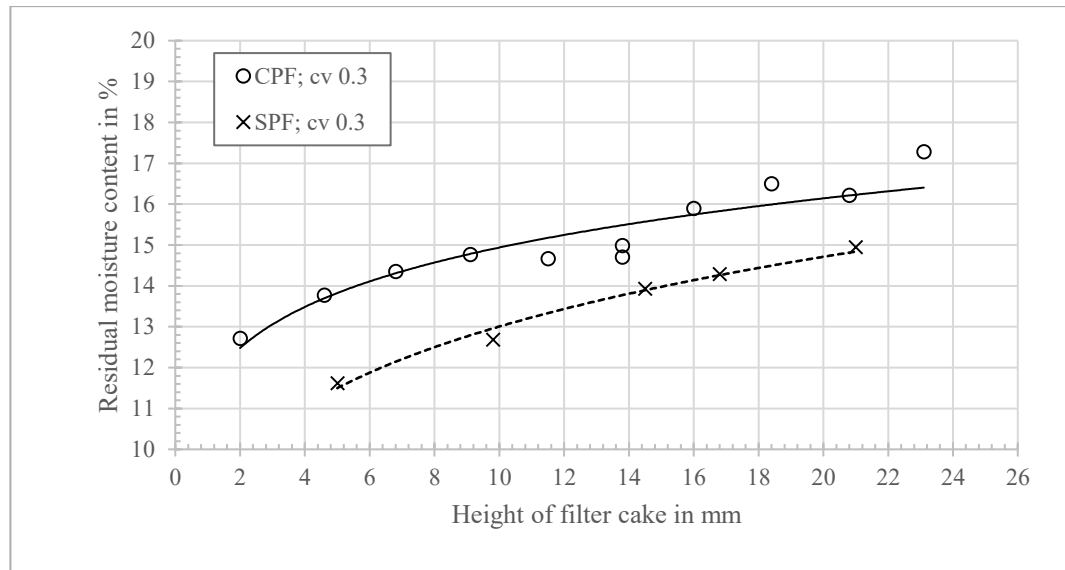


Figure 116. Saturation and residual moisture content of VN coal filter cake in the variety of height ; using SPF and CPF; 0.3 of volume fraction, “1-3 bar” of pressure difference.

Although there is a difference in the permeability ratio of thick filter cake, the saturation level as well as the remaining moisture content of filter cake when using steam pressure filtration is still much lower than that of cake using the conventional pressure filtration. As shown in Figure 116, the saturation value increases from 0.4 to approximately 0.7, equivalent to 11% -14% of residual moisture content when the filter cake height increases to 21 mm. This result is pretty good because only with the mechanical transfer phase, the amount of water is significantly reduced, which cannot be achieved using traditional filtration. The moisture of the material is expected to be further reduced if the drying phase is applied. The remaining water in the filter cake at high temperature, under the effect of the air flowing through it, continues to evaporate and reduce moisture. In the comment of S.Gerl and W.Stahl [52], the dewatering can be further reduced, even attaining the value of 0. The higher the amount of heat, the greater the water transfer capacity. The amount of heat absorbed in the remaining water and in the solid part, caused by condensation, leads to further evaporation of water and further moisture loss.

#### 5.4. General conclusion

In general, the probability and severity of cracks in coal filter cake tend to be similar to limestone.

The permeability ratio tends to decrease when increasing the solid phase content of the suspension. Along with that is the decrease in saturation and moisture. However,

another feature is that while limestone tends to shrink and micro-cracks in dilute suspension, shrinkage cracking is not observed in coal. Cracks on coal filter cake occur in horizontally. They divide the filter cake into two sections. For almost cases, it can be commented they predominate, and they also strongly affect the amount of water remaining in the filter cake. In the case of coal, 0.3 of the solid volume concentration is an appropriate value that should be recommended.

When the height of the filter cake increases, the degree of crack tends to increase, the phenomenon of increasing and explaining mechanisms in the case of limestone is completely acceptable in the case of coal. The solid concentration of 0.3, the height of 15 mm (or even higher) combined with the “1-3 bar” of application pressure difference, provides the best choice for crack prevention and deliquoring efficiency. The achieved residual moisture content attains 16% with a saturation of 0.65.

When application pressure is increased, the efficiency is improved for dilute sludge, but it is almost the same for solid sludge. However, an increase in pressure in economic and technical conditions should also be made.

Although steam filtration does not significantly prevent cracks in the filter cake due to the effects of the drying effect. The degree of saturation and moisture indicates an outstanding value with 0.4 saturation, equivalent to about 11.5% of the moisture with the 2 mm of filter cake thickness, solid volume content of 0.3, and applied pressure “1-3 bar”. Also, steam filtration is expected to reduce moisture significantly as the remaining water in the filter cake continues to evaporate in the next drying phase.

## **6. Overall conclusion and recommendation**

### **6.1. Overall conclusion**

Filtration is a mechanical process in solid-liquid separation, which is widely applied in many areas of life and manufacturing, especially in mineral processing and metallurgical processing industries. The filtration process consists of 3 main phases: cake formation, mechanical displacement (deliquoring), and drying.

Cracks are undesirable phenomena occurring during the mechanical displacement phase of filtration, especially fine-grained filtration. The appearance of cracks, reducing dewatering efficiency, increasing production costs (more pressure is consumed, increasing the amount of washing water), impurity filtration cakes.

The research of this thesis investigates the formation of cracking during filtration and its relationship to the amount of water remaining on filter cake through the test of the effect of close parameters (the solid volume fraction of initial suspension, filter cake deep, applied pressure difference). Otherwise, using steam pressure filtration like new methods improve the dewatering efficiency, avoid the cracks. Two kinds of material are used. The first one is the powder for laboratory: purity limestone. The second one is an industrial material, Vietnam coal, with the main object of residual moisture content lowest possible, improve the current situation. Through testing and interpretation of the phenomenon, the mechanism of cracks is clarified.

The relevance parameter to evaluate the probability and degree of cracks in the filter cake is the permeability ratio, characterized by the ratio of the gas permeability to the liquid permeability. The amount of liquid in the filter cake is represented by two output parameters, residual moisture content and saturation.

There are two main types of cracks: macro cracking and shrinkage micro cracking. Macro cracks are large cracks that can form from the top of the filter cake, spread to the bottom, and have contact with other cracks. This type of crack dramatically affects the efficiency of dewatering as well as subsequent processes. The shapes of the crack are diverse. They can be the cut on the filter cake, which may crack around the filter cake or the tree-branches cracking in the filter cake. The second type is the shrinkage, micro-cracking. These are cracks that form on the surface, bottom or edge of the filter cake, which have little effect on the dewatering efficiency. Also, there is the phenomenon

cracked horizontally of the filter cake (as also called the delamination phenomenon) due to the strong sedimentation and de-mixing of the coarse particles.

For both limestone and coal, the experimental results showed that the increased concentration of solids in the initial suspension leads to the reduction of the probability and the degree of cracks, the improved residual moisture content as well as saturation. In the surveyed range, the suspension concentration can be divided into three zones: the dilute suspension area (sedimentation area), the transfer area, and the concentrate suspension area (homogeneous area). In the homogeneous region, the output parameters (as mentioned above) are stable and achieve the highest filtration efficiency. While moisture and saturation results are significantly improved when using steam filtration, the degree of cracks shown by the permeability ratio does not differ.

About the height of the filter cake, there is a critical point. The filtration results are almost unchanged in the thin filter cake. The output parameters increase significantly when the filter cake height exceeds this critical point.

In general, when the application pressure is increased during the first two phases of the filtration process, the moisture content and the level of crack formation are significantly reduced. Exceptional cases with the opposite trend occurred in ultrafine KS12 material. The application of pressure of “1-3 bar” shows higher efficiency than the pressure levels of “1-1 bar” or “3-3 bar”.

The best results achieve with coarse-grained limestone and fine limestone, which are 8% and 20% of moisture for conventional pressure filtration. The values are 13% for fine limestone filter cake when using steam pressure filtration. For Vietnamese coal, the results are 13% and 11.5% for traditional filtration and steam pressure filtration, respectively. The result is lower than the current situation in the Cua Ong Coal Washing plant (20 - 25 % of residual moisture content). Otherwise, *most results of saturation and moisture are measured when the gas (air, steam) breakthrough the filter cake, not include the drying phase*. Filter cake under this survey conditions was dewatered without cracks. For the further purpose of dewatering, some preliminary tests are executed. The result shows the high efficiency in using steam pressure filtration with the residual moisture content much lower (Appendix C8).

The cracking formation has a number of the main mechanisms:

- The occurrence of weak positions in the filter cake. Under the effect of tensile stress, the weakest places will form a large hollow, thereby forming cracks.

Through the measurement of capillary pressure, tensile stress is also calculated based on previous literature. The tensile stress is significantly high in the capillary state, reduce gradually in the funicular state, and lowest at the pendular state. The cracking occurs when the tensile stress gets high values, especially in the capillary and funicular state. Like the capillary pressure, tensile stress is a function of the degree of saturation. The difference of particle properties, types of material, the solid volume concentration of the initial suspension cause the different values of tensile stress inside the filter cake.

- The sedimentation of particles inside filter cake, which is the main reason for cracking horizontally. Types of crack also effect to dewatering efficiency.

- Due to the wall effect causing wall friction, it affects the packing structure of filter cake. In some places, packing density is lower than in other areas, thereby forming cracks. Also, due to wall effects lead to pressure losses. It results in a loose connection between the particles inside the filter cake, which quickly forms cracks under tensile stress. This effect occurs only in the Nutsche filter and can be avoided in the pilot-scale filter or industrial-filters.

- Due to the agglomeration of the fine particles and packing in the particle network. Because of the weaker bond, the flocs are broken, created the hollow inside the filter cake. Finally, the collapse of the structure of the filter cake leads to the occurrence of cracking.

- For steam pressure filtration, the long steam breakthrough time causes the drying effect, which also one of the reasons for cracking formation. This phenomenon is rarely encountered in conventional pressure filtration.

High filtration efficiency can be achieved when the initial suspension has a high solid volume content (belong to homogeneous areas). The thin filter cake can avoid crack formation through reduced gas breakthrough time and wall effect. Also, the application of high pressure in the mechanical displacement phase leads to the reduction of tensile stress as well as the formation of weak positions in the filter cake. The application of temperature, carefully control the pH, or using surface tension reducers can lead to a reduction in the ability of agglomeration fine particles. Steam filtration applications, with a combination of mechanical and thermal mechanisms, are a suitable solution for dewatering.

## 6.2. Recommendation

Further research should be conducted to provide abundantly clear evidence on the mechanism of cracking formation, hypothesized to explain the phenomena.

Cracks are identified mainly by visual observation. This dramatically affects the extent of cracking and the inability to identify cracks inside the filter cake. Filter cakes should be observed with more modern equipment such as Computed Tomography.

The prevention, as well as countermeasures to cracking formation, require to be accurately assessed.

It is necessary to study different types of material objects, to clarify the formation tendency and degree of cracks. From the obtained results, it is possible to simulate the process as well as forecast the negative impact of the crack on filtration efficiency.

Filtration experiments with a combination of three phases (cake formation, mechanical displacement, and drying phase) are required to make the most accurate assessment of the dewatering efficiency.

For industrial materials such as Vietnamese coal, extra tests on a pilot-scale and industrial-scale are necessary, especially in strict controlling input parameters and assessing the applicability of steam pressure filtration.

Besides using the gravity separation method, coal also is processed using the flotation separation method. This method is particularly useful in improving the quality and reducing the ash of fine coal and ultrafine coals. Further studies are required on the filtration capacity of coal flotation products as well as the interaction effects of flotation chemical (collector, frother) on filtration efficiency and crack formation.

## References

1. A. Rushton, A.S.W., R.G. Holdich, *Solid-liquid Filtration And Separation Technology* 2015, Weinheim, Germany: VCH Verlag.
2. Svarovsky, L., *1 - Introduction to solid-liquid separation*, in *Solid-Liquid Separation (Fourth Edition)*, L. Svarovsky, Editor. 2001, Butterworth-Heinemann: Oxford. p. 1-29.
3. Sparks, C., *Filters and Filtration Handbook*. 2016, USA: Joe Hayton.
4. Barua, A., *Experimental Study of Filter Cake Cracking During Deliquoring*, in *Chemical Engineering & Chemical Technology*. 2014, Imperial College of Science, Technology and Medicine, London.
5. Wiedemann, T. and W. Stahl, *Experimental investigation of the shrinkage and cracking behaviour of fine particulate filter cakes*. Chemical Engineering and Processing: Process Intensification, 1996. **35**(1): p. 35-42.
6. Redeker, D., K.-H. Steiner, and U. Esser, *Das mechanische Entfeuchten von Filterkuchen*. Chemie Ingenieur Technik, 1983. **55**(11): p. 829-839.
7. Darcy, H., *Les fontaines publiques de la ville de Dijon*. Paris, 1856.
8. Peuker, U. and W. Stahl, *Steam pressure filtration: mechanical-thermal dewatering process*. Drying Technology, 2001. **19**: p. 807-848.
9. Anlauf, H., *Mechanische Fest/Flüssig-Trennung im Wandel der Zeit*. Chemie Ingenieur Technik, 2003. **75**(10): p. 1460-1463.
10. Gerl, S., *Dampf-Druckfiltration - Eine kombinierte mechanisch/thermische Differenzdruckentfeuchtung von Filterkuchen*. 1999.
11. Peuker, U. and W. Stahl, *Scale-up and Operation of a Steam Pressure Filter in Pilot Scale*. Chemical Engineering & Technology, 2001. **24**(6): p. 612-616.
12. Esser, S. and U.A. Peuker, *Steam pressure filtration in combination with a water insoluble pore liquid*. Chemical Engineering Science, 2020. **225**.
13. Esser, S. and U.A. Peuker, *Temperature data during steam pressure filtration in combination with a water insoluble pore liquid*. Data in Brief, 2020. **31**.
14. Gerl, S.a.S., W., *Fundamentals of steam pressure filtration*, in *Proc. 10th Annual National Technical Conference , American Filtration & Separations Society*. 1997: Minneapolis, MI, USA.
15. Kozeny, J., *Ueber kapillare Leitung des Wassers im Boden*, in *Sitzungsber Akad. Wiss*. 1927: Wien. p. 136 (2a): 271-306.

16. Anlauf, H., *Wet Cake Filtration: Fundamentals, Equipment, and Strategies*. 2019: Wiley-VCH.
17. Walter Gösele, C.A., *Filtration*, in *Ullmann's Encyclopedia of Industrial Chemistry*. 2005, Wiley\_VCH Verlag GmbH & Co: Weinheim.
18. VDI, *VDI 2762: Mechanical Solid - liquid separation by Cake Filtration, Part 2: Determination of Filter Cake Resistance*. 2010, Beuth-Verlag: Berlin.
19. Bierck, B.R. and R.I. Dick, *In Situ Examination of Effects of Pressure Differential on Compressible Cake Filtration*. Water Science and Technology, 1990. **22**(12): p. 125-134.
20. Tiller, F.M. and T.C. Green, *Role of porosity in filtration IX skin effect with highly compressible materials*. AIChE Journal, 1973. **19**(6): p. 1266-1269.
21. Mattsson, T., M. Sedin, and H. Theliander, *Filtration properties and skin formation of micro-crystalline cellulose*. Separation and Purification Technology, 2012. **96**: p. 139-146.
22. R.J Wakeman, E.S.T., *Filtration Equipment Selection Modelling and Process Simulation*. 1999, Oxford, UK: Elsevier Advanced Technology.
23. Schubert, H., *Kapillarität in porösen Feststoffsystemen*. 1982, Springer-Verlag, Heidelberg. p. p.184.
24. Batel, W., *Aufnahmevermögen körniger Stoffe für Flüssigkeiten, im Hinblick auf verfahrenstechnische Prozesse*. Chemie Ingenieur Technik, 1956. **28**(5): p. 343-349.
25. Batel, W., *Vorausberechnung der Restfeuchtigkeit bei der mechanischen Flüssigkeitsabtrennung*. Chemie Ingenieur Technik, 1955. **27**(8-9): p. 497-501.
26. A.T., B.R.H.a.C., *Hydraulic properties of porous media*. Hydrology papers, Colorado State University, Fort Collins, CO, 1964.
27. Wakeman, R.J., *Vacuum dewatering and residual saturation of incompressible filter cakes*. International Journal of Mineral Processing, 1976. **3**(3): p. 193-206.
28. J., W.R., *An improved analysis for the forced gas deliquoring of filter cakes and porous media*. J. Sep. Proc. Technol., 1982. **3**: p. 32-38.
29. Rhodes, M., *Introduction to Particle Technology*. 2008, England: John Wiley & Sons Ltd.
30. Newitt, D.M.a.C.-J.J.M., *A contribution to the theory and practice of granulation*. Transactions of the Institution of Chemical Engineers, 1958. **36**( 6): p. 422-442.
31. Rumpf, H., *The Strength of Granules and Agglomerates*. Agglomeration, Interscience, New York, 1962: p. 379-413.



32. Schubert, H., W. Herrmann, and H. Rumpf, *Deformation behaviour of agglomerates under tensile stress*. Powder Technology, 1975. **11**(2): p. 121-131.
33. Rumpf, H.C.H., *Zur Theorie der Zugfestigkeit von Agglomeraten bei Kraftübertragung an Kontaktpunkten*. Chemie Ingenieur Technik, 1970. **42**(8): p. 538-540.
34. Schubert, H., *Handbuch der Mechanischen Verfahrenstechnik, Band 1*. 2003, Weinheim: WILEY-VCH Verlag.
35. Schubert, H., *Kapillardruck und Zugfestigkeit von feuchten Haufwerken aus körnigen Stoffen*. Chemie Ingenieur Technik, 1973. **45**(6): p. 396-401.
36. Istitute, W.C., *The coal resource - A comprehensive overview of coal, available at [www.worldcoal.org](http://www.worldcoal.org)*. 2005.
37. MIJAŁ, W., *Coal mining and coal preparation in Vietnam*. Journal of the Polish Mineral Engineering Society, 2018.
38. Baruya, P., *Prospects for coal and clean coal technologies in Indonesia*. 2009.
39. Bui, X.-N. and C. Drebenstedt, *Use of hydraulic backhoe excavator in Vietnam open pit coal mines*. 2004.
40. Wolfgang Ritschel, H.-W.S. *World market for hard coal 2007 edition*. 2007; Available from: <http://www.rwe.com/web/cms/en/235584/rwe-powerag/media-center/hard-coal/>. RWE Power, 102 pp (Oct 2007).
41. Chuan, L.M., *Current status of coal demand and supply in Vietnam and plan of Vinacomin in the coming time, available at [www.jcoal.org.jp](http://www.jcoal.org.jp)*. 2011.
42. H. Anlauf, R.B., W.Stahl, A.Krebber, *The formation of shrinkage cracks in filter cakes during dewatering of fine sized ores*. Aufbereitungstechnik, 1985.
43. Wakeman, R.J., *The Role of Internal Stresses in Filter Cake Cracking*. Filtration and Separation, 1974: p. 357 - 360.
44. R:D.Wyckoff, H.G.B.M.M., D.W.Reed, *The measurement of the Permeability of Porous Media for Homogeneous Fluids*. 1933.
45. VDI, *VDI 2762: Mechanical solid-liquid separation by cake filtration, Part 3: Mechanical deliquoring of incompressible filter cakes by undersaturation using a gas pressure difference*. 2017, Beuth-Verlag: Berlin.
46. Rumpf, H.C.H. and A.R. Gupte, *Einflüsse der Porosität und Korngrößenverteilung im Widerstandsgesetz der Porenströmung*. Chemie Ingenieur Technik, 1971. **43**(6): p. 367-375.

47. Carman, P.C., *Fluid flow through granular beds*. Chemical Engineering Research and Design, 1997. **75**: p. S32-S48.
48. Lala, A., *Modifications to the Kozeny-Carman model to enhance petrophysical relationships*. Exploration Geophysics, 2017. **49**.
49. Gray, W.A., *The packing of solid particles*. 1968.
50. Urs A. Peuker, W.S., *Scale-up of steam pressure filtration*. Chemical Engineering and Processing: Process Intensification, 1999. **38**(4-6): p. 611-619.
51. Burton, G., *A New Process For Reducing the Moisture Content of Filter Cakes*. Proceedings of the Fourth International Coal Preparation Congress, 1962: p. 620-632.
52. Gerl, S. and W. Stahl, *Improved Dewatering of Coal by Steam Pressure Filtration*. Coal Preparation, 1996. **17**(1-2): p. 137-146.

## Appendices

### Appendix A: Data from CCWP.

#### A1. Particle size and solid concentration of the suspension.

Source: the surveyed data of the Coal Washing Science and Technology Department - Cua Ong Coal Washing Company. The samples are collected in surveyed three days (26/3, 31/3, 4/4 /2015).

Input suspension to thickener	Sampling location	Slurry flow rate, m <sup>3</sup> /h (estimated number)	Solid/liquid ratio, g/l	Particle size range (mm), %				
				+1	0.5 -1	0.1 - 0.5	0.074 - 0.1	-0.074
Factory I	Pressure stabilizer tank	1013	122.58	0.63	1.06	11.40	8.80	78.11
Factory II	Pressure stabilizer tank	3040	158.46	0.62	2.81	23.91	9.23	63.43

#### A2. The dimension of thickener.

Source: the surveyed data of the Coal Washing Science and Technology Department - Cua Ong Coal Washing Company.

Size parameters in mm	Factory I	Factory II
The diameter of input pipes to pressure reducing tank	375x2	375; 219
The diameter of pipes between pressure reducing tank and thickener	450	700
Diameter of thickener	10690	21500
Height of thickener	4700	3200
The diameter of input pipes to thickener	600	1800

#### A3. Particle size and solid concentration of suspension.

Source: Report No. 1285/BC-TTCO about the assessment of efficiency of filtration, Cua Ong Coal Washing Company, in April, 11<sup>st</sup> 2018. The samples are collected in surveyed three days (4/4, 5/4, 6/4 /2018).

No.	Content	Particle size range (mm), %				Solid/Liquid ratio
		+1	0.5-1	0.5-0.125	0-0.125	
1	Input suspension to filter	0.29	1.03	13.43	85.23	458.52
2	Filtrate	0.26	0.7	10.49	88.55	122.55

#### A4. Operation parameters of the filter.

Source: Report No. 1285/BC-TTCO about the assessment of efficiency of filtration, Cua Ong Coal Washing Company, in April, 11<sup>st</sup> 2018. The samples are collected in surveyed three days (4/4, 5/4, 6/4 /2018).

No.	Block	Mass in T	Residual moisture content	Working time (hours)	Specific capacity (t/h)
1	1	1823	25.38	98	18.6
2	2	3677	24.86	210.4	17.48
Total		5500	25.03	308.4	17.83

#### A5. The assessment according to the Reportation No. 1285/BC-TTCO.

Source: Report No. 1285/BC-TTCO about the assessment of efficiency of filtration, Cua Ong Coal Washing Company, in April, 11<sup>st</sup> 2018.

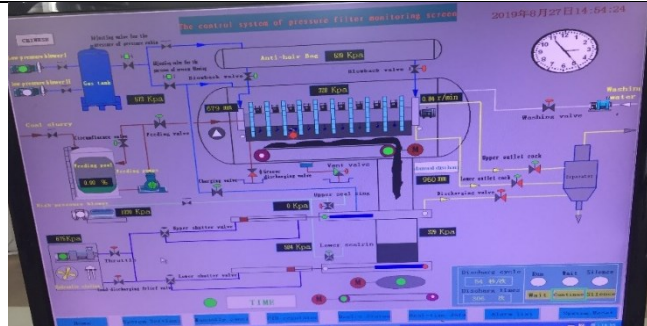
- The solid/liquid ratio of input suspension is suitable (458.52 g/l compared to 420g/l of design).
- The solid/liquid ratio of filtrate is high (122.55 g/l compared to 40g/l of design).
- The high residual moisture content (reach to 27% in some shifts).
- The low efficiency of filtration due to the significant amount of fine particle (below 0.5 mm, especially below 0.125 mm).
- The pressure loss (180-280 Mpa- compared to the 350 Mpa of design).

#### A6. Images for dewatering equipment in Cua Ong Coal Washing Plant.





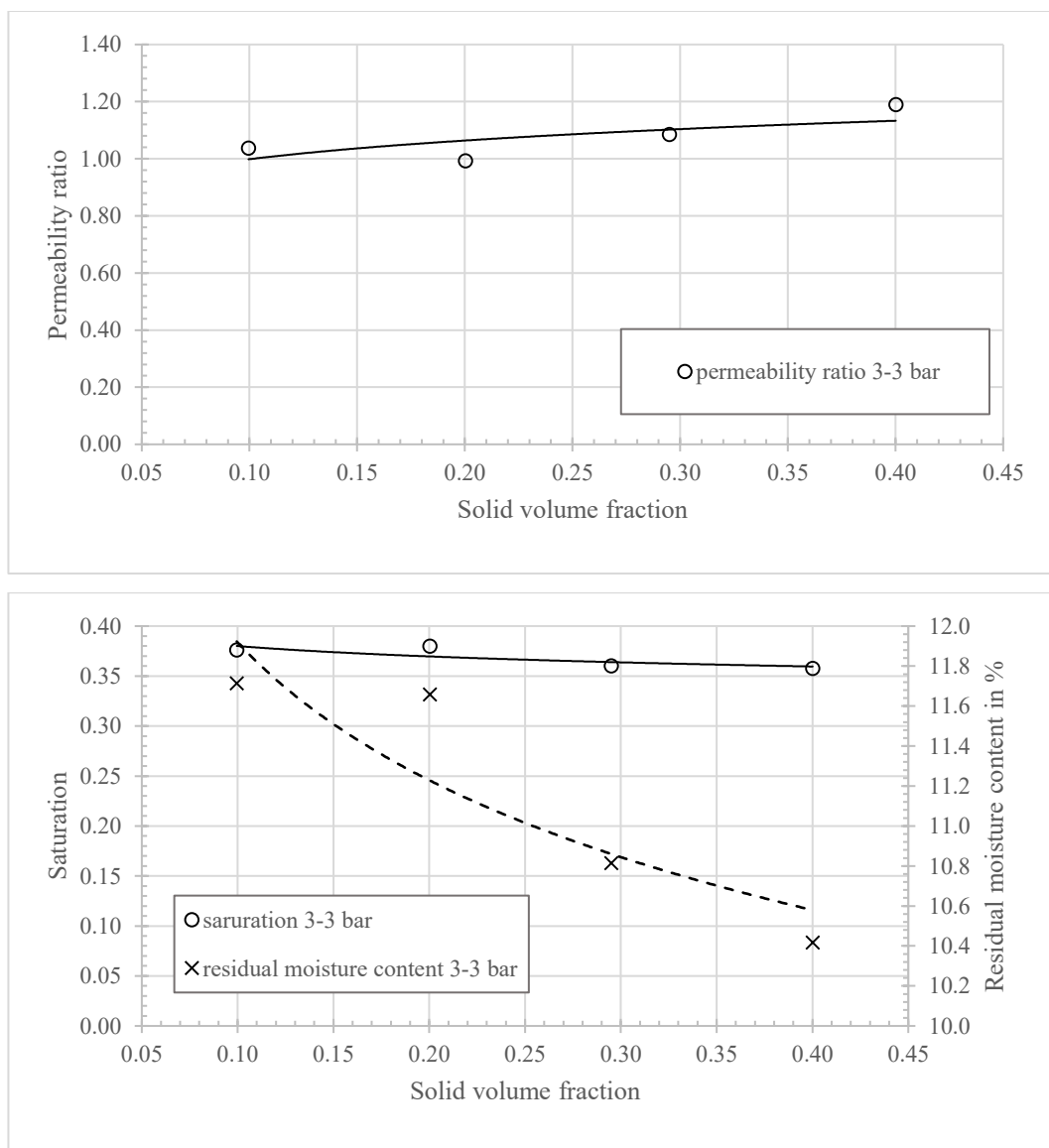
Hyperbaric disk filter

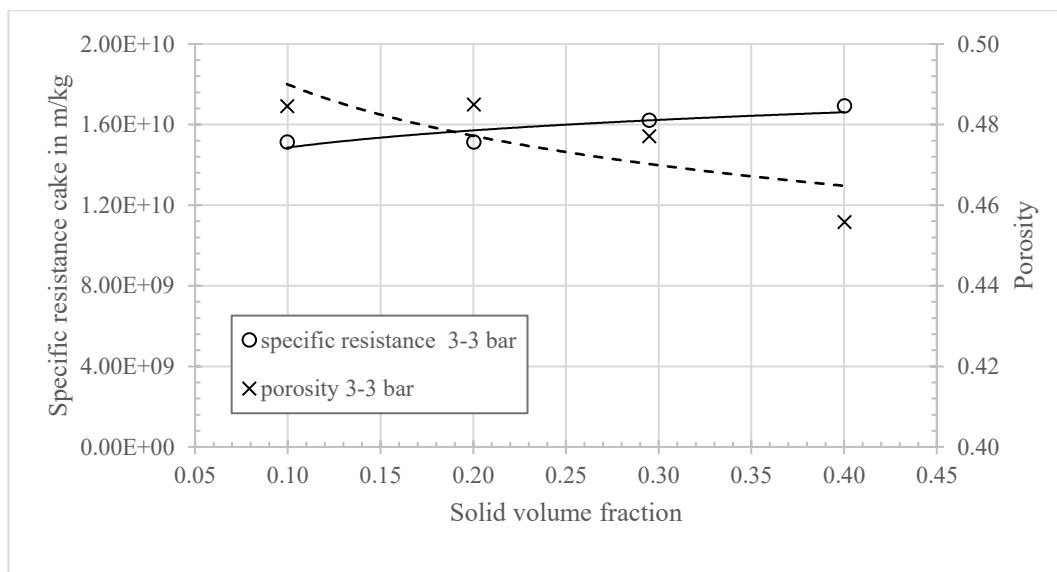


Diagram, parameters of filtration process (upper)  
and Thermal drum dryer (lower)

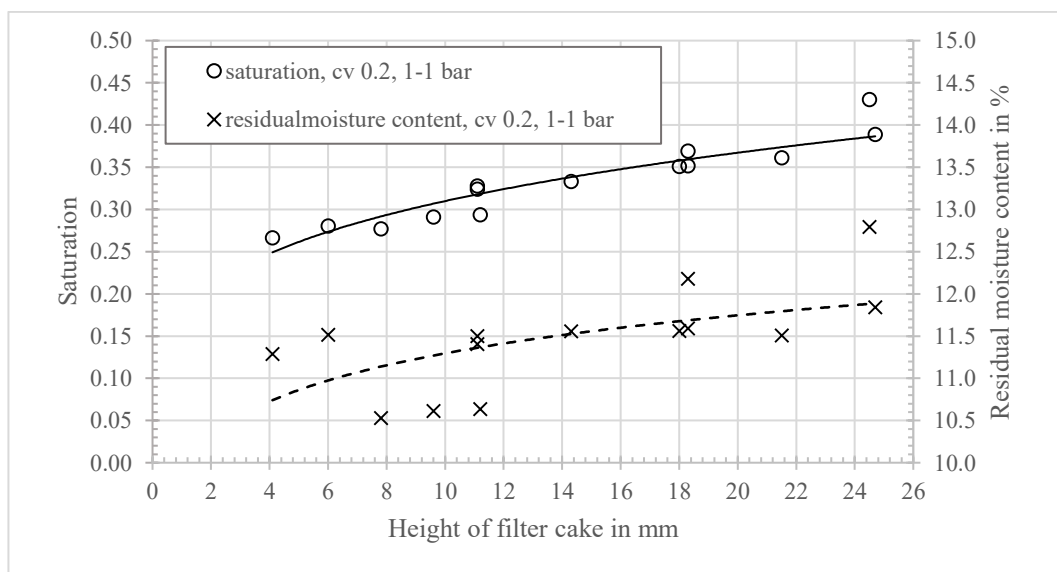
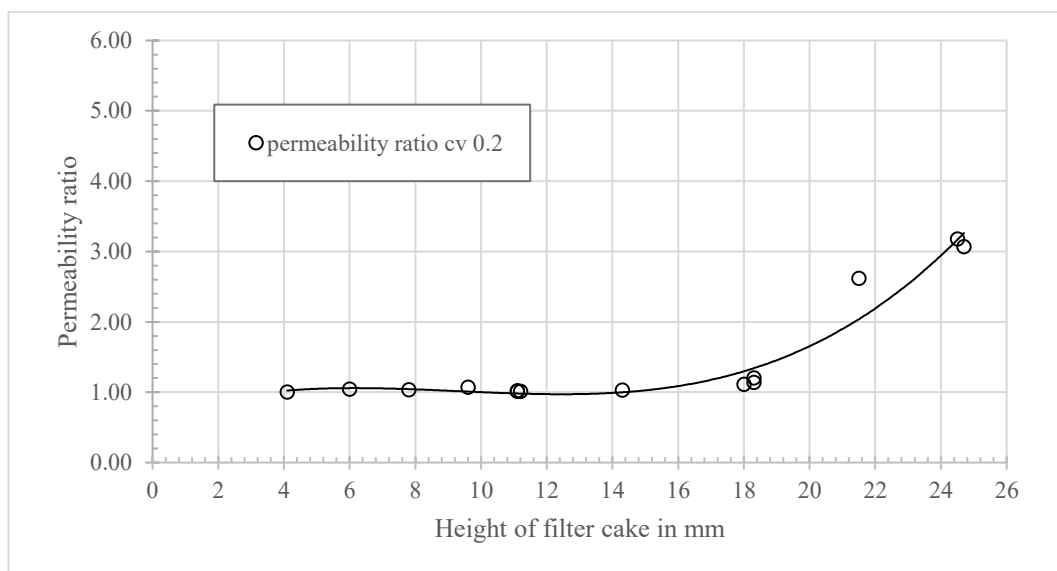
Appendix B: Data from the crack formation with various operation parameters using conventional pressure filtration (CPF).

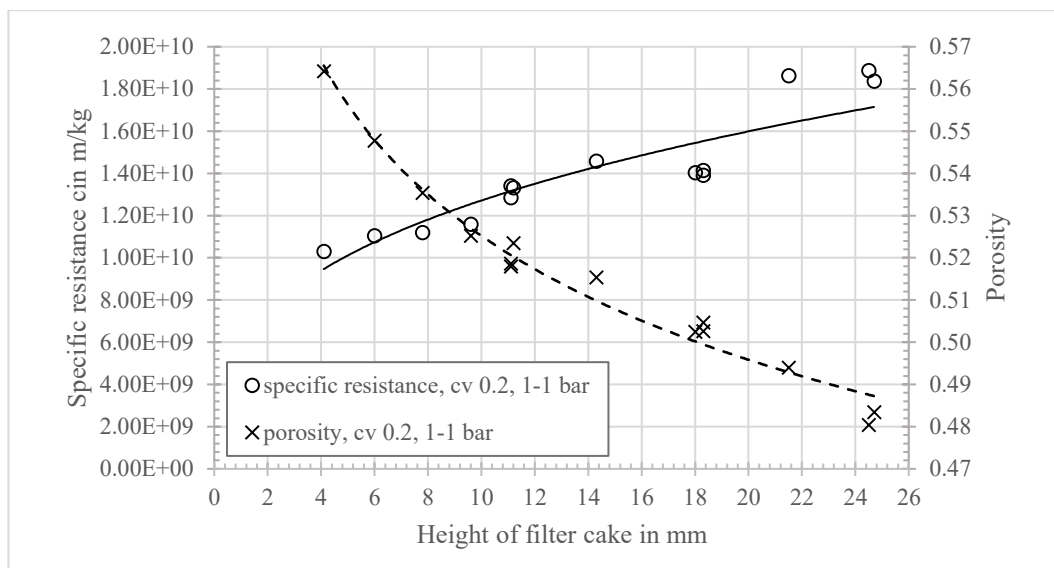
B1. The result of KS100 filtration in the variety of volume fraction; 18 mm of filter cake height, “3-3” of pressure difference.



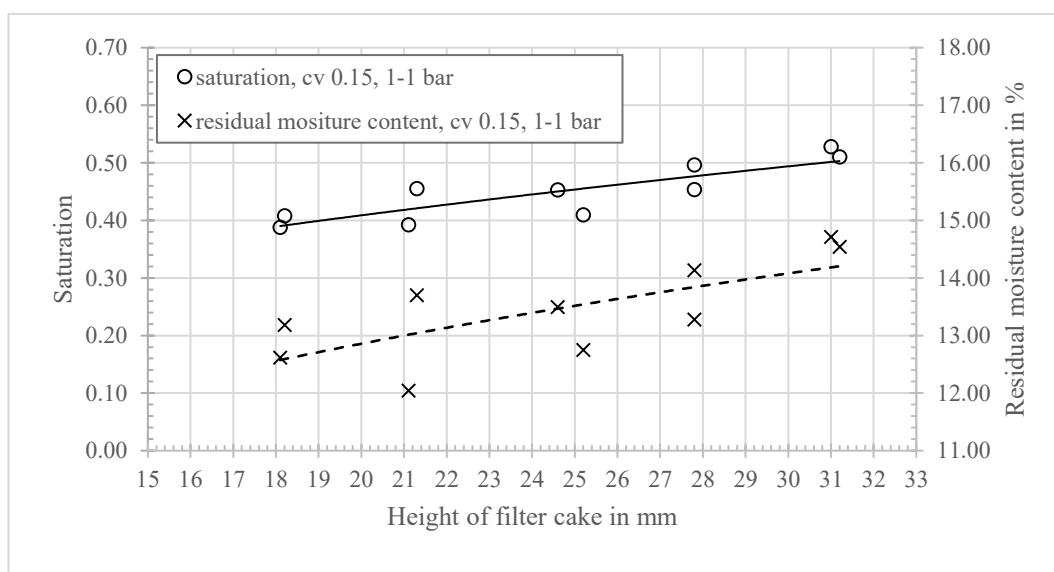
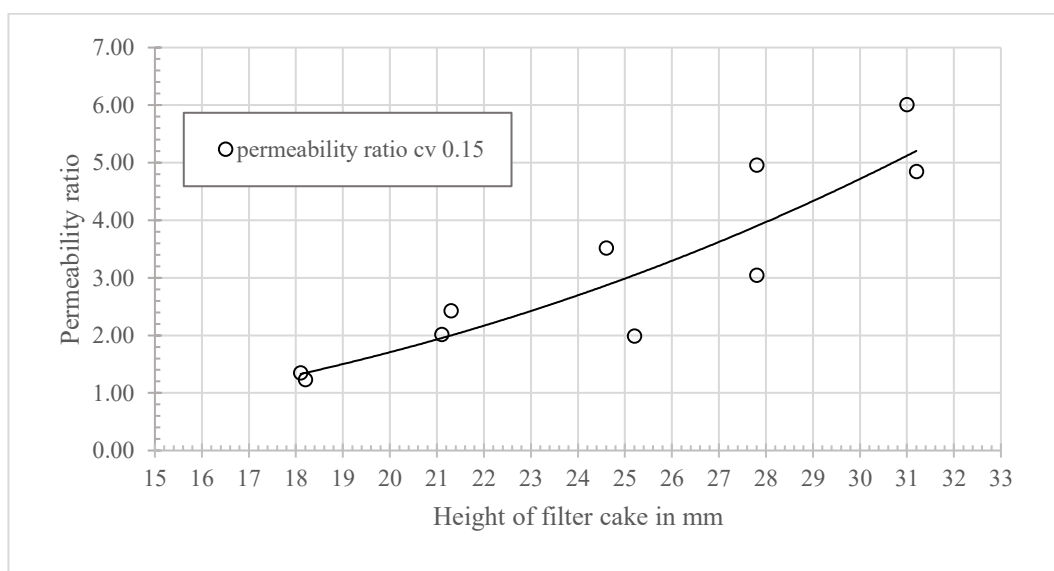


B2. The result of KS100 filtration in the variety of filter cake deep; 0.2 of volume fraction, “1-1 bar” of pressure difference.

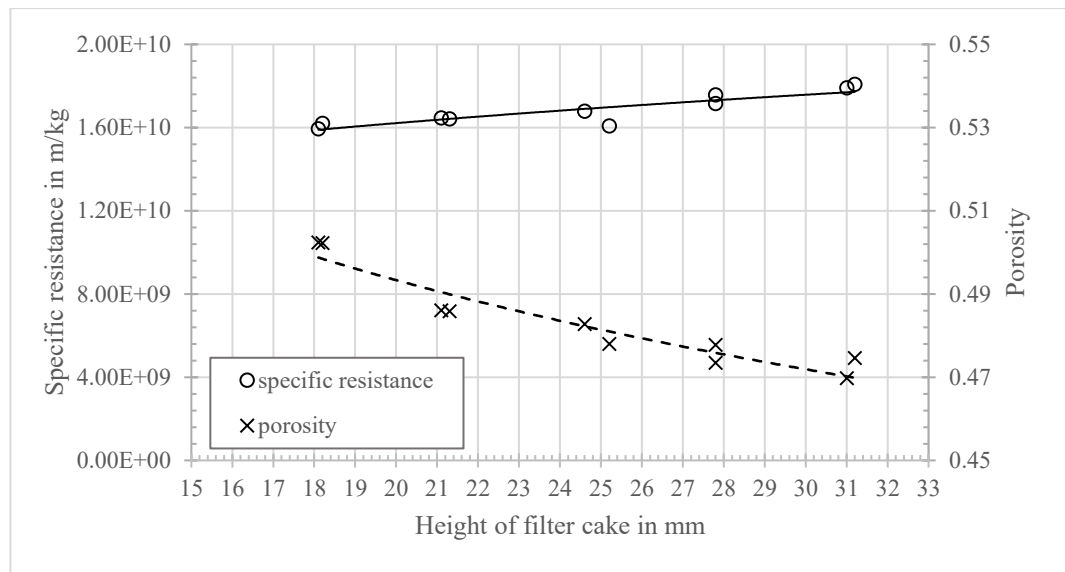




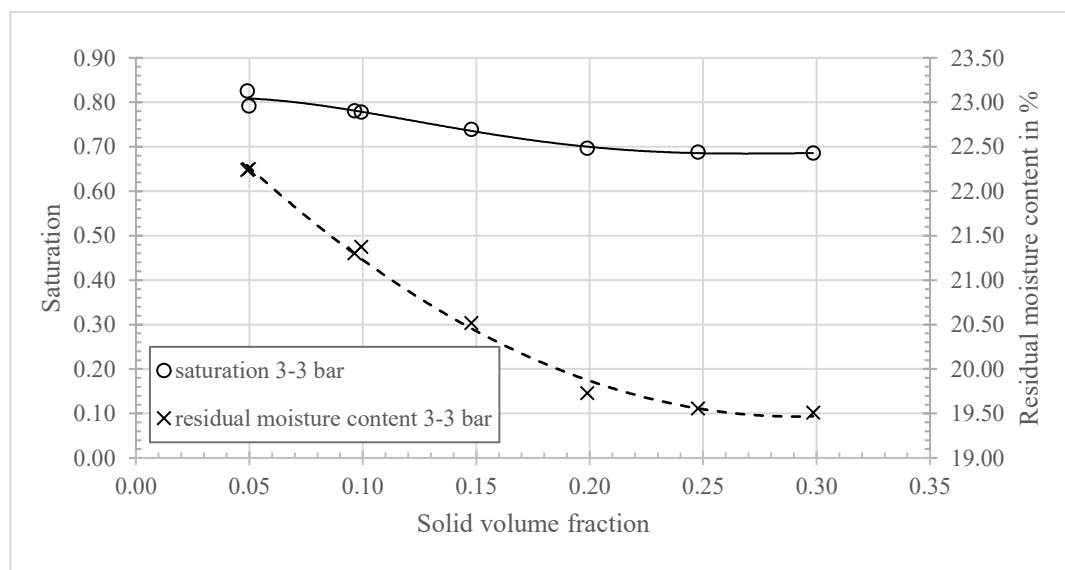
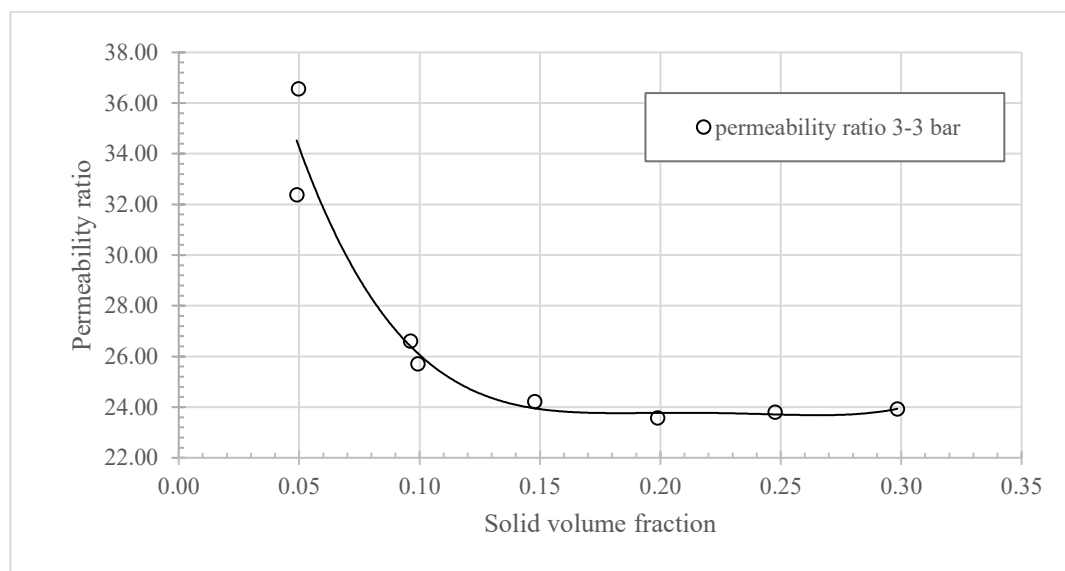
B3. The result of KS100 filtration in the variety of filter cake deep; 0.15 of volume fraction, “1-1 bar” of pressure difference.

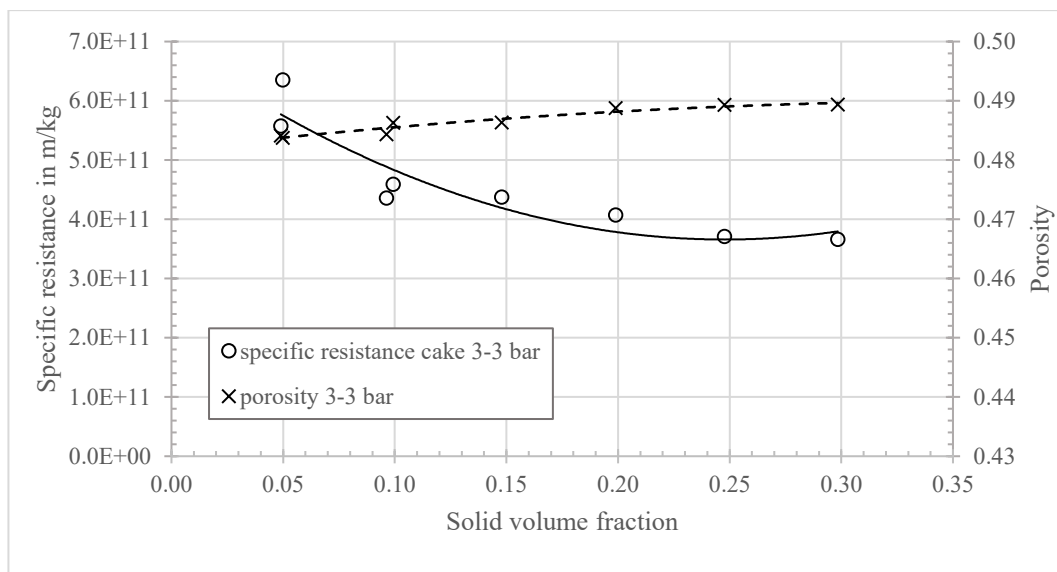




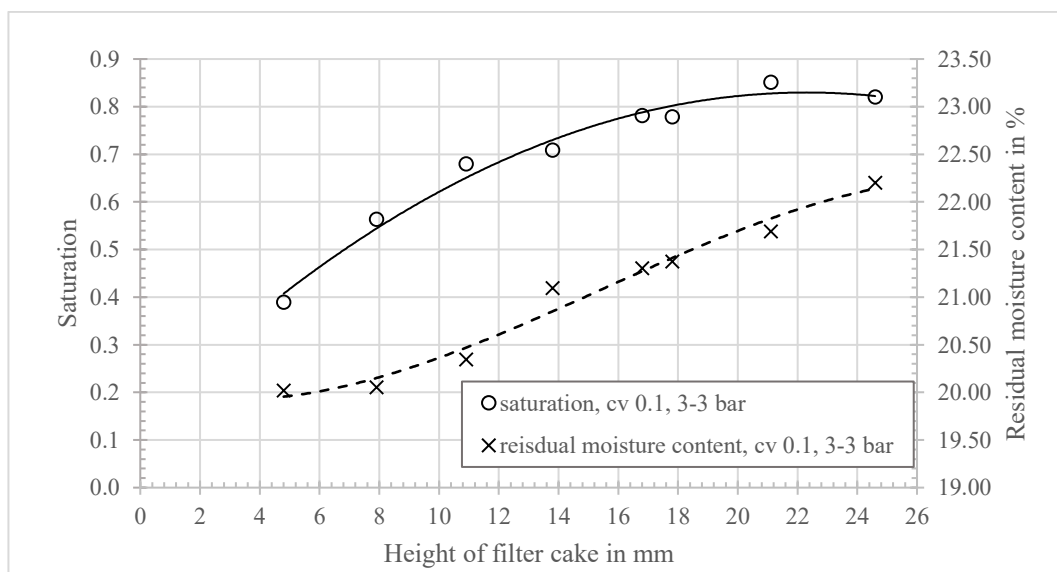
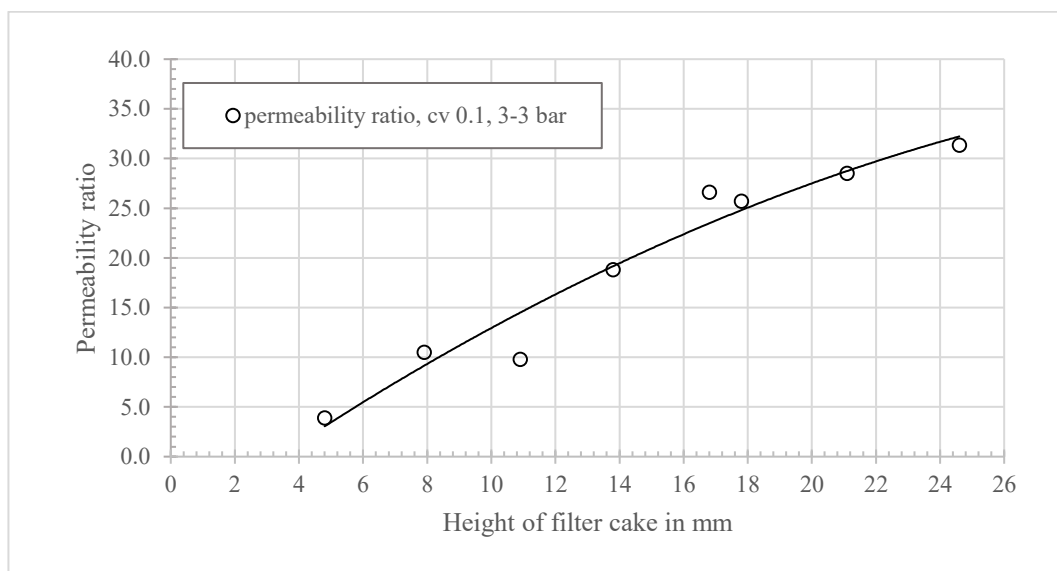


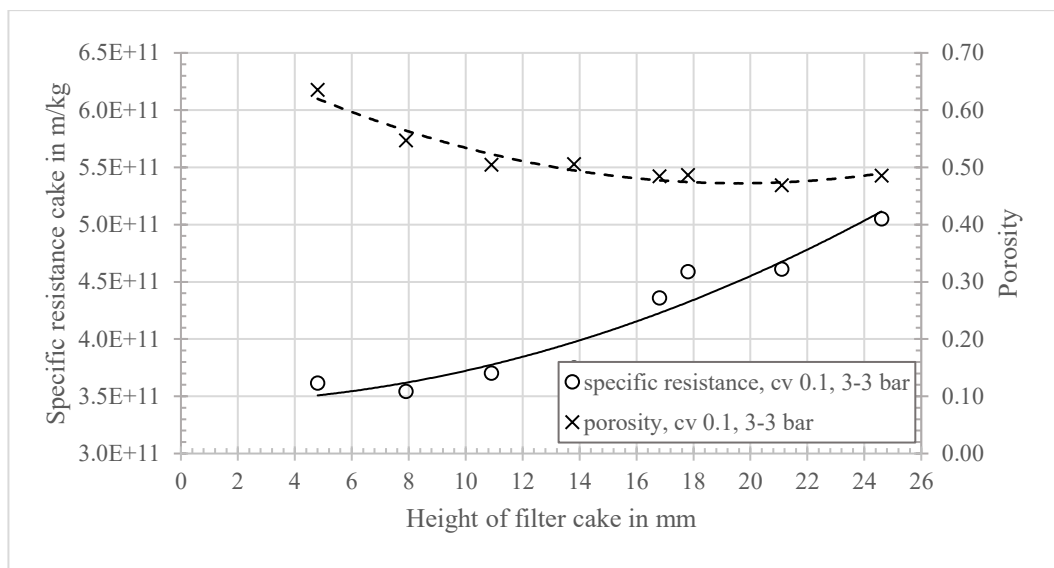
B4. The result of KS12 filtration in the variety of solid volume fraction; 18 mm of filter cake height, “3-3 bar” of pressure difference.



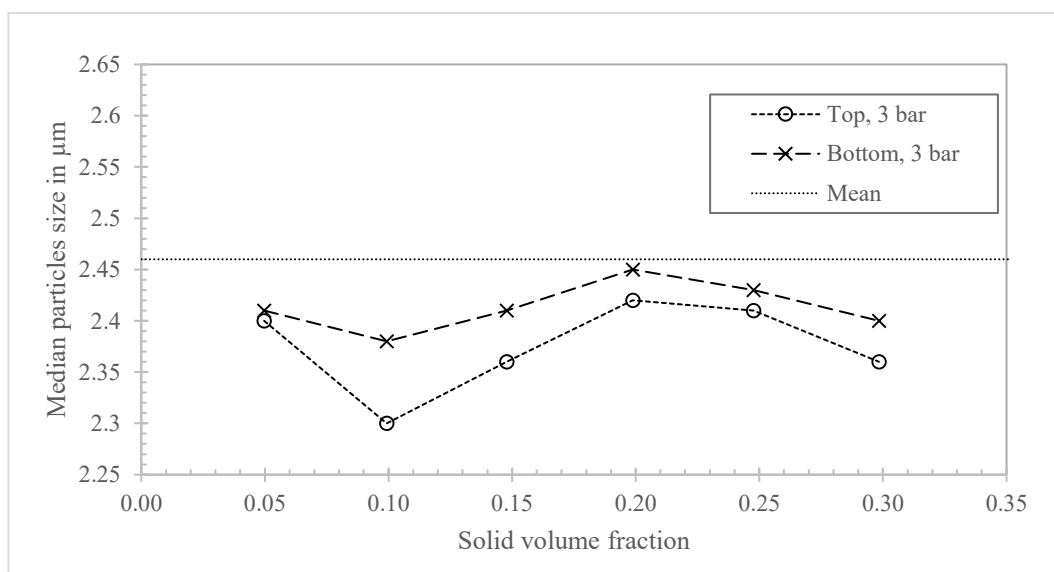


B5. The result of KS12 filtration in the variety of filter cake deep; 0.1 of solid volume fraction, “3-3 bar” of pressure difference.

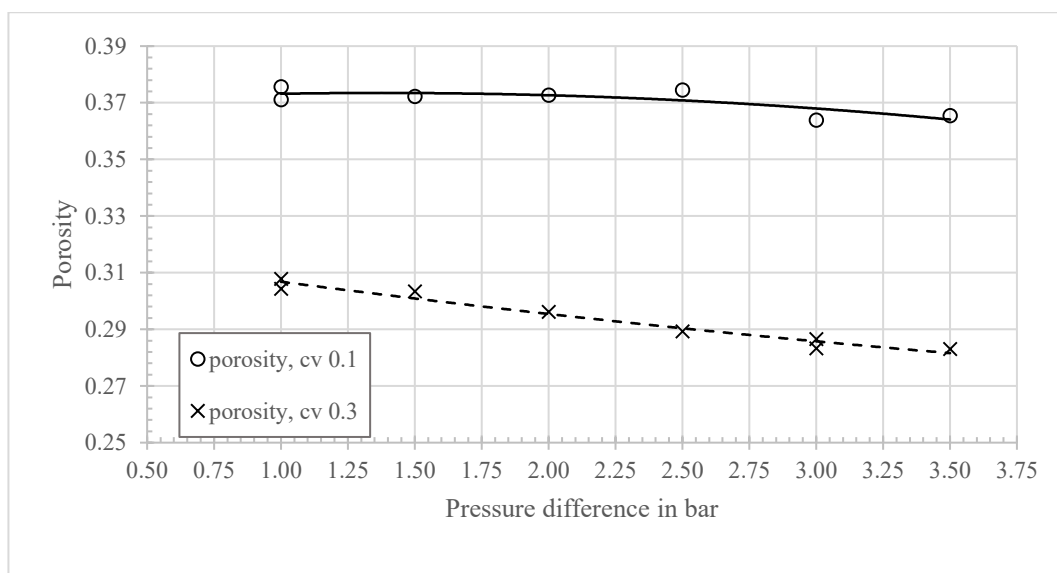
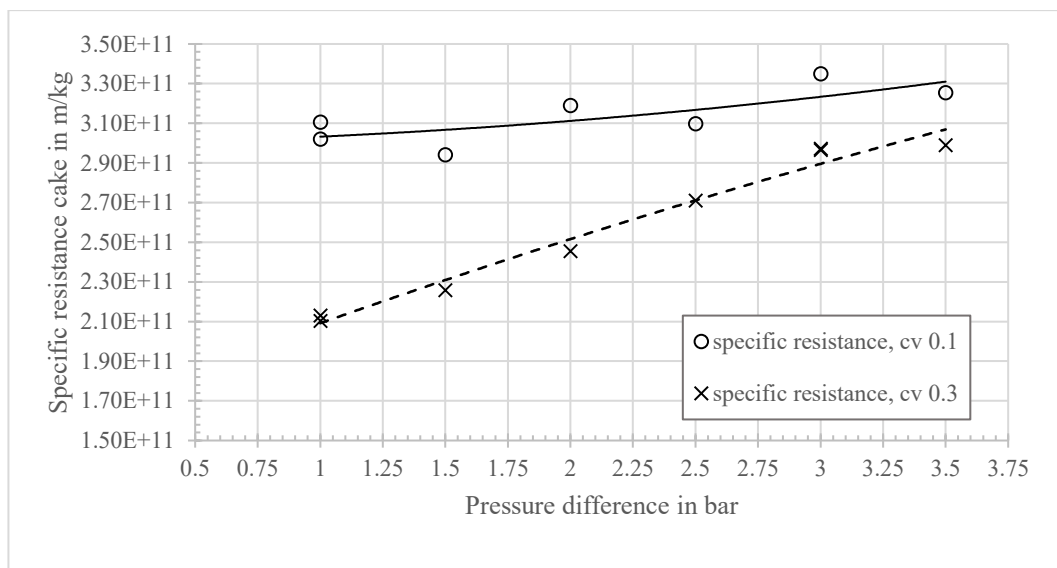




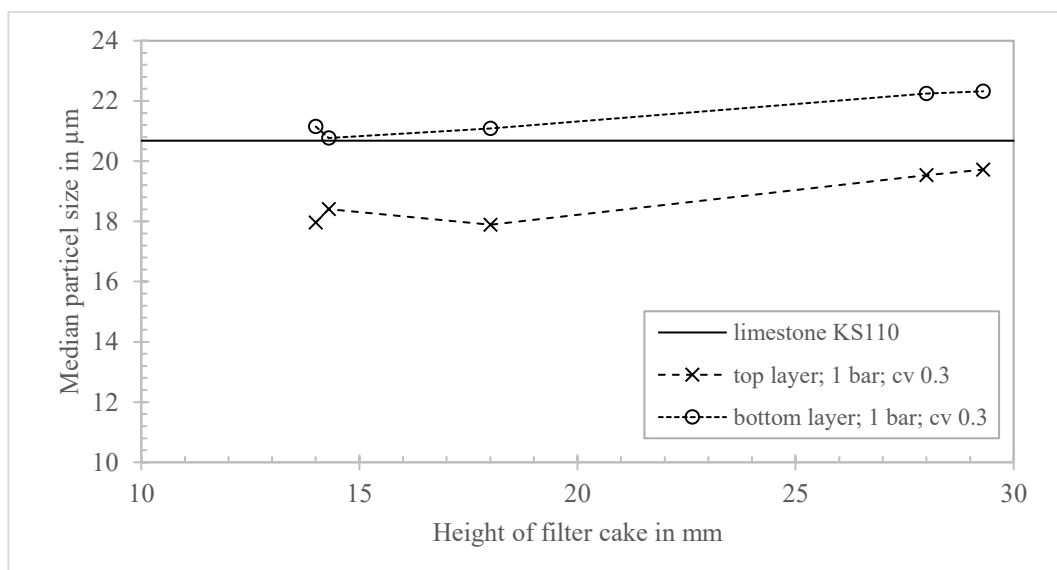
B6. Median particle size on the top and bottom layer of KS12 filter cake in the variety of volume fraction, 18 mm of filter cake height, 3 bar of pressure difference in the cake formation phase.



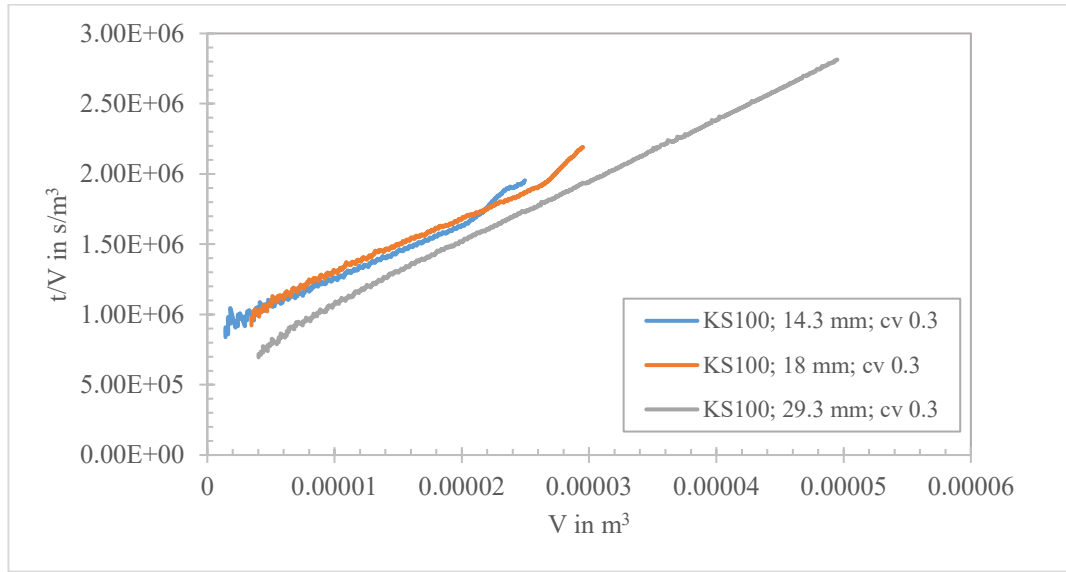
B7. Specific resistance and porosity of VN coal filter cake in the variety of pressure difference, 15 mm of filter cake deep.



B8. Median particle size on the top and bottom layer of KS 12 in a variety of filter cake thickness; 0.3 of volume fraction; 1 bar of pressure difference in the cake formation phase.

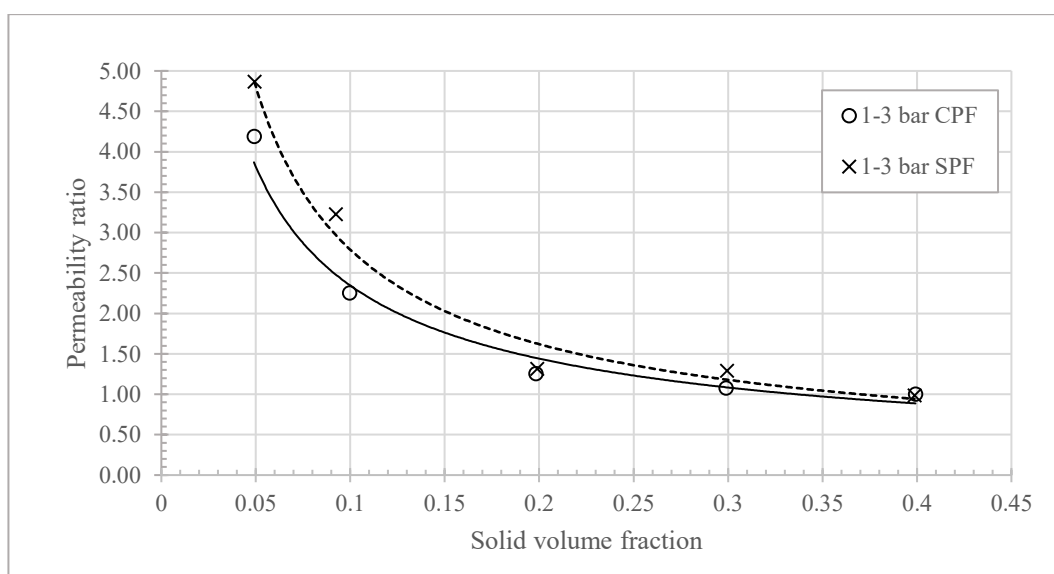
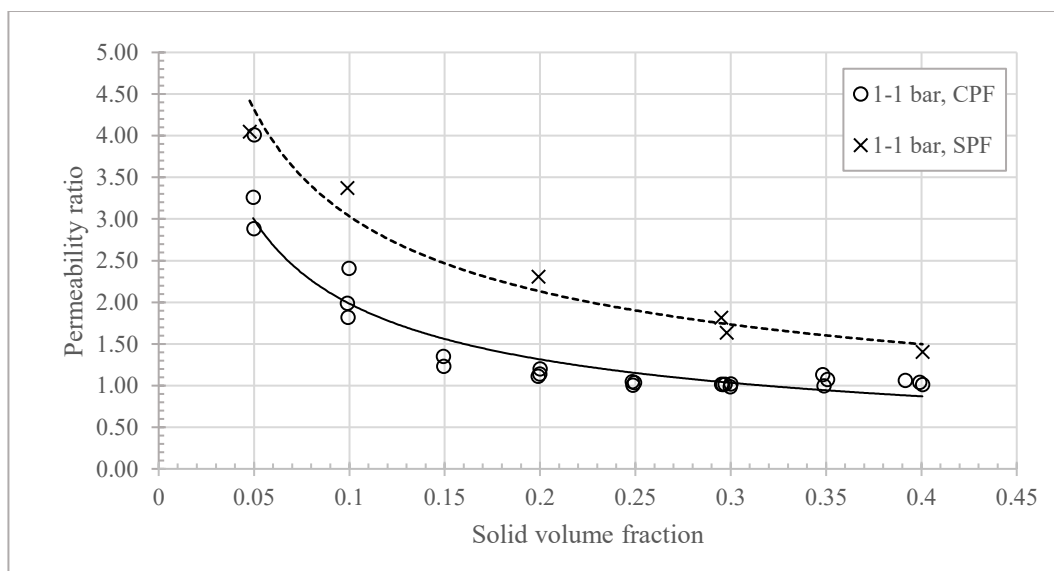


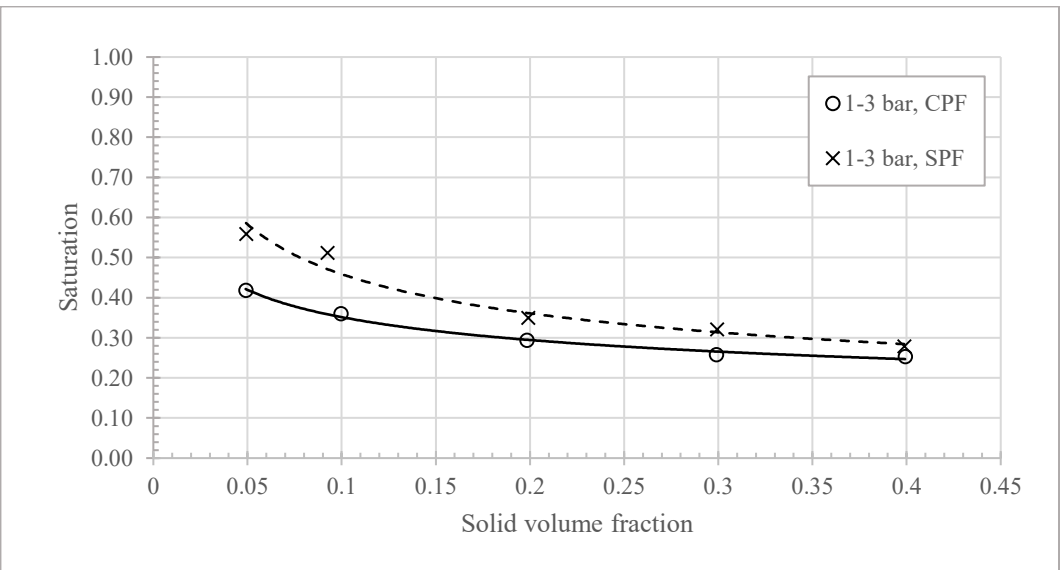
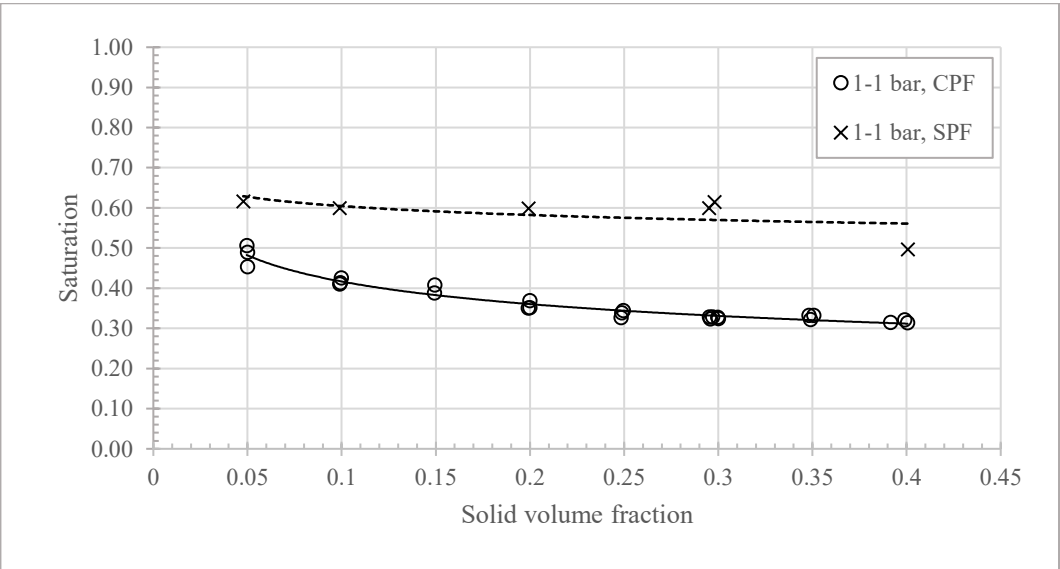
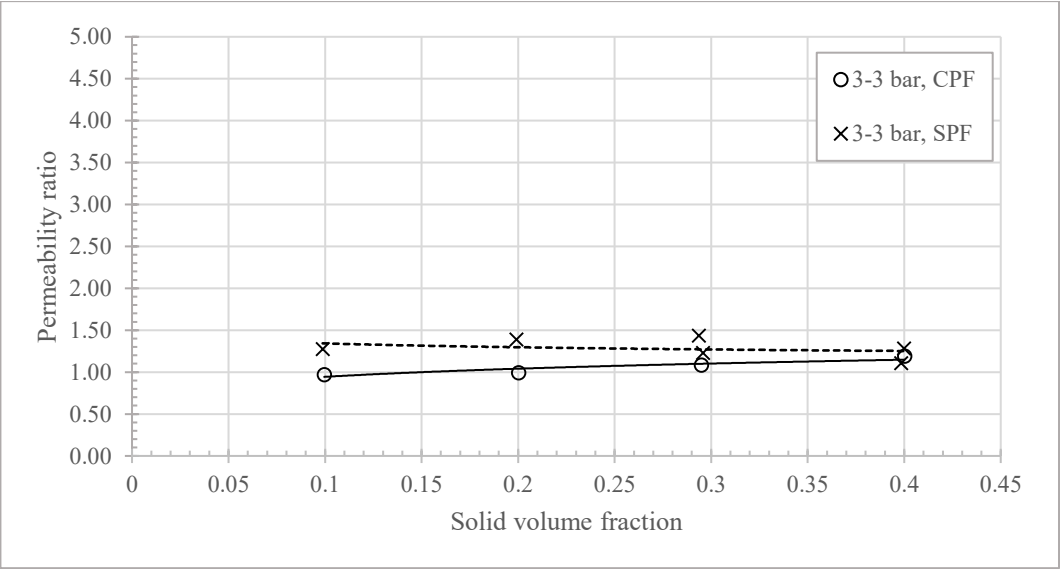
B9. The diagram  $t/V$  vs  $V$  of KS100 filter cake in variety filter cake height; 1 bar of pressure difference in the cake formation phase, 0.3 of volume fraction.

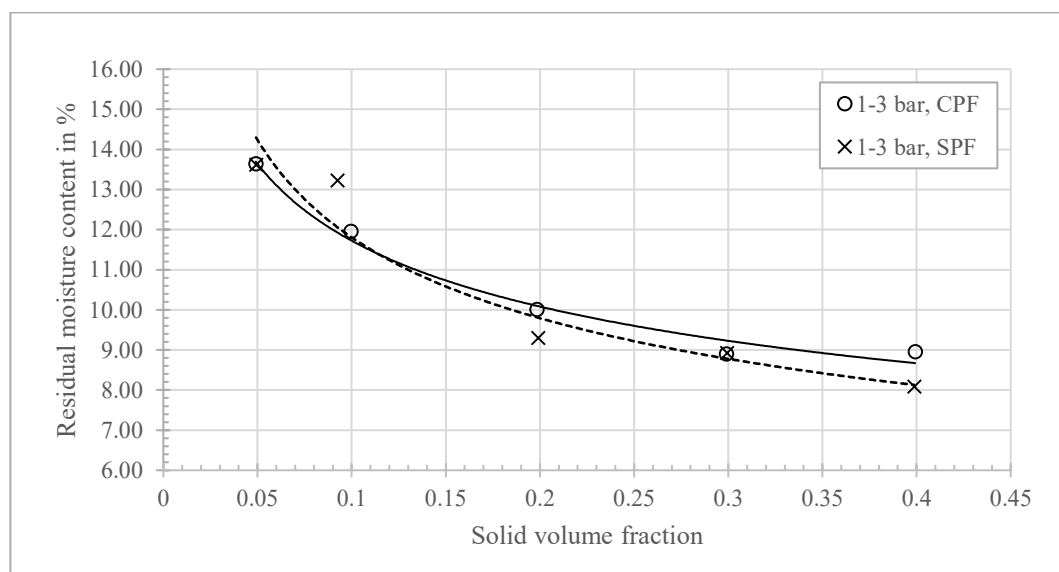
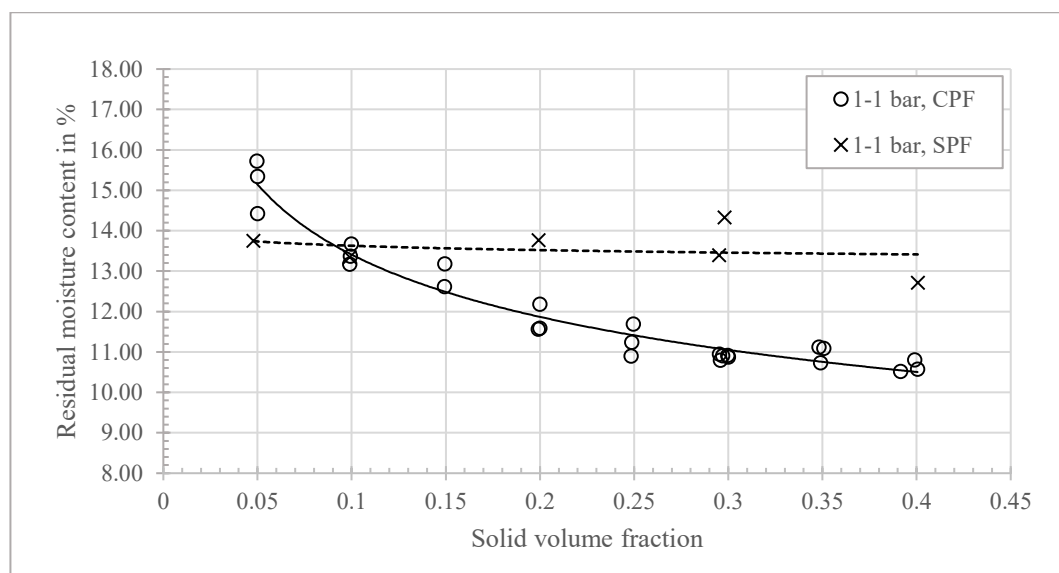
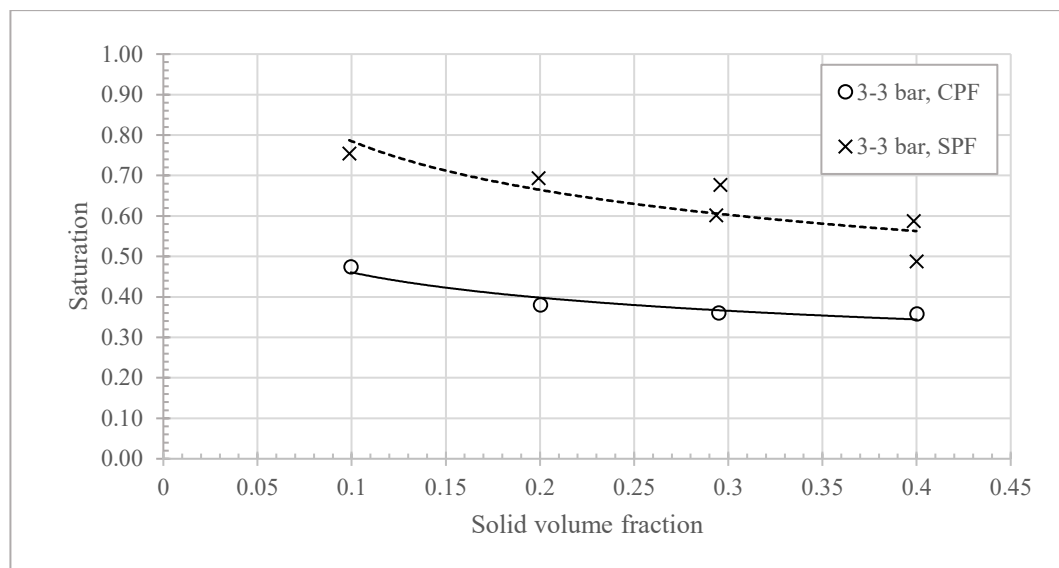


## Appendix C: Data from steam pressure filtration.

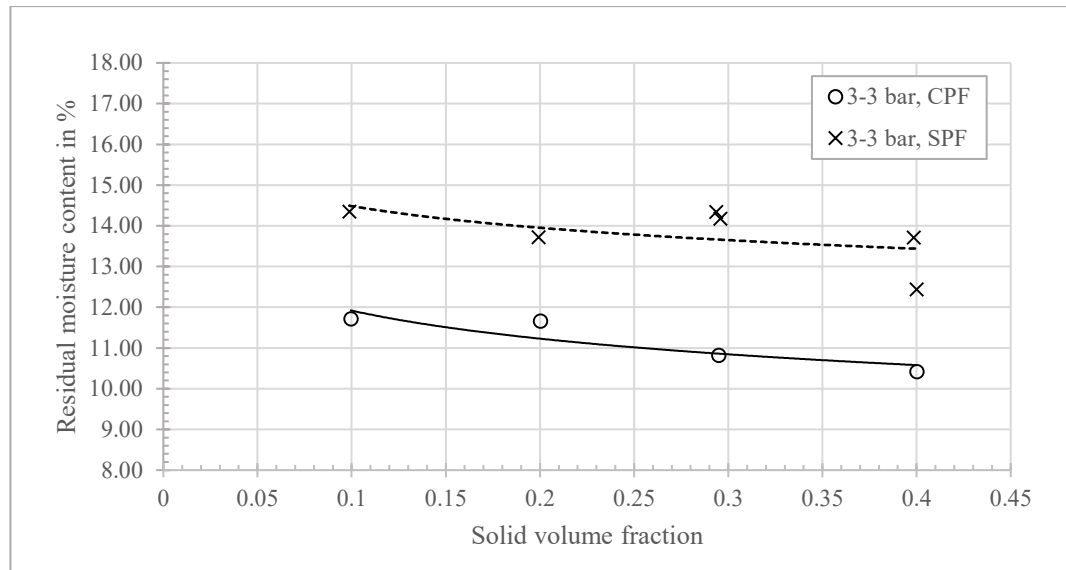
C1. Permeability ratio, saturation and residual moisture content of KS100 filter cake in variety volume fraction using CPF and SPF; 18 mm filter cake deep; “1-1 bar”, “1-3 bar” and “3-3 bar” of pressure difference.



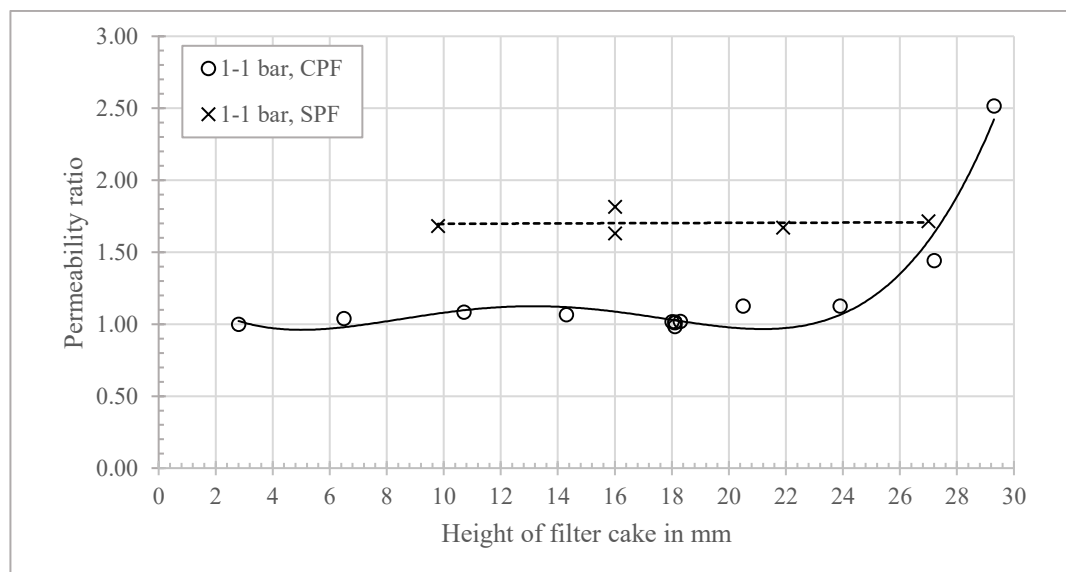


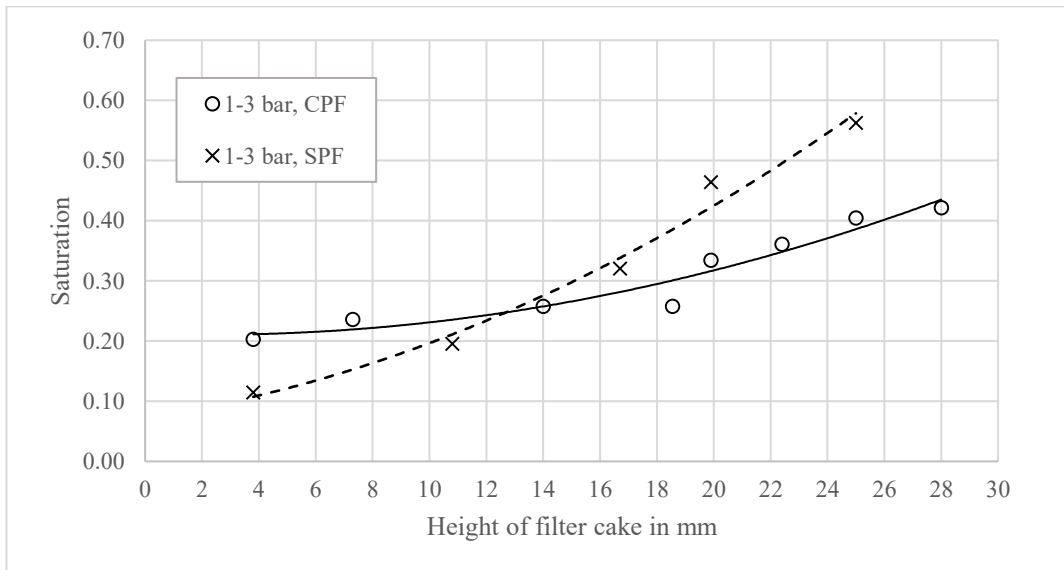
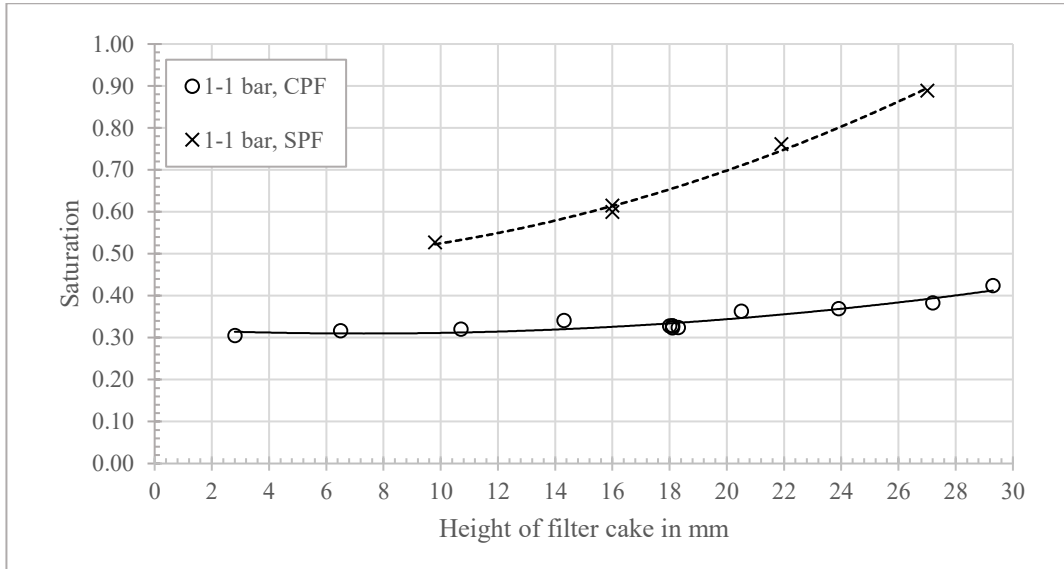
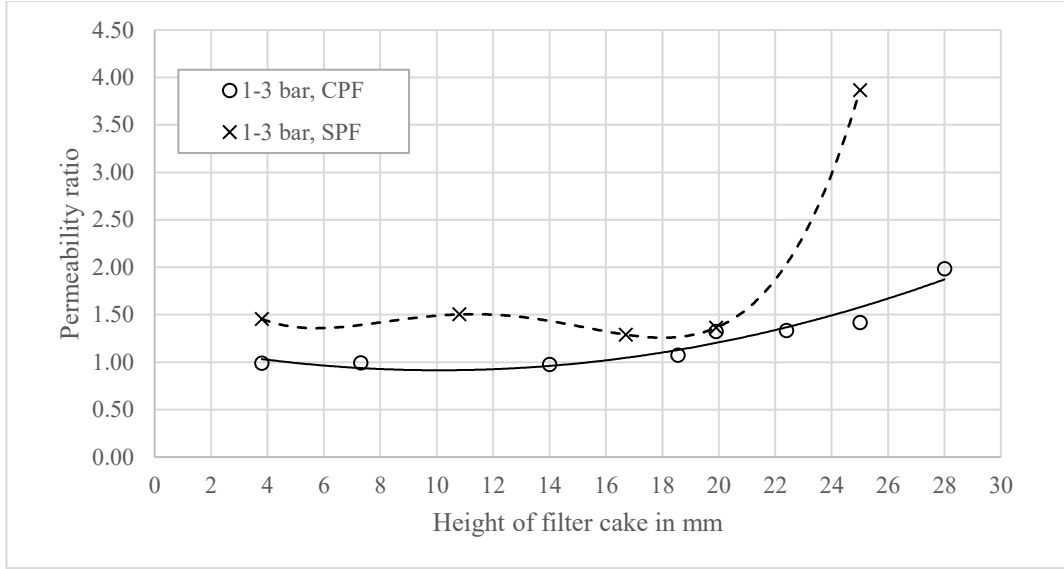


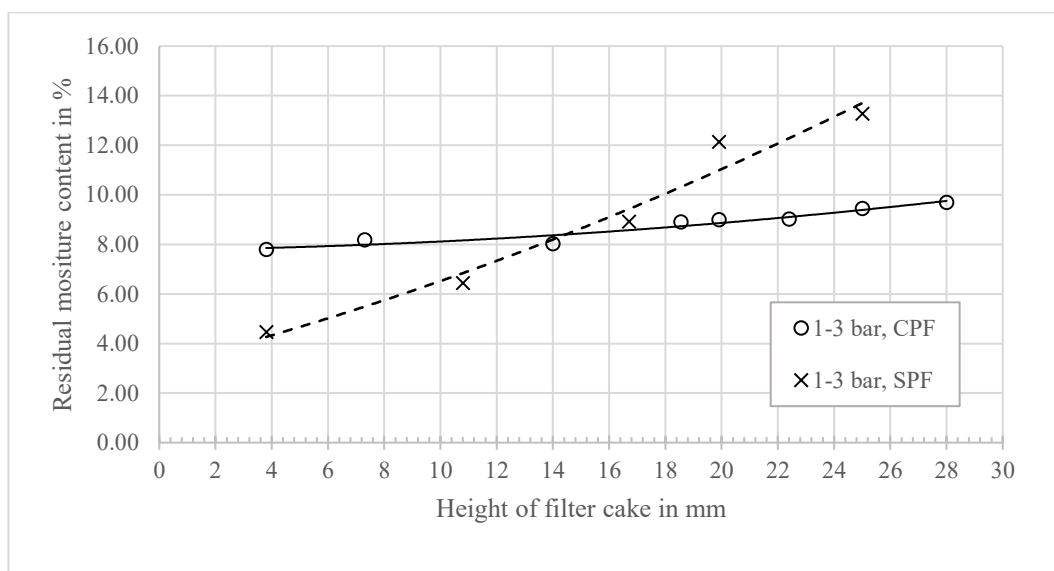
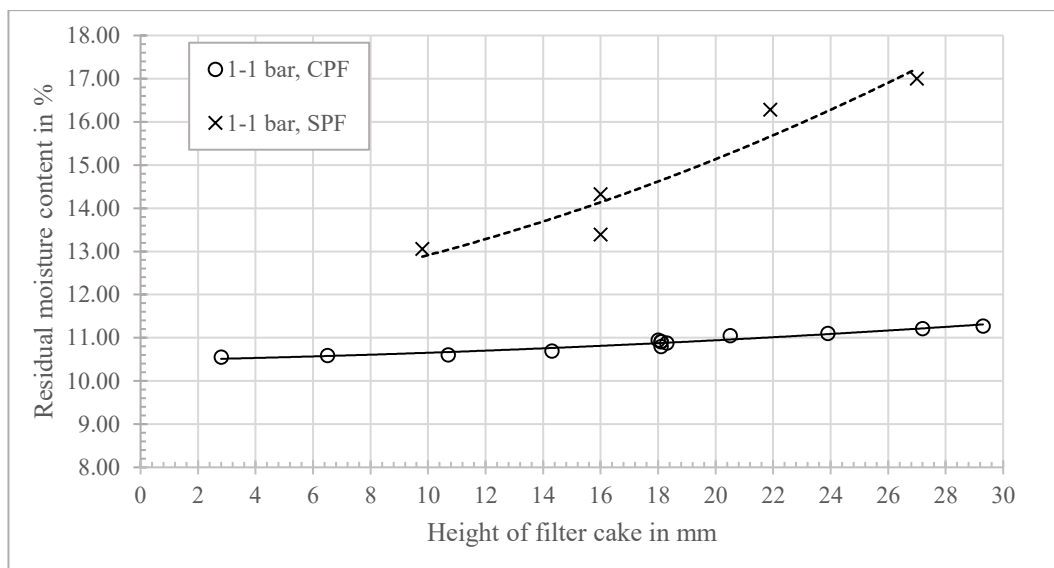




C2. Permeability ratio, saturation and residual moisture content of KS100 filter cake in variety filter cake height using CPF and SPF; 0.3 of volume fraction; “1-1 bar” and “1-3 bar” of pressure difference.



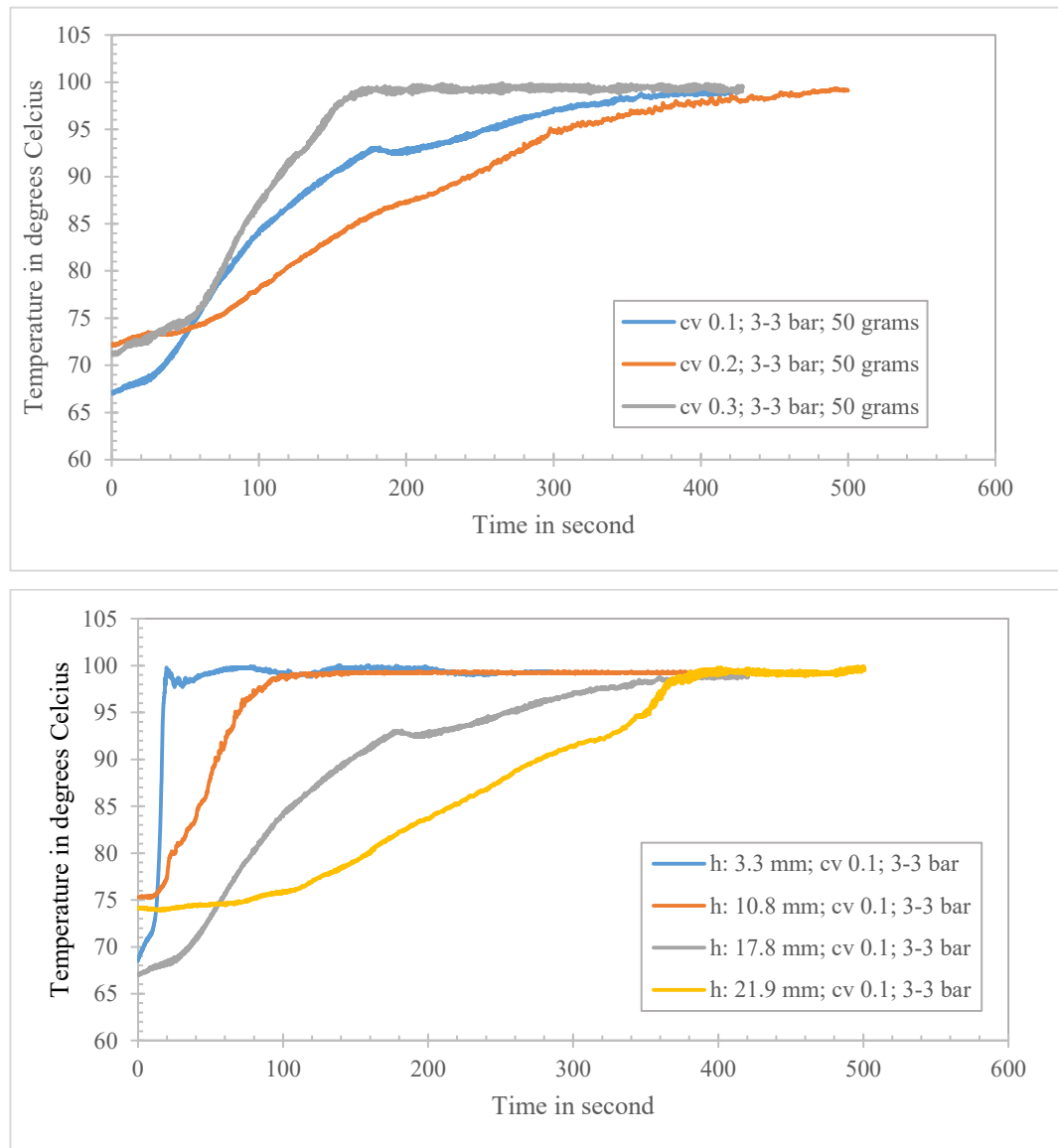




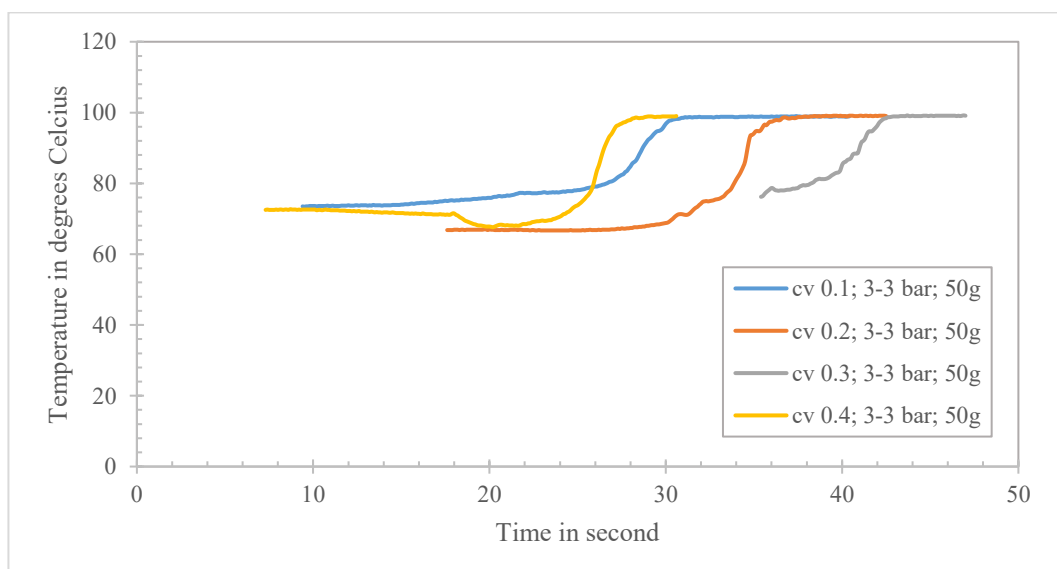
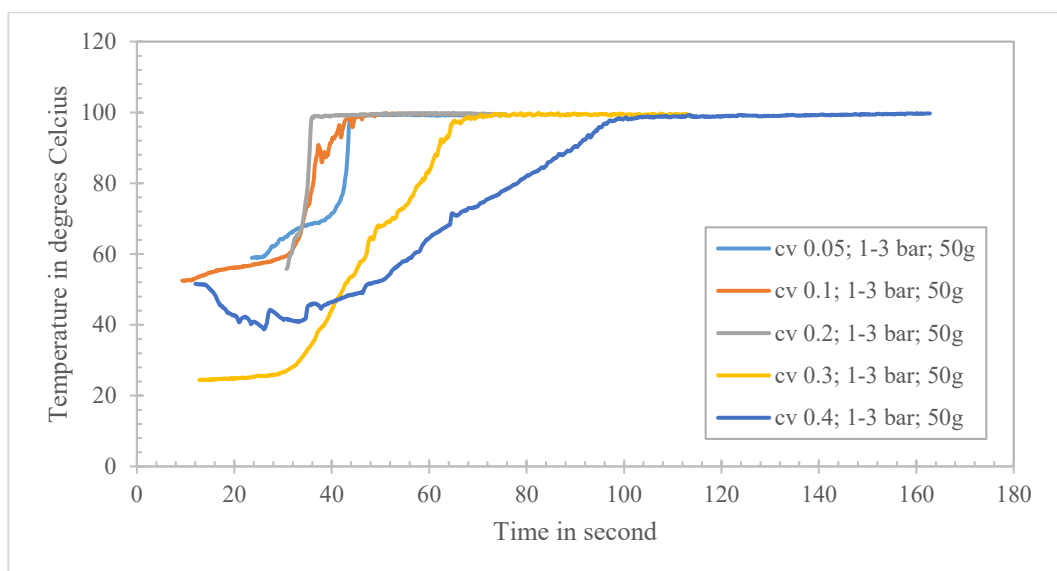
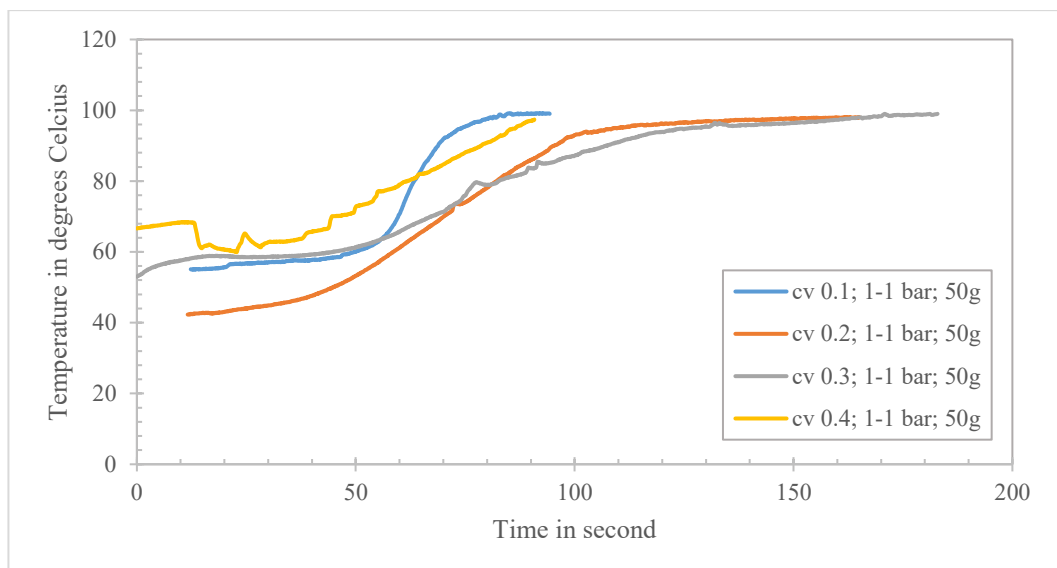
C3. Test for KS100 material result with the highest effort in controlling systematic error, using the steam pressure filtration (similar test procedure that is used for KS12 and VN coal).

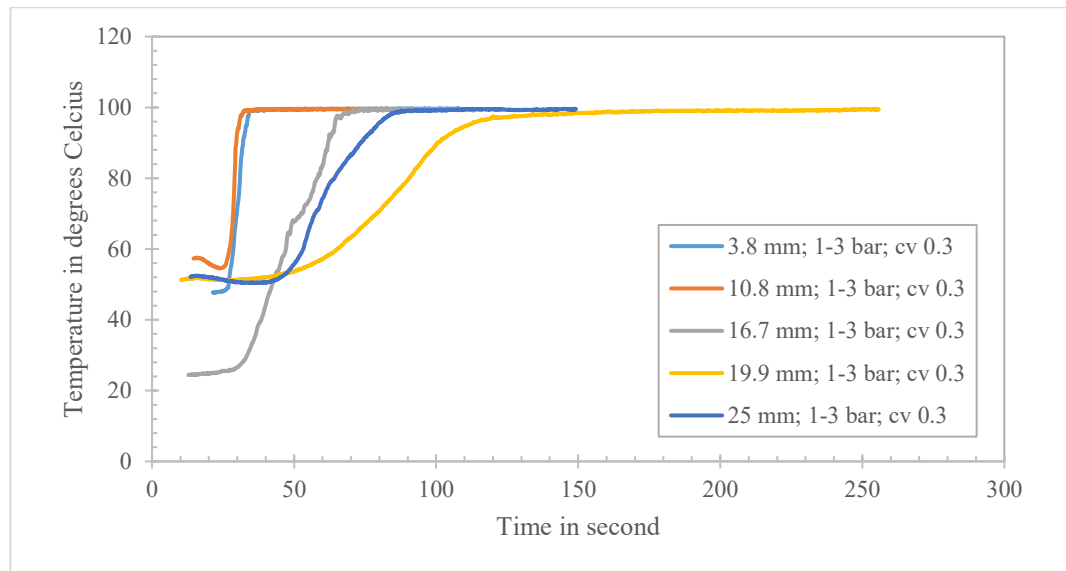
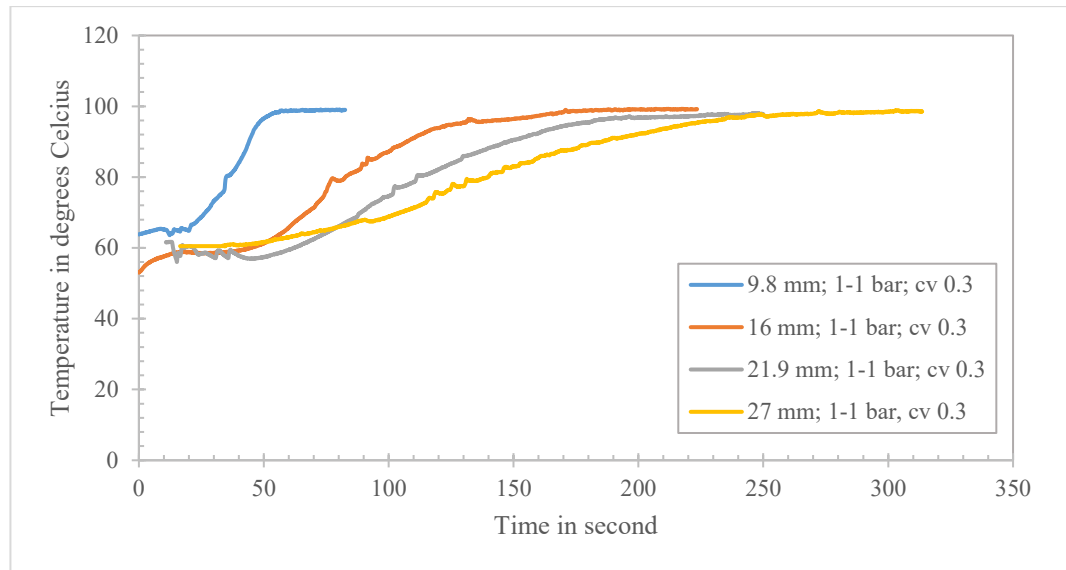
Test parameters		Saturation		Residual moisture content in %	
		New result	Last result	New result	Last result
Volume fraction	0.4	0.30	0.36	8.75	10.42
Pressure difference	3-3 bar				
Height of filter cake	16 mm				
Systematic errors		16.67 %		16.07 %	

C4. The temperature profile of bottom filter cake during the mechanical displacement phase for KS12 in various volume fraction and height of filter cake.

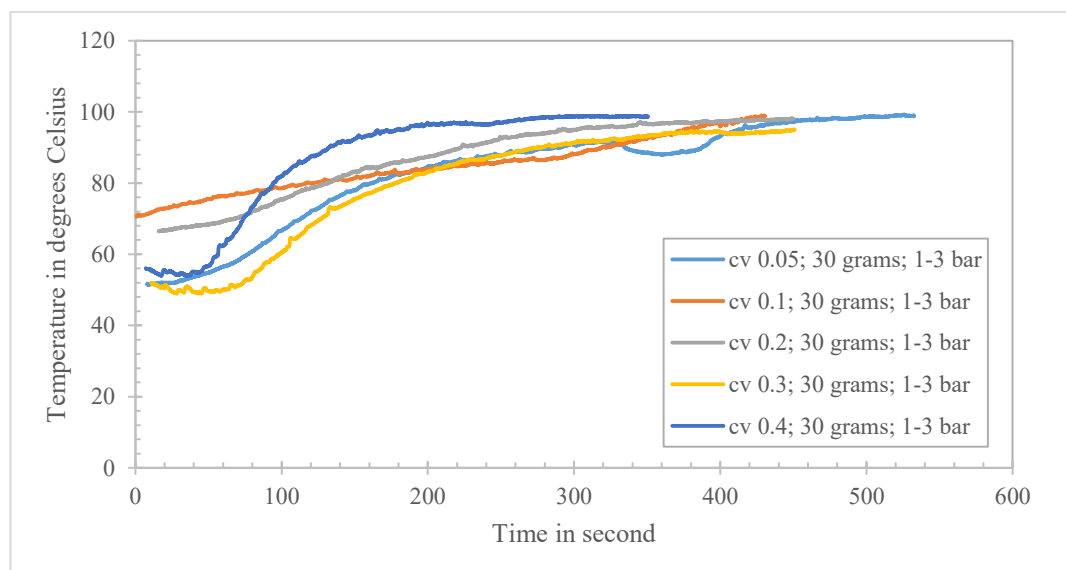


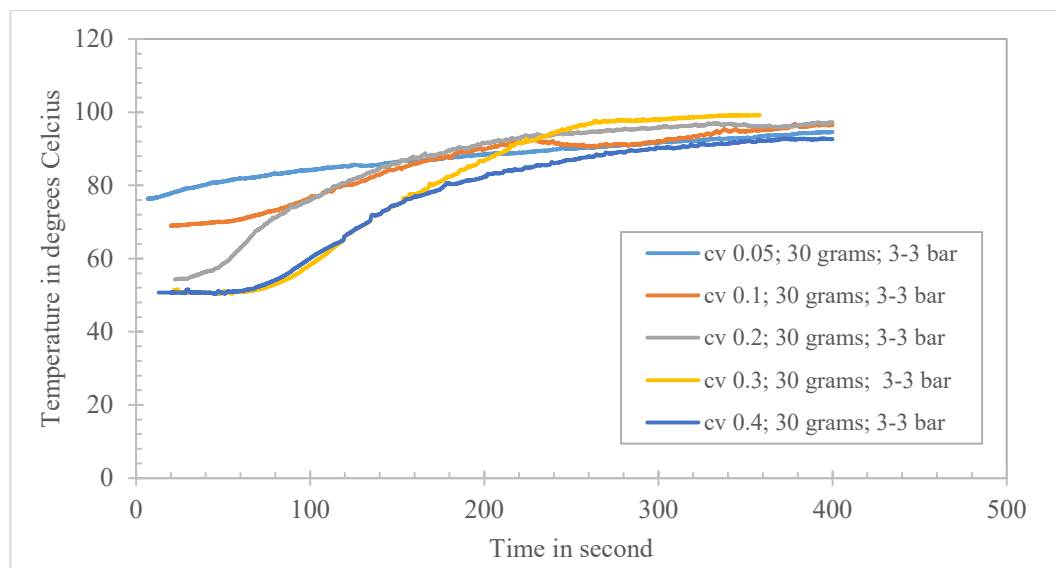
C5. The temperature profile of bottom filter cake during the mechanical displacement phase for KS100 in various volume fraction; filter cake height 15 mm.



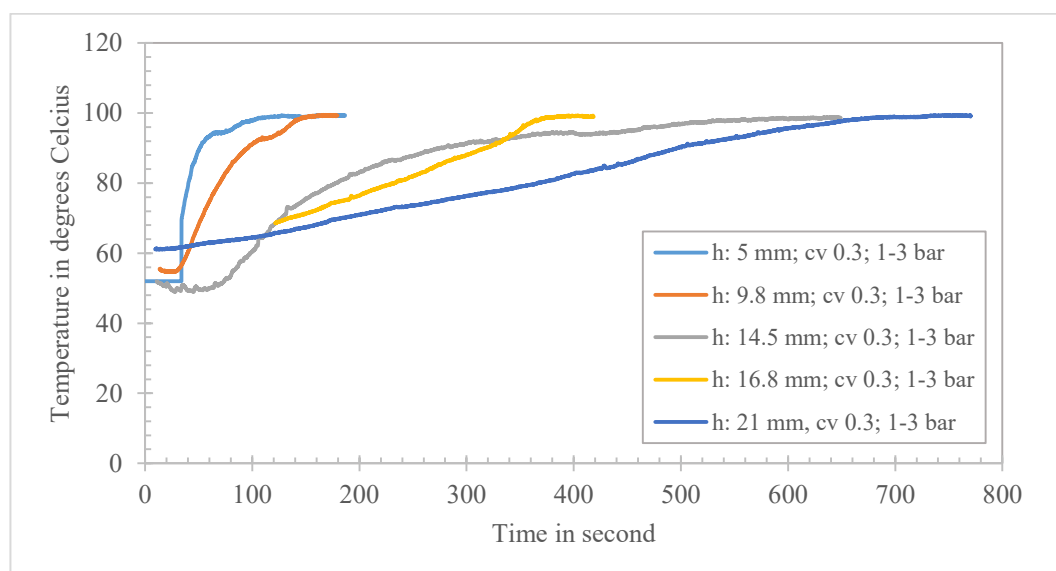


C6. The temperature profile of bottom filter cake during the mechanical displacement phase for VN coal in various volume fractions.





C7. The temperature profile of the bottom filter cake during the mechanical displacement phase for VN coal in a variety of filter cake height.



C8. Pre-test results using steam pressure filtration, including 3 phases: cake formation, mechanical displacement (by steam), drying (by air).

	KS100		KS12	VN coal	
Volume fraction	0.3	0.4	0.3	0.3	0.4
Pressure difference (cake formation-deliquoring-drying)	3-3-3 bar	3-3-3 bar	3-3-3 bar	3-3-3 bar	3-3-3 bar
Mass of solid in gram	50	50	50	30	30
Time of drying in second	150				
<b>Reisidual moisture content in %</b>	<b>9.05</b>	<b>6.73</b>	<b>16.12</b>	<b>13.78</b>	<b>12.65</b>

## Appendix D: Miscellaneous Information.

### D1. The concentration parameter $\kappa$ .

The value:

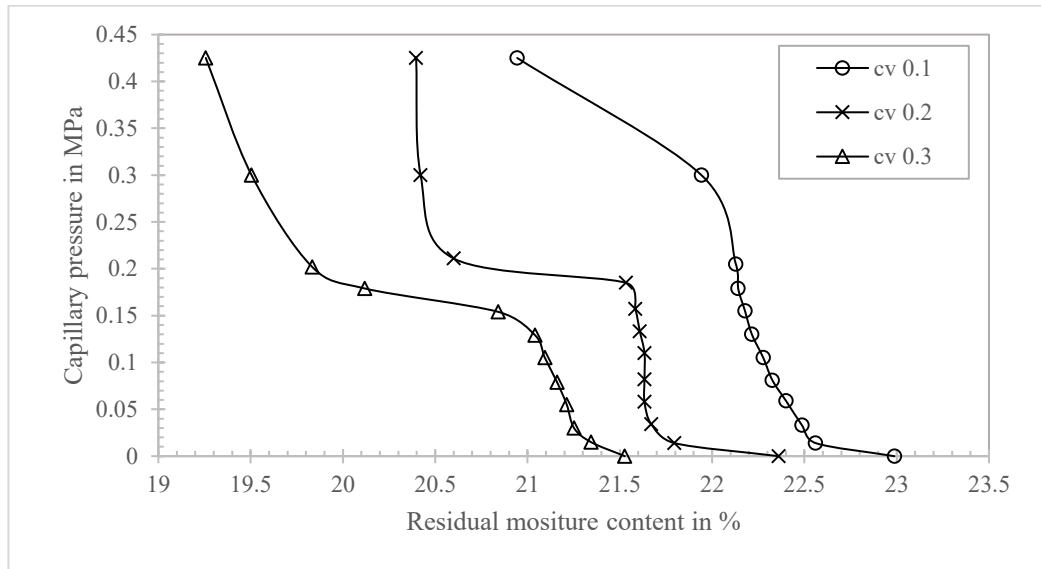
$$c. \frac{H.A}{m} = \frac{m}{V_{\text{filtrate}}} \cdot \frac{H.A}{m} = \frac{H.A}{V_{\text{slurry}} - V_{\text{cake}}} = \frac{V_{\text{cake}}}{V_{\text{slurry}} - V_{\text{cake}}}$$

By multiply  $V_{\text{slurry}}$  and  $V_{\text{solid}}$  to both numerator and denominator of above Equation, the new form can be rewritten:

$$c. \frac{H.A}{m} = \frac{V_{\text{cake}}}{V_{\text{slurry}} - V_{\text{cake}}} \cdot \frac{V_{\text{slurry}} \cdot V_{\text{solid}}}{V_{\text{slurry}} \cdot V_{\text{solid}}} = \frac{V_{\text{solid}}}{V_{\text{slurry}}} \cdot \frac{1}{\frac{(V_{\text{slurry}} - V_{\text{cake}})}{V_{\text{cake}}} \cdot \frac{V_{\text{solid}}}{V_{\text{slurry}}}}$$

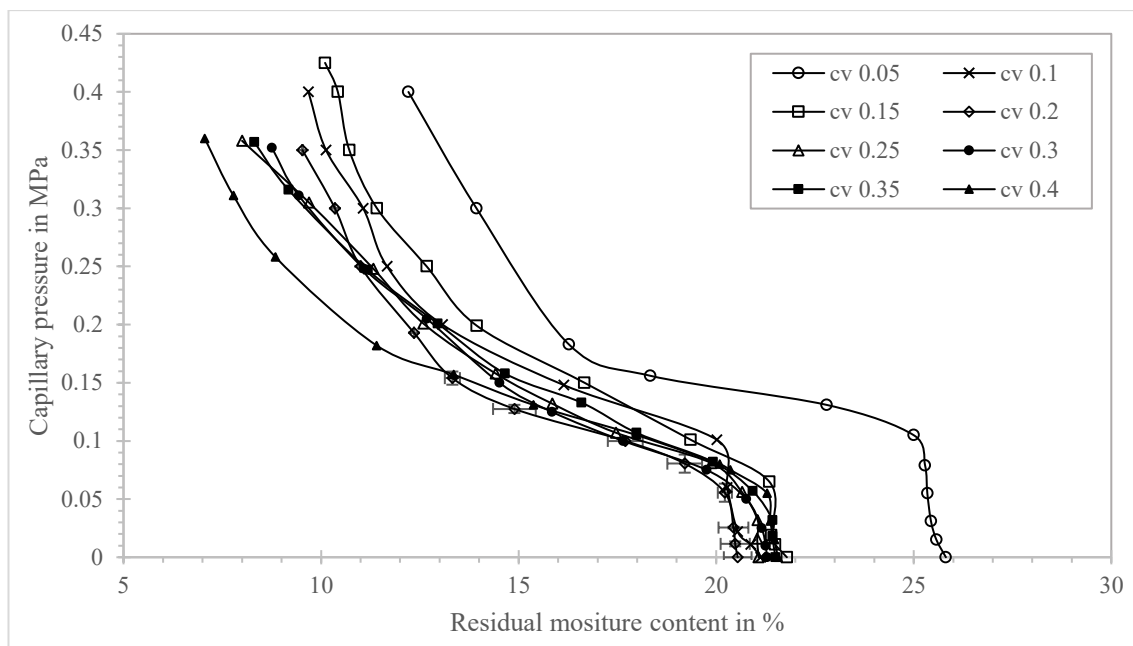
$$= \frac{c_v}{\frac{V_{\text{slurry}} \cdot V_{\text{solid}} - V_{\text{cake}} \cdot V_{\text{solid}}}{V_{\text{cake}} \cdot V_{\text{slurry}}}} = \frac{c_v}{\frac{V_{\text{solid}}}{V_{\text{cake}}} - \frac{V_{\text{solid}}}{V_{\text{slurry}}}} = \frac{c_v}{1 - \varepsilon - c_v} = \kappa$$

### D2. The relationship between the capillary pressure and the residual moisture content of KS12 filter cake in the various solid volume fraction of suspension.

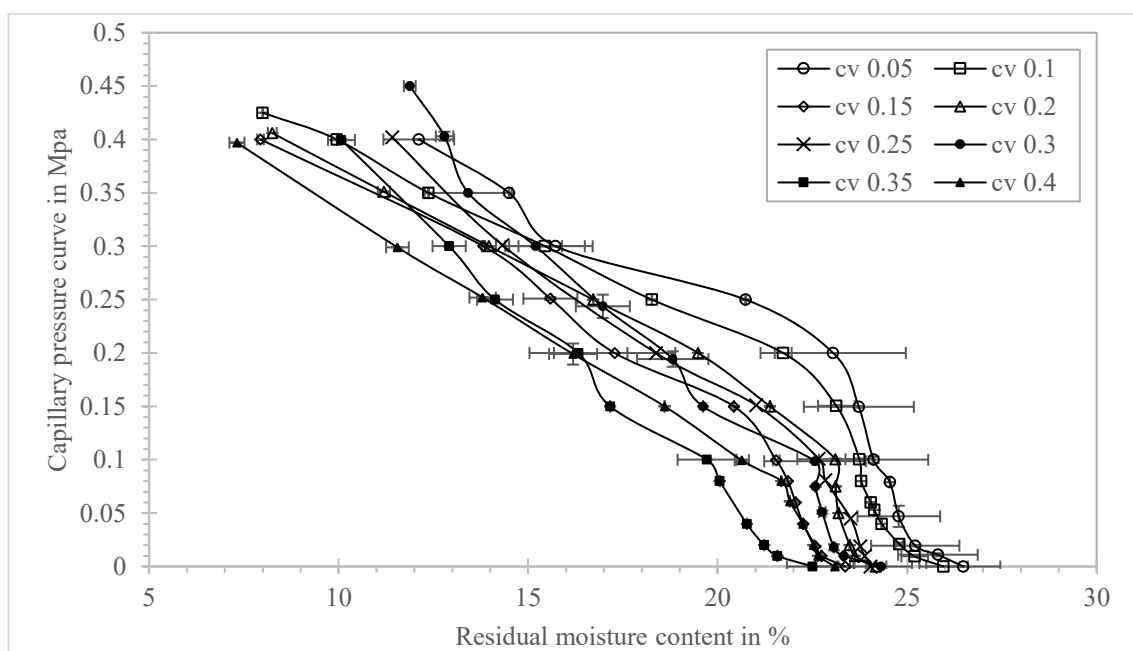


### D3. The relationship between the capillary pressure and the residual moisture content of KS100 filter cake in the various solid volume fraction of suspension.

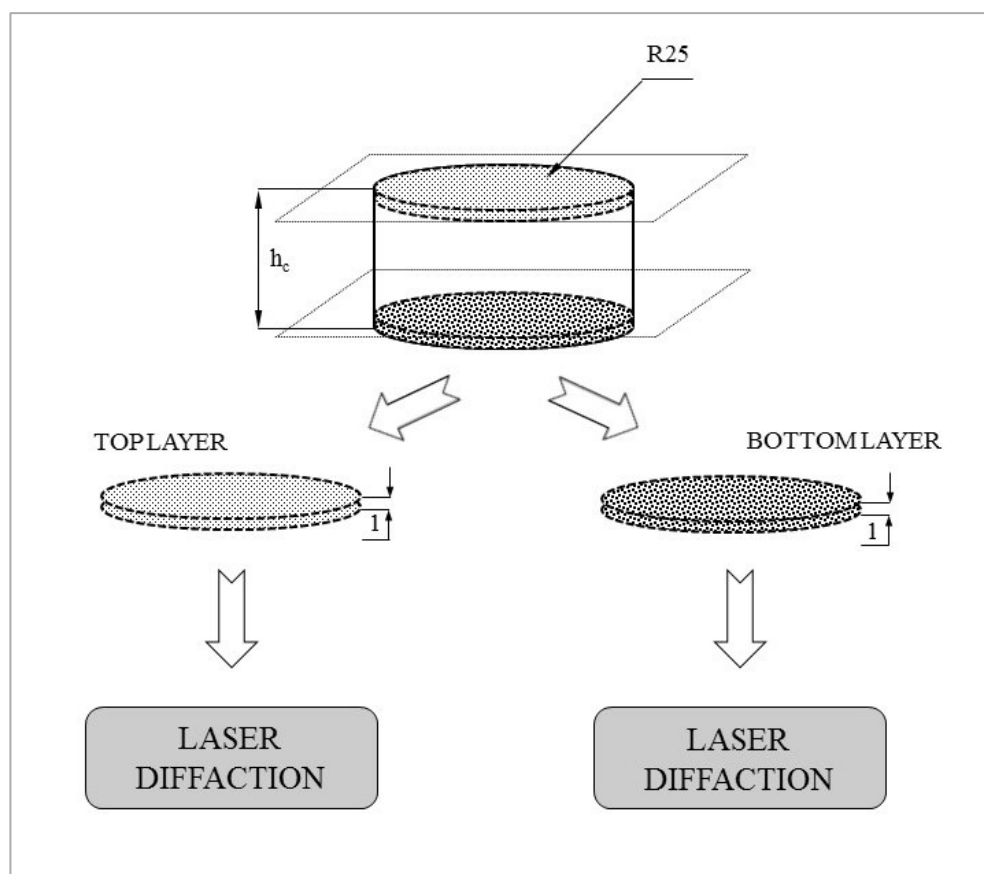




D4. The relationship between the capillary pressure and the residual moisture content of Vietnam coal filter cake in the various solid volume fraction of suspension.



D5. Diagram for sampling procedure from the top and bottom layer of the filter cake.



D6. Zeta potential of KS12 and KS100.

